Molecular thermodynamics using fluctuation solution theory

Ellegaard, Martin Dela

Publication date:
2011

Document Version
Publisher's PDF, also known as Version of record

Molecular thermodynamics using fluctuation solution theory

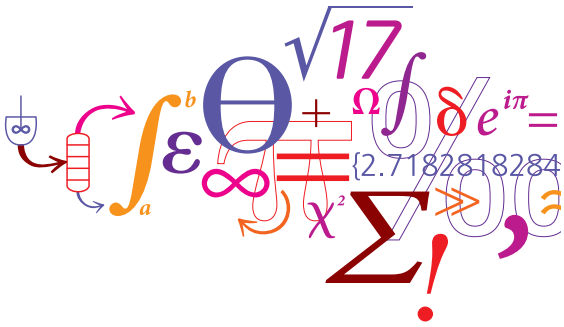

Martin D. Ellegaard
Ph.D. Thesis
April 2011

DTU Chemical Engineering
Department of Chemical and Biochemical Engineering

Molecular thermodynamics using fluctuation solution theory

Martin D. Ellegaard
Ph.D. Thesis
April 2011

DTU Chemical Engineering
Department of Chemical and Biochemical Engineering

Address: Computer Aided Process Engineering Center
Department of Chemical and Biochemical Engineering
Technical University of Denmark
Building 229
DK-2800 Kgs. Lyngby
Denmark
Phone: +45 4525 2800
Fax: +45 4588 4588
Web: www.capec.kt.dtu.dk

Print: J&R Frydenberg A/S
København
September 2011

ISBN: 978-87-92481-47-4

Π

Preface to thesis

This thesis is submitted as partial fulfillment of the requirements for the degree of *philosophiae doctor* at the Technical University of Denmark. The work was carried out between February 2008 and March 2011 at the Department of Chemical and Biochemical Engineering under guidance of associate professor Jens Abildskov, and funded by a scholarship granted by the Technical University of Denmark.

Initially, I wish to express my warmest thanks to my advisor for his large dedication and enthusiasm for the project. Though I was given freedom to pursue paths I thought best, the door was never closed. During the course of the work in this thesis, I was fortunate to be able to return to the University of Virginia for a period of time. I would like to express my sincere graditude and warmest thanks to professor John P. O'Connell for allowing me to return to Charlottesville and hosting me once again at the Department of Chemical Engineering. My gratitude also extends to the good people at the ChE department, as well as the wonderful people at the Lorna Sundberg International Center.

I am indebted to both my advisors for many fruitful investigations and discussions, as well as their tremendous support during the past three years. It is not without sorrow that I now conclude my studies, before entering the "real" world!

As is customary with projects such as these, many people not directly related to the scientific part deserve acknowledgements. The people at

the Computer-Aided Process Engineering Centre,

Kemiteknik,

the Technical University of Denmark, and

the University of Virginia

deserve much appreciation for wonderful friendships during the last eight years. Last, but certainly not least, I wish to express my most sincere gratitude to my wonderful wife, especially for putting up with me during these last (and long) months of writing.

Nørrebro, April 2011

M.D.E.

Abstract

Properties of chemicals and their mutual phase equilibria are critical variables in process design. Reliable estimates of relevant equilibrium properties, from thermodynamic models, can form the basis of good decision making in the development phase of a process design, especially when access to relevant experimental data is limited. This thesis addresses the issue of generating and using simple thermodynamic models within a rigorous statistical mechanical framework, the so-called *fluctuation solution theory*, from which relations connecting properties and phase equilibria can be obtained. The framework relates thermodynamic variables to molecular pair correlation functions of liquid mixtures. In this thesis, application of the framework is illustrated using two approaches:

1. Solubilities of solid solutes in mixed solvent systems are determined from *fluctuation solution theory* application to expression arising from thermodynamics. This results in neat and unusually simple expressions involving molecular correlation functions. These are determined from a combination of experimental data and molecular-based models, and their transferability is analyzed extensively.

2. Solubilities of gases in ionic liquids are described using a simple, yet physically sound, model for molecular correlation functions. The method addresses solubilities of supercritical gases in ionic liquids, as well as volumetric properties of pure fluids.

In both cases, the models require a minimum of input data, and results are not highly sensitive towards parameter values.

Resumé

Kemikaliers egenskaber og deres indbyrdes faseligevægte are kritiske variable i forbindelse med procesdesign. En god beslutningsproces i udviklingsfasen af procesdesign kræver gode estimater af relevante ligevægtsegenskaber fra termdoynamiske modeller. Dette gør sig især gældende, når adgangen til eksperimentelt data er begrænset. Denne afhandling beskriver udvikling, og brug, af termdoynamiske modeller i indenfor rammerne af det rigoristiske statistisk mekaniske *fluctuation solution theory*, hvorfra relationer mellem stofegenskaber og faseligvægte kan fås. Teorien forbinder termodynamiske variable til integraler af molekylære parfordelingsfunktioner for væskeblandinger. Afhandlingern illustrerer anvendelsen af teorien gennem to tilgangsmåder:

1. Opløseligheden af fastformige stoffer i blandede solventer er bestemt fra de fundamentale ligevægtsrelationer, som med *fluctuation solution theory*, resulterer i usædvanligt simple udtryk, som involverer integralerne for parfordelingsfunktioner som modelparametre. Disse bestemmes udfra en kombination af eksperimentelt data og molekylære modeller, og deres indbydes samhørighed er analyseret i stort omfang.

2. Opløseligheder af gasser i ioniske væsker er beskrevet med en simpel, men dog fysisk velfunderet, model for molekylære parfordelingsfunktioner. Metoden er anvendt til såvel gasopløseligheder, som volumetriske egenskaber af rene fluider.

De resulterende modeller kræver i begge tilfælde et minimalt datagrundlag for parameterestimering, og resultaterne udviser ikke stor følsomhed overfor parameterværdierne.

Menu

Nomenclature

Throughout this thesis vectors and matrices are denoted using a boldface sans serif font. Usually, vectors are denoted with lower case letters (**a**) while matrices are marked with upper case (**A**). Unfortunately, as a result of inconsistencies in the standard literature, this is not always followed stringently, and the reader should take care to consider the correct dimension when analyzing equations containing vectors or matrices.

Below is a comprehensive list of all symbols appearing in the thesis, ordered according to different categories, as well as subscripts, superscripts, and abbreviations.

Roman symbols

$a_{0,R}, a_{1,R}, a_{2,R}$	Parameters in expression for Henry's law constant
a_1, a_2	Parameters in expression for hard-sphere second virial coefficient
a_k	Coefficient in Equation (3–2) or parameter in expression for reduced volume
a_{kj}	Parameter in Wilson equation or UNIFAC equation
A	Parameter in the Porter equation
A	Parameter in Margules equation in the unsymmetric convention
A_{12}, A_{21}	Constants appearing in Margules equation
A_{ij}	Matrix element defined in Equation (2–17)
$A_{i,j}$	Margules parameter in the unsymmetric convention for i in pure j
b_1, b_2	Parameters in expression for hard-sphere second virial coefficient
b_i	Parameter in expression for reduced volume
B	Parameter in Margules equation in the unsymmetric convention
B_{12}, B_{21}	Constants appearing in Margules equation
B_{ij}	Matrix element defined on page 34, liquid bulk modulus, or second virial coefficient
$B_{i,j}$	Margules parameter in the unsymmetric convention for i in pure j
c	Constant of integration
c_i	Molar concentration of species i

$c_1, \ldots, c_5$	Parameters in expression for second virial coefficient
c_P	Heat capacity at constant pressure
c_{ij}	Direct correlation function between i and j
C_{ij}	Direct correlation function integral between i and j
$D_{a,i}, D_{c,i}$	Parameters in method of Jacquemim et al.
D_{ij}	Matrix element of Gibbs-Duhem equation in Equation (2–20)
E_j	Energy level of microstate j
f	Fugacity of mixture
f_i	Fugacity of species i
f_{ij}	Difference in total correlation function integrals
F	Objective function for excess solubility parameter estimation
$F^{(k)}$	Variable in modified Margules equation
F_{234}	Function of f_{ij}
$g_{ij}^{(2)}$	Pair correlation function of i and j
g	Molar Gibbs energy
g_1, g_2	Phase equilibrium constraints
g_i	Molar Gibbs energy of species i
G	Total Gibbs energy
G_a, G_c	Parameters in method of Jacquemim et al.
G_i	Variable in modified Margules equation
G_{ki}	Variable in UNIFAC equations
h	Molar enthalpy
h_{ij}	Total correlation function between i and j
H_a, H_c	Parameters in method of Jacquemim et al.
H_i	Henry's law constant of i
$H_{i,j}$	Henry's law constant of i in j
H_{ij}	Total correlation function integral between i and j
J_i	Variable in UNIFAC equations
k	Boltsmann's constant or scale factor for hard-sphere volume
k_{ij}	Binary interaction coefficient
K_i	K-factor for computing liquid miscibility
L_i	Variable in UNIFAC equations
m_i	Molality of i
M_i	Molar mass of i

n	Total number of moles, $n = \sum_i n_i$
n_i	Number of moles of species i of number of points in set i
N	Total number of moles, $N = \sum_i N_i$
N_i	Number of molecules of species i
P	Pressure
$P(\mathbf{N})$	Probability of configuration with $\mathbf{N}$
q	Variable in UNIFAC equations or objective function in data reduction of pure liquids
q_i	Variable in UNIFAC equations
Q	Partition function in the canonical ensemble
Q_k	Volume of group k
r_i	Variable in UNIFAC equations
$\mathbf{r}_i$	Position vector of i, ($\mathbf{r}_i = [r_{x,i}, r_{y,i}, r_{z,i}]$)
R	Ideal gas constant
R_k	Surface area of group k
s	Molar entropy or objective function in gas–ionic liquid data reduction
s_i	Logarithmic mole fraction of i
s_{ki}	Variable in UNIFAC equations
S_1, S_2	Solid phases
t	Dummy variable in density expression
T	Temperature
T_i^*	Characteristic temperature of i
T_{ij}^*	Cross-characteristic temperature of i and j
u	Intermolecular potential energy
v_i	Molar volume of i
v_a^*, v_c^*	Volumes of anion and cation
V	Total system volume
V_i^*	Characteristic volume of i
V_{ij}^*	Cross-characteristic volume of i and j
w_i	Weight fraction of i or weight of data set i
W_{ijk}	Difference in correlation functions for all pairs composed of i, j, and k
x_i	Liquid-phase mole fraction of i
$x_{i,j}$	Solubility of i in j
X_{ii}	Element of diagonal matrix, $X_{ii} = x_i$
y_i	Vapor-phase mole fraction of i

Y_{ii}	Element of diagonal matrix, $Y_{ii} = \rho\bar{v}_i$
z	Coordination number in UNIFAC equations
z_0, z_1, z_2	Parameters in expression for reduced hard-sphere diameter
z_j	Composition of j
Z_{1234}	Difference in correlation functions for all pairs composed of 1, 2, 3, and 4

Greek letters

β	Inverse thermal energy ($\beta^{-1} \equiv \mathrm{k}T$) or isobaric expansivity
γ_i	Activity coefficient of species i
$\gamma_{i,j}$	Activity coefficient of species i in pure species j
δ_{ij}	Kronecker delta ($\delta_{ij} = 1$ if $i = i$, otherwise 0.)
$\delta V_{w,j}$	Van der Waals volume of j
Δ	Used to denote a difference in the property that follows this symbol or a quantity defined on page 59
ϵ_{ki}	Variable in Wilson equation
η	Parameter in modified Margules equation
η_k	Variable in Wilson or UNIFAC equations
ϕ_i	Fugacity coefficient of volume fraction of species i
Φ	Arbitrary thermodynamic variable
κ	Compressibility
λ_{ij}	Parameter in Wilson equation
Λ_{ij}	Variable in Wilson equation
μ_i	Chemical potential of species i
$\nu_k^{(i)}$	Stoichiometry of group k on molecule i
ω_i	Angular orientation of i
Ω	Normalization factor
ρ	Molar density ($\rho = \sum_i \rho_i$)
ρ_i	Molar density of i
$\rho_i(\mathbf{r}_i)$	Molar density of i at position $\mathbf{r}_i$
$\rho_{i,j}$	Molar density of i and j at positions $\mathbf{r}_i$ and $\mathbf{r}_j$
σ_i	Hard-sphere diameter of i
ϑ_k	Variable in UNIFAC equations
Ξ	Partition function in the grand canonical ensemble
ζ_m	Reduced density of degree m

Subscripts

c	Critical variable
i, j, k	Chemical species
m	Melting or mixture property
mix	Mixture property
t	Transition property

Superscripts

$'$	Solute-free composition
$\hat{}$	Model-based value
$\bar{}$	Mean value
$\tilde{}$	Reduced property
$*$	Unsymmetric convention (normalization of γ_i)
∞	Infinite dilution
0	Initial or pure species property
0	Infinite dilution in single solvent
$+$	Infinite dilution in mixed solvent
α, β	Phases
C	Combinatorial term in UNIFAC equation
E	Excess quantity
$h.s.$	Hard-sphere property
id	Ideal property
L	Liquid-phase property
R	Residual term in UNIFAC equation
sat	Saturated property
S	Solid-phase property
V	Vapor-phase property

Miscellaneous symbols

$\langle\rangle$	Average value
T	Transpose of a vector or matrix
$\mathbf{0}$	Zero column vector
$\mathbf{F}$	Matrix defined in Equation (2–39)
$\mathbf{i}$	Unit vector

$\mathbf{I}$	Unit matrix
$\bar{v}_i$	Partial molal volume of i

Abbreviations

AAD	Average absolute deviation
AAPE	Average absolute percentage error
Adj ()	Adjoint matrix
ASOG	Analytical solution of groups
COSMO	Conductor-like screening model
DMSO	Dimethylsulfoxide
FST	Fluctuation solution theory
GC-EOS	Group-contribution equation of state
IUPAC	International Union of Pure and Applied Chemistry
MEK	Methyl ethyl ketone
MOSCED	Modified separation of cohesive energy density
MTBE	Methyl tert-butyl ether
NRTL-SAC	Non-random two-liquid segment activity coefficient
PAH	Polycyclic aromatic hydrocarbon
PC-SAFT	Perturbed-chain SAFT
PCP-SAFT	Pertubed-chain-polar SAFT
POY	Poynting factor
SAFT	Statistical associated-fluid theory
S.D.	Standard deviation
SLE	Solid-liquid equilibria
SRK	Soave-Redlich-Kwong equation of state
UNIFAC	Universal functional activity coefficient
VLE	Vapor-liquid equilibria

1. Introduction

Remember that all models are wrong; the practical question is how wrong do they have to be to not be useful.[1]

Design of chemical products and processes requires accurate knowledge of a variety of thermophysical properties and phase equilibria characterizing the chemical substances and their mixtures of interest. Consulting experimentalists for the required data is time consuming and expensive, especially if the number of mixture combinations is large. Process engineers therefore often resort to models for estimating properties. Examples of these include evaluating volumetric properties needed to properly size a piece of equipment, or enthalpies for calculating heat duties. A problem which often manifests is selection of optimal solvent(s) for enhancing certain properties for a chemical process. This could be boiling point elevation, or lowering of viscosity. Another is the estimation of optimal conditions for a separation process, such as distillation or liquid extraction. Figure 1–1 (roughly) illustrates a production line of a chemical substance. A feed line is connected to a reaction unit, and the result is almost always a mixture of product(s) and commodity species (e.g. solvents, catalysts, additives). During subsequent separation processes, high-value products are separated from those of lesser value. If the product is a liquid, separation from solvents can occur by using differences in boiling points (distillation).

Designing a distillation column involves many variables. Among others estimation of the relative volatility between light and heavy keys. Dohrn and Pfohl[2] pointed out, that a 5% error in the estimation of this quantity can lead to an estimation of more than double the minimum number of stages for the column. With a typical investment cost for a distillation column being around €4500000, designing "safe", i.e., adding

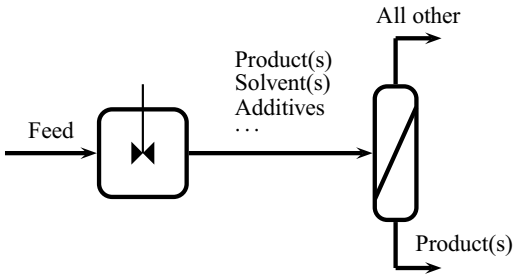

Figure 1–1. Simplified overview of chemical production from feed to purified product(s).

extra stages beyond those required by minimum, can be extremely expensive, and should be avoided when possible. The goal of thermodynamics as an *engineering* discipline is to provide engineers and other model users with reliable estimates of relevant solution properties and phase equilibria in order to facilitate optimal design of chemical processes. Particularly downstream separation processes, since often more than half of investment costs is for equipment in this part of the process.[3] Thermodynamic models must therefore facilitate reliable decision making when facing problems, such as optimizing existing production lines or scale-up of facilities.

1.1. Background

All engineering sciences require knowledge and expertise, but chemical engineering, in addition to these, requires insight into molecular level science. The art of problem solving in this field is therefore often of a complex nature. The scientific/engineering approach to problem solving can be constructed as a three-step process, where a physical problem is dissected into smaller parts, whereafter a final solution of the original problem is obtained from combining the partial results. This requires the ability to

1. formulate a physical problem in mathematical and thermodynamic terms,
2. solve that problem formulation using theoretical insights (e.g. statistical mechanics),
3. and finally translate the solution back into real-world terminology. This is usually in the form of a model describing relations between a set of variables, such as an equation of state.

This three-step process is illustrated in Figure 1–2. Essentially, the first two items have been solved by the pioneering works of Boltzmann, Maxwell, and Gibbs, who formulated the basis of modern-day engineering thermodynamics. The critical part of the process in Figure 1–2, and what has been the basis of much research in thermodynamics since the start of the 20th century, is the translation back into physical terms. This means the development of models describing properties (thermodynamic, thermophysical, ...), which are used to solve the – often complex – problems that arise in chemical thermodynamics, by setting up mathematical relations between relevant variables, such as temperature, pressure, and density. Consider the situation where an engineer in the process design group of a company is required to estimate the solubility of a new high-value pharmaceutical compound X in a mixture of solvents, which will be used to design a chemical separation process for X. Solubilities of X are known in each of the pure solvents, and the solubilities in a few mixtures have been measured as well, in addition to a few thermophysical properties (such as melting point and heat of fusion) of X, that are also known. Otherwise no data for X is known to exist. The engineer is now required to determine the composition of a solvent mixture, which will give the highest solubility of X, in order to minimize crystallization in the

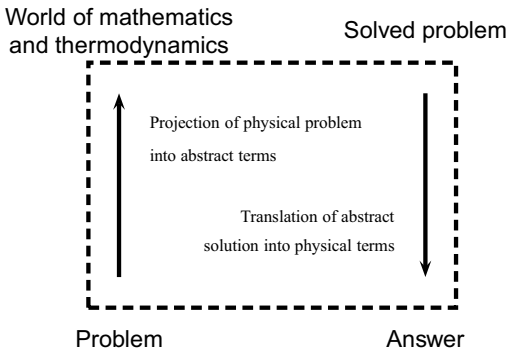

Figure 1–2. Application of thermodynamics for solving real world problems. Adapted freely from Prausnitz et al.[3]

process equipment. The value of X is extremely high, so experimental measurements must be confined to an absolute minimum, and should ideally be used only for confirmation of a candidate process design. The engineer will be interested in a model for determining solubilities in mixtures of solvents. The nature of thermodynamic models can be classified in two ways:

1. Models which are universal in nature, and

2. models which are non-universal in nature.

The first type is a model applicable for many types of properties or phase equilibria. These encompass most contemporary excess Gibbs energy methods and equations of state. They are usually based on very general fluid-phase models, and are therefore able to address a wide variety of problems. The background for making this classification is based on the constant production of new and improved molecular models, aspiring in their generality. There seems to be a quest for a model capable of describing effectively all types of properties, phase equilibria, and molecular species. This is often referred to as *the universal equation of state*. There is a strong desire towards establishing this on the basis of molecular structure, e.g. group contributions.[4–9] Group contribution method assign thermodynamic properties to fragments of a molecule, rather than the entire molecule itself, and calculates a molecular property based on the group stoichiometry. This implies that molecules, for which no data exist, can be built using only their molecular structures as basis. Regardless of the parameterization, being either pure component parameters or group contributions, any such model capable of describing properties of practically all kinds of chemical substances, throughout all relevant state conditions, must be highly complicated and contain many parameters (or other adjustable coefficients). Since the early days of molecular-based theories – springing from the pioneering works of van der Waals in 1879 – models based on molecular-level interactions has grown significantly in complexity and application range. Through the 20th century, equations

of state have evolved from being mere modifications of the attractive term in the van der Waals equation, such as traditional cubic equations like the Redlich-Kwong[10] and Peng-Robinson[11] equations, to more advanced multiterm models, capable of describing hydrogen bonding and other phenomena explicitly. The majority of them are quite parameterized, and parameter determination takes time. The illustration is done based on equations of state, but similar arguments hold for the vast majority of all molecular-based models in the scientific literature. In spite of being complex, there are a few inherent problems with many equations of state and excess Gibbs energy methods. While most parameters for an equation of state can be obtained from regression of pure component data, many equations make use of the one-fluid mixing rule, where binary interaction parameters are used to properly scale interactions between unlike molecular species. Results are often highly sensitive to their values, and their values come only from regression of (at least) binary data. Excess Gibbs energy models usually do not suffer from combining rules, but generally require mixture data for regression of parameters. Unfortunately, parameters are not always consistent when regressed from two- or multicomponent mixtures,[3] especially in highly asymmetric systems.

Non-universal models are capable of addressing delimited problems solely. These are frequently based on empirical observations, but their form can be consistent with rigorous theoretical considerations. Although this latter path might seem inferior to the former, this is not generally the case. For confined problems, it is often advantageous to work with models which are more tuned towards specific problems. Often, the models are less sensitive towards parameter values. Be they either universal or non-universal, it is important not to lose perspective of the role of thermodynamics in process design, i.e., to establish reliable and practical estimates of relevant thermodynamic properties. This will inevitably imply a trade-off between generality and simplicity of the model. It is therefore unrealistic to expect a single model to quantitatively describe everything being used in practice for designing thermodynamic processes.

1.2. Specifying the problem

We now return to the engineer faced with having to determine the maximum solubility of X in solvents A and B. Parameters for X are not known for any thermodynamic model, but A and B are common solvents, so their parameters for a model can be established relatively easy. The engineer has a limited amount of experimental data for testing different thermodynamic models to find the optimal mixture of solvents.

A number of "predictive" models are available for addressing solubilities in solvent mixtures, such as the log-linear method and COSMO*. These do not require estimation of pure component parameters,

* These models are described in Chapter 3. For now they appear as confusing acronyms to the non-expert.

Table 1–1. Methods used for calculating solute solubility in mixed solvent systems.

Method	Example(s)	Comments
Empirical methods	Cosolvency models	Requires substantial amounts of mixture data for parameter estimation.
g^{E}-models	Wilson, NRTL, UNIQUAC	Requires two parameters for each pair ($A_{ij} \neq A_{ji}$). Multicomponent results might not be accurate when using binary-based parameters.
g^{E}-models (predictive)	ASOG, UNIFAC	GC methods are often unable to accurately describe polyfunctional molecules. Often group interactions are missing. Does not make use of available data.
EoS	PR, SRK, SAFT	Requires many parameters regressed from data and k_{ij} from mixtures.

but their estimates of often not very accurate. Group contribution methods, such as ASOG and UNIFAC, also do not require pure component properties. Unfortunately, the "exotic" molecular structures of most pharmaceutical compounds prohibits use of most group contribution methods, since parameters for many functional groups have yet to be estimated. Furthermore, most group contribution methods are unable to accurately address polyfunctional molecules. Neither of these predictive methods makes use of the limited experimental data, which are available.

Equations of state and other advanced models typically require more parameters than what can be obtained from measurements in two single solvents. Even if just two parameters are required for X with A and B, the equation-of-state models require binary interaction coefficients to properly scale the combining rules; coefficients which require mixture data, and have to be known to within a few per cent. This is therefore an unlikely path. Conventional excess Gibbs energy models, such as Wilson, NTRL, and UNIQUAC, require two parameters for each pair interaction. That means, that a single solubility point in a solvent is not enough, and additional mixture data is required. In addition, parameters obtained from binary to represent multicomponent data does often not perform as well as using parameters regressed from multicomponent data.

A large number of empirical correlations do exist for mixture solubilities as function of composition of the solvent mixture. They are typically referred to as cosolvency models. However, the parameters for these come only from regression of multicomponent data, wherefore this is not an option.

Table 1–1 summarizes the arguments in the above discussions.

What seems to be in need is a simple, but accurate method for estimating mixture solubilities of new solids which actually makes use of available (limited) experimental data. The parameters should be based on physical terms, so that they might be calculable from data sources other than solubilities in solvent mixtures, meaning that the parameters are transferable between different data types. This implies, that the method should be based on some degree of rigor.

Table 1–2. Methods used for calculating gas solubilities solubility in ionic liquids.

Method	Example(s)	Comments
g^{E}-models	Wilson, NRTL, UNIQUAC	Poynting factors are used for pressure nonideality. These require $\bar{v}_i(T, P, \mathbf{x})$. These factors tend to cancel the composition nonideality (γ_i) to some extent.
Cubic EoS	RK, PR	Require hypothetical critical parameters for ionic liquids. Results are often very sensitive towards k_{ij}. The density ranges of these models might be limited.
EoS	SAFT	Many parameters, which require much data. Results are very sensitive towards k_{ij}. The association phenomena cannot always be captured.

Consider another example where the engineer is asked to determine the solvent, which gives the highest solubility of a sparingly soluble gas (hydrogen). Ionic liquids are a relatively new class of industrial solvents (practically without vapor pressures), which have shown great potential with gas solubilities, and the optimal design should include an ionic liquid as solvent. The problem arises when facing with the myriad of different molecular structures which exist (this will be explained in more detail in Chapter 8). Selecting the better solvent based on experiment is certainly infeasible when, in 2004,[12] more than one 500 different ionic liquid structures were identified*. Estimates of solubility from thermodynamic models is practically the only feasible option. Gases with small solubilities (such as hydrogen) typically have high equilibrium pressures (often above $100\,\mathrm{bar}$), so applying excess Gibbs energy models, which have no explicit pressure dependence, requires Poynting factors. These, in turn, require partial molal volumes. Furthermore, these factors often counter-effect the influence of gas-solvent nonideality arising from composition, i.e., activity coefficients (elaborated on more closely in Chapter 8).

Conventional cubic equations of state require critical pressures and temperatures, as well as binary interaction parameters (k_{ij}). Ionic liquid do not vaporize, so their critical point is purely hypothetical. Results are often highly sensitive towards k_{ij}, which means that regression may require substantial amounts of mixture data.

Ionic liquids are known to form solvates, so models which account for these phenomena may in principle be advantageous (such as SAFT). However, often many parameters are required, which means that much mixture data is needed for regression of their values. Empirical correlations are likely to exist, but extensions to high pressures makes this an unreliable option. Table 1–2 makes a summary, analogous to that above.

* Today (2011) that number is likely to be in the thousands.

Again, what seems to be needed is a method, which in a fast and reliable manner, can estimate the equilibrium solubility with a minimum of parameters.

1.3. Objectives of this work

The cases above depict a situation, where there is a need for a simple modeling framework, which with a minimum of parameters, are able to accurately describe relevant solution properties. The basis of the framework should be rigorous, partly to ensure consistency, but also to give the resulting model parameters a clear physical meaning. This helps in the development phase, where parameters can be compared and analyzed.

There are quite a few solution theories in the literature, which have resulted in neat and rather simple models. This is illustrated by e.g. *regular solution theory*,[13] which give species activity coefficients in solution. Wilson[14,15] interpreted the *local composition theory* of Guggenheim[16] to develop slightly more advanced, but still relatively simple, thermodynamic models for phase equilibria. These are based on expressing the interactions between molecules in the liquid phase in terms of parameters expressing nonideality in mixtures.

Here, the theory, usually referred to as *fluctuation solution theory*, or sometimes Kirkwood-Buff theory, has been invoked. The choice of this particular theory is motivated by mainly two things:

1. The basis of the theory is rigorous statistical mechanics, but actually results in neat expressions for properties of pure components and mixtures.

2. It is completely general and makes no assumption regarding intermolecular forces and interactions.

Chapter 2 gives an overview of the theory and its many relations. Here, the objectives of the thesis are given.

Objectives: Application of a general, rigorous statistical mechanical framework from which simple, but soundly based models, can be either derived, or used in combination with, for describing and predicting thermodynamic properties and phase equilibria. The framework is then applied for the two general problems illustrated above:

1. Solubilities of solids in mixtures of solvents. A simplified variant of this approach has previously been applied to solubilities of gases in mixed solvents, and it is worthy to test if solid solubilities can be addressed.

2. Solubilities of gases in ionic solvents (ionic liquids). A method, based on *fluctuation solution theory*, has previously been applied for solubilities of gases in pure and mixed organic/aqueous solvents.[17] It is relatively simple, and contain very few parameters. The basis of the

model is general, and is not sensitive to molecular details (polarity, association, etc.). The method is attractive, since it does not require substantial amounts of data for regression, and it not too sensitive towards parameter values. It is therefore attractive to see if the solubilities of gases can be described equally well.

The two problems are very different, and it is not desirable to address them simultaneously. Therefore, the thesis has been divided in two overall parts, and the problems are dealt with separately. The technical details of the two problems are then described in Chapters 3 and 8.

1.4. Overview of thesis

The thesis is organized as follows:

Chapters 1: Here, the overall problem of modeling in engineering thermodynamics is outlined, and the motivation for the thesis work is described by two relevant cases.

Chapter 2: Chapter 2 introduces and details the statistical mechanical framework *fluctuation solution theory*. It provides the basis of the modeling framework which is used throughout the thesis.

Chapter 3: This initiates Part I of the thesis. This chapter introduces the main problems when attempting to model solid solubilities are described. It also presents the traditional thermodynamic framework of solid-liquid equilibrium, and gives a number of relevant relations between properties of solubilities.

Chapter 4: An outline of the modeling framework is given, and is used to develop a model for estimating solubilities in mixtures of solvents. A procedure for obtaining parameters is given, and explains the role of the solvent mixture in the mixed solvent solubility issue.

Chapter 5: Here, reduction of binary vapor-liquid equilibrium data is presented. This is used to describe characteristic features of the solvent mixtures, which are required by the models developed in Chapter 4.

Chapter 6: This is the main results chapter for the mixed solvent solubility part. It presents the application of the developed models for solubilities in two- and three-solvent systems. A detailed analysis of the role of the solvent mixture is given with examples illustrating.

Chapter 7: A summary and discussion of the results obtained is give here, and ending Part I.

Chapter 8: This initiates Part II of the thesis. An introduction to the concept of ionic liquids, their properties, and their phase equilibria is given. The chapter gives an overview of the conventional

approaches to high-pressure gas-liquid systems, and explains why there is a need for a stronger basis when developing models for gas-liquid equilibria.

Chapter 9: Chapter 9 shows how the modeling framework is constructed, and gives an overview of the general thermodynamic relations, which are obtained.

Chapter 10: This chapter highlights application for volumetric properties of pure ionic liquids. Results are presented, which illustrates the simplicity and overall performance of the method.

Chapter 11: This is one of the main results chapters for gas solubility calculations in ionic liquids. Results show how the method estimates gas solubilities, and also illustrates some of the limiting features.

Chapter 12: This is the second chapter with results for gas solubilities. Based on the conclusions from Chapter 11, attempts are made to further optimize the method.

Chapter 13: Here, a general summary and discussion of the results obtained in this part is given, which also ends Part II.

Chapter 14: Overall conclusions of the thesis, and an outlook on some future challenges, which remain.

Each chapter is ended with a small summary to familiarize the reader with the major results obtained. There are a number of appendices, usually derivations of theoretical results, or long parameter tables. These are placed immediately after the relevant chapters. In addition, there are also a few "global" appendices, i.e., appendices not pertaining to one specific chapter, but are drawn upon by several chapters. These are placed after the conclusions, from page 263 and on. They are:

Appendix A: The mathematical framework for linear and nonlinear parameter estimation.

Appendix B: Publications by the author.

The underlying theory, which connects Part I and II of this thesis, is derived and presented in the following chapter. It is given prior to formulating the technical problems of both Part I and II, since it forms the basis of the theory for both parts. Therefore, it seems appropriate to present it at this place.

References

1. G. E. P. Box and N. R. Draper. *Empirical model-building and response surfaces*. Wiley, 1987.
2. R. Dohrn and O. Pfohl. *Fluid Phase Equil.*, 194-197:15–29, 2002.
3. J. M. Prausnitz, R. N. Lichtenthaler, and E. Gomez de Azevedo. *Molecular thermodynamics of fluid-phase equilibria*. Prentice-Hall, 3rd edition, 1999.
4. J. Ahlers and J. G. Gmehling. *Fluid Phase Equil.*, 191:177–188, 2001.
5. L. S. Wang, J. Ahlers, and J. G. Gmehling. *Ind. Eng. Chem. Res.*, 42:6205, 2003.

References

6. J. Ahlers and J. G. Gmehling. *Ind. Eng. Chem. Res.*, 42:7045–7045, 2003.

7. J. Ahlers, J. G. Gmehling, and T. Yamaguchi. *Ind. Eng. Chem. Res.*, 43:6569–6576, 2004.

8. A. Lymperiadis, C. S. Adjiman, A. Galindo, and G. Jackson. *J. Chem. Phys.*, 127:234903 (1–22), 2007.

9. A. Lymperiadis, C. S. Adjiman, G. Jackson, and A. Galindo. *Fluid Phase Equil.*, 274:85–104, 2008.

10. O. Redlich and J. N. S. Kwong. *Chem. Rev.*, 44: 233, 1949.

11. D. Y. Peng and D. B. Robinson. *Ind. Eng. Chem. Res. Fundam.*, 15:59–64, 1976.

12. K. N. Marsh, J. A. Boxall, and R. Lichtenthaler. *Fluid Phase Equil.*, 219:93–98, 2004.

13. J. Hildebrand, J. M. Prausnitz, and R. L. Scott. *Regular and related solutions*. Van Nostrand Reinhold Company, 1970.

14. G. M. Wilson. *J. Am. Chem. Soc.*, 86(2):127–130, 1964.

15. G. M. Wilson and C. H. Deal. *Ind. Eng. Chem. Res. Fundam.*, 1:20–23, 1962.

16. E. A. Guggenheim. *Mixtures*. Oxford University Press, 1952.

17. E. A. Campanella, P. M. Mathias, and J. P. O'Connell. *AIChE J.*, 33:2057–2066, 1987.

2. Fundamentals of fluctuation solution theory

The Kirkwood-Buff theory of solutions (or *fluctuation solution theory*; FST) originates from classical fluctuation theory of statistical mechanics, hence its name. Thus, many of the relations used are in fact fundamental theory, which is used in the teachings of statistical mechanics. Therefore, a brief introduction to some basic concepts from statistical mechanics is provided first, before introducing the expressions first given by Kirkwood and Buff[1] in 1951, and later expanded by O'Connell[2] in 1971. The chapter shows how fluctuation quantities – in terms of correlation function integrals – may be used to derive expressions for density fluctuations of thermodynamic variables in open systems. At the end of the chapter, a few possible ways of estimating the correlation function integrals that yield thermodynamic properties of solutions are discussed.

2.1. Statistical mechanics and fluctuations

Consider an open, homogeneous system in the grand canonical ensemble. Herein, the set of chemical potentials $\boldsymbol{\mu}$, total volume V, and temperature T is fixed, allowing for fluctuations in all other variables, including the number of molecules (and hence the number density). The probability that the M-component system will contain N_1, N_2,…,N_M molecules of the M species is[3]

$$P(\mathbf{N}) = \frac{Q(\mathbf{N},V,T)}{\Xi(\boldsymbol{\mu},V,T)} \exp\{\beta G\}\,, \qquad G = \sum_{i=1}^{M} N_i\mu_i. \tag{2–1}$$

Here, Q and Ξ are the canonical and grand canonical partition functions, respectively, and the chemical potential of i is μ_i. It is customary to denote thermal energy by the symbol β ($\beta^{-1} \equiv \mathsf{k}T$). The partition functions are defined in the classical way[3]

$$Q(\mathbf{N},V,T) = \sum_{j}^{\substack{\text{miro-}\\ \text{states}}} \exp\{-\beta E_j\}\,, \tag{2–2a}$$

$$\Xi(\boldsymbol{\mu},V,T) = \sum_{i=1}^{M} \sum_{N_i} \exp\{\beta G\}\, Q(\mathbf{N},V,T). \tag{2–2b}$$

Here, E_j is the energy level of microstate j. It then follows that the average number of particles in the open system can be written in terms of the grand partition function[3]

$$\langle N_i \rangle = \sum_N N_i P(\mathbf{N}) = \frac{1}{\Xi} \left(\frac{\partial \Xi}{\partial \beta \mu_i} \right)_{T,V,\mu_{j \neq i}}. \tag{2–3}$$

In a similar fashion, the doublet can also be written in terms of Ξ

$$\begin{aligned} \langle N_i N_j \rangle &= \sum_{k=1}^{M} N_i N_j P(\mathbf{N}) = \frac{1}{\Xi} \left(\frac{\partial^2 \Xi}{\partial \beta \mu_i \partial \beta \mu_j} \right)_{T,V,\mu_{k \neq i,j}} = \frac{1}{\Xi} \left(\frac{\partial \langle N_i \rangle \Xi}{\partial \beta \mu_j} \right)_{T,V,\mu_{k \neq j}} \\ &= \langle N_i \rangle \langle N_j \rangle + \left(\frac{\partial \langle N_i \rangle}{\partial \beta \mu_j} \right)_{T,V,\mu_{k \neq j}}. \end{aligned} \tag{2–4}$$

Equation (2–4) relates the average number of singlet and doublet molecules in the open system to the derivative of the singlet taken wrt. the chemical potential of the other. This relation is a fundamental result from statistical mechanics and will be used to derive the theory later in this chapter.

The singlet density of molecular type i, $\rho_i^{(1)}(\mathbf{r}_i, \boldsymbol{\omega})$, is the number of molecular centres* in the system defined by the position vector $\mathbf{r}_i$, and orientation given by ω_i. Similarly, the pair number density $\rho_{ij}^{(2)}(\mathbf{r}_i, \mathbf{r}_j, \boldsymbol{\omega})$ is the average number of molecules of types i at $\mathbf{r}_i$ and j at positions given by $\mathbf{r}_j$. Integration over the entire system volume yields the volume-averaged number of molecules

$$\int_V \rho_i^{(1)}(\mathbf{r}_i, \boldsymbol{\omega}) \mathrm{d}\mathbf{r} = \langle N_i \rangle, \tag{2–5}$$

and

$$\int_V \int_V \rho_{ij}^{(2)}(\mathbf{r}_i, \mathbf{r}_j, \boldsymbol{\omega}) \mathrm{d}\mathbf{r}_i \mathrm{d}\mathbf{r}_j = \langle N_i N_j \rangle - \delta_{ij} \langle N_i \rangle. \tag{2–6}$$

We define a pair correlation function from the left-hand sides of these two equations. Between centres of i and j the pair correlation function is defined through[3]

$$g_{ij}^{(2)}(\mathbf{r}_i, \mathbf{r}_j, \boldsymbol{\omega}) \equiv \frac{\rho_{ij}^{(2)}(\mathbf{r}_i, \mathbf{r}_j, \boldsymbol{\omega})}{\rho_i^{(1)}(\mathbf{r}_i, \boldsymbol{\omega}) \rho_j^{(1)}(\mathbf{r}_j, \boldsymbol{\omega})}. \tag{2–7}$$

Distribution functions for molecular centres, regardless of orientations, are obtained from integration of the angular distribution function over all orientations[4]

$$g_{ij}^{(2)}(\mathbf{r}_i, \mathbf{r}_j) = \langle g_{ij}^{(2)}(\mathbf{r}_i, \mathbf{r}_j, \boldsymbol{\omega}) \rangle_{\omega_1 \ldots \omega_N} \equiv \frac{1}{\Omega^N} \int g_{ij}^{(2)}(\mathbf{r}_i, \mathbf{r}_j, \boldsymbol{\omega}) \mathrm{d}\omega^N, \tag{2–8}$$

with $\Omega = \int \mathrm{d}\omega$. In the proceeding derivation, we will make use of the centres pair correlation function,

* In anisotropic systems this definition of molecular centres is necessary.

defined as the left-hand side of the above equation. The pair correlation function* is a normalized probability density function of finding particle i at $\mathbf{r}_i$ when j is at $\mathbf{r}_j$, and vice versa (subscripts are symmetric). In a homogeneous fluid (which we will consider henceforth) the singlet density $\rho_i^{(1)}$ is actually independent of position,[3] and is simply the bulk molecular density ρ_i. Further simplification stems from the fact that the correlation function depends solely on the separation between i and j, thus being independent of the origin in the coordinate space. Therefore, the distance from $\mathbf{r}_i$ to $\mathbf{r}_j$ is written $\mathbf{r} = |\mathbf{r}_i - \mathbf{r}_j|$. By subtracting unity from the pair correlation function

$$g_{ij}^{(2)}(\mathbf{r}) - 1 = \frac{\rho_{ij}^{(2)}(\mathbf{r}) - \rho_i^{(1)}(\mathbf{r})\rho_j^{(1)}(\mathbf{r})}{\rho_i^{(1)}(\mathbf{r})\rho_j^{(1)}(\mathbf{r})}, \tag{2–9}$$

and integrating twice, using the results above, we find that

$$\int\int \left[g_{ij}^{(2)}(\mathbf{r}) - 1\right] \mathrm{d}\mathbf{r}\mathrm{d}\mathbf{r} = \frac{\langle N_i N_j\rangle - \langle N_i\rangle\langle N_j\rangle}{\langle N_i\rangle\langle N_j\rangle} - \frac{\delta_{ij}}{\langle N_j\rangle}. \tag{2–10}$$

Finally, the second integration on the left-hand side gives

$$\frac{1}{V}\int \left[g_{ij}^{(2)}(\mathbf{r}) - 1\right] \mathrm{d}\mathbf{r} = \frac{\langle N_i N_j\rangle - \langle N_i\rangle\langle N_j\rangle}{\langle N_i\rangle\langle N_j\rangle} - \frac{\delta_{ij}}{\langle N_j\rangle}. \tag{2–11}$$

We notice from Equation (2–11) that the right-hand side contains a difference in averaged numbers. If there are no interactions between molecules i and j – i.e., they are completely uncorrelated – that difference is zero, whence

$$\langle N_i N_j\rangle = \langle N_i\rangle\langle N_j\rangle, \tag{2–12}$$

and the right-hand side of (2–11) is zero, except for a negligible contribution when $i = j$. It is customary to designate the integrand in Equation (2–11) the *total* correlation function,

$$h_{ij}(\mathbf{r}) = g_{ij}^{(2)}(\mathbf{r}) - 1. \tag{2–13}$$

Thus, if $h_{ij} = 0$ the correlation, or interaction, between i and j is effectively zero. This is a statistical mechanical definition of an ideal solution. By combining Equations (2–11) and (2–4), we find that

$$\frac{\delta_{ij}}{\langle N_j\rangle} + \frac{1}{V}\int h_{ij}(\mathbf{r})\mathrm{d}\mathbf{r} = \frac{1}{\langle N_i\rangle\langle N_j\rangle}\left(\frac{\partial\langle N_i\rangle}{\partial\beta\mu_j}\right)_{T,V,\mu_{k\neq j}}. \tag{2–14}$$

* Also referred to as radial distribution function for spherically symmetric systems.

Multiplication by the average total number of molecules $\langle N \rangle$, and rearranging, yields the relation

$$x_i \delta_{ij} + x_i x_j \frac{\langle N \rangle}{V} \int h_{ij}(\mathbf{r}) \mathrm{d}\mathbf{r} = \frac{1}{\langle N \rangle} \left(\frac{\partial \langle N_i \rangle}{\partial \beta \mu_j} \right)_{T,V,\mu_{k \neq j}} . \tag{2–15}$$

By definition, the fraction outside the integral is the singlet number density, ρ, and the ratios of molecular numbers is a mere mole fraction. We may then write the equation as

$$x_i \delta_{ij} + x_i x_j \rho \int h_{ij}(\mathbf{r}) \mathrm{d}\mathbf{r} = \frac{1}{\langle N \rangle} \left(\frac{\partial \langle N_i \rangle}{\partial \beta \mu_j} \right)_{T,V,\mu_{k \neq j}} , \tag{2–16}$$

or in compact matrix notation

$$\mathbf{A} = (\mathbf{BX})^{-1} , \quad A_{ij}^{-1} = \frac{1}{\langle N \rangle} \left(\frac{\partial \langle N_i \rangle}{\partial \beta \mu_j} \right)_{T,V,\mu_{k \neq j}} , \tag{2–17}$$

where $\mathbf{B} = \mathbf{I} + \mathbf{XH}$. In the equation above, $\mathbf{I}$ is the unit diagonal matrix, $\mathbf{X}$ is a diagonal matrix with elements $X_{ii} = \langle N_i \rangle / \langle N \rangle$, and

$$H_{ij} = H_{ji} = \rho \int h_{ij}(\mathbf{r}) \mathrm{d}\mathbf{r} \tag{2–18}$$

is the *total correlation function integral*. Equation (2–16), and its matrix equivalent, was derived by Kirkwood and Buff in 1951.[1] It provides a relation between spatial integrals of pair correlation functions in solution and derivative thermodynamic properties. The derivative in Equation (2–17) may be rewritten using the equality of fluctuations[1] of a thermodynamically open system

$$\left(\frac{\partial \mu_j}{\partial \langle N_i \rangle} \right)_{T,V,N_{k \neq j}} = \left(\frac{\partial \langle N_i \rangle}{\partial \mu_j} \right)^{-1}_{T,V,\mu_{k \neq j}} . \tag{2–19}$$

However, while derivatives in the canonical and grand canonical ensembles result in neat relations between correlation function integrals and derivatives of chemical potentials, their ties to experimentally measurable quantities are not straightforward. While temperature is straightforward to control in both open and closed systems, it is not advantageous to work with chemical systems of finite sizes. Therefore, systems with fixed temperature, set of mole numbers, and total pressure are traditionally the basis. For this reason, the $\mathbf{N}PT$ ensemble – which has the Gibbs energy as its characteristic function, the derivatives of which form activity coefficients of species in solution – is a standard framework for phase equilibria problems, because it constrains pressure rather than density.[5] Since pressure does not appear explicitly in Equation (2–17), we express the derivatives by introducing the Gibbs-Duhem equation at constant T and P

$$\mathbf{0}^{\mathsf{T}} = (\mathbf{Xi})^{\mathsf{T}} \mathbf{D}, \qquad D_{ij} = N \left(\frac{\partial \beta \mu_i}{\partial N_j} \right)_{T,P,N_{k \neq j}} , \tag{2–20}$$

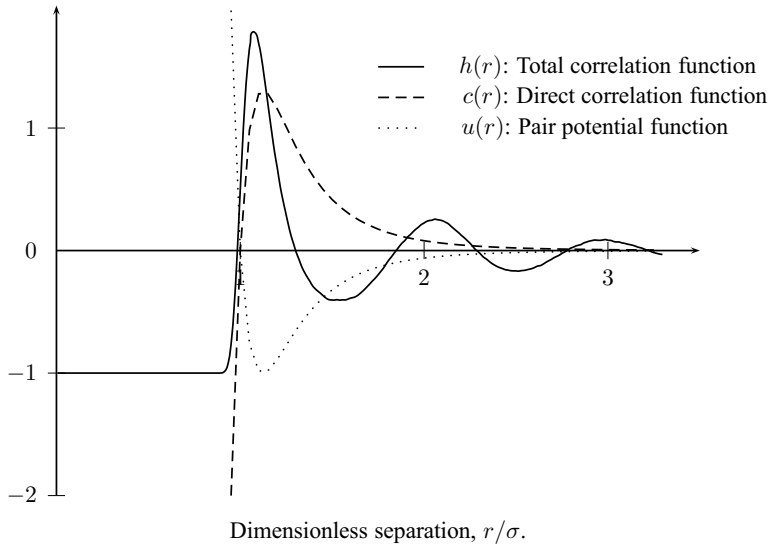

Figure 2–1. Molecular pair correlation functions for dense fluids. The total correlation function, h, is a long-ranged function, which takes into account indirect effects from third molecules. The fluctuations in this function are likely to exist for several molecular diameters. The direct correlation function excludes that, and gives only the direct effect of 1 on 2 (or vice versa). It is of short range, comparable to the pair potential function, u, given here by a simple 12-6 Lennard-Jones expression.

where $\mathbf{0}$ is the zero vector column vector, and $\mathbf{i}$ is the unit column vector. The derivatives in the different ensembles are then connected by

$$\mathbf{A} = \mathbf{D} + \frac{\beta}{\rho\kappa}\mathbf{Y}\mathbf{i}\left(\mathbf{Y}\mathbf{i}\right)^{\mathsf{T}}, \qquad \left(\frac{\partial\beta\mu_i}{\partial N_j}\right)_{T,V,N_{k\neq j}} = \left(\frac{\partial\beta\mu_i}{\partial N_j}\right)_{T,P,N_{k\neq j}} + \beta\rho\frac{\bar{v}_i\bar{v}_j}{\kappa}, \tag{2–21}$$

where $\kappa \equiv \rho^{-1}(\partial\rho/\partial P)_{T,N}$ is the compressibility of the solution. $\mathbf{Y}$ is a diagonal matrix, the elements of which are $Y_{ii} = \rho\bar{v}_i$, where $\bar{v}_i$ is the partial molal volume of species i. Combining Equations (2–17), (2–20), and (2–21) yields the expression at constant pressure

$$\mathbf{X}\mathbf{D} = \left[\mathbf{I} - \frac{\mathbf{X}\left(\mathbf{B}^{-1}\right)^{\mathsf{T}}\mathbf{i}\mathbf{i}^{\mathsf{T}}}{\mathbf{i}^{\mathsf{T}}\mathbf{B}^{-1}\mathbf{X}\mathbf{i}}\right]\mathbf{B}^{-1}, \qquad [\mathbf{X}\mathbf{D}]_{ij} = N_i\left(\frac{\partial\beta\mu_i}{\partial N_j}\right)_{T,P,N_{k\neq j}}. \tag{2–22}$$

Equation (2–22) offers a relation between the chemical potential at constant pressure and temperature, a quantity which is experimentally accessible, and the pair correlation function integrals. This can lead to expressions for component activity coefficients. Another property is the partial molal volumes of species in solution

$$\rho\bar{v}_i = \sum_{j=1}^{M}\frac{|\mathbf{B}|_{ji}}{\mathbf{i}\mathbf{B}^{-1}\mathbf{X}\mathbf{i}}, \tag{2–23}$$

where $|\mathbf{B}|_{ji}$ is the (j,i)-element of the matrix. The compressibility, κ, can be found from the denomina-

tor of Equation (2–22)

$$\frac{\beta}{\rho\kappa} = \mathbf{i}^{\mathsf{T}}\mathbf{B}^{-1}\mathbf{X}\mathbf{i}. \tag{2–24}$$

The magnitudes of the integrals describe the degree of correlation, or interaction, between molecular pairs. Figure 2–1 exemplifies the total correlation function for a spherically symmetric, pure-fluid system as function of separation (reduced by molecular diameter, σ). This behavior is descriptive for dense fluids, and reveals that the value of h – unlike the pair potential energy function – does not converge until a distance of several molecular diameters. For a system of spherically symmetric molecules, the total correlation function integral, Equation (2–18), can be rewritten in terms of the scalar distance between molecular centres

$$H_{ij} = \rho \int h_{ij}(r) 4\pi r^2 \mathrm{d}r. \tag{2–25}$$

The integrand contains the product of correlation function and separation squared. This can cause severe fluctuations in the integrand, and will propagate through Equation (2–22). Figure 2–2 shows fluctuations in the integrand as function of radial separation. The slow decay of the amplitude makes the integral a quantity that is not straightforward to obtain. In addition to being sensitive towards fluctuations in correlation function values, Equation (2–22) suffers from severe complexity when addressing higher-order mixtures (three or more components). Although matrix inversion is standard procedure, it will often lead to results being highly complicated. Moreover, the total correlation function integral will diverge at the critical point. This can be seen by writing the compressibility for a pure fluid. At the critical point this approaches zero,

$$-\frac{\beta V}{\rho}\left(\frac{\partial V}{\partial P}\right)_{T,N} = [1+H]^{-1} \to 0 \quad \text{for} \quad T \to T_c. \tag{2–26}$$

Thus, H approaches infinity. Therefore, standard treatments of fluid systems has concentrated on conditions far from the critical point. For this reason, among others, it is convenient to introduce another correlation function; one that is inversely proportional to the total correlation function. It is of shorter range than the pair correlation function (similar to the pair potential function), and is more likely to be approximated accurately for that reason.

2.2. The direct correlation function

Ornstein and Zernike [6] defined the direct correlation function in an integral equation to describe direct and indirect correlations. The "molecular" representation of this is sketched below. The total correlation function between molecules 1 and 2 can be separated by two parts:

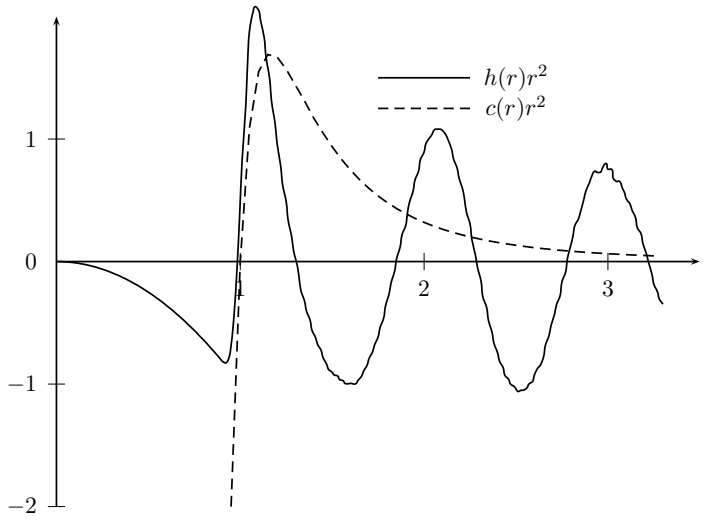

Figure 2–2. Fluctuations in integrands of molecular correlation functions, h and c. The fluctuations in product of the total correlation function and r^2 are often severe, since h does not converge until several molecular diameters. The direct correlation function converges much more rapidly, resulting in no fluctuation due to the short-ranged nature of this function.

i. A short-ranged, direct effect of 1 on 2, which has similar range as the pair potential function.

ii. An indirect effect, where 1 influences 2 through other molecules (3).

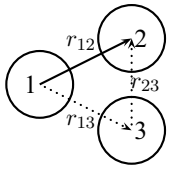

In simplified notation the Ornstein-Zernike equation is

$$h(12) = c(12) + \rho \int c(13)h(23)\mathrm{d}3 \tag{2–27}$$

Here, "12" refers to the correlation between molecules 1 and 2. Thus, the total correlation is given by a direct contribution plus indirect effects stemming from interactions with third molecules. The multicomponent analogy for hard spheres was given by Lebowitz,[7] and removes the indirect effects from all other molecular species:

$$h_{ij}(\mathbf{r},\boldsymbol{\omega}) = c_{ij}(\mathbf{r},\boldsymbol{\omega}) + \sum_{k=1}^{M} \rho_k \int \langle c_{ik}(\mathbf{r},\boldsymbol{\omega}) h_{jk}(\mathbf{r},\boldsymbol{\omega})\rangle_{\omega_k} \mathrm{d}\mathbf{r}_k. \tag{2–28}$$

In dense fluids, the angular indirect correlations (integral of (2–28)) do not contribute greatly. As a results of that, we concern ourselves with the direct correlation function for molecular centres, defined

in a similar way as the pair correlation function, i.e.,

$$c_{ij}(\mathbf{r}) = \langle c_{ij}(\mathbf{r},\omega)\rangle_{\omega_1 \ldots \omega_N}. \tag{2–29}$$

The integral defined above has some unique features. In addition to the contributions of the terms (as outlined above), the products in the integrand are separable. Taking the Fourier transform,[4] the convolution term factorizes, and the equation can be integrated to give

$$\rho \int h_{ij}(\mathbf{r})\mathrm{d}\mathbf{r} = \rho \int c_{ij}(\mathbf{r})\mathrm{d}\mathbf{r} + \sum_{k=1}^{M} x_k \left\{ \left[\rho \int c_{ik}(\mathbf{r})\mathrm{d}\mathbf{r} \right] \left[\rho \int h_{jk}(\mathbf{r})\mathrm{d}\mathbf{r} \right] \right\}. \tag{2–30}$$

Equivalently, in the present notation, the spatially integrated Ornstein-Zernike equation can be written in matrix notation as

$$\mathbf{H} = \mathbf{C} + \mathbf{HXC}, \tag{2–31}$$

where

$$C_{ij} = C_{ji} = \rho \int c_{ij}(\mathbf{r})\mathrm{d}\mathbf{r}. \tag{2–32}$$

Rearranging Equation (2–31)

$$\mathbf{I} + \mathbf{HX} = (\mathbf{I} - \mathbf{CX})^{-1}, \tag{2–33}$$

and substituting into (2–17) gives

$$\mathbf{A}^{-1} = (\mathbf{I} - \mathbf{CX})\,\mathbf{X}^{-1}. \tag{2–34}$$

The elements of this equation are

$$\left|\mathbf{A}^{-1}\right|_{ij} = N \left(\frac{\partial \beta \mu_i}{\partial N_j} \right)_{T,V,N_{k\neq j}} = \rho \left(\frac{\partial \beta \mu_i}{\partial \rho_j} \right)_{T,\rho_{k\neq j}} = \frac{\delta_{ji}}{x_i} - C_{ji}. \tag{2–35}$$

A more convenient quantity to be used for phase equilibria is the species activity coefficient, γ_i. Rewriting Equation (2–35) gives

$$\rho \left(\frac{\partial \ln \gamma_i}{\partial \rho_j} \right)_{T,\rho_{k\neq j}} = 1 - C_{ji}. \tag{2–36}$$

Now, for an isothermal change in pressure, the Gibbs-Duhem relation is

$$\mathrm{d}P = \sum_{i=1}^{M} \rho_i \mathrm{d}\mu_i, \tag{2–37}$$

and if we couple this with the foregoing analysis, we can write the the change in pressure as

$$\left(\frac{\partial P\beta}{\partial \rho_i}\right)_{T,\rho_{j\neq i}} = 1 - \sum_{j=1}^{M} x_j C_{ji}. \tag{2–38}$$

Another derivative of the chemical potential is obtained by utilizing the Gibbs-Duhem equation at constant pressure and temperature. We then obtain the equivalent of Equation (2–22).

$$\mathbf{XD} = \left[\mathbf{I} - \frac{\mathbf{XF^{\mathsf{T}}ii^{\mathsf{T}}}}{\mathbf{i^{\mathsf{T}}FXi}}\right]\mathbf{F}, \qquad \mathbf{F} = \mathbf{I} - \mathbf{XC}. \tag{2–39}$$

The elements of the above equation are

$$N_i\left(\frac{\partial \beta\mu_i}{\partial N_j}\right)_{T,P,N_{k\neq j}} = \delta_{ij} - \frac{x_i\left\{1 + C_{ij} - \sum_{n=1}^{M} x_n(C_{in}+C_{jn}) + \sum_{n=1}^{M}\sum_{m=1}^{M} x_n x_m (C_{in}C_{jm} - C_{ij}C_{nm})\right\}}{1 - \sum_{n=1}^{M}\sum_{m=1}^{M} x_n x_m C_{nm}} \tag{2–40}$$

Partial molal volumes and isothermal compressibilities are given by

$$\rho\bar{v}_i = \frac{1 - \sum_{j=1}^{M} x_j C_{ij}}{1 - \sum_{j=1}^{M}\sum_{k=1}^{M} x_j x_k C_{jk}}, \qquad \frac{\beta}{\rho\kappa} = 1 - \sum_{i=1}^{M}\sum_{j=1}^{M} x_i x_j C_{ij}. \tag{2–41}$$

Notice, that unlike Equation (2–22), Equation (2–39) does not require inversion of a matrix. Furthermore, as Figure 2–2 shows, the integrand decays in a monotonic fashion. Although the direct correlation function is not *directly* calculable from molecular simulation*, its integral is more well-behaved than the total correlation function, and is therefore more likely to be accurately approximated using either experiment[8] or model.[9]

2.3. Calculation of thermodynamic properties

The practicality of FST can be significant. The derivations above reveal some resemblances to classical thermodynamics, in that the value of such a number of relations is zero, unless attempts to quantify matters are made. In the following subsections, a few attempts to quantify molecular correlation function integrals will be explained.

* c is a hypothetical function defined by Ornstein and Zernike.

2.3.1. Correlation function integrals from molecular simulation

The theoretical achievements sketched above attracts particular interest in the context of molecular simulation techniques. With the rise of highly advanced computational facilities in the 1990s and 2000s, molecular simulation – either molecular dynamics, where Newton's equations of motion are solved with a molecular force field, or Monte Carlo methods, where equilibrium is reached from statistical principles – has the field of computational thermodynamics has grown considerably.

Perhaps most notably, and also in the context of FST, Christensen [10] and Christensen et al. [11] used molecular dynamics simulations to compute the integrals of binary mixtures of subcritical organic systems. These would then yield derivatives of species activity coefficients, through the chemical potential. These values would then, in turn, be used to estimate parameters in an expression for the activity coefficient. Comparison with vapor pressure data revealed this approach could accurately predict the phase equilibria for a variety of systems. One fundamental concern was the integration scheme of the total correlation function. The fluctuating values at high separations, was found to contribute significantly to the integral. Moreover, simulations of dense systems is extremely time consuming, and a simulation may take as much as a week to complete. Thus, for practical purposes, molecular simulation is still not a widely recommended tool for process design.

2.3.2. Correlation function integrals from data

It is also possible to conceive the above correlation function integrals from analysis of experimental data. There are a few studies in the open literature, but the works of Wooley [8,12] seem to be the most thorough. Wooley compiled a data bank of correlation function integrals for a large variety of binary mixtures by estimating of their values from reliable data sources. Using the Ornstein-Zernike equation with Equation (2–21), the direct correlation function integrals in a binary mixture can be expressed as

$$1 - C_{11} = \frac{\rho \bar{v}_1^2}{\kappa \mathsf{R} T} + x_2 \left(\frac{\partial \ln \gamma_1}{\partial x_1} \right)_{T,P,N_2}, \tag{2–42a}$$

$$1 - C_{12} = \frac{\rho \bar{v}_1 \bar{v}_2}{\kappa \mathsf{R} T} - x_1 \left(\frac{\partial \ln \gamma_1}{\partial x_1} \right)_{T,P,N_2}, \tag{2–42b}$$

$$1 - C_{22} = \frac{\rho \bar{v}_2^2}{\kappa \mathsf{R} T} + x_1 \left(\frac{\partial \ln \gamma_2}{\partial x_2} \right)_{T,P,N_1}. \tag{2–42c}$$

As previously, κ is the compressibility at constant temperature, and $\bar{v}_i$ is the partial molal volume of i. The species activity coefficients are γ_i. Wooley used experimental values for compressibilities and partial molal volumes, whereas the activity coefficient derivatives were found from conventional excess

Gibbs energy models, with parameters fitted to vapor-liquid equilibrium data on the specific mixtures. 26 binary mixtures, comprising of traditional organic solvents and water, were examined, and their correlation function integrals were published. The purpose was to provide reliable estimates for comparison with molecular theories, solution models, or equation-of-state mixing rules, in addition to verifying experimental data obtained from e.g. light scattering and sedimentation studies. It was found that the integrals often varied strongly with composition, and were greatly affected by the derivative terms.

2.3.3. Traditional engineering approaches

While simulation and experimental data may give accurate estimates of the correlation function integrals, they are not directly applicable for practical purposes. Simulation methods take much too long for completion, and experimental studies do not really pose as attractive, since the modeling issues are restricted to being correlations. Instead, what is often resorted to (and was also explored by Kirkwood and Buff[1] and O'Connell[2]), is the traditional engineering approach.

From an engineering perspective, there are basically two ways of estimating a function (property) from its derivative

1. Series expansion.

2. Integration.

Frequently, a series expansion to second order sufficiently describes the variation of a property within a margin of a reference point. This requires partial derivatives of first and second order. A first derivative value is obtained directly from theory, whereas higher order terms are obtained from differentiation of correlation functions. Well-known relations have been established,[13,14] which gives expressions for partial derivatives of correlation functions. Unfortunately, this results in generation of higher-order correlation functions, i.e. triplets and quadruplets. Approximate theories (such as PY and CHNC*) can be helpful in addressing these, but they are derived on the basis of hard spheres, and therefore not representative of real-fluid systems. In Part I, it will be shown how this treatment can result in a simple model for solubilities of solids in mixtures of solvents.

The latter item above require *integrals* of correlation functions somehow be expressed in terms of measurable state variables. This path is often less sensitive to model formulations/approximations than taking derivatives. Nevertheless, integration requires a model that connects the thermodynamic variables. In the present derivation, the variables temperature and component number densities arises naturally from the statistical mechanical ensemble. The details of such a treatment is presented in Part II.

* PY: Percus-Yevick, CHNC: Convolution-hypernetted chain.[4,15]

2.4. Summary

This chapter has seen the derivation of the statistical mechanical *fluctuation solution theory* (FST), which connects integrals of molecular correlation functions to derivative thermodynamic properties. It was found, that based on the*total* correlation function, an expression between derivatives of chemical potential, partial molal volumes, and compressibilities required the inversion of a matrix correlation function integrals. Introducing the Ornstein-Zernike equation, and redoing the analysis based on the *direct* correlation function, the expressions were much simpler, and did not require matrix inversion. Finally, a few options for obtaining correlation function integrals were discussed.

In the following chapter, the topic of Part I is introduced. The method developed in that part, requires the framework of FST, which was provided by this chapter.

References

1. J. G. Kirkwood and F. P. Buff. *J. Chem. Phys.*, 19 (8):774–777, 1951.
2. J. P. O'Connell. *Mol. Phys.*, 20(1):27–33, 1971.
3. D. A. McQuarrie. *Statistical mechanics*. University Science Books, 2000.
4. C. G. Gray and K. E. Gubbins. *Theory of molecular fluids*, volume 1: Fundamentals. Oxford University Press, 1984.
5. J. M. Prausnitz, R. N. Lichtenthaler, and E. Gomez de Azevedo. *Molecular thermodynamics of fluid-phase equilibria*. Prentice-Hall, 3rd edition, 1999.
6. L. S. Ornstein and F. Zernike. *Proc. Kon. Akad. Wetenschap. (Amst.)*, 17:793–806, 1914.
7. J. L. Lebowitz. *Phys. Rev.*, 133:A895–A899, 1964.
8. R. J. Wooley. *Fluctuation thermodynamic properties of nonelectrolyte liquid mixtures*. PhD thesis, University of Florida, Gainesville, FL, USA, 1987.
9. P. M. Mathias. *Thermodynamic properties of high-pressure liquid mixtures containing supercritical components*. PhD thesis, University of Florida, Gainesville, FL, USA, 1978.
10. S. Christensen. *Thermodynamic models from fluctuation solution theory analysis of molecular simulations*. PhD thesis, Technical University of Denmark, Kgs. Lyngby, Denmark, 2007.
11. S. Christensen, G. H. Peters, F. Y. Hansen, and J. Abildskov. *Fluid Phase Equil.*, 261:185–190, 2007.
12. R. J. Wooley and J. P. O'Connell. *Fluid Phase Equil.*, 66:233–261, 1991.
13. F. P. Buff. *J. Chem. Phys.*, 23:419–427, 1955.
14. R. J. Baxter. *J. Chem. Phys.*, 41:553–558, 1964.
15. H. L. Frisch and J. L. Lebowitz, editors. *The equilibrium theory of classical fluids*. Benjamin, 1964.

PART I

SOLUBILITIES OF SOLIDS IN MIXED SOLVENTS

3. Introduction and thermodynamics of solid solubility

This chapter gives an overview of existing methods for estimating solubilities in mixed solvents. This is followed by an outline of the conventional framework for solid solubility. Fundamental concepts, such as *ideal* and *excess* solubilities, are introduced and their relations to other properties are explored.

3.1. Background

Designing optimal separation processes for solids has been a mile stone for many chemical processing units for many years. Water is a desirable solvent due to its benign nature, but poor aqueous solubilities can often cause difficulties in the processing.[1] Therefore, many separations for production of solid substances can be more effective when mixtures of solvents are employed compared to using pure solvents. Also the functionality of chemical products can depend strongly upon formulations with mixed solvents. This means, that specific properties can be enhanced (or suppressed) by appropriate solvent selection. The term co- and antisolvents are often used when referring to solvents which are capable of enhancing or suppressing solubility. However, selection of appropriate solvents has been the topic of many research directions, as will be seen below. Solvent selection can be complicated by specific chemical phenomena, which occur between solid and solvents. This is especially found in pharmaceutical processing. Here, the solid substance is often a complex active ingredient with

1. more than a single functional group,
2. molecular weights above a few hundred grams per mole,
3. multiple conformations and isomers
4. complex interaction schemes, such as dipole-dipole interactions, hydrogen bonding, and formation of solvates and/or hydrates (in aqueous solutions), and
5. limited amounts of (reliable) data.

These phenomena complicate selection of optimal solvents substantially. A wide range of solvents and solvent mixtures (especially aqueous) are of interest. There are substantial compilations of experimental data,[2–8] and data for new systems continue to appear in the scientific literature. Solubilities of solids in single solvents have been reported extensively, but there are fewer literature values for solubilities in mixed solvents, and the large number of available solvent mixtures makes thorough experimental testing infeasible. Solvent selection is essentially a thermodynamic problem, since it can be formulated in terms of relevant state variables (e.g. T, P, and $\mathbf{x}$), but more than 30% of the efforts of industrial thermodynamics groups can be related to different aspects of solvent selection.[9] Experience and empirical descriptions of experimental results have often formed the basis for selecting candidate solvents, but this form of trial-and-error approach is time consuming and not as systematic as we would like as engineers. When minimum time-to-market is a primary concern of industries, such as especially the pharmaceutical, rapid and reliable property predictions, thereby facilitating a more systematic approach, would be highly desirable.

Recent modeling approaches to solubility in pure and mixed solvent systems[10–14] reveal a great and growing interest in the applied thermodynamics community in solubility calculations for such systems. However, accurate prediction is not straightforward since the dependence of solubilities on solvent composition can be quite complex, ranging from a linear variation to multiple extrema. Below, an overview of the modeling attempts that have been made for mixed solvent solubilities is presented. It is not exhaustive, but should offer the reader a useful classification of previous methods.

3.2. Existing methods for solid-liquid equilibria

The established methods for solid solubility in solvent mixtures in the open literature seem to fall under the categories given below.

3.2.1. Excess Gibbs energy methods

There is a variety of modeling approaches using conventional g^{E}-models to the solid-liquid phase equilibrium (SLE) by solving the relations that arise from equating fugacities in solid and liquid phases. Gmehling et al.[15] are frequently given credit for the first UNIFAC application for SLE in both pure and mixed solvents. They concluded that UNIFAC, with group parameters obtained from regression of vapor-liquid equilibrium data (typically taken at higher temperatures), could be used for solid-liquid equilibrium at lower temperatures. UNIFAC has since been used extensively for computation of solubilities in single solvents,[16–22] but less activity has been seen in the area of mixed solvent solubility. Some works are summarized in the following.

Fu and Luthy [23,24] conducted a significant study to determine the solubilities of aromatics in aqueous mixtures of organic solvents and the ability of UNIFAC to describe these, concluding that the model overestimates the solubility in pure solvents by a factor of nearly two. Domańska [25,26] also demonstrated that UNIFAC generally was unable to yield acceptable solubility predictions of organics in binary mixtures of paraffins and alcohols. The fundamental issues when applying UNIFAC can be summarized as UNIFAC being unable to:

1. Distinguish between isomers,
2. accurately describe properties of polyfunctional molecular structures,
3. describe proximity effects, i.e., interactions between neighboring functional groups,
4. and account for effects of directional forces (such as hydrogen bonding).

These inherent deficiencies arise from the solution-of-groups concept, as discussed by Currier and O'Connell. [27] Furthermore, parameters for group-group interactions are often not available, especially with atoms such as P and S. Nevertheless a UNIFAC model particularly developed for pharmaceutical functionalities is presented recently by Diedrichs and Gmehling. [28] Inclusion of higher-order groups, i.e., defining additional, larger fragments, to account for isomeric effects and polyfunctionality have been proposed previously, [29] but requires no less data for correlation. Furthermore, aqueous systems still remain to be dealt with, e.g. simultaneous representation of infinite dilution activity coefficients and composition dependencies.

MOSCED (modified separation of cohesive energy density) [30–33] estimates activity coefficients by extending Scatchard and Hildebrand's regular solution theory. The method requires a set of five parameters for each molecular substance to characterize dispersion, induction, polarity, and hydrogen bonding (acidic and basic). Often, not all parameters are needed, i.e., for nonpolar organics, only dispersion appears, and for solutions with polar compounds, only dispersion and induction characteristics are required. The estimated activity coefficients are used to compute solubilities as a function of solvent composition (if more than one solvent is in the system) and temperature. The MOSCED model generally describes liquid-phase nonideality well, but a large amount of input data is needed to find parameters for new substances. Draucker et al. [33] also note that the MOSCED model is generally poor in describing solubilities that do not change linearly with temperature.

On the basis of the *conductor-like screening model* (COSMO) framework, Lin and Sandler [34] developed the concept of segment contributions towards pure component properties (COSMO-SAC), inspired by the success of UNIFAC. Their initial work considered vapor-liquid equilibria of water and organic liquids, but gave rise to application of the segment concept into other models. This includes a version

of the NTRL g^{E}-model (NTRL-SAC) for drug solubilities in pure solvents.[12,35] Chen and Crafts[36] successfully extended this method to solubilities of drugs in mixed solvents, primarily aqueous and mixtures of polar components. The NRTL-SAC method may require up to four parameters characterizing each pure component. They found that accurate predictions of mixed solvent solubilities could be obtained from regression of solubilities in single solvents. Shu and Lin[37] extended COSMO-SAC to solubilities of aromatic substances and drugs in binary solvent mixtures. Their analysis revealed that binary correction terms, calculated from solubilities in pure solvents, were needed for every pair in order to lower the disagreement with experimental mixture data. However, even in that case the average error in the 235 solubility data sets they analyzed was 88%.

3.2.2. Equation-of-state methods

Application of an equation of state is done by writing the activity coefficient of i in terms of liquid-phase fugacity coefficients

$$\gamma_i(T, P, \mathbf{x}) = \frac{\phi_i(T, \rho, \mathbf{x})}{\phi_i(T, \rho, x_i = 1)} \tag{3–1}$$

Equations of state are given in terms of the residual Helmholtz energy, whose independent variables are temperature T, overall solution density ρ and composition $\mathbf{x}$. The SLE framework is no different than application of a conventional g^{E}-model as above, but differs in the sense that γ_i is obtained as a ratio of two functions constrained by the equation of state solution density, from which fugacity coefficients are obtained. The suitability of equations of state to global phase equilibrium calculations has always motivated attention to new model variants. Particularly in recent years, advanced equations of state have received much attention in academic research programs. Mainly motivated by the advent of models based on the statistical-associated fluid theory (SAFT). Thus several testings of equations of state on SLE problems using Equation (3–1) are now published. Most activities have been on solubilities of solids in single solvents,[13,38–40] but there are also examples of mixed solvent applications. Ferreira et al.[41] used PC-SAFT to model solubilities of amino acids in aqueous alkanol mixtures. In addition to the pure component parameters required for the model, including hydrogen bonding characteristics, binary interaction parameters were often required to properly scale interactions between unlike molecular species. Ruether and Sadowski[42] also used PC-SAFT for solubilities of drugs in solvent mixtures of water and various alcohols, using temperature dependent binary interaction parameters. Although an equation of state approach enables calculation of mixture properties when parameters are based on pure component information, in many cases estimates are better when parameters are evaluated using mixture information. This is likely to result from inadequate combining rules. An advantage of working with models based on rigorous theory is that parameters are often calculable from other sources. Cassens et al.[14] attempted to use quantum mechanics to generate parameters for the PCP-SAFT model, and subsequently

use these for estimating the solubilities of a range of pharmaceutical solutes in pure solvents. Although potentially a completely predictive method, experimental data are required to determine accurate association parameters, in addition to binary interaction coefficients.

3.2.3. Reference solvent methods

Abildskov and O'Connell [43–45] used a reference solvent approach for estimating solubilities of solids in pure and mixed solvents. That method required infinitely diluted activity coefficients and a known solubility in a reference solvent to compute the solubility in another. UNIFAC was used to compute solute-solvent activity coefficients. Applying UNIFAC requires fitting of a large number of unknown group interaction parameters. By using the infinite dilution state as reference, the reference solvent methods gave a theoretically well-founded basis for selecting only the most vital parameters. Thus, much parameter fitting efforts could be eliminated. This makes the method quite effective for quickly rationalizing data taken on a complex solute in series of solvents. Recently, Diedrichs and Gmehling [28] seem to have adopted the same ideas and concepts in the development of their *Pharma* UNIFAC method.

3.2.4. Excess solubility methods

Models based on the *excess* solubility* concept divide into two different categories. One frequently cited approach is the algebraic mixing rule (otherwise referred to as the log-linear model), where the solubility of a solid in the mixed solvent is given by a linear combination of the pure solvent solubilities, weighted with respect to solvent composition. This allows the mixed solvent solubility to be predicted from the solubilities of the solute in the pure species alone, i.e. ideal mixing. It is often associated with Yalkowsky and co-workers,[46] but its essentials were employed to gas solubility (and outlined for solid solubility) studies already in the 1960s by Kehiaian [47–50] and by O'Connell and Prausnitz.[51] Most real systems do not conform to the underlying assumptions inherent in the log-linear approach and experimental drug solubilities can differ significantly from its estimates. A similar form for solid solubilities was later implemented by Williams and Amidon.[52–54] They used a Wohl expansion for the activity coefficients and devised methods for estimating parameters for the resulting expression. Their method was completely general, and applied for solubilities in binary and ternary solvent systems. While parameters for specific solvent-solvent terms were calculable from data sources other than solubility, such as low-pressure vapor-liquid equilibrium data, solute-solvent parameters required mixed solvent solubility data. Attempts were made to compute these from partition coefficients, but the data used for regression was limited. Furthermore, extension to ternary solvent mixtures requires parameters fitted to binary solvent solubilities. Nitta and Katayama [55] were among the first to explore ways of estimating the excess solu-

* This quantity and its relations to other properties are explained in detail later in this chapter.

bility by means of a model with specific chemical interactions, including differences in size and shape and association.

The other approach expresses the excess solubility as function of solvent composition such as with polynomials ranging from one to six adjustable parameters as reviewed by Jouyban et al..[56,57] Fundamentally, they all describe the (excess) solubility in a binary solvent mixture as function of solute-free composition. In a binary solvent system, one independent variable is used to describe the solute-free composition, z_j, where j is a solvent index. The choice of mole fraction, volume fraction, or mass fraction, is essentially arbitrary. Common to all of the models described by Jouyban et al. is that they can be put on a standard polynomial form

$$\ln x_{1,m} - x_2 \ln x_{1,2} - x_3 \ln x_{1,3} = \sum_k a_k z_j^{(k)}. \tag{3–2}$$

Here, $x_{1,m}$ is the solubility of the solute, 1, in the mixed solvent, and $x_{1,2}$ and $x_{1,3}$ are the solubilities in pure solvents, 2 and 3. The coefficients a_k come only from regression of mixture data, since they are specific to combinations of solute and solvents. These methods can describe a wide variety of mixed solvent solubility behavior, but are not applicable for systems where mixture data are either scarce or nonexisting. Furthermore, the transferability of the parameters is not fully accounted for. Models with less than two parameters are rarely adequate for generalizations. While for the more parameterized versions, the parameters might be interpreted as characterizing solute- and solvent-solvent interactions, their values come only from regression to experimental data on multicomponent systems. Thus, the major limitation of excess solubility models is the availability of parameters for systems with limited or no data.

Methods for multisolvent systems

The generic g^{E}-models and equations of state from above are able to address solubilities in mixtures beyond binary solvents. That said, the focus of these models have been on solubilities in pure and binary solvent mixtures. Ochsner et al.[58] attempted UNIFAC for a three solvent system of 4-hexylresorcinol in ethyl acetate–ethyl myristate–hexane mixtures, but found that the solubility profile was not generally successful over the entire composition range. However, it is difficult to make conclusions based on this single case. Williams and Amidon[54] made estimates of a few pharmaceuticals in water–propylene glycol–ethanol mixtures using their model, which was discussed above. They concluded, that multisolvent data was necessary to estimate solute-solvent interaction parameters.

While purely empirical methods, such as those reviewed by Jouyban et al., offer simple models, esti-

mation of their parameters is impossible without solubility data in solvent mixtures. Many of the models, which are based on more rigorous theory, are quite heavy to work with for non-experts. Obtaining reliable solubility estimates from a minimum of input data is not straightforward, and not currently offered by any one single method, and certainly not methods that are easily parameterized.

In the section to follow, a thorough introduction to the thermodynamics of solid solubility is given. The insights gained will be used to form the basis for a model, which is constructed in the next chapter.

3.3. Thermodynamic framework for solid solubility

The solubility of solids in liquids is a function of the intermolecular forces between solute and solvent(s), and in the absence of specific chemical phenomena (such as association or steric hindrance effects), the intermolecular forces between similar species are lower than those between dissimilar species. The rule of thumb "like dissolves like" is an empirical statement of this fact.[59] But this is only true in some cases, in fact intermolecular forces can be dominated by an often overlooked phenomenon; the solubility depends not only on the activity coefficient of the solute (which is representative of the intermolecular forces) but also on the standard-state fugacity of the liquid solution and the fugacity of the pure solid.[59] This means, that it is important to properly characterize the standard states of a solid phase and the liquid solution in which it is dissolved.

The starting point for any phase equilibrium specification is the equality of fugacities of species in each phase. We consider the equilibrium at temperature T and pressure P between a solid phase, with composition $\mathbf{z}$, and a liquid solution in which the solid is dissolved, with composition $\mathbf{x}$

$$f_i^S(T, P, \mathbf{z}) = f_i^L(T, P, \mathbf{x}). \tag{3–3}$$

The solid phase is assumed to be pure solute i. In that case, with the Lewis-Randall framework, the fugacities in each phase can be written as

$$f_i^{0,S}(T, P) = x_i \gamma_i(T, P, \mathbf{x}) f_i^{0,L}(T, P). \tag{3–4}$$

The standard-state fugacity $f_i^{0,L}$, to which γ_i refers, can be arbitrary, requiring only same temperature as the solution. The effect of pressure on very subcritical species is negligible. A convenient choice of liquid reference state is the (hypothetical) fugacity of the pure, subcooled liquid, denoted $f_i^{0,L}$. While the two standard-state fugacities ($f_i^{0,S}, f_i^{0,L}$) cannot be evaluated separately, their ratio can be well approximated. The isofugacity criterion reveals a relation to the molar change in free energy for a pure

component* by

$$\ln \frac{f_i^{0,S}(T)}{f_i^{0,L}(T)} = \ln x_i \gamma_i(T, \mathbf{x}) \equiv \ln x_i^{\mathrm{id}}(T) = -\frac{g_i^L - g_i^S}{\mathsf{R}T} \tag{3–5}$$

The quantity x_i^{id} is called the ***ideal*** solubility, since it is the solubility in the ideal solution ($\gamma_i = 1$). The fugacity ratio on the left-hand side can be evaluated from a thermodynamic process on the pure solute involving six states ($a - f$) as depicted in Figure 3–1. This process relates the fugacities to measurable thermophysical properties. A similar derivation was also given by Prausnitz et al.,[59] but they considered a homomorph solute, i.e., a solid phase with no transition(s) between T and the melting point. Here, the derivation is redone, but for a solute which undergoes a first-order phase transition. Many solids exhibit phase transitions, and their contribution to the overall change in free energy can sometimes be significant. Therefore, it is relevant to include its effect into the process depicted below. The solid is warmed from phase S_1 through a solid phase transition at $T_{t,i}$ and melted at the fusion point, $T_{m,i}$. Finally, the liquid is hypothetically cooled below melting and transition points. In the absence of a phase

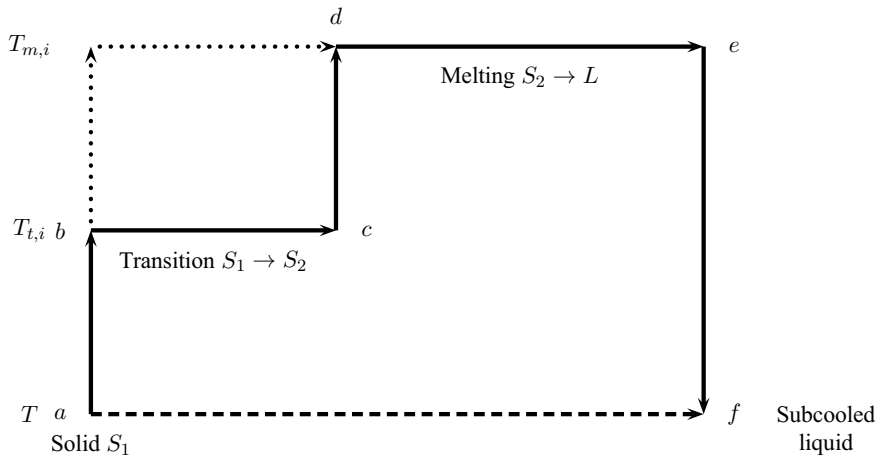

Figure 3–1. Thermodynamic cycle for solubilization of a pure solid i. Vertical distances denote a change in temperature, while horizontal arrows denote phase transitions.

transition, the dotted line from $b \rightarrow d$ must be followed instead of $b \rightarrow c \rightarrow d$, which is identical to that

* This is done by writing the free energy (or chemical potential, μ_i) as: $\mu_i = \mu_i^0 + \mathsf{R}T \ln f_i$.

of Prausnitz et al. The difference in free energies between states a and f is

$$
\begin{aligned}
-\frac{g^L - g^S}{\mathsf{R}T} = \frac{g_f(T) - g_a(T)}{\mathsf{R}T} = \left(\frac{g_b^{S_1}(T_{t,i})}{\mathsf{R}T_{t,i}} - \frac{g_a^{S_1}(T)}{\mathsf{R}T}\right) + \underbrace{\left(\frac{g_c^{S_2}(T_{t,i}) - g_b^{S_1}(T_{t,i})}{\mathsf{R}T_{t,i}}\right)}_{=0} \\
+ \left(\frac{g_d^{S_2}(T_{m,i})}{\mathsf{R}T_{m,i}} - \frac{g_c^{S_1}(T_{t,i})}{\mathsf{R}T_{t,i}}\right) + \underbrace{\left(\frac{g_e^{L}(T_{m,i}) - g_d^{S_2}(T_{m,i})}{\mathsf{R}T_{m,i}}\right)}_{=0} + \left(\frac{g_f^{L}(T)}{\mathsf{R}T} - \frac{g_e^{L}(T_{m,i})}{\mathsf{R}T_{m,i}}\right).
\end{aligned}
\tag{3–6}
$$

The free energies of transition and melting (steps $b \to c$ and $d \to e$) are zero since transition occurs spontaneously. The difference in Gibbs energies of the remaining steps are evaluated by integrating the Gibbs-Helmholtz equation at constant pressure

$$
-\frac{h}{T^2} = \left(\frac{\partial}{\partial T}\frac{g}{T}\right)_P. \tag{3–7}
$$

Integration yields

$$
\begin{aligned}
\frac{g}{T} &= -\int_{T_0}^{T} \frac{h(T)}{T^2}\mathrm{d}T = -\int_{T_0}^{T} \frac{h(T_0)}{T^2}\mathrm{d}T - \int_{T_0}^{T}\int_{T_0}^{T} \frac{c_P(T)}{T^2}\mathrm{d}T\mathrm{d}T \\
&= h(T_0)\left(\frac{1}{T_0} - \frac{1}{T}\right) - c_P\int_{T_0}^{T}\frac{1}{T}\mathrm{d}T - c_P\int_{T_0}^{T}\frac{1}{T_0}\mathrm{d}T \\
&= h(T_0)\left(\frac{1}{T_0} - \frac{1}{T}\right) - c_P\left(\ln\frac{T}{T_0} + 1 - \frac{T}{T_0}\right).
\end{aligned}
\tag{3–8}
$$

It is assumed here, that the heat capacities are independent of temperature; a reasonable assumption as long as $T < T_{m,i}$. For the terms above we get, by adding and subtracting $h_4^{S_2}/\mathsf{R}(1/T - 1/T_{m,i})$

$$
\begin{aligned}
-\frac{g^L - g^S}{\mathsf{R}T} = \frac{h_b^{S_1}}{\mathsf{R}}\left(\frac{1}{T_{t,i}} - \frac{1}{T}\right) - \frac{c_P^{S_1}}{\mathsf{R}}\left(\ln\frac{T_{t,i}}{T} + 1 - \frac{T_{t,i}}{T}\right) + \frac{h_c^{S_2}}{\mathsf{R}}\left(\frac{1}{T_{m,i}} - \frac{1}{T_{t,i}}\right) \\
- \frac{c_P^{S_2}}{\mathsf{R}}\left(\ln\frac{T_{m,i}}{T_{t,i}} - 1 + \frac{T_{t,i}}{T_{m,i}}\right) + \frac{h_d^{S_2}}{\mathsf{R}}\left(\frac{1}{T} - \frac{1}{T_{m,i}}\right) + \frac{h_e^{L}}{\mathsf{R}}\left(\frac{1}{T} - \frac{1}{T_{m,i}}\right) \\
- \frac{c_P^{L}}{\mathsf{R}}\left(\ln\frac{T}{T_{m,i}} - 1 + \frac{T_{m,i}}{T}\right) - \frac{h_d^{S_2}}{\mathsf{R}}\left(\frac{1}{T} - \frac{1}{T_{m,i}}\right).
\end{aligned}
\tag{3–9}
$$

The enthalpy change, for the second solid phase (S_2), resulting from changing temperature from the solid transition temperature to the melting point can be written as

$$
h_d^{S_2}(T_{m,i}) = h_c^{S_2}(T_{t,i}) + \int_{T_{t,i}}^{T_{m,i}} c_P^{S_2}\mathrm{d}T \approx h_c^{S_2}(T_{t,i}) + c_P^{S_2}\left(T_{m,i} - T_{t,i}\right). \tag{3–10}
$$

By inserting this above, we find that

$$-\frac{g^L - g^S}{\mathsf{R}T} = \frac{h_e^L - h_d^{S_2}}{\mathsf{R}}\left(\frac{1}{T} - \frac{1}{T_{m,i}}\right) - \frac{c_P^L - c_P^{S_2}}{\mathsf{R}}\left(\ln\frac{T}{T_{m,i}} - 1 + \frac{T_{m,i}}{T}\right) + \frac{h_b^{S_1} - h_c^{S_2}}{\mathsf{R}}\left(\frac{1}{T_{t,i}} - \frac{1}{T}\right) - \frac{c_P^{S_1} - c_P^{S_2}}{\mathsf{R}}\left(\ln\frac{T_{t,i}}{T} + 1 - \frac{T_{t,i}}{T}\right). \tag{3–11}$$

We now define the enthalpy and heat capacity differences as

$$\begin{aligned} \Delta h_{m,i} &\equiv h_e^L - h_d^{S_2}, \qquad & \Delta c_{P,m,i} &\equiv c_P^L - c_P^{S_2} \\ \Delta h_{t,i} &\equiv h_b^{S_1} - h_c^{S_2}, \qquad & \Delta c_{P,t,i} &\equiv c_P^{S_1} - c_P^{S_2}, \end{aligned} \tag{3–12}$$

so that the final expression becomes

$$\frac{g_i^L - g_i^S}{\mathsf{R}T} = -\frac{\Delta h_{m,i}}{\mathsf{R}}\left(\frac{1}{T} - \frac{1}{T_{m,i}}\right) + \frac{\Delta c_{P,m,i}}{\mathsf{R}}\left(\ln\frac{T}{T_{m,i}} - 1 + \frac{T_{m,i}}{T}\right) - \frac{\Delta h_{t,i}}{\mathsf{R}}\left(\frac{1}{T_{t,i}} - \frac{1}{T}\right) + \frac{\Delta c_{P,t,i}}{\mathsf{R}}\left(\ln\frac{T_{t,i}}{T} + 1 - \frac{T_{t,i}}{T}\right). \tag{3–13}$$

The assumptions required in order to derive Equation (3–13) can be summarized as

1. There are no pressure effects on the properties of condensed matter.

2. The heat capacities are independent of temperature.

3. Solid-phase transitions are first order in the Ehrenfest sense.

While the first and second items are reasonable for most substances, the latter requirement means that the equation is not generally applicable to all solids, unless they are known to exhibit first-order transitions only. Those which undergo second order phase transitions (such as a lambda transition[60,61]) require modified forms. Derivation of its contribution to the free energy change is not complicated, and was done by Preston et al. [60] and Choi and McLaughlin. [61] Fortunately, second order transitions are not as frequent as first order. Substances which may undergo second order phase transitions include substances such as methane, butane, cyclohexane, and phenantracene,[60,61] although this may well depend on the medium.

The full form of Equation (3–13) is rarely used. If there are no known phase transitions between T and $T_{m,i}$ then

$$\ln x_i\gamma_i(T, \mathbf{x}) = -\frac{\Delta h_{m,i}}{\mathsf{R}}\left(\frac{1}{T} - \frac{1}{T_{m,i}}\right) + \frac{\Delta c_{P,m,i}}{\mathsf{R}}\left(\ln\frac{T}{T_{m,i}} - 1 + \frac{T_{m,i}}{T}\right). \tag{3–14}$$

If $\Delta c_{P,m} \approx 0$ or $T_{m,i} - T$ is small, a good approximation is

$$\ln x_i \gamma_i(T, \mathbf{x}) \approx -\frac{\Delta h_{m,i}}{\mathsf{R}} \left(\frac{1}{T} - \frac{1}{T_{m,i}} \right) \tag{3–15}$$

Alternatively, if $T_{m,i}$ is much larger than T, the contribution from the heat capacity term can be significant. This means that the change in heat capacity needs to be accounted for. There are essentially four options:

1. The term is negligible.
2. Experimental values are used.
3. A model is used to estimate its value.
4. Approximation by the entropy of fusion: $\Delta c_{P,m,i} \approx \Delta s_{m,i} = \Delta h_{m,i}/T_{m,i}$.

The first item was discussed above, and is reasonable if the change in heat capacity is small. Furthermore, if $T_{m,i} - T$ is small, then the terms within the parenthesis multiplied onto $\Delta c_{P,m,i}$ approach zero. This is the suggestion by Prausnitz et al.,[59] and is widely used in the thermodynamic community.[10,17–19,62] Ideally, in the case of a significant contribution from $\Delta c_{P,m,i}$ an experimental value is preferable, but measurements are scarce and do not cover a very large range of solutes. Selection of an appropriate value for $\Delta c_{P,m,i}$ occasionally relies on comparison with experimental solubility data to determine the "best fit", as was done by Grant et al.[63] However, there are also theoretical considerations to support some values over others. The heat capacity is a measure of how much energy a molecule can absorb in its phase. This means, that it is related to the degrees of rotational freedom within the molecule. It is often negligible for flat, rigid molecules, e.g. anthracene, naphthalene, pyrene, and other polycyclic aromatic hydrocarbons (PAHs). The approximation to the molar entropy of fusion is related to this fact. Extensive discussions regarding the entropy of fusion for rigid versus nonrigid molecules is made by Prigogine and Defay.[64] Models for heat capacities of liquids and solids are appearing in the literature, but their estimates are not generally successful for all molecular types.[65,66] The final approximation listed above, $\Delta c_{P,m,i} = \Delta h_{m,i}/T_{m,i}$, gives[67]

$$\ln x_i \gamma_i(T, \mathbf{x}) \approx -\frac{\Delta h_{m,i}}{\mathsf{R} T_{m,i}} \ln \frac{T_{m,i}}{T} = -\frac{\Delta s_{m,i}}{\mathsf{R}} \ln \frac{T_{m,i}}{T}. \tag{3–16}$$

Equations (3–15) and (3–16) have been evaluated extensively. Yalkowsky[68] concluded that Equation (3–15) is a good approximation for the solubilities of naphthalene, anthracene, phenanthracene, and flourene in solutions of benzene. Neau and Flynn[69] concluded that Equation (3–16) is generally better than (3–15), except for flat, rigid molecules, such as those studied by Yalkowsky. In the absence of

heat capacities from either data or estimation methods, it is not obvious how to obtain values for the estimation of the ideal solubility in Equation (3–13) when dealing with nonrigid molecular structures. Obviously, when experimental data is available for comparison, the results from both approximations can be directly compared. However, this is not possible when there are no measurements. Furthermore, as noted elsewhere,[70] the transition point is not always independent of solvent, but may differ slightly.

Solving Equation (3–5) for the solubility, x_i, can be constructed as locating the zero of a function f:

$$f(x_i) = \ln x_i \gamma_i(T, \mathbf{x}) - \ln x_i^{\mathrm{id}}(T) = 0, \qquad \text{s.t.} \quad T, \mathbf{x}'. \tag{3–17}$$

Here, we have used $\mathbf{x}'$ to denote solvent composition, i.e., solute-free*. Solving this equation for the equilibrium composition requires:

* Thermophysical properties of melting (and transition), and
* parameters for a g^{E}-model.

Even if the thermophysical properties are available, these may be associated with large uncertainties, since literature values of these are frequently conflicting. The second issue is obtaining relevant model parameters. These need to be found from regression of mixture data – data which is frequently not available, or only available in limited amounts. Therefore, for systems with little or no measured mixture data, the practicality of this approach is often limited. In the section to follow, another approach to mixed solvent solubility will be presented.

3.4. Excess solubility

Thermodynamic properties such as solubility can, like other properties, be dealt with in the context of "ideality" and "nonideality". The difference between the two is defined as the *excess* property. Often the "ideal" state, or reference state, is that of a pure substance or an ideal gas or liquid at similar T and P. The definition of the excess solubility is less rigorous than classical thermodynamics. In what follows, we shall define an excess solubility for a solute in a *mixed* solvent. Rather than using the definition above for the ideal solubility, x_i^{id}, we define an excess solubility relative to the average solubility in the pure solvents,

$$s_i^{\mathrm{E}} = \ln x_1^{\mathrm{E}} \equiv \ln x_{i,m} - \sum_{j \neq i}^{M} x'_j \ln x_{i,j}, \tag{3–18}$$

where $x_{i,m}$ is the solubility of i in the solvent mixture. The "ideal" term of Equation (3–18) is the interpolated solubility from each pure solvent. It is not to be confused with an ideal solution which, in

* For solvent species j, $x'_j = x_j/(1 - x_i)$, and $\sum_j x'_j = 1$.

the context of Lewis and Randall, is defined by an excess Gibbs energy equal to zero. It is noteworthy here to point out that when the solvent mixture forms an ideal *solution* the excess solubility is forced to zero, but the opposite need not be true, i.e., an excess solubility of zero does not imply an ideal (solvent) solution. In the limit of a single solvent, the excess solubility goes to zero, regardless of ideal solution or not.

The definition excess solubility above means that the quantity x_1^{E} is a ratio between the ideal-mixing estimate and the actual mixture mole fraction solubilities. While this formulation might seem awkward, it provides an interesting relation to some other thermodynamic mixture properties, as will be shown below. A fluid mixture can be assigned a mixture fugacity from its corresponding partial molal value[71]

$$\ln \frac{f_i}{x_i} = \left(\frac{\partial n \ln f}{\partial n_i} \right)_{T,P,n_{j\neq i}} , \tag{3–19}$$

where $n = \sum_i n_i$. By means of partial molal terms, the fugacity can be written as

$$\ln f = \sum_{i=1}^{M} x_i \ln \frac{f_i}{x_i}. \tag{3–20}$$

Using the symmetric (Lewis-Randall) and unsymmetric (Henry's law) normalizations for the species activity coefficients, the right-hand side term can be written in two equivalent ways

$$f_i = \begin{cases} x_i \gamma_i(T, \mathbf{x}) f_i^0(T) \\ x_i \gamma_i^*(T, \mathbf{x}) H_i(T) \end{cases} , \tag{3–21}$$

where H_i is Henry's law constant, defined by

$$\lim_{x_i \to 0} (\gamma_i f_i^0) \equiv \lim_{x_i \to 0} (\gamma_i^* H_i) = H_i. \tag{3–22}$$

Though usually defined as the reference fugacity in a single solvent, this definition applies for i in both single and mixed solvents. This means that the Henry's constant refers to a solute-free mixture. As a result of this, we can therefore write $\ln f$ in two ways

$$\ln f = \sum_{i=1}^{M} x_i \ln \frac{f_i}{x_i} = \begin{cases} g^{\mathrm{E}}/\mathsf{R}T + \sum_i x_i \ln f_i \\ g^{\mathrm{E}}/\mathsf{R}T + \sum_i x_i \ln H_i/\gamma_i^{\infty} \end{cases} , \tag{3–23}$$

where g^{E} is the excess Gibbs energy with all species normalized using the Lewis-Randall standard

state,[59] and $\gamma_i^\infty = \lim_{x_i \to 0} \gamma_i$. For a solute i dissolved in a mixed solvent, we can write

$$\ln \frac{f_i}{x_i} = \ln f + (1 - x_i) \left(\frac{\partial \ln f}{\partial x_i} \right)_{T,P,\mathbf{x}'}, \tag{3–24}$$

where $'$ denotes solute-free composition of the solvent. If we now take the limit as $x_i \to 0$ the left-hand side approaches the Henry's constant in the solvent mixture, defined from Equation (3–22), $\ln H_{i,m}$

$$\ln H_{i,m} = \ln f' + \lim_{x_i \to 0} \left(\frac{\partial \ln f}{\partial x_i} \right)_{T,P,\mathbf{x}'}, \tag{3–25}$$

where f' is the fugacity of the solute-free mixture. Both terms of the right-hand side are functions of solvent composition at constant T and (to a lesser extent) P, and this is a general expression for the Henry's constant of a solute dissolved in a solvent mixture. If the solvent is pure j we have for the solute

$$\ln H_{i,j} = \ln f_j + \left(\frac{\partial \ln f_i}{\partial x_i} \right)_{T,P,x_j=1}, \tag{3–26}$$

where f_j is the fugacity of the pure solvent species j at T. Multiplication by x'_j and summing over all species gives

$$\sum_{j \neq i} x'_j \ln H_{i,j} = \sum_{j \neq i} \ln f_j + \sum_{j \neq i} x'_j \left(\frac{\partial \ln f_i}{\partial x_i} \right)_{T,P,x_j=1}. \tag{3–27}$$

Subtraction from Equation (3–25) gives

$$\ln H_{i,m} - \sum_{j \neq i} x'_j \ln H_{i,j} = \ln f' - \sum_{j \neq i} \ln f_j + \lim_{x_i \to 0} \left(\frac{\partial \ln f}{\partial x_i} \right)_{T,P,\mathbf{x}'} - \sum_{j \neq i} x'_j \left(\frac{\partial \ln f_i}{\partial x_i} \right)_{T,P,x_j=1}. \tag{3–28}$$

The left-hand side is the excess Henry's constant and the first two terms of the right-hand side represent the excess free energy of the *solvent* mixture, $g^{\mathrm{E}}(\text{solvents})/\mathsf{R}T$. Rewriting gives

$$\ln H_{i,m} - \sum_{j \neq i} x'_j \ln H_{i,j} = \frac{g^{\mathrm{E}}(\text{solvents})}{\mathsf{R}T} + \lim_{x_i \to 0} \left(\frac{\partial \ln f}{\partial x_i} \right)_{T,P,\mathbf{x}'} - \sum_{j \neq i} x'_j \left(\frac{\partial \ln f_i}{\partial x_i} \right)_{T,P,x_j=1}. \tag{3–29}$$

The left-hand side can, in view of Equation (3–22), also be formulated as

$$\ln H_{i,m} - \sum_{j \neq i} x'_j \ln H_{i,j} = \lim_{x_i \to 0} (\ln \gamma_i) - \sum_{j \neq i} x'_j \lim_{x_i \to 0} (\ln \gamma_{i,j}). \tag{3–30}$$

Thus,

$$\ln H_{i,m} - \sum_{j \neq i} x'_j \ln H_{i,j} = \frac{g^{\mathrm{E}}(\text{solvents})}{\mathsf{R}T} + \Delta^\infty, \tag{3–31}$$

where Δ^∞ is the difference among the derivative terms in Equation (3–29). Further, we can relate this

equation to the excess solubility above. Inserting Equation (3–5) into (3–18) gives

$$\ln x_{i,m} - \sum_{j\neq i} x'_j \ln x_{i,j} = \ln x_i^{\mathrm{id}} - \ln \gamma_i - \sum_{j\neq i} x'_j (\ln x_i^{\mathrm{id}} - \ln \gamma_{i,j}) = -\ln \gamma_i + \sum_{j\neq i} x'_j \ln \gamma_{i,j}, \quad (3\text{–}32)$$

assuming that the solute forms *identical* crystal structures in all solvents (thus x_i^{id} is the same in all solvents). Taking the limit of infinite dilution, we find that

$$\ln x_{i,m} - \sum_{j\neq i} x'_j \ln x_{i,j} = -\lim_{x_i\to 0}(\ln \gamma_i) + \sum_{j\neq i} x'_j \lim_{x_i\to 0}(\ln \gamma_{i,j}) = -\ln H_{i,m} + \sum_{j\neq i} x'_j \ln H_{i,j}. \quad (3\text{–}33)$$

Therefore, we may subsequently write

$$\ln x_{i,m} - \sum_{j\neq i} x'_j \ln x_{i,j} = \frac{g^{\mathrm{E}}(\text{solvents})}{\mathrm{R}T} + \Delta^{\infty}. \quad (3\text{–}34)$$

So if the difference among the derivative terms in Δ^{∞} are small, the excess solubility is approximately equal to the negative excess free energy of the solvent mixture, *independent* of the solute! It

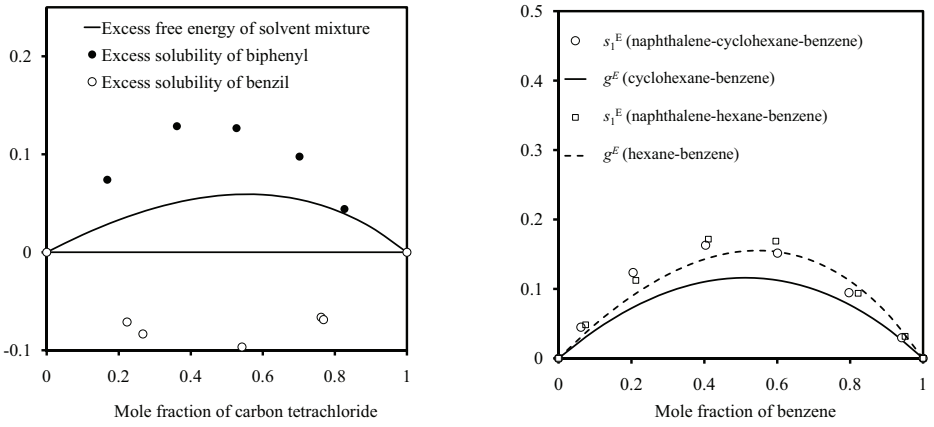

Figure 3–2. Left: Excess solubilities of biphenyl[72] and benzil[73] in hexane–carbon tetrachloride and their excess free energy.[74] The excess solubilities of biphenyl and benzil are of opposite sign, although they are dissolved in the same solvent mixture. Right: Excess solubilities of naphthalene[75] in cyclohexane–benzene and hexane–benzene and the solvent excess free energy.[76,77] Consistent behavior between excess solubility and excess Gibbs energies of solvent mixtures is observed.

is usually referred to as the first-order approach (zeroth being ideal mixture), and was introduced by O'Connell and Prausnitz[51] for gas solubilities in mixed solvent systems in 1964. Kehiaian[47–50] outlined a method based on these principles for solids in the mid-1960s. Although a potentially powerful method, solute-independent excess solubility is an infrequent experimental observation. The left plot of Figure 3–2 shows the excess free energy ($g^{\mathrm{E}}/\mathrm{R}T$) of hexane and carbon tetrachloride and excess

solubilities of biphenyl and benzil herein. The nonideality of the solvent mixture is estimated from data of Bissell and Williamson.[74] The two excess solubility profiles are of opposite sign, and significantly larger than the excess free energy of the solvent mixture. However, there are also examples of systems where the solvent excess free energy is consistent with the excess solubility of a solid. The right plot of Figure 3–2 shows an example of this, for naphthalene in the moderately nonideal solvent mixtures cyclohexane–benzene and hexane–benzene. The first order approach also predicts that the excess solubility is of equal sign as the excess free energy of the solvent mixture. This is not always the case with experimental data. Consider Figure 3–3 which shows the excess solubility of naphthalene in mixtures of water and ethylene glycol (data of Lepree et al.[78]) and water and dimethylsulfoxide (DMSO; data of Lepree et al.[78]). The solvent nonideality here was estimated from the data of Lai et al.[79] and Lancia et al..[80] There are a wide number of approaches to mixed solvent solubility, in binary solvent

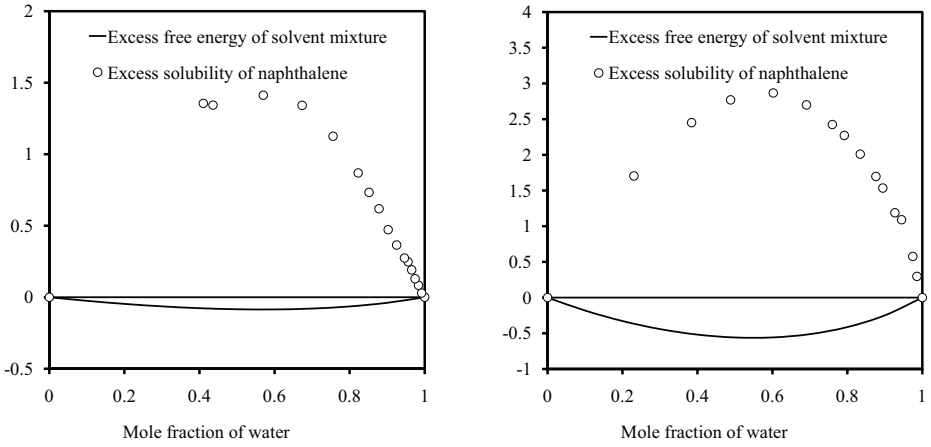

Figure 3–3. Excess solubilities of naphthalene in water–ethylene glycol and water–DMSO mixtures. Notice that in both systems the excess Gibbs energy of the solvent mixtures are of opposite sign to the excess solubility.

mixtures, in the engineering literature which makes use of the excess solubility.[81–83] This is partly because the definition of the excess removes the effect of pure solvent. This means that for modeling, only the direct effect of mixing remains. This is often advantageous when dealing with solubilities in pure solvent which differs by several orders of magnitude (e.g. aqueous–organic systems). For a binary solvent system, the excess solubility can be written as

$$s_1^{\mathrm{E}} = \ln \frac{x_{1,m}}{x_{1,3}} + x_2 \ln \frac{x_{1,3}}{x_{1,2}}. \tag{3–35}$$

The latter fraction is constant, while the former contains the ratio of solubility to the solubility in pure

3. Expressing a function/model for this is easier than solving the equilibrium problem, especially since the nonideality of the solvent mixture greatly (but not solely) determines the magnitude of the excess solubility. Therefore, the modeling basis in this thesis is also based on the excess approach, as will become apparent in Chapter 4. Though this increases the amount of model input, it may also increase the accuracy of the output, and decrease the complexity of the modeling.

3.5. Summary

This chapter has given an overview of the state-of-the-art in the field of mixed solvent solubility. The current methods, which are available for solid-liquid equilibrium in mixed solvents, are often based on expressions which require large amounts of data for regression of good parameter values. The chapter also presented the thermodynamic framework which governs solid solubility in liquids. The traditional equal-fugacity approach requires the thermophysical properties characterizing the melting process of the solid. These are frequently not available, or may be associated with large degrees of uncertainty. Therefore, it might sometimes be advantageous to not base a thermodynamic method on these properties. The chapter also defined the *excess* solubility, and useful relations for this quantity were found. This means, that if the excess solubility can be estimated, the actual mole fraction solubility can be found from the solubility of the solute in each of the pure solvents.

In the following chapter, we will explore a method for estimating the excess solubility of a solid solute in a mixed solvent based on the *fluctuation solution theory* principles, which were derived in Chapter 2.

References

1. J. W. Millard, F. A. Alvarez-Núnez, and S. H. Yalkowsky. *Int. J. Pharm.*, 245:153–166, 2002.
2. T. L. Nielsen, J. Abildskov, P. M. Harper, I. Papaeconomou, and R. Gani. *J. Chem. Eng. Data*, 46: 1041–1044, 2001.
3. J. Marrero and J. Abildskov. *Solubility and related properties of large complex chemicals*, volume 15 of *DECHEMA Chemistry Data Series*. DECHEMA, Frankfurt am Main, 2003.
4. J. Abildskov. *Solubility and related properties of large complex chemicals*, volume 15 of *DECHEMA Chemistry Data Series*. DECHEMA, Frankfurt am Main, 2005.
5. S. H. Yalkowsky and Y. He. *Handbook of aqueous solubility data*, volume 1. CRC Press, 2003.
6. W.E. Acree Jr. *Polycyclic Aromatic Hydrocarbons in Pure and Mixed Solvents*, volume 54. IUPAC Solubility Data Series, 1994.
7. W. E. Acree Jr. *Polycyclic Aromatic Hydrocarbons: Binary Nonaqueous Systems, Part I: Solvents A-E*, volume 58. IUPAC Solubility Data Series, 1995.
8. W. E. Acree Jr. *Polycyclic Aromatic Hydrocarbons: Binary Nonaqueous Systems, Part II: Solvents F-Z*, volume 59. IUPAC Solubility Data Series, 1995.
9. P. Kolár, J. W. Shen, A. Tsuboi, and T. Ishikawa. *Fluid Phase Equil.*, 194-197:771–782, 2002.
10. H. Modaressi, E. Conte, J. Abildskov, R. Gani, and P. Crafts. *Ind. Eng. Chem. Res.*, 47:5234, 2008.
11. M. H. Abraham, R. E. Smith, R. Luchtefeld, A. J. Boorem, and W. E. Acree Jr. R. Luo. *J. Pharm. Sci.*, 99:1500–1515, 2010.
12. F. L. Mota, A. P. Carneiro, A. J. Queimada, S. P. Pinho, and E. A. Macedo. *Eur. J. Pharm. Sci.*, 37: 499–507, 2009.
13. F. L. Mota, A. J. Queimada, S. P. Pinho, and E. A. Macedo. *Fluid Phase Equil.*, 298:75–82, 2010.
14. J. Cassens, F. Ruether, K. Leonhard, and G. Sadowski. *Fluid Phase Equil.*, 299:161–170, 2010.
15. J. G. Gmehling, T. F. Anderson, and J. M. Prausnitz. *Ind. Eng. Chem. Res. Fundam.*, 17:269–273, 1978.
16. S. Gracin, T. Brinck, and Å. C. Rasmuson. *Ind. Eng. Chem. Res.*, 41:5114–5124, 2002.

References

17. I. Hahnenkamp, G. Graubner, and J. G. Gmehling. *Int. J. Pharm.*, 388:73–81, 2010.

18. A. T. Kan and M. B. Tomson. *Environ. Sci. Technol.*, 30:1369–1376, 1996.

19. W. B. Arbuckle. *Environ. Sci. Technol.*, 20:1060–1064, 1986.

20. A. Martin, P. L. Wu, A. Adjei, A Beerbower, and J. M. Prausnitz. *J. Pharm. Sci.*, 70:1260–1264, 1981.

21. A. Li, W. J. Doucette, and A. W. Andren. *Chemosphere*, 29:657–669, 1994.

22. J. A. P. Coutinho, S. I. Andersen, and E. H. Stenby. *Fluid Phase Equil.*, 103:23–39, 1995.

23. J. K. Fu and R. G. Luthy. Pollutant sorption to soils and sediments in organic/aqueous solvent systems. Technical report, EPA, Athens, GA, USA,, 1985.

24. J. K. Fu and R. G. Luthy. *J. Environ. Eng.*, 112: 328–345, 1986.

25. U. Domańska. *Fluid Phase Equil.*, 35:217–236, 1987.

26. U. Domańska and T. Hofman. *J. Sol. Chem.*, 14: 531–547, 1985.

27. R. P. Currier and J. P. O'Connell. *Fluid Phase Equil.*, 33:245–265, 1987.

28. A. Diedrichs and J. G. Gmehling. *Ind. Eng. Chem. Res.*, 50:1757–1769, 2011.

29. J. Abildskov, R. Gani, P. Rasmussen, and J. P. O'Connell. *Fluid Phase Equil.*, 158-160:349–356, 1999.

30. E. R Thomas and C. A. Eckert. *Ind. Eng. Chem. Proc. Des. Dev.*, 23:194–209, 1984.

31. M. J. Lazzaroni, D. Bush, C. A. Eckert, T. C. Frank, S. Gupta, and J. D. Olson. *Ind. Eng. Chem. Res.*, 44:4075–4083, 2005.

32. T. C. Frank, J. J. Anderson, J. D. Olson, and C. A. Eckert. *Ind. Eng. Chem. Res.*, 46:4621–4625, 2007.

33. L. C. Draucker, M. Janakat, M. J. Lazzaroni, D. Bush, C. A. Eckert, T. C. Frank, and J. D. Olson. *Ind. Eng. Chem. Res.*, 46:2198–2204, 2007.

34. S. T. Lin and S. I. Sandler. *Ind. Eng. Chem. Res.*, 41:899–913, 2002.

35. C. C. Chen and Y. Song. *Ind. Eng. Chem. Res.*, 43: 8354–8362, 2004.

36. C. C. Chen and P. A. Crafts. *Ind. Eng. Chem. Res.*, 45:4816–4824, 2006.

37. C. C. Shu and S. T. Lin. *Ind. Eng. Chem. Res.*, 50: 142–147, 2011.

38. I. V. PrikhodŠko, F. Tumakaka, and G. Sadowski. *Russ. J. Appl. Chem.*, 80:542–548, 2007.

39. M. B. Oliveira, V. L. Oliveira, J. A. P. Coutinho, and A. J. Queimada. *Ind. Eng. Chem. Res.*, 48: 5530–5536, 2009.

40. I. Tsivintzelis, I. G. Economou, and G.M. Kontogeorgis. *AIChE J.*, 55:756–770, 2009.

41. L. A. Ferreira, M. P. Breil, S. P. Pinho, E. A. Macedo, and J. M. Mollerup. *Ind. Eng. Chem. Res.*, 48:5498Ü5505, 2009.

42. F. Ruether and G. Sadowski. *J. Pharm. Sci.*, 98: 4205–4215, 2009.

43. J. Abildskov and J. P. O'Connell. *Ind. Eng. Chem. Res.*, 42:5622–5634, 2003.

44. J. Abildskov and J. P. O'Connell. *Fluid Phase Equil.*, 228-229:395–400, 2005.

45. J. Abildskov and J. P. O'Connell. *Mol. Sim.*, 30: 367–378, 2004.

46. S. H. Yalkowsky, editor. *Techniques of solubilization of drugs*. Marcel Dekker, New York, 1981.

47. H. Kehiaian. *Bull. Acad. Pol. Sci. Ser. Sci. Chim.*, 12:323, 1964.

48. H. Kehiaian. *Bull. Acad. Pol. Sci. Ser. Sci. Chim.*, 14:153, 1966.

49. H. Kehiaian. *Rev. Chim., Rep. Populaire, Roumaine*, 31:299, 1966.

50. H. Kehiaian. *Bull. Acad. Pol. Sci. Ser. Sci. Chim.*, 13:425, 1965.

51. J. P. O'Connell and J. M. Prausnitz. *Ind. Eng. Chem. Res. Fundam.*, 2:347–351, 1964.

52. N. A. Williams and G. L. Amidon. *J. Pharm. Sci.*, 73:9–13, 1984.

53. N. A. Williams and G. L. Amidon. *J. Pharm. Sci.*, 73:14–18, 1984.

54. N. A. Williams and G. L. Amidon. *J. Pharm. Sci.*, 73:18–23, 1984.

55. T. Nitta and T. Katayama. *J. Chem. Eng. Jpn.*, 8: 175–180, 1975.

56. A. Jouyban, N. Y. K. Chew, H. K Chan, M. Sabour, and W. E. Acree Jr. *Chem. Pharm. Bull.*, 53(6): 634–637, 2005.

57. A. Jouyban, L. Valaee, M. Barzegar-Jalali, B. J. Clark, and W. E. Acree Jr. *Int. J. Pharm.*, 177:93, 1999.

58. A. B. Ochsner, R. J. Belloto Jr., and T. D. Sokoloski. *J. Pharm. Sci.*, 74:132–135, 2985.

59. J. M. Prausnitz, R. N. Lichtenthaler, and E. Gomez de Azevedo. *Molecular thermodynamics of fluid-phase equilibria*. Prentice-Hall, 3rd edition, 1999.

60. G. T. Preston, E. W. Funk, and J. M. Prausnitz. *J. Chem. Phys.*, 75:2345–2352, 1971.

61. P. B. Choi and E. McLaughlin. *AIChE J.*, 29:150–153, 1983.

62. C. Fan and C. Jafvert. *Environ. Sci. Tech.*, 31:3516–3522, 1997.

63. D. J. W. Grant, M. Mehdizadeh, A. H. L. Chow, and J.E. Fairbrother. *Int. J. Pharm.*, 18:25–38, 1984.

64. I. Prigogine and R. Defay. *Chemical thermodynamics*. Longmans Green and co, 2nd edition, 1954.

65. G. D. Pappa, E. C. Voutsas, K. Magoulas, and D. P. Tassios. *Ind. Eng. Chem. Res.*, 44:3799–3906, 2005.

66. M. Wu and S. H. Yalkowsky. *Ind. Eng. Chem. Res.*, 48:1063–1066, 2009.

67. J. Hildebrand, J. M. Prausnitz, and R. L. Scott. *Regular and related solutions*. Van Nostrand Reinhold Company, 1970.

68. S. H. Yalkowsky. *J. Pharm. Sci.*, 70:971, 1981.

69. S. H. Neau and G. L. Flynn. *Pharm. Res.*, 7:1157, 1990.

70. U. Domańska, A. Pobudkowska, and P. Gierycz. *Fluid Phase Equil.*, 289:20–31, 2010.

71. H. C. Van Ness and M. M. Abbott. *Classical thermodynamics of nonelectrolyte solutions: With applications to phase equilibra*. McGraw-Hill, 2nd edition, 1982.

72. W. E. Acree Jr. *Int. J. Pharm.*, 18:47–52, 1975.

73. W. E. Acree Jr. and G. L. Bertrand. *J. Sol. Chem.*, 12:101, 1983.

74. T. G. Bissell and A. G. Williamson. *J. Chem. Thermodyn.*, 7:131–136, 1975.

75. E. L. Heric and C. D. Posey. *J. Chem. Eng. Data*, 9:35, 1964.

76. M. Goral. *Fluid Phase Equil.*, 102:275, 1994.

77. L. M. Lozano, E. A. Montero, M. C. Martin, and M. A. Villamanan. *Fluid Phase Equil.*, 110:219–230, 1995.

78. J. M. Lepree, M. J. Mulski, and K. A. Connors. *J. Chem. Soc., Perk. Trans.*, 2:1491–1497, 1994.

79. J. T. W. Lai, F. W. Lau, D. Robb, P. Westh, G. Nielsen, C. Trandum, A. Hvidt, and Y. Koga. *J. Sol. Chem.*, 24:89–102, 1995.

80. A. Lancia, D. Musmarra, and F. Pepe. *J. Chem. Eng. Jpn.*, 29(3):449–455, 1996.

81. C. J. Orella and D. J. Kirwan. *Ind. Eng. Chem. Res.*, 30:1040–1045, 1991.

82. M. T. Gude, H. H. J. Meuwissen, L. A. M. van der Wielen, and K. Ch. A. M. Luyben. *Ind. Eng. Chem. Res.*, 35:4700–4712, 1996.

83. M. T. Gude, L. A. M. van der Wielen, , and K. Ch. A. M. Luyben. *Fluid Phase Equil.*, 116:110–117, 1996.

4. Fluctuation solution theory method for solid solubility in mixed solvents

This chapter outlines and derives expressions for the excess solubility of a solid in a mixed solvent using fluctuation solution theory relations from Chapter 2. These are then used to express the excess solubility as function of correlation function integrals. Finally, we parameterize the expressions, and show how to estimate the resulting parameters.

4.1. General relations

Chapter 3 showed how the *excess* solubility of a solute in a solvent mixture relates to the *excess* Henry's law constant and the activity coefficients at infinite dilution in Equation (3–33). The following chapters will build upon this relation. The activity coefficients in the symmetric (Lewis-Randall) standard state is related to those in the unsymmetric by[1]

$$\lim_{x_i \to 0} \ln \gamma_i = \ln(\gamma_i / \gamma_i^*) = - \lim_{x_i \to 1} \ln \gamma_i^*. \tag{4–1}$$

The excess solubility can therefore also be formulated in terms of the difference in the activity coefficients in the unsymmetric convention by invoking the relation from Equation (3–32)

$$\ln x_{i,m} - \sum_{j \neq i}^{M} x'_j \ln x_{i,j} = - \lim_{x_i \to 0} \ln \gamma_{i,m} + \sum_{j \neq i}^{M} x'_j \lim_{x_i \to 0} \ln \gamma_{i,j} = \lim_{x_i \to 1} \ln \gamma^*_{i,m} - \sum_{j \neq i}^{M} x'_j \lim_{x_i \to 1} \ln \gamma^*_{i,j}. \tag{4–2}$$

In the following derivation, we show how to establish useful relations to γ_i^*.

The Margules relation for the excess free energy in a binary mixture is given by an empirical expression[2,3]

$$\frac{g^{\mathrm{E}}}{\mathsf{R}Tx_1x_2} = (A_{21}x_1 + A_{12}x_2) + x_1x_2\,(B_{21}x_1 + B_{12}x_2) + \ldots \tag{4–3}$$

This resembles the expansion technique by Wohl.[4] By truncating the series after the first term and

differentiating properly, the activity coefficient of species 1 becomes

$$\ln \gamma_1 = \frac{\partial}{\partial n_1}\left(n\frac{g^{\mathrm{E}}}{\mathsf{R}T}\right)_{T,P,n_{i\neq 1}} = A_{12}x_2^2 + 2\left(A_{21} - A_{12}\right)x_1 x_2^2, \tag{4–4}$$

where $n = \sum_i n_i$. As 1 vanishes the limiting value becomes

$$\lim_{x_1 \to 0} \ln \gamma_1 = A_{12}. \tag{4–5}$$

The activity coefficient in the unsymmetric convention, by combining Equations (4–1) and (4–4), becomes

$$\ln \gamma_1^* = A_{12}x_2^2 + 2\left(A_{21} - A_{12}\right)x_1 x_2^2 - A_{12}, \tag{4–6}$$

which can be put into a more convenient form (using $x_2 = 1 - x_1$)

$$\ln \gamma_1^* = -x_1\left(-2A_{21} + 4A_{12}\right) - x_1^2\left(4A_{21} - 5A_{12}\right) - x_1^3\left(-2A_{21} + 2A_{12}\right). \tag{4–7}$$

This is essentially a polynomial expansion for $\ln \gamma_1^*$. By adding and subtracting $x_1^2\left(A_{21} - 2A_{12}\right)$ we can rewrite to get

$$\ln \gamma_1^* = -A\left(x_1 - \frac{x_1^2}{2}\right) - B\left(\frac{x_1^2}{2} - \frac{x_1^3}{3}\right), \tag{4–8}$$

with

$$A = -2A_{21} + 4A_{12}; \qquad B = -6A_{21} + 6A_{12}.$$

If additional terms are included in Equation (4–3) then (4–8) extends to higher orders. Equation (4–8) is derived for binaries, but may be generalized to multicomponent systems, if composition dependence is imposed on the coefficients A and B. This is written as $A(\mathbf{x}^+)$ and $B(\mathbf{x}^+)$. From Equation (4–8) the excess solubility of a single solute i in an M-component mixture becomes

$$\begin{aligned}
\ln x_{i,m} - \sum_{j\neq i}^{M} x_j' \ln x_{i,j} &= \lim_{x_1\to 1}\gamma_{i,m}^* - \sum_{j\neq i}^{M} x_j' \lim_{x_1\to 1}\gamma_{i,j}^* \\
&= -\lim_{x_1\to 1}\left[A_{i,m}\left(x_1 - \frac{x_1^2}{2}\right) - B_{i,m}\left(\frac{x_1^2}{2} - \frac{x_1^3}{3}\right)\right] \\
&\quad - \sum_{j\neq i}^{M} x_j' \lim_{x_1\to 1}\left[A_{i,j}\left(x_1 - \frac{x_1^2}{2}\right) - B_{i,j}\left(\frac{x_1^2}{2} - \frac{x_1^3}{3}\right)\right] \\
&= -\sum_{j\neq i}^{M} x_j'\left\{\frac{1}{2}\left[A_{i,j} - A_{i,m}(\mathbf{x}^+)\right] + \frac{1}{6}\left[B_{i,j} - B_{i,m}(\mathbf{x}^+)\right]\right\}.
\end{aligned} \tag{4–9}$$

Here, subscript m refers to a property in the mixed solvent with solute-free composition $\mathbf{x}^+$, while j

denotes a property of i in pure j. Obviously, in the limit of a single solvent j

$$A_{i,j} = A_{i,m} \quad \text{and} \quad B_{i,j} = B_{i,m}.$$

Thus, the excess solubility in any multicomponent solvent system is given straightforwardly if the coefficients $A_{i,j}$ and $B_{i,j}$ can be found. In the following, we will establish general relations to these from fluctuation solution theory.

4.2. Series expansion

We estimate the coefficients by using the relation to the activity coefficient, $\mu_i(T,P,\mathbf{x}) - \mu_i(T,P,x_i = 1) = \mathsf{R}T \ln x_i \gamma_i(T,P,\mathbf{x})$. Here, μ_i is the chemical potential of component i, and γ_i is the activity coefficient, normalized using the Lewis-Randall standard state. Consider the Taylor expansion of the activity coefficient, written in terms of the chemical potential, about a state of infinite dilution

$$\begin{aligned}\frac{\mu_i}{\mathsf{R}T} - \ln x_i - \left(\frac{\mu_i}{\mathsf{R}T} - \ln x_i\right)_{x_i=0} &= n_i \left(\frac{\partial \mu_i/\mathsf{R}T}{\partial n_i} - \frac{\mathrm{d}\ln x_i}{\mathrm{d}n_i}\right)_{T,P,n_{j\neq i},x_i=0} \\ &+ \frac{n_i^2}{2}\left(\frac{\partial^2 \mu_i/\mathsf{R}T}{\partial n_i^2} - \frac{\mathrm{d}^2 \ln x_i}{\mathrm{d}n_i^2}\right)_{T,P,n_{j\neq i},x_i=0} + \frac{n_i^3}{6}\left(\frac{\partial^3 \mu_i/\mathsf{R}T}{\partial n_i^3} - \frac{\mathrm{d}^3 \ln x_i}{\mathrm{d}n_i^3}\right)_{T,P,n_{j\neq i},x_i=0} + \dots\end{aligned} \tag{4–10}$$

with all derivatives at fixed temperature and pressure. The left-hand side yields – with Equation (4–1) – the unsymmetric activity coefficient

$$\begin{aligned}\ln \gamma_i^* = x_i \left(n\frac{\partial \mu_i/\mathsf{R}T}{\partial n_i} - \frac{1}{x_i} + 1\right)_{T,P,n_{j\neq i},x_i=0} + \frac{x_i^2}{2}\left(n^2\frac{\partial^2 \mu_i/\mathsf{R}T}{\partial n_i^2} + \frac{1}{x_i^2} - 1\right)_{T,P,n_{j\neq i},x_i=0} \\ + \frac{x_i^3}{6}\left(n^3\frac{\partial^3 \mu_i/\mathsf{R}T}{\partial n_i^3} - \frac{2}{x_i^3} + 2\right)_{T,P,n_{j\neq i},x_i=0}.\end{aligned} \tag{4–11}$$

By rewriting the derivatives into

$$n^2\frac{\partial^2 \mu_i}{\partial n_i^2} = n\frac{\partial}{\partial n_i}\left(n\frac{\partial \mu_i}{\partial n_i}\right) - n\frac{\partial \mu_i}{\partial n_i} \tag{4–12a}$$

$$n^3\frac{\partial^3 \mu_i}{\partial n_i^3} = n\frac{\partial}{\partial n_i}\left(n\frac{\partial}{\partial n_i}\left(n\frac{\partial \mu_i}{\partial n_i}\right)\right) - 3n\frac{\partial}{\partial n_i}\left(n\frac{\partial \mu_i}{\partial n_i}\right) + 2n\frac{\partial \mu_i}{\partial n_i}, \tag{4–12b}$$

and collect the terms to see that the resulting equation is exactly of the form indicated by Equation (4–8):

$$\begin{aligned}\ln \gamma_i^* = \left(x_i - \frac{x_i^2}{2}\right)\left[n\frac{\partial \mu_i/\mathsf{R}T}{\partial n_i} - \frac{1}{x_i} + 1\right]_{T,P,n_{j\neq i},x_i=0} \\ + \left(\frac{x_i^2}{2} - \frac{x_i^3}{3}\right)\left[n\frac{\partial}{\partial n_i}\left(n\frac{\partial \mu_i/\mathsf{R}T}{\partial n_i}\right) + \frac{1}{x_i^2} - 1\right]_{T,P,n_{j\neq i},x_i=0}.\end{aligned} \tag{4–13}$$

This means, that the coefficients in the Margules relation for γ_i^* can be given by

$$\begin{aligned} A_{i,m} &= -\left[n\frac{\partial \mu_i/\mathsf{R}T}{\partial n_i} - \frac{1}{x_i} + 1\right]_{T,P,n_{j\neq i},x_i=0} = \lim_{x_i\to 0}\left(n\frac{\partial \ln \gamma_i}{\partial n_i}\right)_{T,P,n_{j\neq i}} \\ B_{i,m} &= -\left[n\frac{\partial}{\partial n_i}\left(n\frac{\partial \mu_i/\mathsf{R}T}{\partial n_i}\right) + \frac{1}{x_i^2} - 1\right]_{T,P,n_{j\neq i},x_i=0} \\ &= \lim_{x_i\to 0}\left(n\frac{\partial \ln \gamma_i}{\partial n_i}\right)_{T,P,n_{j\neq i}} + \lim_{x_i\to 0}\left(n\frac{\partial}{\partial n_i}\left(n\frac{\partial \ln \gamma_i}{\partial n_i}\right)\right)_{T,P,n_{j\neq i}}. \end{aligned} \tag{4–14}$$

The expansion is built on the derivative $n(\partial \ln \gamma_i/\partial n_i)_{T,P,n_{j\neq i}}$, but this is not the most convenient quantity to obtain relations for. The quantity $(\partial \ln \gamma_i/\partial x_i)_{T,P,n_{j\neq i}}$ is in fact more convenient in relations to fluctuation solution theory. Applying the chain rule of partial differentiation, the derivative can be written as

$$\left(\frac{\partial \ln \gamma_i}{\partial x_j}\right)_{T,P,n_{k\neq j}} = \sum_{m=1}^{M}\left(\frac{\partial \ln \gamma_i}{\partial n_m}\right)_{T,P,n_{k\neq j}}\left(\frac{\partial n_m}{\partial x_j}\right)_{T,P,n_{k\neq j}}. \tag{4–15}$$

Since all other mole numbers than j is fixed, the derivative turns out to be

$$\left(\frac{\partial \ln \gamma_i}{\partial x_j}\right)_{T,P,n_{k\neq j}} = \left(\frac{\partial \ln \gamma_i}{\partial n_j}\right)_{T,P,n_{k\neq j}}\left(\frac{\partial n_j}{\partial x_j}\right)_{T,P,n_{k\neq j}} = \frac{n}{1-x_j}\left(\frac{\partial \ln \gamma_i}{\partial n_j}\right)_{T,P,n_{k\neq j}}. \tag{4–16}$$

It turns out, that the right-hand side derivative has the same mathematical properties as a derivative with respect to n_j. In the limit as j vanishes the two are identical

$$\lim_{x_j\to 0}\left(\frac{\partial \ln \gamma_i}{\partial x_j}\right)_{T,P,n_{k\neq j}} = \lim_{x_j\to 0} n\left(\frac{\partial \ln \gamma_i}{\partial n_j}\right)_{T,P,n_{k\neq j}}. \tag{4–17}$$

Returning to the derivation at hand, we truncate the series in Equation (4–13) after the first term, and find

$$\ln \gamma_i^* = -\left(x_i - \frac{x_i^2}{2}\right)\left(\frac{\partial \ln \gamma_i}{\partial x_i}\right)_{T,P,n_{j\neq i},x_i=0} \tag{4–18}$$

The required derivatives are then obtained from their relations to integrals of molecular pair correlation function, which was outlined in Chapter 2.

4.3. Excess solubility and correlation function integrals

We consider a liquid mixture of solvents, in which a solid solute is dissolved. Index 1 denotes solute while 2 and above denote solvent species. So to advance, we need to formulate expressions for derivatives of species activity coefficients, in order to express the excess solubility from Equation (4–2). The relations between derivatives of activity coefficients and molecular correlation function integrals are derived rigorously in Appendix 4.A. We give here the expressions for the derivative for Equation (4–18)

and the resulting excess solubilities in binary and ternary solvent systems.

4.3.1. System with two solvents

In a ternary system, i.e., a system with two solvents, the derivative of $\ln \gamma_1$ is

$$\left(\frac{\partial \ln \gamma_1}{\partial x_1}\right)_{T,P,n_{j\neq 1}} = \frac{\dfrac{x_2 x_3 f_{23}}{x_2 + x_3} - x_2 f_{12} - x_3 f_{13} - x_2 x_3 W_{123}}{1 + x_1 x_2 f_{12} + x_1 x_3 f_{13} + x_2 x_3 f_{23} + x_1 x_2 x_3 W_{123}}, \tag{4–19}$$

where the elements of the matrix **f** are defined as

$$f_{ij} \equiv H_{ii} + H_{jj} - 2H_{ij}, \tag{4–20}$$

H_{ij} being the *total correlation function integral* between i and j, which was defined in Equation (2–18). The off-diagonal elements of the symmetric matrix **f** describe deviations from ideal correlation between molecular pairs. The term W_{123} contains multiple pair products of correlation function integrals, and is given by

$$\begin{aligned} W_{123} =& H_{11}H_{22} + H_{11}H_{33} + H_{22}H_{33} - 2H_{12}H_{33} - 2H_{13}H_{22} - 2H_{11}H_{23} \\ &+ 2H_{12}H_{23} + 2H_{13}H_{23} + 2H_{12}H_{13} - H_{12}^2 - H_{13}^2 - H_{23}^2. \end{aligned} \tag{4–21}$$

The activity coefficient of the solute in the ternary mixture becomes, when taking the limit of infinite dilution, as indicated in Equation (4–18)

$$\ln \gamma_1^* = \left(x_1 - \frac{x_1^2}{2}\right) \frac{x_2 x_3 f_{23}^+ - x_2 f_{12}^+ - x_3 f_{13}^+}{1 + x_2 x_3 f_{23}^+}. \tag{4–22}$$

Here, $^+$ denotes that component 1 is at infinite dilution in the mixed solvent, implying that the f_{ij}^+ are functions of solvent composition. The term W_{123} contains products of H_{ij}s and cannot be factorized into f_{ij}s. It is a function of species 1, 2, and 3, and is – in principle – composition dependent. It may be regarded as a ternary parameter, but ternary mixture data is required to estimate its value. This means, that it appears as an adjustable parameter pertaining to each triplet of solute and solvents. This is an unattractive approach, since the parameter is not transferable. Therefore, W_{123} has been discarded since (as will be shown later) it is unrealistic to approximate it within reasonable accuracy without obtaining all values of H_{ij}. It should also be less significant since it is multiplied by two mole fractions. For a single solvent ($x_3 = 0$), we obtain the exact relation

$$\left(\frac{\partial \ln \gamma_1}{\partial x_1}\right)_{T,P,n_2} = -\frac{x_2 f_{12}}{1 + x_1 x_2 f_{12}}, \tag{4–23}$$

This means, that the activity coefficient of the solute in pure solvent 2 becomes

$$\ln \gamma_1^* = \left(x_1 - \frac{x_1^2}{2} \right) f_{12}^0. \tag{4–24}$$

Here, ^{0} denotes infinite dilution in pure solvent. We recognize this equation as the familiar one-term Margules relation in the unsymmetric convention, or Porter equation, since f_{12}^0 is independent of composition. The Lewis-Randall normalized version is obtained from applying Equation (4–1)

$$\ln \gamma_1 = \frac{1}{2} f_{12}^0 (1 - x_1)^2. \tag{4–25}$$

As noted by O'Connell,[5] inclusion of higher order terms in Equation (4–18) involves rather complicated expressions, and contains triplet (and higher order) distribution function integrals, which are not as well accounted for. The triplet correlation function, h_{ijk}, describes the correlation between molecules i, j, and k. Theoretical considerations[6,7] for liquid-phase distribution functions, such as Percus-Yevick $(h_{ijk} = 0)$ or convolution-hypernetted chain approximations $(h_{ijk} = -h_{ij}h_{jk})$ may be used as an immediate remedy. However, they are essentially hard-sphere theories, and as such are only valid in the absence of strong intermolecular forces, and cannot sufficiently describe real-fluid behavior. Therefore, it makes sence to initially investigate the implications of a simple formulation.

In lieu of additional rigor and complexity, the excess solubility, when inserting into Equation (4–2) becomes

$$\ln x_{i,m} - \sum_{j \neq i}^{M} x_j' \ln x_{i,j} = \frac{1}{2} \frac{x_2 x_3 f_{23}^+ - x_2 f_{12}^+ - x_3 f_{13}^+}{1 + x_2 x_3 f_{23}^+} - \frac{1}{2} \left[x_2 f_{12}^0 + x_3 f_{13}^0 \right], \tag{4–26}$$

which, together with Equation (4–23) for the solvent-binary, may be rearranged to yield

$$\begin{aligned} \ln x_{i,m} - \sum_{j \neq i}^{M} x_j' \ln x_{i,j} = & -\frac{x_3}{2} \left(\frac{\partial \ln \gamma_3}{\partial x_3} \right)_{T,P,n_2}^{+} \\ & - \frac{x_2}{2} \left[\frac{f_{12}^+}{1 + x_2 x_3 f_{23}^+} - f_{12}^0 \right] - \frac{x_3}{2} \left[\frac{f_{13}^+}{1 + x_2 x_3 f_{23}^+} - f_{13}^0 \right]. \end{aligned} \tag{4–27}$$

The derivative term in this equation is independent of solute, and represents a property of the solvent mixture alone. The emphasis towards component 3 is intended, but this does not imply that the equation is biased towards the selection of solvent indices. The Gibbs-Duhem equation at constant T and P can be written

$$x_1 \left(\frac{\partial \ln \gamma_1}{\partial n_2} \right)_{T,P,n_1,n_3} + x_2 \left(\frac{\partial \ln \gamma_2}{\partial n_2} \right)_{T,P,n_1,n_3} + x_3 \left(\frac{\partial \ln \gamma_3}{\partial n_2} \right)_{T,P,n_1,n_3} = 0. \tag{4–28}$$

Taking the limit of infinite dilution of 1, and transforming into a derive taken with respect to mole fraction, the result is

$$x_2(1-x_2)\left(\frac{\partial \ln \gamma_2}{\partial x_2}\right)^+_{T,P,n_3} + x_3(1-x_2)\left(\frac{\partial \ln \gamma_3}{\partial x_2}\right)^+_{T,P,n_3} = 0. \tag{4–29}$$

Since $\mathrm{d}x_2 = -\mathrm{d}x_3$ in a binary, the equation becomes

$$x_2\left(\frac{\partial \ln \gamma_2}{\partial x_2}\right)^+_{T,P,n_3} = x_3\left(\frac{\partial \ln \gamma_3}{\partial x_3}\right)^+_{T,P,n_2}, \tag{4–30}$$

revealing that the product of mole fraction and derivative is completely symmetric with respect to solvent indices. Equation (4–27) expresses the excess solubility with three terms:

i. A term for the solvent-solvent nonideality (2-3): $\frac{x_3}{2}\left(\frac{\partial \ln \gamma_3}{\partial x_3}\right)^+_{T,P,n_2}$

ii. A term for the solute-solvent nonideality (1-2): $\frac{x_2}{2}\left[\frac{f^+_{12}}{1+x_2x_3f^+_{23}} - f^0_{12}\right]$

iii. A term for the solute-solvent nonideality (1-3): $\frac{x_3}{2}\left[\frac{f^+_{13}}{1+x_2x_3f^+_{23}} - f^0_{13}\right]$

The first term on the right-hand side of Equation (4–27) is correct to all orders of the expansion in Equation (4–10), indicating that its contribution is more than just empirical. This implies, that even if the solute forms ideal solutions with both solvent species ($f_{12} = f_{13} = 0$) the solvent-solvent term alone can induce a contribution to the excess solubility. Curiously, if the solvent mixture excess free energy can be described with the Porter equation

$$g^{\mathrm{E}}(\text{solvents}) = Ax_2x_3 \quad \Rightarrow \quad \ln \gamma^+_3 = \frac{A}{\mathsf{R}T}x_2^2, \tag{4–31}$$

then the derivative above can be written as

$$-\frac{x_3}{2}\left(\frac{\partial \ln \gamma_3}{\partial x_3}\right)^+_{T,P,n_2} = -\frac{x_3}{2}\left(-2\frac{A}{\mathsf{R}T}x_2\right) = \frac{A}{\mathsf{R}T}x_2x_3 = \frac{g^{\mathrm{E}}}{\mathsf{R}T}(\text{solvents}) \tag{4–32}$$

This result is identical to that derived in Equation (3–34), when assuming the term Δ^∞ is zero. As pointed out when deriving Equation (3–34), the contribution from the excess free energy of the solvent mixture is usually too small in magnitude (or of opposite sign) compared to observed excess solubilities. Therefore, the form of Equation (4–27) seems qualitatively correct, since additional terms to the excess solubility, which also contains information about solute-solvent interactions, can contribute.

While Equation (4–27) offers an expression for the excess solubility, it is not very practical. The $f^+_{1j}, (j = 2, 3)$ change with solvent composition, and are therefore dependent on the nature of the other

solvent. This is not the case with f_{1j}^0. Its value is constant for each $(1,j)$ pair at constant temperature. The total correlation function between i and j, and thus its integral, is a measure of their total correlations, including indirect effects. However, the fact that the elements in **f** are differences, suggests that it might be reasonable to assume that the mixture terms are equal to the pure solvent terms, i.e.,

$$f_{1j}^{+} \triangleq f_{1j}^{0}, \qquad \forall j \neq 1. \tag{4–33}$$

Molecular correlation functions are strong functions of density,[7,8] so this approximation should be reasonable, except when solution density varies strongly with solvent composition. This is rarely the case with organic solvent mixtures, though the density variation of aqueous mixtures with organics might be large. The result of Equation (4–33) in Equation (4–27) is that the expression for the excess solubility simplifies to

$$\ln x_{i,m} - \sum_{j\neq i}^{M} x_j' \ln x_{i,j} = -\frac{x_3}{2}\left(\frac{\partial \ln \gamma_3}{\partial x_3}\right)_{T,P,n_2}^{+} \left[1 + x_2 f_{12}^0 + x_3 f_{13}^0\right]. \tag{4–34}$$

Equation (6–6) offers a direct, and practical way, of assessing the excess solubility in a binary solvent mixture. The solvent-solvent term can be obtained independently of the solute, usually from low-pressure binary vapor-liquid equilibrium data forming the basis of a g^{E}-model (this is discussed later). The solute-solvent parameters are independent of the nature of the other solvent, and suggests that these may be obtained independently. Details regarding estimation of both solvent-solvent derivative and solute-solvent parameters are discussed later in this chapter. First, we apply the same procedure for mixtures comprised of three solvents.

4.3.2. System with three solvents

From Appendix 4.A the derivative of species 1 in a quaternary mixture can be approximated by

$$\left(\frac{\partial \ln \gamma_1}{\partial x_1}\right)_{T,P,n_2,n_3,n_4} = \frac{\dfrac{x_2x_3}{1-x_1}f_{23} + \dfrac{x_2x_4}{1-x_1}f_{24} + \dfrac{x_3x_4}{1-x_1}f_{34} - x_2f_{12} - x_3f_{13} - x_4f_{14}}{1 + \displaystyle\sum_{i>j} x_ix_jf_{ij} + \sum_{i>j>k} x_ix_jx_kW_{ijk} + x_1x_2x_3x_4Z_{1234}} - \frac{x_2x_3W_{123} + x_2x_4W_{124} + x_3x_4W_{134} + x_2x_3x_4Z_{1234}}{1 + \displaystyle\sum_{i>j} x_ix_jf_{ij} + \sum_{i>j>k} x_ix_jx_kW_{ijk} + x_1x_2x_3x_4Z_{1234}} \tag{4–35}$$

Note that this expression is an approximation, since the full, rigorous expression is expected to be complicated beyond practical applications. Similar to W_{123} above, W_{ijk} contains multiple products of pair

TCFIs, as do Z_{1234}. In the case of two ($x_4 = 0$) or one solvent ($x_4 = x_3 = 0$) this equation reduces to the previous expressions. At infinite dilution, we obtain

$$\left(\frac{\partial \ln \gamma_1}{\partial x_1}\right)^+_{T,P,n_2,n_3} = \frac{F^+_{123}}{1+F^+_{234}} - \frac{x_2 f^+_{12} + x_3 f^+_{13} + x_4 f^+_{13} + x_2 x_3 W^+_{123} + x_2 x_4 W^+_{124} + x_3 x_4 W^+_{134} + x_2 x_3 x_4 Z_{1234}}{1+F^+_{234}}, \quad \text{(4–36)}$$

$$\text{with} \quad F^+_{234} = 1 + x_2 x_3 f^+_{23} + x_2 x_4 f^+_{24} + x_3 x_4 f^+_{34}.$$

In the continuing derivation, the presence of the W terms and Z will be ignored. The reason is similar to than when disregarding the W_{123} term in the binary solvent case above. The values of the W terms and Z can only come from multicomponent data. Thus, when forming $\ln \gamma_1^*$ and subtracting the mole fraction-averaged pure solvent terms, we get for the excess solubility in a ternary solvent mixture

$$\ln x_{i,m} - \sum_{j\neq i}^{M} x'_j \ln x_{i,j} = \frac{F^+_{234}}{1+F^+_{234}} - \frac{x_2}{2}\left[\frac{f^+_{12}}{1+F^+_{234}} - f^0_{12}\right] - \frac{x_3}{2}\left[\frac{f^+_{13}}{1+F^+_{234}} - f^0_{13}\right] - \frac{x_4}{2}\left[\frac{f^+_{14}}{1+F^+_{234}} - f^0_{14}\right] \quad \text{(4–37)}$$

Utilizing the approximation in Equation (4–33), the expression simplifies to

$$\ln x_{i,m} - \sum_{j\neq i}^{M} x'_j \ln x_{i,j} = \frac{x_2 x_3 f^+_{23} + x_2 x_4 f^+_{24} + x_3 x_4 f^+_{34}}{1 + x_2 x_3 f^+_{23} + x_2 x_4 f^+_{24} + x_3 x_4 f^+_{34}} \left[1 + x_2 f^0_{12} + x_3 f^0_{13} + x_4 f^0_{14}\right] \quad \text{(4–38)}$$

Equations (6–6) and (4–38) describe excess solubilities by separating contributions from solvent-solvent nonideality and those from solute-solvent pairs. In the case of a binary solvent mixture, the resulting equation contains only pair-interaction terms and no triplet-interactions. When extending to three solvents, the solvent-solvent terms, i.e., f^+_{ij}), are functions of composition in the three-component solvent mixture. This means that the relation in Equation (4–23) is not directly applicable. In the following section we will explore different ways of estimating the various terms in the expressions for the excess solubilities in two- and three-solvent mixtures.

4.4. Estimation of terms in excess solubility expressions

There are two types of terms in the final expressions for the excess solubility:

1. Solvent-solvent interactions, and
2. solute-solvent interactions.

Here, we will explore ways of estimating their values from different sources.

4.4.1. Solvent-solvent terms

The solvent-solvent terms in the models, i.e., the derivative term on the right-hand side of Equation (6–6) and the f_{ij}^{+} in (4–38) can be obtained independently of the solute, since they appear at infinite dilution of 1. The first item, $(\partial \ln \gamma_3/\partial x_3)^{+}$, is found directly from an excess free energy model (suitably differentiated), which describes the binary solvent mixture

$$\left(\frac{\partial \ln \gamma_3}{\partial x_3}\right)^{+}_{T,P,n_2} = f(T, P, x_3'). \tag{4–39}$$

There are several options, depending on the availability of data. If vapor-liquid equilibrium data is available, the parameters for an excess Gibbs energy model can be regressed. If no data is available, the predictive methods, such as UNIFAC or COSMO, may be utilized. The details of this treatment are given in Chapter 5. We continue with the three-solvent model.

In that model expression, the fraction

$$\frac{x_2x_3f_{23}^{+} + x_2x_4f_{24}^{+} + x_3x_4f_{34}^{+}}{1 + x_2x_3f_{23}^{+} + x_2x_4f_{24}^{+} + x_3x_4f_{34}^{+}}. \tag{4–40}$$

appears. The f_{ij}^{+} contain correlation function integral pairs in the ternary mixture of 2,3, and 4. Thus, the pair values are affected by the presence of the third solvent species, but not the solute (since this is infinitely diluted). Unfortunately, calculation of f_{ij}^{+} is not straightforward, since the relation in Equation (4–23) used for binary mixtures does not hold for ternary mixtures. One way to circumvent this is to write the derivative in Equation (4–19) for the three different solvent species and then use the Gibbs-Duhem equation at constant T and P to solve for the elements in $\mathbf{f}$ at a specified composition. This means setting up the relations,

$$\left(\frac{\partial \ln \gamma_2}{\partial x_2}\right)^{+}_{T,P,n_3,n_4} = f_1(T, P, \mathbf{x}^{+}, \mathbf{H}^{+}). \tag{4–41a}$$

$$\left(\frac{\partial \ln \gamma_3}{\partial x_3}\right)^{+}_{T,P,n_2,n_4} = f_2(T, P, \mathbf{x}^{+}, \mathbf{H}^{+}). \tag{4–41b}$$

$$\left(\frac{\partial \ln \gamma_4}{\partial x_4}\right)^{+}_{T,P,n_2,n_3} = f_3(T, P, \mathbf{x}^{+}, \mathbf{H}^{+}). \tag{4–41c}$$

The 4×4 matrix $\mathbf{H}^{+}$ contains 10 unique values (since $H_{ij} = H_{ji}$), which all go into the f_{ij}^{+} and the W term. This means, that it is not possible to estimate the values in $\mathbf{H}^{+}$. It is unlikely, that a method be devised, which allows calculating f_{ij}^{+} rigorously. Therefore, we adopt another path. That is to treat the values of f_{ij}^{+} as if they were independent of species other than i and j, i.e., as binary functions. The argument for doing this is as follows: Since all terms in the numerator and denominator of the fraction

in Equation (4–40) consists of products of pairs of two mole fractions, it seems reasonably to assume that the contribution from the (i,j) pair dominates the value of f_{ij}^{+}. We can calculate the values of f_{ij}^{+} from rearranging Equation (4–23)

$$f_{ij}^{+} \approx -\frac{\dfrac{1}{x_i'}\left(\dfrac{\partial \ln \gamma_j}{\partial x_j}\right)^{+}_{T,P,n_{k\neq j}}}{1 + x_j'\left(\dfrac{\partial \ln \gamma_j}{\partial x_j}\right)^{+}_{T,P,n_{k\neq j}}}, \qquad x_i' = \frac{x_i}{x_i + x_j} = 1 - x_j', \qquad \{i,j\} \in [2,3,4]. \tag{4–42}$$

Its value is calculated on a "binary" basis, indicated by primes on the mole fractions. This is to ensure thermodynamic consistency in the expression, i.e., that the limiting value of the fraction is given by the derivative in the numerator when $x_j' \to 0$. In the following, three ways of estimating the solute-solvent terms will be discussed.

4.4.2. Solute-solvent parameters from mixed solvent data – regression

Having addressed the solvent-solvent terms in the excess solubility expressions, we now turn to the solute-solvent terms, f_{1j}^{0}. These are regarded as parameters of the model, and here we explain how to estimate their values from data. This is done by minimizing a sum of squares. The least-squares estimate of the excess solubility parameters is

$$F = \min_{\mathbf{z}} \sum_{k=1}^{m} (\delta s_1^{\mathrm{E}})_k^2 = \min_{\mathbf{z}} \sum_{k=1}^{m} (\hat{s}_1^{\mathrm{E}} - s_1^{\mathrm{E}})_k^2. \tag{4–43}$$

where $\mathbf{z}$ contains values of f_{1j}^{0} relevant to the problem considered, and s_1^{E} denotes an experimental value, whereas $\hat{s}_1^{\mathrm{E}}$ is the excess solubility calculated from the model. Appendix A details the procedure of minimizing F to obtain the least-squares estimate of $\mathbf{z}$. Variances of parameter estimates are found from the underlying variance-covariance matrix, obtained as a byproduct of the optimization. These can then, in turn, be used in an propagation-of-errors expression to estimate the standard deviation of the model estimate induced by the uncertainty in the parameters[9] (see also Appendix A). Graphically, this can be displayed as error bars on a model estimate, as will be shown in Chapter 6.

4.4.3. Solute-solvent parameters from pure solvent data – prediction

While the regression above may provide accurate values of $\mathbf{f}^0$, it is more advantageous to obtain them directly from binary data when possible, in order to avoid relying fundamentally on mixture data. Consider Equation (4–23) for the case of 1 in 2

$$f_{12}^{0} = -\lim_{x_i \to 0} \left(\frac{\partial \ln \gamma_1}{\partial x_1}\right)_{T,P,n_2}. \tag{4–44}$$

Thus, obtaining values of the solute-solvent parameters requires derivatives of activity coefficients in pure solvents. A single solubility point allows for a single parameter of a g^{E}-model to be determined. The simplest model of this form is the Porter equation. We write this for a $(1,2)$-binary as

$$\ln\gamma_1 = B_{12}(1-x_1)^2 \quad \Rightarrow \quad -\lim_{x_i\to 0}\left(\frac{\partial\ln\gamma_1}{\partial x_1}\right)_{T,P,n_2} = 2B_{12} = f_{12}^0. \tag{4–45}$$

A value for B_{12} can be obtained from the solubility of 1 in 2, $x_{1,2}$, and a form of Equation (3–13), giving

$$\ln x_{1,2} + B_{12}(1-x_{1,2})^2 = \ln x_1^{\mathrm{id}} \quad \Rightarrow \quad f_{12}^0 = 2\frac{\ln x_1^{\mathrm{id}}(T) - \ln x_{1,2}(T)}{(1-x_{1,2}(T))^2}. \tag{4–46}$$

Similarly for all other solute-solvent pairs. This connects the mixed solvent solubility models from Equations (6–6) and (4–38) to $\mathbf{f}^0$. Values of these parameters can be regressed from either ternary data with Equation (4–43) or estimated from binary data with Equation (4–46). Note that determining the Porter coefficient requires the thermophysical characteristics for Equation (3–13) in addition to the experimental solubility. Obviously, a more accurate g^{E}-model for Equation (4–44) would be expected to provide better results, especially if the symmetric composition dependence required of the Porter is incorrect. However, such models require more than a single parameter, adding to the requirements of model input.

4.4.4. Solute-solvent parameters from UNIFAC

Obtaining $\mathbf{f}^0$ from binary data, as described above, can be a good alternative to fitting values to mixture data. However, this requires the thermophysical properties characterizing the melting process for the solute, values which frequently are not available. Group contribution methods may be used to estimate $T_{m,i}$ and $\Delta h_{m,i}$ in such cases,[10,11] but the uncertainty associated with their estimates may be substantial. Thus, it would be advantageous if $\mathbf{f}^0$ could be found independently of these parameters. Furthermore, the approach in Equation (4–45) has the limitation that the derivative is formed based on data that really have no composition dependence included. This is not the case if for example a method such as UNIFAC is employed. If the molecular structure of the solute and solvent(s) can be constructed from UNIFAC groups, then UNIFAC can in principle be used to calculate the derivative required. The mole number derivative of the species activity coefficient, according to UNIFAC, is (see Chapter 5.A for details of this treatment)

$$\begin{aligned} n\left(\frac{\partial\ln\gamma_i}{\partial n_j}\right)_{T,P} = &-(1-J_i)(1-J_j) - 5(J_i-L_i)(J_j-L_j)\bar{q} \\ &+ L_iL_j\bar{q} + \sum_k^{NSG}\left[\vartheta_k\frac{s_{ki}s_{kj}}{\eta_k^2} - \frac{G_{kj}s_{ki}+G_{ki}s_{kj}}{\eta_k}\right], \end{aligned} \tag{4–47}$$

and so

$$f_{12}^0 = (1 - J_1^0)^2 - 5(J_1^0 - L_1^0)^2\bar{q} + (L_i^0)^2\bar{q} + \sum_k^{NSG}\left[\vartheta_k \frac{s_{k1}}{\eta_k} - 2G_{k1}\right]\frac{s_{k1}}{\eta_k}. \tag{4–48}$$

Provided the composition derivatives of activity coefficients from UNIFAC are reliable, this is a convenient way to determine parameters.

4.5. Summary

Two models expressing the excess solubility in terms of molecular correlation function integrals were developed from the principles of *fluctuation solution theory*. The models separated the excess solubility into contributions from nonideality in the solvent mixture, as well as terms coming from solute-solvent interactions. Several methods for obtaining the solute-solvent parameters were discussed, including estimation from data, as well as UNIFAC. The solvent-solvent contributions require a model expressing the excess Gibbs energy of the solvent mixture. This is the subject in the following chapter, so the route into solubility estimates is departed for a while.

4.A. Activity coefficients from total correlation function integrals

This appendix give relations between derivatives of species activity coefficients and integrals of molecular pair correlation functions. The theoretical background is presented in Chapter 2, where the required properties, i.e., partial derivatives of chemical potentials with respect to number of moles, are given in compact matrix notation. Here, the equations are written out explicitly for systems of two, three, and four components.

We seek the derivative of the species activity coefficient with respect to mole fraction at constant temperature and pressure and mole number of other species

$$\left(\frac{\partial \ln \gamma_i}{\partial x_j}\right)_{T,P,n_{k\neq j}}, \tag{4–49}$$

which is related to the chemical potential derivative through

$$\left(\frac{\partial \ln \gamma_i}{\partial x_j}\right)_{T,P,n_{k\neq j}} = \frac{n}{1 - x_j}\left(\frac{\partial \beta\mu_i}{\partial n_j}\right)_{T,P,n_{k\neq j}} - \frac{1}{x_i}\frac{\delta_{ij} - x_i}{1 - x_j}. \tag{4–50}$$

Particularly, we seek the derivative of species 1 in a mixture taken with respect to itself, meaning the

$(1,1)$-term from this equation. This simplifies the relation

$$\left(\frac{\partial \ln \gamma_1}{\partial x_1}\right)_{T,P,n_{k\neq 1}} = \frac{n}{1-x_1}\left(\frac{\partial \beta\mu_1}{\partial n_1}\right)_{T,P,n_{k\neq 1}} - \frac{1}{x_1}. \tag{4–51}$$

Using the notation of Chapter 2, the derivative is given by

$$\mathbf{XD} = \left[\mathbf{I} - \frac{\mathbf{X}\left(\mathbf{B}^{-1}\right)^{\mathsf{T}}\mathbf{i}\mathbf{i}^{\mathsf{T}}}{\mathbf{i}^{\mathsf{T}}\mathbf{B}^{-1}\mathbf{X}\mathbf{i}}\right]\mathbf{B}^{-1}, \tag{4–52}$$

where the elements of the matrix product of the left-hand side is

$$[\mathbf{XD}]_{ij} = n_i\left(\frac{\partial \beta\mu_i}{\partial n_j}\right)_{T,P,n_{k\neq j}}. \tag{4–53}$$

$\mathbf{X}$ is a diagonal matrix with elements $X_{ii} = x_i$, the mole fraction of component i in the mixture. $\mathbf{I}$ is the unit matrix, and $\mathbf{i}$ is the unit vector. $\mathbf{B}$ is a matrix with elements

$$B_{ij} = \delta_{ij} + x_i H_{ij}, \tag{4–54}$$

with δ_{ij} being the (i,j) element of $\mathbf{I}$. H_{ij} is the integral of the total correlation function, defined in Chapter 2.

4.A.1. Binary mixture

For a binary mixture, we first note that the inverse of $\mathbf{B}$ is given by

$$\mathbf{B}^{-1} = \frac{1}{\det \mathbf{B}}\begin{bmatrix} B_{22} & -B_{12} \\ -B_{21} & B_{11} \end{bmatrix} = \frac{1}{\det \mathbf{B}}\begin{bmatrix} 1+x_2H_{22} & -x_1H_{12} \\ -x_2H_{21} & 1+x_1H_{11} \end{bmatrix}, \tag{4–55}$$

where the determinant is

$$\det \mathbf{B} = 1 + x_1H_{11} + x_2H_{22} + x_1x_2(H_{11}H_{22} - H_{12}H_{21}). \tag{4–56}$$

The matrix equation above then becomes

$$\begin{bmatrix} n_1\left(\frac{\partial\beta\mu_1}{\partial n_1}\right)_{T,P,n_2} & n_1\left(\frac{\partial\beta\mu_1}{\partial n_2}\right)_{T,P,n_1} \\ n_2\left(\frac{\partial\beta\mu_2}{\partial n_1}\right)_{T,P,n_2} & n_2\left(\frac{\partial\beta\mu_2}{\partial n_2}\right)_{T,P,n_1} \end{bmatrix} = \\ \left(\begin{bmatrix} 1 & 0 \\ 0 & 1 \end{bmatrix} - \frac{\begin{bmatrix} x_1 & 0 \\ 0 & x_2 \end{bmatrix} \begin{bmatrix} B_{22} & -B_{21} \\ -B_{12} & B_{11} \end{bmatrix} \begin{bmatrix} 1 \\ 1 \end{bmatrix} \begin{bmatrix} 1 & 1 \end{bmatrix}}{\begin{bmatrix} 1 & 1 \end{bmatrix} \begin{bmatrix} B_{22} & -B_{12} \\ -B_{21} & B_{11} \end{bmatrix} \begin{bmatrix} x_1 & 0 \\ 0 & x_2 \end{bmatrix} \begin{bmatrix} 1 \\ 1 \end{bmatrix}} \right) \frac{1}{\det \mathbf{B}} \begin{bmatrix} B_{22} & -B_{12} \\ -B_{21} & B_{11} \end{bmatrix}. \tag{4–57}$$

The denominator term in the parenthesis becomes

$$\begin{bmatrix} 1 & 1 \end{bmatrix} \begin{bmatrix} B_{22} & -B_{12} \\ -B_{21} & B_{11} \end{bmatrix} \begin{bmatrix} x_1 & 0 \\ 0 & x_2 \end{bmatrix} \begin{bmatrix} 1 \\ 1 \end{bmatrix} = \sum_{i,j} \left[\text{Adj}\,(\mathbf{B})\,\mathbf{X}\right]_{ij} \\ = x_1B_{22} + x_2B_{11} - x_1B_{21} - x_2B_{12} = x_1 + x_2 + x_1x_2(H_{11} + H_{22} - H_{12} - H_{21}) \\ = 1 + x_1x_2f_{12}. \tag{4–58}$$

Here, we have defined $f_{ij} \equiv H_{ii} + H_{jj} - 2H_{ij}$, and used that $\mathbf{H}$ is symmetric (though $\mathbf{B}$ is not). The resulting matrix in Equation (4–57) is somewhat complicated, but we focus on the $(1,1)$-term and find

$$n_1\left(\frac{\partial\beta\mu_1}{\partial n_1}\right)_{T,P,n_2} = \frac{1}{\det \mathbf{B}}\left(B_{22} - \frac{x_1(B_{22} - B_{21})^2}{1 + x_1x_2f_{12}}\right) \\ = \frac{1}{\det \mathbf{B}}\left(1 + x_2H_{22} - x_1\frac{1 + x_2^2(H_{22} - H_{21}) + 2x_2(H_{22} - H_{21})}{1 + x_1x_2f_{12}}\right) \\ = \frac{(1 + x_2H_{22})(1 + x_1x_2f_{12}) - x_1 1 + x_2^2(H_{22} - H_{21}) + 2x_2(H_{22} - H_{21})}{\det \mathbf{B}(1 + x_1x_2f_{12})}. \tag{4–59}$$

If we now expand all parentheses and remember the definition of f_{12}, we see that by collecting within orders of mole fraction

$$n_1\left(\frac{\partial\beta\mu_1}{\partial n_1}\right)_{T,P,n_2} \\ = \frac{x_2(1 + H_{22}) + x_1x_2\begin{pmatrix} H_{11} + H_{22} - 2H_{12} \\ -2H_{22} + 2H_{12} \end{pmatrix} + x_1x_2^2\begin{pmatrix} H_{22}(H_{11} + H_{22} - 2H_{12}) - \\ H_{22}^2 - H_{12}^2 + 2H_{21}H_{22} \end{pmatrix}}{\det \mathbf{B}(1 + x_1x_2f_{12})} \tag{4–60}$$

Putting x_2 outside the fraction and removing the parenthesis yields after some rearranging

$$n_1\left(\frac{\partial\beta\mu_1}{\partial n_1}\right)_{T,P,n_2} = x_2\frac{1 + x_1H_{11} + (1 - x_1)H_{22} + x_1x_2(H_{11}H_{22} - H_{12}H_{21})}{\det \mathbf{B}(1 + x_1x_2f_{12})}, \tag{4–61}$$

where we immediately recognize the entire numerator as the determinant in Equation (4–56), which cancels with that in the denominator. Thus leaving

$$n_1 \left(\frac{\partial \beta \mu_1}{\partial n_1} \right)_{T,P,n_2} = \frac{x_2}{1 + x_1 x_2 f_{12}}. \tag{4–62}$$

Now, the derivative in Equation (4–51) becomes

$$\begin{aligned} \left(\frac{\partial \ln \gamma_1}{\partial x_1} \right)_{T,P,n_2} &= \frac{n}{1 - x_1} \left(\frac{\partial \beta \mu_1}{\partial n_1} \right)_{T,P,n_2} - \frac{1}{x_1} = \frac{1}{x_1} \left(\frac{n_1}{1 - x_1} \left(\frac{\partial \beta \mu_1}{\partial n_1} \right)_{T,P,n_2} - 1 \right) \\ &= \frac{1}{x_1} \left(\frac{x_2}{1 - x_1} \frac{1}{1 + x_1 x_2 f_{12}} - 1 \right) = \frac{1}{x_1} \left(\frac{-x_1 x_2 f_{12}}{1 + x_1 x_2 f_{12}} \right) \\ &= -\frac{x_2 f_{12}}{1 + x_1 x_2 f_{12}} \end{aligned} \tag{4–63}$$

This is the expression given by Kirkwood and Buff[12] and O'Connell[5] for a binary mixture. Similar results are found for the remaining terms in Equation (4–57)

$$\left(\frac{\partial \ln \gamma_1}{\partial x_2} \right)_{T,P,n_1} = \frac{x_2 f_{12}}{1 + x_1 x_2 f_{12}}, \tag{4–64a}$$

$$\left(\frac{\partial \ln \gamma_2}{\partial x_1} \right)_{T,P,n_1} = \frac{x_1 f_{12}}{1 + x_1 x_2 f_{12}}, \tag{4–64b}$$

$$\left(\frac{\partial \ln \gamma_2}{\partial x_2} \right)_{T,P,n_1} = \frac{x_1 f_{12}}{1 + x_1 x_2 f_{12}}, \tag{4–64c}$$

which all satisfy the Gibbs-Duhem equation. Next, we consider a ternary mixture.

4.A.2. Ternary mixture

The inverse of $\mathbf{B}$ in a ternary mixture is

$$\mathbf{B}^{-1} = \frac{1}{\det \mathbf{B}} \begin{bmatrix} B_{22}B_{33} - B_{32}B_{23} & -B_{12}B_{33} + B_{13}B_{32} & B_{21}B_{32} - B_{13}B_{22} \\ -B_{21}B_{33} + B_{31}B_{23} & B_{11}B_{33} + B_{13}B_{31} & -B_{23}B_{11} + B_{21}B_{13} \\ B_{21}B_{23} - B_{31}B_{22} & -B_{32}B_{11} + B_{31}B_{12} & B_{22}B_{11} - B_{21}B_{12} \end{bmatrix}, \tag{4–65}$$

where the determinant becomes

$$\begin{aligned} \det \mathbf{B} = x_1 x_2 x_3 \Big(& 1 + x_1 H_{11} + x_2 H_{22} + x_3 H_{33} + x_1 x_2 f_{12} + x_1 x_3 f_{13} + x_2 x_3 f_{23} \\ & + x_1 x_2 x_3 (H_{11} H_{22} H_{33} + 2 H_{12} H_{13} H_{23} - H_{11} H_{23}^2 - H_{13}^2 H_{22} - H_{12}^2 H_{33}) \Big) \end{aligned} \tag{4–66}$$

The matrix equation is now

$$
\begin{bmatrix}
n_1\left(\frac{\partial\beta\mu_1}{\partial n_1}\right)_{T,P,n_2,n_3} & n_1\left(\frac{\partial\beta\mu_1}{\partial n_2}\right)_{T,P,n_1,n_3} & n_1\left(\frac{\partial\beta\mu_1}{\partial n_3}\right)_{T,P,n_1,n_2} \\
n_2\left(\frac{\partial\beta\mu_2}{\partial n_1}\right)_{T,P,n_2,n_3} & n_2\left(\frac{\partial\beta\mu_2}{\partial n_2}\right)_{T,P,n_1,n_3} & n_2\left(\frac{\partial\beta\mu_2}{\partial n_3}\right)_{T,P,n_1,n_2} \\
n_3\left(\frac{\partial\beta\mu_3}{\partial n_1}\right)_{T,P,n_2,n_3} & n_3\left(\frac{\partial\beta\mu_3}{\partial n_2}\right)_{T,P,n_1,n_3} & n_3\left(\frac{\partial\beta\mu_3}{\partial n_3}\right)_{T,P,n_1,n_2}
\end{bmatrix}
= \frac{1}{\det \mathbf{B}}
\begin{bmatrix}
B_{22}B_{33} - B_{32}B_{23} & -B_{12}B_{33} + B_{13}B_{32} & B_{21}B_{32} - B_{13}B_{22} \\
-B_{21}B_{33} + B_{31}B_{23} & B_{11}B_{33} + B_{13}B_{31} & -B_{23}B_{11} + B_{21}B_{13} \\
B_{21}B_{23} - B_{31}B_{22} & -B_{32}B_{11} + B_{31}B_{12} & B_{22}B_{11} - B_{21}B_{12}
\end{bmatrix}
-
$$

$$
\frac{\begin{bmatrix} x_1 & 0 & 0 \\ 0 & x_2 & 0 \\ 0 & 0 & x_3 \end{bmatrix}
\begin{bmatrix}
B_{22}B_{33} - B_{32}B_{23} & -B_{21}B_{33} + B_{31}B_{23} & B_{21}B_{23} - B_{31}B_{22} \\
-B_{12}B_{33} + B_{13}B_{32} & B_{11}B_{33} + B_{13}B_{31} & -B_{32}B_{11} + B_{31}B_{12} \\
B_{21}B_{32} - B_{13}B_{22} & -B_{23}B_{11} + B_{21}B_{13} & B_{22}B_{11} - B_{21}B_{12}
\end{bmatrix}
\begin{bmatrix} 1 \\ 1 \\ 1 \end{bmatrix}
\begin{bmatrix} 1 & 1 & 1 \end{bmatrix}
\begin{bmatrix}
B_{22}B_{33} - B_{32}B_{23} & -B_{12}B_{33} + B_{13}B_{32} & B_{21}B_{32} - B_{13}B_{22} \\
-B_{21}B_{33} + B_{31}B_{23} & B_{11}B_{33} + B_{13}B_{31} & -B_{23}B_{11} + B_{21}B_{13} \\
B_{21}B_{23} - B_{31}B_{22} & -B_{32}B_{11} + B_{31}B_{12} & B_{22}B_{11} - B_{21}B_{12}
\end{bmatrix}
\begin{bmatrix} x_1 & 0 & 0 \\ 0 & x_2 & 0 \\ 0 & 0 & x_3 \end{bmatrix}
\begin{bmatrix} 1 \\ 1 \\ 1 \end{bmatrix}}{\det \mathbf{B} \begin{bmatrix} 1 & 1 & 1 \end{bmatrix}
\begin{bmatrix}
B_{22}B_{33} - B_{32}B_{23} & -B_{12}B_{33} + B_{13}B_{32} & B_{21}B_{32} - B_{13}B_{22} \\
-B_{21}B_{33} + B_{31}B_{23} & B_{11}B_{33} + B_{13}B_{31} & -B_{23}B_{11} + B_{21}B_{13} \\
B_{21}B_{23} - B_{31}B_{22} & -B_{32}B_{11} + B_{31}B_{12} & B_{22}B_{11} - B_{21}B_{12}
\end{bmatrix}
\begin{bmatrix} x_1 & 0 & 0 \\ 0 & x_2 & 0 \\ 0 & 0 & x_3 \end{bmatrix}
\begin{bmatrix} 1 \\ 1 \\ 1 \end{bmatrix}}. \tag{4–67}
$$

4. Fluctuation solution theory method for solid solubility in mixed solvents

As before, we first calculate the denominator term and find

$$\begin{aligned}\sum_{i,j}\left[\text{Adj}\left(\mathbf{B}\right)\mathbf{X}\right]_{ij} &= x_1\big(B_{22}B_{33} - B_{32}B_{23} - B_{12}B_{33} + B_{13}B_{32} + \\ B_{21}B_{32} - B_{13}B_{22}\big) &+ x_2\left(-B_{21}B_{33} + B_{31}B_{23} + B_{11}B_{33} + B_{13}B_{31} - B_{23}B_{11} + B_{21}B_{13}\right) \\ &+ x_3\left(B_{21}B_{23} - B_{31}B_{22} - B_{32}B_{11} + B_{31}B_{12} + B_{22}B_{11} - B_{21}B_{12}\right).\end{aligned} \tag{4–68}$$

Inserting the expression for B_{ij} gives the final result after rearranging and listing within orders of mole fractions, we get an expression that resembles that from before

$$\begin{aligned}\sum_{i,j}\left[\text{Adj}\left(\mathbf{B}\right)\mathbf{X}\right]_{ij} &= x_2x_3\Big\{1 + x_1x_2f_{12} + x_1x_3f_{13} + x_2x_3f_{23} \\ &+ x_1x_2x_3\big(H_{11}H_{22} + H_{11}H_{33} + H_{22}H_{33} - 2H_{12}H_{33} - 2H_{13}H_{22} - 2H_{11}H_{23} \\ &+ 2H_{12}H_{23} + 2H_{13}H_{23} + 2H_{12}H_{13} - H_{12}^2 - H_{13}^2 - H_{23}^2\big)\Big\}.\end{aligned} \tag{4–69}$$

Again, remembering the quantity of interest, we focus on the $(1,1)$-term, which gives

$$\begin{aligned}n_1\left(\frac{\partial\beta\mu_1}{\partial n_1}\right)_{T,P,n_2,n_3} &= \frac{1}{\det\mathbf{B}}\Big\{B_{22}B_{33} - B_{32}B_{23} \\ &- x_1\frac{\left(B_{22}B_{33} - B_{23}B_{32} - B_{21}B_{33} + B_{23}B_{31} + B_{21}B_{32} - B_{22}B_{31}\right)^2}{x_2x_3(1 + x_1x_2f_{12} + x_1x_3f_{13} + x_2x_3f_{23} + x_1x_2x_3W_{123})}\Big\}\end{aligned} \tag{4–70}$$

Here, W_{123} is the sum of products of pairs

$$\begin{aligned}W_{123} =& H_{11}H_{22} + H_{11}H_{33} + H_{22}H_{33} - 2H_{12}H_{33} - 2H_{13}H_{22} - 2H_{11}H_{23} \\ &+ 2H_{12}H_{23} + 2H_{13}H_{23} + 2H_{12}H_{13} - H_{12}^2 - H_{13}^2 - H_{23}^2.\end{aligned} \tag{4–71}$$

Putting terms on a common denominator, factorizing the B_{ij}s and substituting with the H_{ij}s gives

$$\begin{aligned}n_1\left(\frac{\partial\beta\mu_1}{\partial n_1}\right)_{T,P,n_2,n_3} &= \frac{1}{\det\mathbf{B}x_2x_3(1 + x_1x_2f_{12} + x_1x_3f_{13} + x_2x_3f_{23} + x_1x_2x_3W_{123})}\Big\{ \\ &(1 + x_2H_{22} + x_3H_{33} + x_2x_3(H_{22}H_{33} - H_{23}^2))x_2x_3(1 + x_1x_2f_{12} + x_1x_3f_{13} \\ &+ x_2x_3f_{23} + x_1x_2x_3W_{123}) - x_1\left(x_3(H_{33} - H_{31}) + x_2x_3(H_{22} - H_{21})(H_{33} - H_{32})\right)^2\Big\},\end{aligned} \tag{4–72}$$

which can be reduced to the following

$$n_1\left(\frac{\partial\beta\mu_1}{\partial n_1}\right)_{T,P,n_2,n_3} = \frac{1}{\det\mathbf{B}x_2x_3(1+x_1x_2f_{12}+x_1x_3f_{13}+x_2x_3f_{23}+x_1x_2x_3W_{123})}\Bigg\{ (x_2x_3(x_2+x_3)+x_2^2x_3^2f_{23})\Bigg(1+x_1H_{11}+x_2H_{22}+x_3H_{33}+x_1x_2f_{12}+x_1x_3f_{13} + x_2x_3f_{23}+x_1x_2x_3(H_{11}H_{22}H_{33}+2H_{12}H_{13}H_{23}-H_{11}H_{23}^2-H_{13}^2H_{22}-H_{12}^2H_{33})\Bigg)\Bigg\}. \tag{4–73}$$

We immediately recognize the second parenthesized term of this equation as the determinant of Equation (4–66), which means that the equation reduces to

$$n_1\left(\frac{\partial\beta\mu_1}{\partial n_1}\right)_{T,P,n_2,n_3} = \frac{x_2+x_3+x_2x_3f_{23}}{1+x_1x_2f_{12}+x_1x_3f_{13}+x_2x_3f_{23}+x_1x_2x_3W_{123}}. \tag{4–74}$$

Thus, when forming the derivative in Equation (4–51) we get

$$\begin{aligned}&\left(\frac{\partial\ln\gamma_1}{\partial x_1}\right)_{T,P,n_2,n_3} = \\ &= \frac{1}{x_1}\frac{\frac{x_2+x_3}{1-x_1}+\frac{x_2x_3}{1-x_1}f_{23}-1-x_1(x_2f_{12}+x_3f_{13})-x_2x_3f_{23}-x_1x_2x_3W_{123}}{1+x_1x_2f_{12}+x_1x_3f_{13}+x_2x_3f_{23}+x_1x_2x_3W_{123}}\end{aligned} \tag{4–75}$$

By remembering that $x_2+x_3=1-x_1$ we get

$$\begin{aligned}\left(\frac{\partial\ln\gamma_1}{\partial x_1}\right)_{T,P,n_2,n_3} &= \frac{1}{x_1}\frac{\left(\frac{x_2x_3}{x_2+x_3}-x_2x_3\right)f_{23}-x_1(x_2f_{12}+x_3f_{13})-x_1x_2x_3W_{123}}{1+x_1x_2f_{12}+x_1x_3f_{13}+x_2x_3f_{23}+x_1x_2x_3W_{123}} \\ &= \frac{1}{x_1}\frac{\frac{x_1x_2x_3}{x_2+x_3}f_{23}-x_1(x_2f_{12}+x_3f_{13})-x_1x_2x_3W_{123}}{1+x_1x_2f_{12}+x_1x_3f_{13}+x_2x_3f_{23}+x_1x_2x_3W_{123}} \\ &= \frac{\frac{x_2x_3}{x_2+x_3}f_{23}-x_2f_{12}-x_3f_{13}-x_2x_3W_{123}}{1+x_1x_2f_{12}+x_1x_3f_{13}+x_2x_3f_{23}+x_1x_2x_3W_{123}}.\end{aligned} \tag{4–76}$$

As with the binary case, the originally complicated expressions from the matrix inversion reduces significantly due to a large degree of cancelation. Furthermore, setting $x_3=0$ recovers the expression for a binary in Equation (4–63). However, unlike Equation (4–63) this expression contains more than just differences in correlation function integrals: The term W_{123} contains products of H_{ij}s and cannot be factorized into f_{ij}s. It is important to note that the f_{12} from Equation (4–63) is different from that in Equation (4–76). The reason for this is that the f_{12} from the ternary mixture contains a contribution from species 3 from indirect correlation, as discussed in the context of the direct correlation function in Chapter 2.

4.A.3. Quaternary mixture

The complexity increases significantly when extending to mixtures of four components. The adjoint matrix of **B** becomes the 4×4 matrix, the columns of which are:

$\text{Adj}\,(\mathbf{B})_{:,1}$

$$\begin{bmatrix} B_{22}B_{33}B_{44} - B_{22}B_{34}B_{43} - B_{32}B_{23}B_{44} + B_{32}B_{24}B_{43} + B_{42}B_{23}B_{34} - B_{42}B_{24}B_{33} \\ -B_{21}B_{33}B_{44} + B_{21}B_{34}B_{43} + B_{31}B_{23}B_{44} - B_{31}B_{24}B_{43} - B_{41}B_{23}B_{34} + B_{41}B_{24}B_{33} \\ B_{21}B_{32}B_{44} - B_{21}B_{34}B_{42} - B_{31}B_{22}B_{44} + B_{31}B_{24}B_{42} + B_{41}B_{22}B_{34} - B_{41}B_{24}B_{32} \\ -B_{21}B_{32}B_{43} + B_{21}B_{33}B_{42} + B_{31}B_{22}B_{43} - B_{31}B_{23}B_{42} - B_{41}B_{22}B_{33} + B_{41}B_{23}B_{32}. \end{bmatrix} \tag{4–77}$$

$\text{Adj}\,(\mathbf{B})_{:,2}$

$$\begin{bmatrix} -B_{12}B_{33}B_{44} + B_{12}B_{34}B_{43} + B_{32}B_{13}B_{44} - B_{32}B_{14}B_{43} - B_{42}B_{13}B_{34} + B_{42}B_{14}B_{33} \\ B_{11}B_{33}B_{44} - B_{11}B_{34}B_{43} - B_{31}B_{13}B_{44} + B_{31}B_{14}B_{43} + B_{41}B_{13}B_{34} - B_{41}B_{14}B_{33} \\ -B_{11}B_{32}B_{44} + B_{11}B_{34}B_{42} + B_{31}B_{12}B_{44} - B_{31}B_{14}B_{42} - B_{41}B_{12}B_{34} + B_{41}B_{14}B_{32} \\ B_{11}B_{32}B_{43} - B_{11}B_{33}B_{42} - B_{31}B_{12}B_{43} + B_{31}B_{13}B_{42} + B_{41}B_{12}B_{33} - B_{41}B_{13}B_{32}. \end{bmatrix} \tag{4–78}$$

$\text{Adj}\,(\mathbf{B})_{:,3}$

$$\begin{bmatrix} B_{12}B_{23}B_{44} - B_{12}B_{24}B_{43} - B_{22}B_{13}B_{44} + B_{22}B_{14}B_{43} + B_{42}B_{13}B_{24} - B_{42}B_{14}B_{23} \\ -B_{11}B_{23}B_{44} + B_{11}B_{24}B_{43} + B_{21}B_{13}B_{44} - B_{21}B_{14}B_{43} - B_{41}B_{13}B_{24} + B_{41}B_{14}B_{23} \\ B_{11}B_{22}B_{44} - B_{11}B_{24}B_{42} - B_{21}B_{12}B_{44} + B_{21}B_{14}B_{42} + B_{41}B_{12}B_{24} - B_{41}B_{14}B_{22} \\ -B_{11}B_{22}B_{43} + B_{11}B_{23}B_{42} + B_{21}B_{12}B_{43} - B_{21}B_{13}B_{42} - B_{41}B_{12}B_{23} + B_{41}B_{13}B_{22}. \end{bmatrix} \tag{4–79}$$

$\text{Adj}\,(\mathbf{B})_{:,4}$

$$\begin{bmatrix} -B_{12}B_{23}B_{34} + B_{12}B_{24}B_{33} + B_{22}B_{13}B_{34} - B_{22}B_{14}B_{33} - B_{32}B_{13}B_{24} + B_{32}B_{14}B_{23} \\ B_{11}B_{23}B_{34} - B_{11}B_{24}B_{33} - B_{21}B_{13}B_{34} + B_{21}B_{14}B_{33} + B_{31}B_{13}B_{24} - B_{31}B_{14}B_{23} \\ -B_{11}B_{22}B_{34} + B_{11}B_{24}B_{32} + B_{21}B_{12}B_{34} - B_{21}B_{14}B_{32} - B_{31}B_{12}B_{24} + B_{31}B_{14}B_{22} \\ B_{11}B_{22}B_{33} - B_{11}B_{23}B_{32} - B_{21}B_{12}B_{33} + B_{21}B_{13}B_{32} + B_{31}B_{12}B_{23} - B_{31}B_{13}B_{22}. \end{bmatrix} \tag{4–80}$$

Therefore, results obtained from procedures like before are expected to be of a complexity much larger than that encountered in the ternary case. Due to this, and the fact that any results obtained have to be useful in terms of modeling, this path does not appear feasible. Instead, a simpler, but more empirical, expression may be obtained by recognizing that:

1. The denominator is composed entirely of pairs of TCFI-collections (f_{ij}) plus additional terms

which take into account multicomponent interactions. These cover all levels of interactions, i.e., from binary to quaternary.

2. The numerator is composed of pairs of TCFI-collections with the single f_{1j} subtracted, in addition to the multicomponent terms.

This means that an expression of the form

$$\left(\frac{\partial \ln \gamma_1}{\partial x_1}\right)_{T,P,n_2,n_3,n_4} = \frac{\frac{x_2x_3}{1-x_1}f_{23} + \frac{x_2x_4}{1-x_1}f_{24} + \frac{x_3x_4}{1-x_1}f_{34} - x_2f_{12} - x_3f_{13} - x_4f_{14}}{1 + \sum_{i>j} x_ix_jf_{ij} + \sum_{i>j>k} x_ix_jx_kW_{ijk} + x_1x_2x_3x_4Z_{1234}} - \frac{x_2x_3W_{123} + x_2x_4W_{124} + x_3x_4W_{134} + x_2x_3x_4Z_{1234}}{1 + \sum_{i>j} x_ix_jf_{ij} + \sum_{i>j>k} x_ix_jx_kW_{ijk} + x_1x_2x_3x_4Z_{1234}} \quad (4\text{–}81)$$

should approximate the rigorous solution that would be obtained from Equation (4–52). The denominator term, when written out, becomes $\sum_{i>j} x_ix_jf_{ij} + \sum_{i>j>k} x_ix_jx_kW_{ijk} = x_1x_2f_{12} + x_1x_3f_{13} + x_1x_4f_{14} + x_2x_3f_{23} + x_2x_4f_{24} + x_3x_4f_{34} + x_1(x_2x_3W_{123} + x_2x_4W_{124} + x_3x_4W_{134})$. The W terms represent ternary interactions, while Z in Equation (4–81) represents four component interactions. Equation (4–81) reduces to the ternary based expression when setting $x_4 = 0$ and, of course, the binary when $x_3 = x_2 = 0$.

Equation (4–81) is a simple approximation to the solution, which *can* be obtained. However, from a practical point of view, and in light of the context in which the derivative terms are used, the approximation seems reasonable.

4.A.4. Higher order mixtures

The approach taken in order to arrive at Equation (4–81) can straightforwardly be extended to higher order mixtures.

References

1. I. Prigogine and R. Defay. *Chemical thermodynamics*. Longmans Green and co, 2nd edition, 1954.
2. M. Margules. *Sitz. Akad. Wiss. Wien Math. Nat. Kl. IIa*, 104:1243, 1895.
3. N. A. Gokcen. *J. Chim. Phys.*, 94:817–843, 1997.
4. K. Wohl. *Trans. AIChE*, 42:215, 1946.
5. J. P. O'Connell. *AIChE J.*, 17(3):658–663, 1971.
6. H. L. Frisch and J. L. Lebowitz, editors. *The equilibrium theory of classical fluids*. Benjamin, 1964.
7. C. G. Gray and K. E. Gubbins. *Theory of molecular fluids*, volume 1: Fundamentals. Oxford University Press, 1984.
8. D. A. McQuarrie. *Statistical mechanics*. University Science Books, 2000.
9. R. Fletcher. *Practical methods of optimization*. Wiley, 1987.

References

10. R. S. Boethling and D. Mackay, editors. *Handbook of property estimation methods for chemicals*. Lewis Publishers, 2000.

11. J. Marrero and R. Gani. *Fluid Phase Equil.*, 183-184:183–208, 2001.

12. J. G. Kirkwood and F. P. Buff. *J. Chem. Phys.*, 19 (8):774–777, 1951.

5. Vapor-liquid equilibria in solvent mixtures

This chapter is concerned with the representation of the solute-free (i.e., solvent) mixtures in which solids are dissolved. First the conditions necessary for equilibrium are stated, so that estimates of Equation (5–1) may be obtained. This is followed by a brief explanation of the procedure used to obtain the characteristics for the models. Much of this is standard procedure, but some fundamental concepts are repeated here for the sake of completeness, and will be referred to later in the thesis.

5.1. Introduction

Chapter 4 derived expressions for the excess solubility of a solid solute in a mixture of two and three solvents. Those models require the derivative

$$\left(\frac{\partial \ln \gamma_i}{\partial x_j}\right)_{T,P,n_{k\neq j}} = \frac{n}{1-x_j}\left(\frac{\partial \ln \gamma_i}{\partial n_j}\right)_{T,P,n_{k\neq j}}, \tag{5–1}$$

for the solvent species in a binary mixture. For this purpose, we require a model which describes the excess free energy of the solvent mixture. Three models are considered for this:

1. The Wilson [1] equation.
2. Modified Margules equation of Abbott and Van Ness. [2]
3. The UNIFAC model. [3,4]

The equation details of the models are given in the appendix at the end of this chapter. The relative merits of all threes models are discussed extensively in standard textbook literature, [5,6] and since it is not the principal subject of this investigation, the discussion of the models given here is not in depth. The two former models express the nonideality in terms of interactions between unlike molecular species, which in turn are characterized by parameters. These are system specific, and their values come only from regression of data. In systems where there are no data, either of these two models can be used. Instead, group contribution methods, such as UNIFAC [3,4] can be used to estimate the nonideality of a mixture. UNIFAC also expresses the nonideality in terms of molecular interactions, not between the

molecules of the system, but rather between fragments (or groups) on each molecule. UNIFAC divides molecules into smaller groups and use these to express the excess free energy by assigning thermodynamic properties to the molecular fragments. This is known as the "solution-of-groups" concept, and was formerly introduced by Wilson and Deal.[7] UNIFAC has, since its birth in 1975,[3] evolved in many different directions in terms of group definitions and model expressions. Most importantly is the evolution in terms of the group-group interaction parameters, the parameters of the model, which come from regression of substantial amounts of data. There are several versions of UNIFAC, which are standard today. The version implemented here is that of Hansen et al.[4] from 1991.

5.2. Vapor-liquid equilibrium (VLE)

The fundamental relation for equilibrium between a liquid mixture and its vapor phase is the equality of fugacities of every species in each phase. For a liquid phase with composition **x** in equilibrium with its vapor phase, composition **y**, the isofugacity criterion is[5]

$$\forall i \qquad f_i^V(T,P,\mathbf{y}) = f_i^L(T,P,\mathbf{x}). \tag{5–2}$$

This leads to

$$y_i\varphi_i(T,P,\mathbf{y})P = x_i\gamma_i(T,P,\mathbf{x})f_i^{0,L}(T,P). \tag{5–3}$$

φ_i is the fugacity coefficient of i, and γ_i is the Lewis-Randall normalized activity coefficient. At conditions far below the critical point, typically at low to moderate pressures and temperatures, the fugacity coefficient is approximately unity (corresponding to an ideal gas), and the pressure dependence of the liquid-phase activity coefficient is negligible. The reference fugacity, $f_i^{0,L}$, is the fugacity of i as a pure liquid at the reference pressure. This is frequently approximated by the saturation pressure for substances that are liquids at T. These approximations yield the *modified* Raoult's law

$$y_iP = x_i\gamma_i(T,\mathbf{x})P_i^{\text{sat}}(T), \tag{5–4}$$

where $P_i^{\text{sat}}(T)$ is the saturated vapor pressure of i at T. Summing over all M components gives the total pressure above a liquid mixture,

$$P = \sum_{i=1}^{M} x_i\gamma_i(T,\mathbf{x})P_i^{\text{sat}}(T). \tag{5–5}$$

Total pressure data as function of T and liquid-phase composition, **x**, enables estimation of parameters for an expression of the excess free energy of the mixture. This is usually referred to as *Barker's*

method[8]*. The pure component vapor pressures were taken from the original data sources, and not from correlations or tabulations, to ensure a consistent reference fugacity. If a measured value was not provided by the authors, its value was obtained from fitting to the experimental data along with the model parameters, as recommended by Abbott and Van Ness.[9] The uncertainty in vapor pressures are critical for the correlation of VLE data, and it is best if their values come from regression of isothermal experimental data†. Estimation of parameters for any thermodynamic model is based on solving

$$\min s = \sum_{k}^{\substack{\text{data}\\ \text{points}}} (\delta P)_k^2, \tag{5–6}$$

where δP is the difference in calculated and observed pressure. This is standard procedure for reducing VLE data.[6] Note here that the estimation is nonlinear (as a result of the expression for $\ln \gamma_i$). The details of nonlinear estimation are given in Appendix A at the end of the thesis.

5.3. Binary mixtures

A large data base of binary vapor-liquid equilibria data have been processed. These span a wide range of conditions, ranging from nearly ideal to systems with two liquid phases. Both Wilson and modified Margules models are capable of correlating strongly nonideal systems (e.g. alkane-alcohol) and relatively ideal (e.g. alkane-alkane) systems as well. In the event of no experimental data for correlation, UNIFAC estimates liquid-phase activity coefficients using transferrable parameter values, which come from regression of mixture data, and does therefore not require input data other than group stoichiometries. Although UNIFAC can describe mixtures of organic solvents, UNIFAC is not well suited for mixtures which have very high limiting activity coefficients, γ_i^∞. If γ_i^∞ is too high, then the slope with changing composition is too steep, and may result in false miscibility gaps. The stability criterion (for a binary mixture) is

$$\left(\frac{\partial \ln \gamma_1}{\partial x_1}\right)_{T,P} < \frac{1}{x_1}. \tag{5–7}$$

If this relation is satisfied then the mixture enters the metastable region of the phase diagram, i.e., the region beyond the spinodal. Further increase in nonideality can result in a two-phase region, wherefore UNIFAC will predict liquid-liquid miscibility. Thus, care must be taken when applying UNIFAC for strongly nonideal mixtures, if those are known to be miscible.

* Barker used the three-suffix Margules equation for γ_i, but the terminology in this thesis is used regardless of model for γ_i.
† The correlation of vapor pressures using an Antoine-like expression can cause significant error.

Table 5–1. Binary systems at temperature T, no. data points, and errors of correlation with Wilson and modified Margules equations.

					AAD (%)		
#	Component 1	Component 2	T(°C)	n	Wilson	Margules	Reference
1	2-Propanol	Water	80	21	1.19	2.42	[10]
2	Water	1,2-Propanediol	98	9	0.97	1.37	[11∗,†]
3	Ethanol	Water	25	14	0.76	0.27	[12∗]
4	1-Propanol	Octane	85	25	0.53	1.63	[13∗]
5	Cyclohexane	Acetone	50	27	0.10	0.48	[14∗]
6	Acetone	Toluene	45	20	0.87	0.86	[15]
7	Cyclohexane	Methyl-ethyl-ketone	50	32	0.08	0.26	[14∗]
8	Methyl-ethyl-ketone	Toluene	57	15	0.07	0.09	[16∗]
9	1-Butanol	Heptane	50	14	0.55	1.49	[17]
10	1-Propanol	Heptane	30	21	0.83	3.05	[18∗]
11	Methylcyclohexane	1-Butanol	90	21	0.58	0.80	[19]
12	1-Butanol	Octane	100	14	0.29	0.14	[20]
13	Acetone	Hexane	45	16	0.60	0.42	[21∗]
14	Heptane	Dibutyl ether	90	9	0.98	0.98	[22∗,†]
15	Hexane	Dibutyl ether	35	14	0.03	0.03	[23†]
16	Methyl-ethyl-ketone	Hexane	65	9	0.43	0.44	[24∗]
17	1-Butanol	Hexane	25	17	2.53	5.49	[25∗,†]
18	1-Propanol	Hexane	30	15	0.42	4.15	[26∗]
19	2-Butanol	Hexane	25	15	1.28	2.27	[25∗]
20	2-Methyl-1-propanol	Hexane	59	23	0.49	1.63	[27∗]
21	Water	1-Propanol	40	25	0.67	1.39	[28†]
22	Heptane	Hexane	30	10	0.33	0.29	[29]
23	Heptane	Butyl acetate	75	18	0.94	0.89	[30∗]
24	Cyclohexane	1-Butanol	80	9	31.86	11.60	[31∗,†]
25	Cyclohexane	2-Butanol	50	18	1.53	1.18	[32∗]
26	Heptane	2-Methyl-1-propanol	40	20	0.15	0.47	[33∗,†]
27	Heptane	3-Methyl-1-butanol	75	25	0.55	1.77	[34∗]
28	1-Propanol	2-Pentanol	40	24	0.17	0.17	[35]
29	2-Propanol	2-Pentanol	40	24	0.39	0.41	[35]

Continues on next page

Continued from last page

30	Benzene	Hexane	40	17	0.05	0.10	36∗
31	Benzene	Toluene	52	6	2.62	2.29	37
32	Benzene	Hexadecane	35	21	0.16	1.82	38†
33	Carbon tetrachloride	Hexane	25	12	0.05	0.05	39∗
34	Carbon tetrachloride	Heptane	25	14	0.09	0.09	39∗
35	Carbon tetrachloride	Benzene	40	8	0.01	0.61	40∗,†
36	Carbon tetrachloride	Isooctane	35	7	0.03	2.92	41∗,†
37	Methyl-ethyl-ketone	Water	50	18	15.04	2.69	42∗
38	Acetonitrile	Water	50	10	16.49	4.36	43∗,†
39	Water	Ethylene glycol	98	12	3.20	1.00	11∗,†
40	Water	1-Butanol	50	45	1.82	4.92	44
41	1,4-dioxane	Water	25	11	0.28	0.49	45
42	2-Methyl-2-butanol	1-Pentanol	100	20	0.67	0.39	46∗
43	1-Propanol	Isooctane	72	20	0.29	0.37	47∗,†
44	1-Propanol	Cyclohexane	25	29	0.82	2.97	48
45	Ethanol	Hexane	45	40	0.38	3.81	49∗
46	Benzene	Cyclohexane	40	22	0.02	0.02	50∗
47	Heptane	Cyclohexane	25	21	0.07	0.07	50∗
48	Methyl-t-butyl ether	Cyclohexane	40	23	0.02	0.02	50∗
49	Cyclooctane	Cyclohexane	25	13	0.05	9.34	51†
50	Cyclohexane	Hexane	40	11	0.02	0.02	52
51	Cyclohexane	Isooctane	35	6	0.01	1.20	53∗,†
52	Ethyl acetate	Cyclohexane	40	17	0.43	0.54	54∗
53	2-Methyl-1-butanol	1-Pentanol	0	18	0.08	0.09	46∗
54	2-Methyl-2-butanol	1-Pentanol	100	20	0.67	0.39	46∗
55	3-Methyl-2-butanol	1-Pentanol	100	19	0.46	0.46	46∗
56	Acetone	Water	50	17	0.30	1.91	55
57	Ethylbenzene	Benzene	20	5	1.73	1.70	56
58	Carbon tetrachloride	Octane	40	16	0.06	0.12	57
59	Carbon tetrachloride	Nonane	40	16	0.12	0.22	57
60	Carbon tetrachloride	Decane	40	16	0.11	0.20	57
61	Carbon tetrachloride	Toluene	40	16	0.02	0.02	57

Continues on next page

Continued from last page

62	Carbon tetrachloride	*o*-Xylene	40	16	0.19	0.15	[57]
63	Carbon tetrachloride	*p*-Xylene	40	15	0.23	0.25	[57]
64	Dimethylsulfoxide	Water	25	47	10.57	1.49	[58]
65	Methyl-t-butyl ether	Hexane	40	23	0.02	0.02	[50]*
66	Cyclohexane	Octane	25	28	0.10	0.14	[59]*
67	Methanol	Ethyl acetate	55	11	0.09	0.83	[60]*,†
68	Ethanol	Ethyl acetate	55	11	0.20	0.43	[60]*,†
69	Methyl acetate	1-Propanol	318	10	0.31	0.29	[61]*,†
70	Methyl acetate	2-Propanol	318	11	0.33	0.32	[61]*,†
71	Heptane	2-Butanol	30	24	0.51	1.71	[62]
72	Carbon tetrachloride	Cyclohexane	40	9	0.01	0.53	[63]*,†
73	3-Methyl-1-butanol	Hexane	25	11	0.54	2.97	[64]*
74	3-Pentanone	Water	70	19	3.64	2.80	[65]*
75	N,N-Dimethylformamide	Water	40	20	0.66	14.88	[28]*,†
76	Benzene	1,4-Dioxane	25	19	0.81	0.85	[66]
77	Chloroform	Benzene	50	19	0.28	3.73	[67]*,†
78	Chloroform	1,4-Dioxane	50	22	0.50	0.13	[68]
79	Ethanol	1,2-Propanediol	25	12	1.80	2.12	[69]

*: Vapor phase composition included in data set.

†: Vapor pressures of pure components not included in data set.

The entire data base of solubility data comprises a large number of solvent mixtures. We have extracted 79 isothermal data sets from the scientific literature. Table 5–1 lists these, along with the number of data points and the temperature at which they were measured. Also indicated in Table 5–1 is whether or not the vapor phase composition is included in the experimental observations. Although this quantity is not necessary for regression,[70] its value may be used to express the level of thermodynamic consistency of the data-model agreement, following Van Ness.[8] Consistency checks of the experimental data has not been made, this is a possible improvement for future directions. Table 5–1 also gives the average absolute relative error in the regression for both models. This statistic is defined as

$$\text{AAD} = \frac{100\%}{n} \sum_{k}^{n} \left| \frac{\delta P}{P} \right|_k . \tag{5–8}$$

The resulting parameter values are given in the appendix towards the end of this chapter. In addition to the Wilson and Margules values, the coefficient for the Porter equation is also provided for a few systems.

The Wilson equation generally correlates the data better than the modified Margules equation apart from a few exceptions, which will be addressed below. Most notably entries # 24, 37, and 38. In the system cyclohexane–1-butanol the authors of the data[31] did not provide vapor pressures. Here, regression with

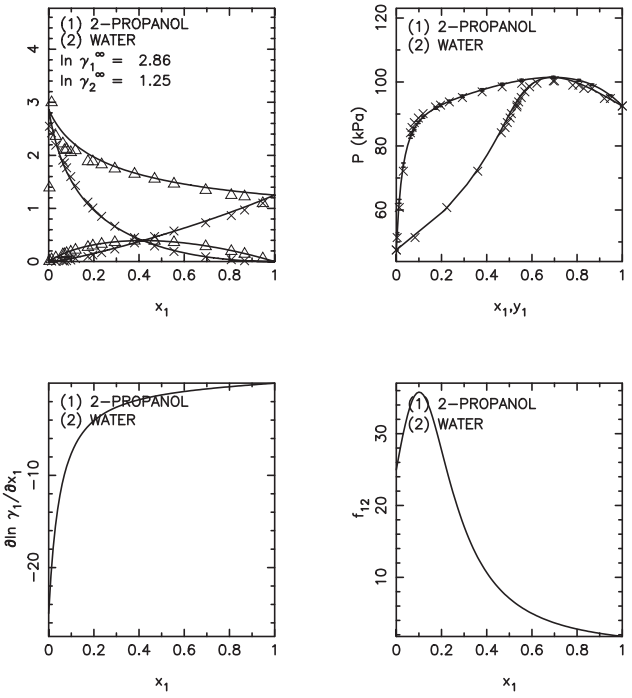

Figure 5–1. Reduction of 2-propanol–water VLE with the Wilson equation. The binary forms a highly nonideal solution, which is correlated well with this model.

the modified Margules equation gives a negative vapor pressure of 1-butanol of $-3.55\,\mathrm{kPa}$, whereas regressing with the Wilson equation gives $20.09\,\mathrm{kPa}$. For cyclohexane the regressed values are 21.78 and 13.19, respectively. Thus, a significant difference is found in the two methods for this particular system. There are also other sets where the two methods are not fully consistent with each other, e.g. # 49 and 51. In these two, the vapor pressures of cyclooctane and cyclohexane using the Wilson equation give 13.01 and $20.22\,\mathrm{kPa}$, respectively, while the modified Margules with two adjustable parameters (in addition to the values of P_i^{sat}) give -0.63 and $-0.15\,\mathrm{kPa}$. Negative vapor pressures are of course not realistic, but the values minimize the function in Equation (5–6).

Though, from a first glance in Table 5–1 the two models might seem very similar, this is not always the case. Since the method outlined for the excess solubility of a solid solute in a mixed solvents require *derivatives* of activity coefficients, it is necessary to examine these in more detail. Figure 5–1 shows the results of reducing the set of 2-propanol and water, reported by Wu et al.,[10] using the Wilson equation.

The system is quite nonideal, as indicated by the large values of γ_1^∞ on the upper left diagram. The

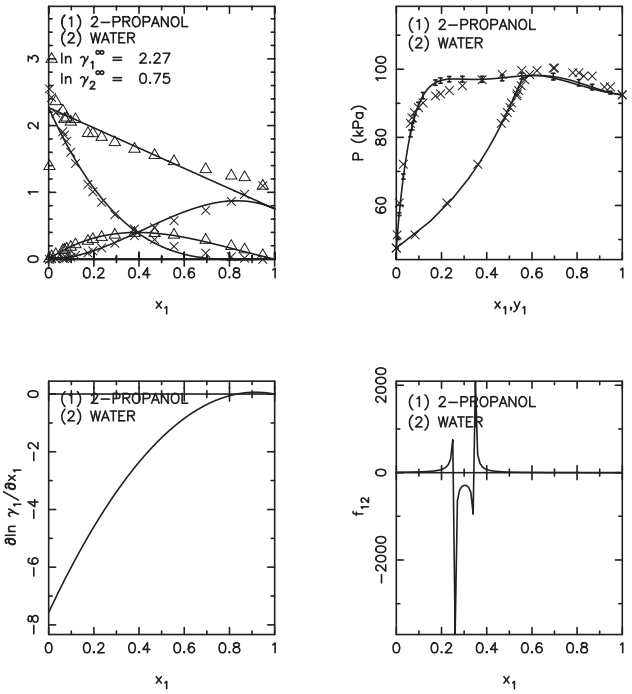

Figure 5–2. Reduction of 2-propanol–water VLE with the modified Margules equation. The data is correlated slightly worse than with the Wilson equation. This is partly indicated by the discontinuities in the plot of f_{23}^+ versus solvent composition.

upper right shows the phase diagram, and reveals that the components form an azeotrope. The lower left diagram shows the derivative given in Equation (5–1), and the lower left shows the quantity f_{12}, as defined in Chapter 4. If we rearrange Equation (4–23) in order to get f_{12}:

$$f_{12} = -\frac{\dfrac{1}{x_2}\left(\dfrac{\partial \ln \gamma_1}{\partial x_1}\right)_{T,P,n_2}}{1 + x_1\left(\dfrac{\partial \ln \gamma_1}{\partial x_1}\right)_{T,P,n_2}}. \tag{5–9}$$

This behavior of f_{12} is characteristic of all systems of water with polar species. A significant peak is found towards the aqueous side. Similarly, Figure 5–2 shows the results using the modified Margules equation with two adjustable parameters. The Margules equation gives slightly lower values of the activity coefficients at infinite dilution, but is unable to correlate the data. The behavior of f_{12} is very different. At $x_1 \approx 0.25$, a discontinuity is encountered and the sign is reversed, with a peculiar new variation. At $x_1 \approx 0.35$, the opposite occurs. The reason for this is found in the expression for f_{12}. We

notice that the denominator is identical to Equation (5–7), which means that at the *spinodal* point, where the mixture enters a meta stable region, the denominator changes sign, which causes f_{12} to approach $\pm\infty$, pending in what direction composition is changed. This type of behavior is a frequent observation with the Margules equation, especially in mixtures with strong nonideality, such as in alkane–alcohol systems. The Wilson equation generally produces smoother curves. The implications of these features are not obvious yet, but must be judged on the basis of their performance with the excess solubility models.

5.3.1. Liquid-liquid equilibria

Throughout this thesis, we consider only single-phase solubilities, i.e., solutes which are dissolved in one liquid phase. There are also solvent mixtures which separates in two phases. Among the examples are MEK–water, water–1-butanol and 3-pentanone–water (# 37, 40, and 74 in Table 5–1). The VLE data of water–1-butanol of Fischer and Gmehling [44] was correlated with a two-parameter Margules equation, using the method described in Appendix 5.C for estimating the phase boundaries, giving Figure 5–3. The calculated phase boundaries are $x_1^\alpha = 0.64$ and $x_1^\beta = 0.89$, which is consistent with the observations of Fischer and Gmehling. This is indicated by the absence of measurements in this range. Immiscible

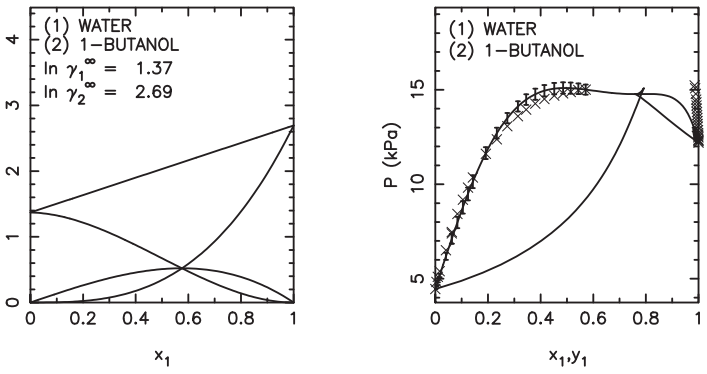

Figure 5–3. Excess free energy and activity coefficients of 1-butanol and water. This mixture has a miscibility gap calculated with the Margules equation.

solvent systems are not uncommon, since extraction, which relies on differences in solubilities in two liquid phases, is a standard unit operation. However, we will limit this thesis to solubilities in a single phase. Dickhut et al. [71] measured solubilities of naphthalene in this solvent mixture (water–1-butanol), but measurements are limited to the water-rich end, outside the binodal. Solvent systems with miscibility gaps do not pose substantial difficulties generally. The Wilson equation is actually particularly useful in these situations, since it does not provide false phase splits. Sometimes simple models are preferable.

5.4. Ternary mixtures

Equation (4–38) expresses the excess solubilities in ternary solvent mixtures. Above binary systems, Margules-type equations are generally not available. Although investigators, such as Chien and Null,[72] have pursued the idea of multicomponent versions, we will not consider them at this point. VLE data of ternary liquid mixtures are scarce in the open literature, and specific mixtures are generally not easy to find data for. Fortunately, the parameters of the Wilson equation are often transferrable from binary

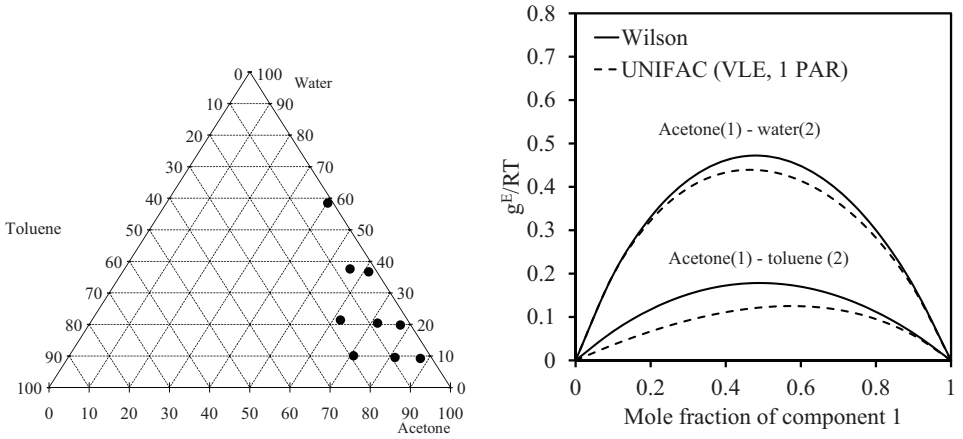

Figure 5–4. Mole fraction compositions in the ternary mixture, at which solubility is measured, and nonideality in the binaries with the Wilson and UNIFAC equations. In the regions where the solubility of toluene is measured the UNIFAC model gives an excess Gibbs energy which is very comparable to that computed by the Wilson equation.

to multicomponent systems when the components are liquids.[5] So if VLE data for all three pairs of solvents are known, then they can be used to estimate nonideality in the multicomponent system. Here, we will examine a ternary solvent mixture, for which solid solubility data exists, and will be the subject of investigations in Chapter 6. The example is water–acetone–toluene, in which solubilities of paracetamol was measured by Granberg and Rasmuson.[73] Water and toluene form two immiscible liquid phases across most of the concentration range, sof solubility measurements are done in almost pure acetone, as shown on left plot in Figure 5–4, in which water and toluene both are completely miscible. However, being that the water–toluene system cannot be correlated, since no data exist, we cannot use the Wilson equation for this system. Instead, we may rely on UNIFAC. If UNIFAC is capable of describing the individual binaries, then the ternary mixtures is likely to be well described also. The mixture is composed of nearly pure acetone, so the simultaneous presence of water and toluene is small. Therefore, a significant contribution from this pair is not expected. The right plot of Figure 5–4 shows the excess free energy for the binaries acetone–water and acetone–toluene estimated using the Wilson equation with

parameters regressed from data, and estimates from UNIFAC. Although the Wilson equation does not seem to be in full agreement with UNIFAC, the agreement within the concentration range in which solubilities are measured ($> 80\%$ acetone) is good. This means, that UNIFAC is a suitable model for this particular ternary system. Similar arguments apply to the ternary of benzene–1,4-dioxane–chloroform, where UNIFAC is a viable model for the nonideality of this ternary solution. The remaining solvent mixtures studied in Chapter 6 are composed on mainly hydrocarbons (alkanes), alkanols, ethers, and esters. These are mixtures, which UNIFAC is fully able to address.

5.5. Summary

This chapter has examined the regression of binary vapor-liquid equilibrium data for estimation of parameters for excess Gibbs energy models. These are used to express the solvent-solvent contributions to the excess solubility models developed in the previous chapter. Binaries formed the basis of the majority of the chapter, but ternary mixtures were also discussed. Generally, if VLE data can be found for a particular solvent mixture, it is regressed to obtain parameters for the Wilson and modified Margules equations. If no data is found, the contributions are estimated with UNIFAC.

The next chapter details the mixed solvent solubility results, by applying the excess solubility models.

5.A. Activity coefficients and derivatives from excess Gibbs energy models

The derivative required is that

$$\left(\frac{\partial \ln \gamma_i}{\partial x_j}\right)_{T,P,n_{k\neq j}} = \frac{n}{1-x_j}\left(\frac{\partial \ln \gamma_i}{\partial n_j}\right)_{T,P,n_{k\neq j}}, \tag{5–10}$$

with all expressions being symmetric with respect to i and j.

For the two-parameter Wilson equation the activity coefficient is

$$\ln \gamma_i = 1 - \ln \eta_i - \sum_k x_k \epsilon_{ki}, \qquad \epsilon_{ki} = \frac{\Lambda_{ik}}{\eta_i}, \qquad \eta_k = \sum_j x_j \Lambda_{kj}. \tag{5–11}$$

The derivative taken with respect to mole number is

$$n\left(\frac{\partial \ln \gamma_i}{\partial n_j}\right)_{T,P,n_{k\neq j}} = 1 - (\epsilon_{ij} + \epsilon_{ji}) + \sum_k x_k \epsilon_{ki}\epsilon_{kj}. \tag{5–12}$$

with

$$\Lambda_{kj} = \frac{v_j}{v_k} \exp\left[-\frac{\lambda_{kj} - \lambda_{kk}}{\mathsf{R}T}\right] = \frac{v_j}{v_k} \exp\left[-\frac{a_{kj}}{T}\right]. \tag{5–13}$$

Here, the off-diagonal elements of **a** are the model parameters which characterizes the interaction between unlike molecular species. Note that $a_{jk} \neq a_{jk}$, and have units of kelvin. In addition to the interactions, the Wilson equation also require the pure component molar volumes. Naturally these depend on temperature, but assuming that they are constant over a limited temperature range is usually a valid approximation. Their values are not crucial for the performance of the Wilson equation, and are taken from the DIPPR compilations.[74]

The five-parameter modified Margules equation is (for a binary only)

$$\ln \gamma_i = G_i(1 - x_i)^2, \quad x_i + x_j = 1, \quad i \neq j \in \{1, 2\}, \tag{5–14}$$

where

$$G_i = A_{ij} + 2(A_{ji} - A_{ij})x_i - 2F^{(1)}x_i x_j + F^{(2)}(\alpha_{ij} + \eta x_j^2)x_i^2,$$

and we have defined

$$F^{(k)} \equiv \frac{\alpha_{ij}\alpha_{ji}x_i x_j}{(\alpha_{ij}x_i + \alpha_{ji}x_j + \eta x_i x_j)^k}. \tag{5–15}$$

The parameters of the model is the set $\{A_{ij}, A_{ji}, \alpha_{ij}, \alpha_{ji}, \eta\}$. Frequently, only the fist two are required. The remaining are only included if the solvent mixture if highly nonideal, and η only if the mixture is close to the miscibility limit. The compositional derivatives are

$$\left(\frac{\partial \ln \gamma_i}{\partial x_i}\right)_{T,P} = x_j^2 \frac{\partial G_i}{\partial x_i} - 2x_j G_i, \tag{5–16}$$

where $\mathrm{d}x_i = -\mathrm{d}x_j$. The derivative of G_i is

$$\begin{aligned}\frac{\partial G_i}{\partial x_i} =& 2(A_{ji} - A_{ij}) + F^{(1)}(x_j - x_i) + F^{(2)}\left[\alpha_{ij}x_1(1 + x_j) - \alpha_{ji}x_i x_j + 2\eta(x_j - x_i)x_i x_i\right] \\ & - F^{(3)}(\alpha_{ij} + \eta x_j^2)x_i^2.\end{aligned} \tag{5–17}$$

For the UNIFAC method, the activity coefficient is given by a combinatorial term, accounting for differences in size and shape, and a energetic term (or residual) which describes the interactions

$$\ln \gamma_i = \ln \gamma_i^C + \ln \gamma_i^R. \tag{5–18}$$

The combinatorial part is given by

$$\ln \gamma_i^C = 1 - J_i + \ln J_i - \frac{z}{2} q_i \left(1 - \frac{J_i}{L_i} + \ln \frac{J_i}{L_i}\right). \tag{5–19}$$

Here, the coordination number z is usually set to 10* The residual part is given by

$$\ln \gamma_i^R = q_i(1 - \ln L_i) - \sum_k^{NSG} \left[\vartheta_k \frac{s_{ki}}{\eta_k} + G_{ki} \ln \frac{s_{ki}}{\eta_k}\right] \tag{5–20}$$

Index k sums the contribution from all subgroups in the mixture (denoted by NSG). We have used the following definitions for the average surface area and volume

$$J_i = \frac{r_i}{\sum_j x_j r_j} = \frac{r_i}{\bar{r}}, \quad L_i = \frac{q_i}{\sum_j x_j q_j} = \frac{q_i}{\bar{q}} \tag{5–21}$$

These are related to the van der Waals surface areas and volumes of the subgroups, which make up the mixture

$$r_i = \sum_k \nu_k^{(i)} R_k, \quad q_i = \sum_k \nu_k^{(i)} Q_k, \tag{5–22}$$

where $\nu_k^{(i)}$ is the stoichiometry of group k on molecule i. Other variables are given by

$$G_{ki} = \nu_i^{(i)} Q_k, \quad s_{ki} = \sum_m^{NSG} G_{mi} \exp\left[-\frac{a_{mk}}{T}\right], \quad \vartheta_k = \sum_j x_j G_{jk}, \quad \eta_k = \sum_j x_j s_{kj}. \tag{5–23}$$

The input parameters to the model are the group stoichiometries $(\nu_k^{(i)})$, pure group areas (R_k) and volumes (Q_k), and the group-group interaction parameters $(a_{mk} \neq a_{km})$. Equation (5–1) becomes

$$\begin{aligned} n \left(\frac{\partial \ln \gamma_i}{\partial n_j}\right)_{T,P,n_{k\neq j}} = &- (1 - J_i)(1 - J_j) - 5(J_i - L_i)(J_j - L_j)\bar{q} \\ &+ L_i L_j \bar{q} + \sum_k^{NSG} \left[\vartheta_k \frac{s_{ki} s_{kj}}{\eta_k^2} - \frac{G_{kj} s_{ki} + G_{ki} s_{kj}}{\eta_k}\right]. \end{aligned} \tag{5–24}$$

5.B. Parameter table for solvent mixtures

* This is the average number of molecules surrounding i in the mixture. Most methods based on the local composition concept assume that this is 10.

Table 5–2. Binary systems and parameters for Wilson, modified Margules, and Porter equations. The number in the left-most column is the number of the system in Table 5–1.

	Wilson		Modified Margules					Porter
#	a_{12}(K)	a_{21}(K)	A_{12}	A_{21}	α_{12}	α_{21}	η	B_{12}
1	400.9	626.8	2.6264	1.1664	3.1604	1.0227		
2	377.2	-294.2	0.0028	-0.2400				-0.1721
3	57.3	431.8	1.4795	0.9157				
4	820.8	193.1	2.3000	2.1353	1.6200	1.1100		
5	214.3	467.8	1.5605	1.6134				
6	254.3	-17.2	0.6925	0.6565				
7	286.4	221.6	1.3727	1.1076				
8	198.9	-87.6	0.3218	0.2534				
9	920.4	71.4	2.8408	1.5518	4.8900	1.0100		
10	1048.1	120.8	3.6833	1.9913	15.3700	1.7600		
11	67.3	743.3	1.2173	1.8336				
12	690.3	108.0	1.7001	1.4683				
13	485.3	202.1	1.5309	1.6878				
14	-194.7	386.6	-0.1054	0.1442				
15	80.8	-63.5	0.0547	0.0561				
16	140.3	99.0	1.0202	1.1463				
17	937.7	54.9	3.1814	1.6722	6.2912	1.8884		
18	965.1	-19.7	3.3905	1.4137	14.7780	1.6065		
19	747.4	69.4	2.8328	1.5468	6.0454	1.2875		
20	757.2	97.3	2.7313	1.5151	6.3944	1.1088		
21	630.7	352.8	1.3556	3.1724	1.0484	5.5998		
22	-130.6	130.6	-0.0351	-0.0730				
23	52.3	216.5	0.6457	0.7365				
24	456.1	255.4	1.6687	4.3116				
25	18.9	964.4	0.8754	2.0557				
26	376.1	423.6	1.7110	1.4926				
27	76.8	719.1	1.2218	1.8376				
28	80.8	-87.7	-0.0265	-0.0284				
29	-15.9	62.5	0.0148	0.0545				

Continues on next page

Continued from last page

	Wilson		Modified Margules					Porter
#	a_{12}(K)	a_{21}(K)	A_{12}	A_{21}	α_{12}	α_{21}	η	B_{12}
30	106.4	111.8	0.4624	0.6640				
31	136.4	-136.4	-0.1813	0.0773				
32	123.1	171.6	-0.1514	0.2217				
33	14.0	86.4	0.1834	0.2846				
34	44.3	42.4	0.1470	0.2427				
35	-34.3	75.8	0.1200	0.1317				
36	56.6	70.9	0.1303	0.3009				
37	15539.3	705.7	3.5857	2.1363	4.8184	1.3925	1.9801	
38	273.0	1054.9	2.2947	1.4522	-0.0272	0.4850		
39	89.1	-89.1	0.0123	-0.4665				-0.2714
40	774.3	891.8	1.3707	2.6935				
41	919.4	-154.6	1.6595	1.9122				
42	112.4	-112.4	-0.1286	0.0020				
43	613.9	121.7	2.4780	1.7287	2.9162	0.8922		
44	873.6	192.7	3.9613	1.9115	21.4454	2.0599		
45	1145.9	175.7	3.5427	2.2308	9.1214	1.6408		
46	105.2	51.8	0.4403	0.4884				
47	-187.0	235.3	0.0572	0.0999				
48	-11.2	84.3	0.2181	0.2317				
49	-57.2	64.9	3.5140	4.4674				
50	28.1	7.0	0.0904	0.1057				
51	382.4	-277.6	3.1287	2.5698				
52	301.3	128.6	1.5778	1.1580				
53	98.8	-98.8	-0.0210	0.0017				
54	112.4	-112.4	-0.1286	0.0020				
55	138.0	-122.7	0.0189	0.0125				
56	91.7	758.7	2.0612	1.5032				
57	-32.7	50.4	0.0518	0.0337				
58	31.4	50.2	0.0596	0.1457				
59	12.9	89.6	-0.0062	0.1039				

Continues on next page

Continued from last page

	Wilson		Modified Margules					Porter
#	a_{12}(K)	a_{21}(K)	A_{12}	A_{21}	α_{12}	α_{21}	η	B_{12}
60	14.6	91.9	-0.0594	0.0392				
61	63.6	-22.9	0.1296	0.1243				
62	-1.5	1.5	-0.0161	-0.0296				
63	142.2	-142.2	-0.0391	-0.0153				
64	-574.9	39.8	-2.8141	-1.3100				
65	48.6	24.6	0.2181	0.2317				
66	-29.5	94.9	-0.0019	0.0560				
67	357.3	799.8	1.0275	2.5614				
68	319.3	118.0	0.8602	2.0320				
69	521.9	249.8	1.0770	0.8432				
70	245.1	334.8	0.8315	0.8650				
71	100.7	767.2	1.5294	2.0834				
72	31.4	2.1	0.0756	2.5781				
73	859.6	89.8	2.1556	1.1940				
74	20806.3	913.1	4.9968	1.6715				
75	104.2	82.9	4.3238	3.1120				
76	263.5	-147.0	0.1654	0.0846				
77	-47.1	-24.8	-0.2294	3.8047				
78	-253.6	-32.1	-0.7704	-1.3203				
79	-288.7	574.1	0.0441	0.5587				

5.C. Algorithm for liquid-liquid equilibria computation

The rigorous approach to liquid-liquid equilibria (LLE) is done by equating the fugacities of all species in the two phases (α, β) and solving

$$\forall i \quad (x_i \gamma_i)^\alpha = (x_i \gamma_i)^\beta. \tag{5–25}$$

However, the solution is not straightforward and requires tedious attention to the solving procedure. A simpler way of dealing with binary LLE at constant pressure and temperature is through the K-factor

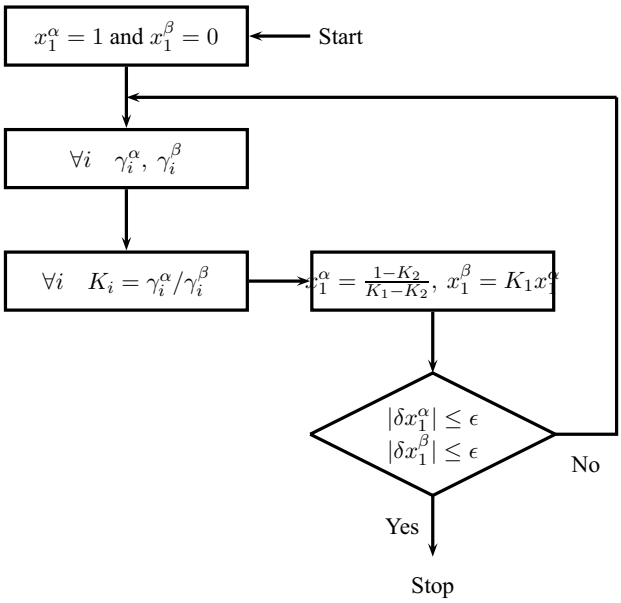

Figure 5–5. Algorithm for computing binary liquid-liquid equilibria using the K-factor method.

approximation. We define a ratio between the compositions of each species in the two phases

$$K_i \equiv \frac{x_i^\beta}{x_i^\alpha} = \frac{\gamma_i^\alpha}{\gamma_i^\beta}. \tag{5–26}$$

The algorithm for computing the compositions in each phase is given in Figure 5–5.

References

1. G. M. Wilson. *J. Am. Chem. Soc.*, 86(2):127–130, 1964.
2. M. M. Abbott and H. C. Van Ness. *AIChE J.*, 21: 62–71, 1975.
3. Aa. Fredenslund, R. L. Jones, and J. M. Prausnitz. *AIChE J.*, 21:1086–1099, 1975.
4. H. K. Hansen, P. Rasmussen, Aa. Fredenslund, M. Schiller, and J. G. Gmehling. *Ind. Eng. Chem. Res.*, 30:2352–2355, 1991.
5. J. M. Prausnitz, R. N. Lichtenthaler, and E. Gomez de Azevedo. *Molecular thermodynamics of fluid-phase equilibria*. Prentice-Hall, 3rd edition, 1999.
6. J. M. Smith, H. C. Van Ness, and M. M. Abbott. *Introduction to chemical engineering thermodynamics*. McGraw-Hill, seventh edition, 2005.
7. G. M. Wilson and C. H. Deal. *Ind. Eng. Chem. Res. Fundam.*, 1:20–23, 1962.
8. H. C. Van Ness. *J. Chem. Thermodyn.*, 27:113–134, 1995.
9. M. M. Abbott and H. C. Van Ness. *Fluid Phase Equil.*, 1:3–11, 1977.
10. H. S. Wu, Hagewiesche D., and Sandler S. I. *Fluid Phase Equil.*, 43:77–89, 1988.
11. A. Lancia, D. Musmarra, and F. Pepe. *J. Chem. Eng. Jpn.*, 29(3):449–455, 1996.
12. R. C. Phutela, Z. S. Kooner, and D. V. Fenby. *Aust. J. Chem.*, 32:2353, 1979.
13. T. Hiaki, K. Takahashi, T. Tsuji, M. Hongo, and Kojima K. *J. Chem. Eng. Data*, 40:271–273, 1995.
14. A. C. Colin, A. Compostizo, and M. D. Pena. *J. Chem. Thermodyn.*, 16:497–502, 1984.
15. R. V. Orye and J. M. Prausnitz. *Trans. Faraday Soc.*, 61:1338, 1965.
16. D. Naumann and H. G. Wagner. *J. Chem. Thermodyn.*, 18:81–87, 1986.
17. C. P. Smyth and E. V. Engel. *J. Am. Chem. Soc.*, 51:2660–2670, 1929.
18. H. C. Van Ness, A. Soczek, G. L. Peloquin, and R. L. Machado. *J. Chem. Eng. Data*, 12:217–224, 1967.
19. V. Seetharamaswamy, V. Subrahmanyam, C. Chiranjivi, and P. Dakshinamurty. *J. Appl. Chem.*, 19: 258–262, 1969.

References

20. P. Gierycz, J. Gregorowicz, and S. Malanowski. *J. Chem. Thermodyn.*, 20:285–388, 1988.

21. K. Schaefer and W. Rall. *Z. Elektrochem.*, 62:1090, 1958.

22. V. O. Maripuri and G. A. Ratcliff. *J. Chem. Eng. Data*, 17:454, 1972.

23. K. N. Marsh, J. B. Ott, and M. J. Costigan. *J. Chem. Thermodyn.*, 12:857–862, 1980.

24. V. O. Maripuri and G. A. Ratcliff. *J. Appl. Chem. Biotechnol.*, 22:899, 1972.

25. V. Rodriguez, J. Pardo, M. C. Lopez, F. M. Royo, , and J. S. Urieta. *J. Chem. Eng. Data*, 38:350–352, 1993.

26. M. Ronc and G. A. Ratcliff. *Can. J. Chem. Eng.*, 54:326, 1976.

27. C. Berro, M. Rogalski, and A. Peneloux. *J. Chem. Eng. Data*, 27:352–355, 1982.

28. J. Zielkiewicz and A. Konitz. *J. Chem. Thermodyn.*, 23:59–65, 1991.

29. C. P. Smyth and E. W. Engel. *J. Am. Chem. Soc.*, 51:2646–2660, 1929.

30. W. A. Scheller, A .R. Torres-Soto, and K. J. Daphtary. *J. Chem. Eng. Data*, 14:17–19, 1969.

31. R. S. Ramalho and J. Delmas. *J. Chem. Eng. Data*, 13:161, 1968.

32. M. E. Araujo, M. R. W. Maciel, and A. Z. Francesconi. *J. Chem. Thermodyn.*, 25:1295–1299, 1993.

33. J. Zielkiewicz. *J. Chem. Thermodyn.*, 26:919–923, 1994.

34. I. Machova, J. Linek, and I. Wichterle. *Fluid Phase Equil.*, 41:257–267, 1988.

35. K. Mara, V. R. Bhethanabotla, and S. W. Campbell. *Fluid Phase Equil.*, 127:147–153, 1997.

36. M. Goral. *Fluid Phase Equil.*, 102:275, 1994.

37. S. M. Klara, R. S. Mohamed, D. M. Dempsey, and G. D. Holder. *J. Chem. Eng. Data*, 32:143–147, 1987.

38. R. L. Snow, J. B. Ott, J. R. Goates, K. N. Marsh, S. Oshea, and R. H. Stokes. *J. Chem. Thermodyn.*, 18:107–130, 1986.

39. T. G. Bissell and A. G. Williamson. *J. Chem. Thermodyn.*, 7:131–136, 1975.

40. G. Scatchard, S. E. Wood, and J. M. Mochel. *J. Am. Chem. Soc.*, 62:712–716, 1940.

41. R. Battino. *J. Phys. Chem.*, 72:4503, 1968.

42. J. Gaube, S. Hammer, and A. Pfennig. *Fluid Phase Equil.*, 123:245–257, 1996.

43. S. J. Park, B. H. Choi, and B. S. Rhee. *J. KIChE*, 25:512, 1987.

44. K. Fischer and J. G. Gmehling. *J. Chem. Eng. Data*, 39:309, 1994.

45. F. Hovorka, R. A. Schaefer, and D. Dreisbach. *J. Am. Chem. Soc*,, 58:2264, 1936.

46. A. Aucejo, M. C. Burguet, J. B. Monton, R. Munoz, M. Sanchotello, and M. I. Vazquez. *J. Chem. Eng. Data*, 39:578–580, 1994.

47. T. Hiaki, K. Takahashi, T. Tsuji, Hongo M., and K. Kojima. *J. Chem. Eng. Data*, 39:605–607, 1994.

48. R. Q. Hwang and S. L. Robinson. *J. Chem. Eng. Data*, 22:319, 1977.

49. S. J. O'Shea and R. H. Stokes. *J. Chem. Thermodyn.*, 18:691, 1986.

50. L. M. Lozano, E. A. Montero, M. C. Martin, and M. A. Villamanan. *Fluid Phase Equil.*, 110:219–230, 1995.

51. M. B. Ewing and K. N. Marsh. *J. Chem. Thermodyn.*, 6:395–306, 1974.

52. M. Goral, P. Oracz, and S. Warycha. *Fluid Phase Equil.*, 81:261–272, 1992.

53. R. Battino. *J. Phys. Chem.*, 70:3408–3416, 1966.

54. H. S. Wu and S. I. Sandler. *J. Chem. Eng. Data*, 33: 157, 1988.

55. M. M. Chaudry, H. C. Van Ness, and M. M. Abbott. *J. Chem. Eng. Data*, 25:254, 1980.

56. T. Bell and R. J. Wright. *J. Phys. Chem.*, 31:1884, 1927.

57. M. Goral and S. Zawadzki. *Fluid Phase Equil.*, 90: 355, 1993.

58. J. T. W. Lai, F. W. Lau, D. Robb, P. Westh, G. Nielsen, C. Trandum, A. Hvidt, and Y. Koga. *J. Sol. Chem.*, 24:89–102, 1995.

59. M. L. Martin and J. C. Youngs. *Aust. J. Chem.*, 33: 2133–2138, 1980.

60. I. Nagata, T. Yamada, and S. Nakagawa. *J. Chem. Eng. Data*, 20:271, 1975.

61. I. Nagata, T. Ohta, and S. Nakagawa. *J. Chem. Eng. Jpn.*, 9:276–281, 1976.

62. J. R. Powell, K. A. Fletcher, W. E. Acree Jr. K. S. Coym, V. G. Varanasi, and S. W. Campbell. *Int. J. Thermophys.*, 18:1495–1520, 1997.

63. G. Scatchard, S. E. Wood, and J. M. Mochel. *J. Am. Chem. Soc.*, 61:3206–3210, 1939.

64. S. G. Sayegh and G. A. Ratcliff. *J. Chem. Eng. Data*, 21:74, 1976.

65. P. O. Haddad and W. C. Edmister. *J. Chem. Eng. Data*, 17:275, 1972.

66. D. D. Deshpande and S. L. Oswal. *J. Chem. Soc. Faraday Trans. I*, 68:1059, 1972.

67. I. Nagata and H. Hayashida. *J. Chem. Eng. Jpn.*, 3: 161, 1970.

68. C. Gonzalez and H. C. Van Ness. *J. Chem. Eng. Data*, 28:407–409, 1983.

69. N. A. Williams and G. L. Amidon. *J. Pharm. Sci.*, 73:18–23, 1984.

70. H. C. Van Ness, F. Pedersen, and P. Rasmussen. *AIChE J.*, 24:1055–1063, 1978.

71. R. M. Dickhut, A. W. Andren, and D. E. Armstrong. *J. Chem. Eng. Data*, 34:438–443, 1989.

72. H. H. Y. Chien and H. R. Null. *AIChE J.*, 18:1177–1183, 1977.

73. R. A. Granberg and Å. C. Rasmuson. *J. Chem. Eng. Data*, 45:478–483, 2000.

74. DIPPR 801 project. Design institute for physical properties, americal institute for chemical engineers, 2005-2010.

6. Solubilities of solids in solvent mixtures

This chapter will

* highlight some fundamental concepts associated with excess solubilities in solvent mixtures,
* explain the (important) role of the nonideality of the solvent mixture to excess solubilities,
* show results for correlating and predicting excess solubilities in binary solvent mixtures,
* show provisional results for correlating and predicting excess solubilities in ternary solvent mixtures, and
* discuss an approach of predicting solute-solvent parameters from reference solvents.

At the end of the chapter, the major results are summarized.

6.1. Solubilities in binary solvent mixtures

A data base of solubilities of solids in solvent mixtures has been compiled from the open literature, covering wide ranges of solutes and solvent mixtures. These range from being nearly ideal to strongly nonideal. The types of solvent systems include:

* Nonpolar species with nonpolar species (e.g. hydrocarbons),
* polar species with polar species (e.g. alkanols, ethers, and esters),
* polar species with nonpolar species,
* aqueous systems, and
* associating systems.

The solutes range from traditional petrochemically based (fused aromatics) to polyfunctional pharmaceuticals. Table 6–1 lists the solutes studied, with their corresponding thermophysical properties, which are required to calculate the solid-state activity in Equation (3–13). The discussion in Chapter 3 revealed,

that the expression used to calculate the ideal solubility depends on the availability of thermophysical property data, as well as the chemical nature of the solid. However, what form of Equation (3–13) to use is not always obvious, and is explained later, when the results pertaining to each solute are presented and discussed.

Table 6–1. Thermophysical properties of solutes. Values listed with more than a single reference represents an unweighted average.

Solute, i	$T_{m,i}$ (K)	Ref.	$\Delta h_{m,i}$ (kJ/mol)	Ref.	$\Delta c_{P,m,i}$ (kJ/mol/K)	Ref.
4-Hexylresorcinol	341	[1]	19.047	[1]		
4-Hydroxybenzoic acid	486	[2–4]	31.420	[3,4]		
Anthracene	490	[5]	28.601	[5]		
Beta carotene	455	[6]	48.498	[6]		
Cholesterol	421	[7–10]	26.634	[7,10]	8.8	[11]
Desmosterol	388	[10]	15.901	[10]		
Mefenamic acid	504	[12]	38.240	[12]		
Naphthalene	353	[13–15]	18.239	[14]		
Paracetamol	443	[16–18]	27.850	[16–18]	99.8	[19]
Phenacetin	407	[20]	28.750	[21]		
Pyrene	424	[22]	17.359	[22]		
Sulfamethazine	471	[23–25]	31.140	[23,25]		
Sulfamethoxypyridazine	454	[26–28]	30.070	[26–28]		
Sulfanilamide	437	[25]	23.650	[25]		
Testosterone	427	[29,30]	26.179	[29]		
Theophylline	547	[13,29,31,32]	29.650	[31,32]		

6.2. Data of different units

The method presented assumes mole fractions as composition variables. Not all data in the literature are given in mole fractions, so it is necessary to convert these. Units such as molarity and mass fractions are frequently reported for solubilities, while fractions of volume or mass are often used for solvent composition. Here, the conversions into mole fractions are given.

For the solvent composition in a binary (2,3), conversion from mass fractions into molar fractions is done by

$$x'_3 = \frac{w'_3 M_2}{M_3 + w'_3(M_2 - M_3)}, \tag{6–1}$$

where M_j is the molar mass of j. For units of volume fractions a similar transformation is applied

$$x_3' = \frac{\phi_3' \bar{v}_2}{\bar{v}_3 + \phi_3'(\bar{v}_2 - \bar{v}_3)}. \tag{6–2}$$

Here, $\bar{v}_j$ is the partial molal volume of j. Partial molal volumes are rarely available for all solvent mixtures. With negligible difference the molar volume is a suitable replacement, since excess molar volumes are usually (relatively) small. Relating the solubility of the solute(1) in mole fraction into mass fraction is obtained by

$$x_1 = \frac{w_1/M_1}{1 - w_1} \sum_{j \neq 1} x_j M_j, \tag{6–3}$$

If the composition is given in molarity-based units, the transformation is

$$x_1 = c_1 \sum_{j \neq 1} x_j' \bar{v}_j \approx c_1 \sum_{j \neq 1} x_j' v_j. \tag{6–4}$$

Here, c_1 is the concentration of 1 in units of moles per volume. As before, molar volumes are suitable approximations to the partial molar quantities. Note that if the solubility is given on a solute-free basis, i.e., (amount of solute) per (amount of solvent) the resulting mole fraction unit will also be on a solute-free basis. In that case, the actual mole fraction is calculated from

$$x_1 = \frac{x_1'}{1 + x_1'}, \tag{6–5}$$

where x_1' indicates solute-free basis.

6.3. Validation of method

A preliminary application of the model is presented in order to provide the reader with some basic concepts which will be used later on. Recall, that the model for excess solubilities in binary solvent mixtures is

$$s_1^{\mathrm{E}} = -\frac{x_3}{2} \left(\frac{\partial \ln \gamma_3}{\partial x_3} \right)^{+}_{T,P,n_2} \left[1 + x_2 f_{12}^0 + x_3 f_{13}^0 \right]. \tag{6–6}$$

There is a number of comparable results, which are relevant. One can for a given set compare the performance of different approaches to excess solubilities, such as

0. Ideal mixture,

1. FST model with $\mathbf{f}^0$ from fit to ternary data,

2. FST model with $\mathbf{f}^0$ from Porter parameter fit to binary data,

3. FST model with $\mathbf{f}^0$ from UNIFAC,

4. UNIFAC regular computation of excess solubility.

The differences in these approaches are explained in more detail below. The first approach assumes the excess solubility is zero, i.e. the solubility is obtained by interpolation of the two pure-solvent solubilities. Figure 6–1(a) illustrates this for cholesterol(1) dissolved in mixtures of dioxane(2) and hexane(3). The lower part of the figure represents the actual solubility as function of solute-free solvent composition. The upper part is the excess solubility, obtained by subtracting the ideal mixture solubility (dashes).

Table 6–2. UNIFAC group stoichiometry of solutes.

Solute \ sub group	CH_3	CH_2	CH	C	CH=CH	CHC	C=C	ACH	AC	$ACCH_2$	OH	ACOH	CH_2CO	CH_3CO_2	$ACNH_2$
4-Hydroxybenzoic acid	0	0	0	0	0	0	0	4	1	0	0	1	0	0	1
4-Hexylresorcinol	1	4	0	0	0	0	0	3	0	1	0	2	0	0	0
Anthracene	0	0	0	0	0	0	0	10	4	0	0	0	0	0	0
Beta carotene	10	6	0	2	5	4	2	0	0	0	0	0	0	0	0
Cholesterol	5	11	7	2	0	1	0	0	0	0	1	0	0	0	0
Desmosterol	5	10	6	2	2	0	0	0	0	0	1	0	0	0	0
Hydrocortisone acetate	1	6	4	3	1	0	0	0	0	0	2	0	2	1	0
Naphthalene	0	0	0	0	0	0	0	8	2	0	0	0	0	0	0
Pyrene	0	0	0	0	0	0	0	10	6	0	0	0	0	0	0
Testosterone	2	7	4	2	0	1	0	0	0	0	1	0	1	0	0

The squares represent experimental values of Weicherz and Marschik,[33] and shows that the effect of mixing solvents increases the solubility substantially. A measure of error is defined to compare the different approaches. This is the average absolute deviation

$$\text{AAD} = \frac{1}{n}\sum_{k}^{n}\left|\frac{\delta x_1}{x_1}\right|_k . \tag{6–7}$$

Here, δx_1 is the difference in solubility from model to experiment. In this case, its value is 0.54, indicating that this system does not conform to the ideal mixture approach. The next illustration is application of the excess solubility model parameterized with three different methods (items $1-3$ above). Figure 6–1(b) shows the results for the cholesterol case. When fitting $\mathbf{f}^0$ to the experimental excess solubilities, the AAD drops to 0.10 with $f_{12}^0 = 2.86$ and $f_{13}^0 = 2.46$. The model gives a quantitative correlation of the data in the dioxane-rich end, but underestimates the data slightly as the composition of hexane is increased. This is contrary to using parameters obtained from applying the Porter equation for the solubilities in single solvents, Equation (4–46), which underestimates the data closer to pure dioxane slightly, but gives a quantitative estimation as hexane is added to the solution. This approach does not require ternary mixture data, but relies solely on the experimental solubilities in the pure solvents and the melting characteristics, required for calculating the ideal solubility. This is done by using the full Equation (3–13), since $\Delta c_{P,m,i} = 8.8\,\text{J/mol/K}$ for cholesterol, reported by Labowitz.[11] $f_{12}^0 = 0.93$ and $f_{13}^0 = 4.46$ is found using this method. These are different than those obtained from regression, but the results are quite similar to fitting the data, and gives an AAD $= 0.11$. Since f_{12}^0 is smaller than the ternary-based fit, the model underestimates the data slightly. In contrast, the f_{13}^0 is larger, giving a better estimation near pure hexane. Using UNIFAC to obtain the solute-solvent parameters in Equation (4–48) give poorer estimates of the excess solubility. UNIFAC gives $f_{12}^0 = 35.42$ and $f_{13}^0 = 16.42$, which disagrees significantly with those from ternary and binary data. UNIFAC frequently gives high values of limiting activity coefficients, γ_i^∞, in nonideal mixtures. This means, that the slope of γ_i must be high to compensate, which causes UNIFAC to overestimate the derivative in the dilute region. The final item listed above involves solving the isofugacity relation, Equation (3–13), for the solubilities and activity coefficients. The only input required for UNIFAC to generate activity coefficients are stoichiometries of groups in each molecule. These are given in Table 6–2 for the solute species.

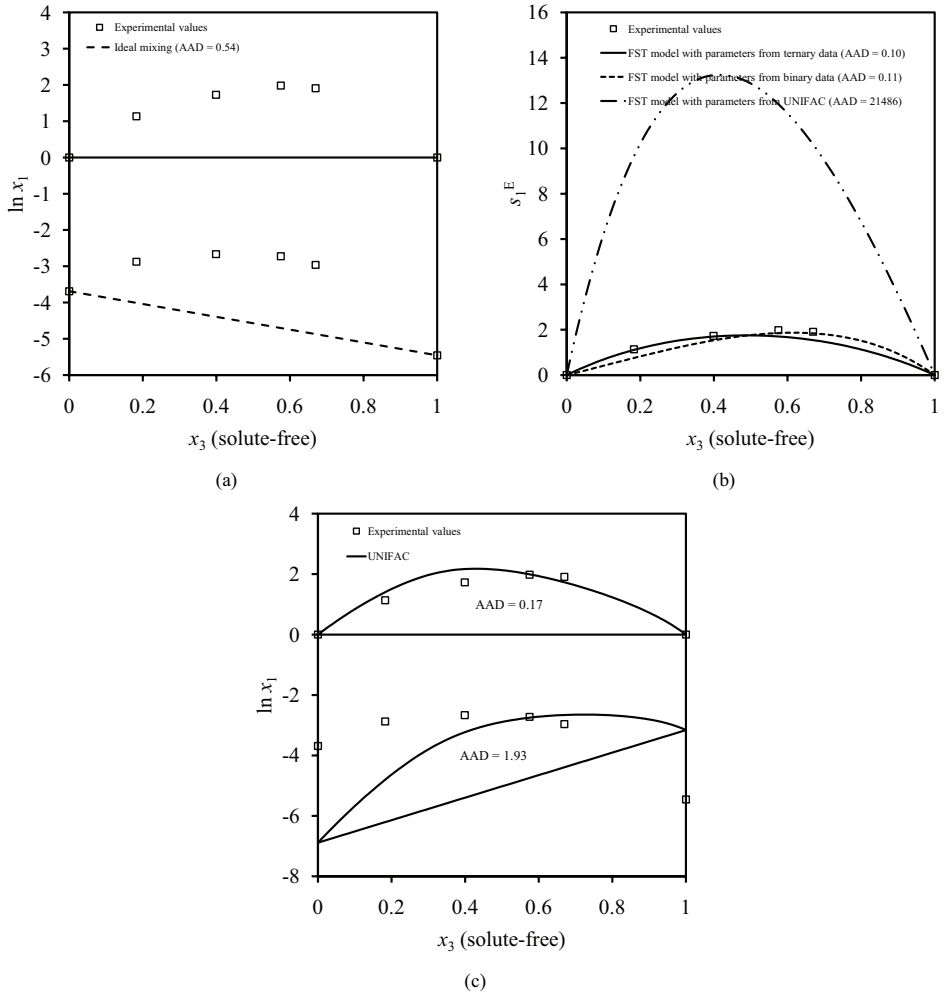

Figure 6–1. Solubility and excess solubility profiles of cholesterol(1) in a mixture of dioxane(2) and hexane(3) at 293 K. (a): Assuming ideal mixture. (b): Using the model outlined in this work with three different methods for solute-solvent parameters. (c): Using UNIFAC to solve Equation (3–13) for the solubility. Data of Weicherz and Marschik.[33]

Figure 6–1(c) shows the result for the cholesterol-dioxane-hexane case. Most notably is that UNIFAC is unable to accurately estimate either of the two single-solvent solubilities. UNIFAC estimates the solubility of cholesterol(1) in dioxane(2) to be $x_{1,2} = 0.001$, and in pure hexane(3) the estimate is $x_{1,3} = 0.042$. The experimental values are 0.025 and 0.0043, respectively, giving an AAD of 1.93. Remarkably, the excess solubility is much better described with UNIFAC. The error, when forming

$$\mathrm{AAD} = \frac{1}{n}\sum_{k}^{n}\left|\frac{\delta x_1}{x_1}\right|_k = \frac{1}{n}\sum_{k}^{n}\left|\frac{\bar{x}_1\hat{x}_1^{\mathrm{E}} - \bar{x}_1 x_1^{\mathrm{E}}}{\bar{x}_1 x_1^{\mathrm{E}}}\right|_k = \frac{1}{n}\sum_{k}^{n}\left|\frac{\delta x_1^{\mathrm{E}}}{x_1^{\mathrm{E}}}\right|_k . \tag{6–8}$$

is 0.17 and similar to applying the FST model, parameterized using either binary or ternary solubility data. In this equation, $\bar{x}_1$ is the ideal mixing term (summation over single-solvent solubilities) in the definition of the excess solubilities, while circumflex denotes a model-calculated value. This is an interesting feature of UNIFAC, and illustrates one of the main advantages when formulating solubilities in terms of mixing properties.

6.3.1. Transferability of parameters

The cholesterol case above reveals that the method is able to correlate $\mathbf{f}^0$ from a data set successfully. While this analysis can reveal much information about the data and the method, it limits the applicability unless the solute-solvent characteristics can assume universal values, i.e., that they are transferable for a solute in combinations of solvents. In order for the method presented here to apply generally, it is necessary that experimental excess solubilities follow certain trends. The structure of the model facilitates large excess solubilities in solvent mixtures which are more nonideal, due to the solvent-solvent term, which is large in nonideal mixture, and zero in ideal mixtures. The left plot of Figure 6–2 shows

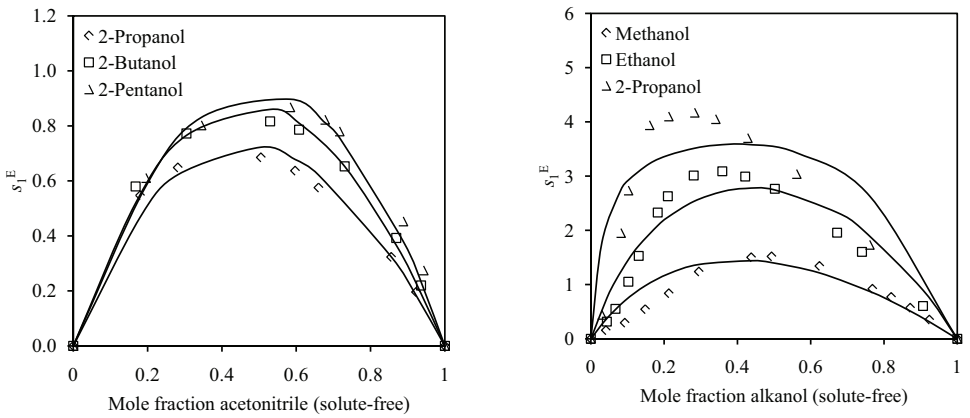

Figure 6–2. Excess solubility profiles of anthracene in mixture of acetonitrile and varying alkanol[34] (left) and naphthalene in aqueous alkanol mixtures[35] (right). Data for both solutes appear to be smooth, and suggests that the data is of good quality.

the excess solubility profiles of anthracene in mixtures of acetonitrile and alkanols of increasing chain lengths. The data points form smooth profiles, suggesting that the data is of high quality. It is difficult to make suggestions of thermodynamic consistency of solid-liquid equilibrium data,[36] but the profiles of the excess solubilities may help in identify potentially unreliably data. If the excess solubilities appear as erratic points, then it is likely to be flawed somehow. As the chain length of the alkanol solvent species increases, the solvent mixture becomes increasingly nonideal, which is in qualitative agreement with the data showing larger excess solubilities. The full-drawn curves in Figure 6–2 are model estimates us-

ing the same anthracene-acetonitrile parameter in all three mixtures. These, and the anthracene-alkanol parameters, are found by minimizing Equation (4–43). The right part of Figure 6–2 shows a similar plot, but for naphthalene in mixture of water and varying alkanols. As before, the data points form neat profiles with only minor scatter. The effects of solvent mixing is much more severe in these systems, indicated by the maximum excess solubility, which increases from 1 (methanol) to above 4 (2-propanol). This corresponds to a factor of more than 50 when converting to x_1^{E}. Using the same naphthalene-water parameter in all three systems, and regressing the remaining alkanol values along with the naphthalene–water value, the model is able to correlate much of the data. The excess solubility is very steep in the water rich end of the plot (left side), requiring a large value of f_{1j}^0 between solute and water. The model actually overestimates the data near pure water. However, in order for the model not to overestimate the data in the organic-rich side, the value is damped. This causes the model to underestimate the maxima in water–2-propanol and water–ethanol mixtures. These examples of systems with moderate and high excess solubilities demonstrate that the model is capable of correlating the data, within a margin of error, using transferable parameter values. The correlations of nonaqueous anthracene data sets were done quantitatively, while the errors in the aqueous systems were larger. The reasons for this are not clear at this point, but may involve the representation of the solvent mixture contribution to the excess solubility, i.e., $\partial \ln \gamma_3 / \partial x_3$. In the following, the role of the solvent mixture will be investigated. Figure 6–3 shows excess solubility profiles of anthracene in solvent mixtures of hexane, heptane, and octane with varying third component, measured by Acree Jr. and coworkers.[37–39] The first three plots (a-c) show systems, which similar to above, have clear trends in the variation of the excess solubility data. As the carbon chain length of the hydrocarbon solvent increases, the excess solubilities decrease, consistent with the solvent mixture being less nonideal. In the fourth system (d), the trend is not obviously consistent with the carbon number of the solvent. The order of increasing excess solubility appears to be octane > hexane > heptane. This is in contrast to the remaining three systems. The solid lines represent modes estimates using transferable solute-solvent parameters*. That means, that the same anthracene–hexane parameter

Table 6–3. Parameters for anthracene with solvent species in Figure 6–3.

Solvent, j	$f_{1j}^{0,a}$	$f_{1j}^{0,b}$	$f_{1j}^{0,c}$
Diethyl adipate	3.29	2.33	3.25
Ethyl acetate	0.28	-0.21	0.28
Butyl acetate	0.89	0.25	0.09
3-m-1-butanol	-0.66	-0.66*	n/a
Hexane	0.09	1.30	-0.10
Heptane	-0.20	0.57	-0.22
Octane	-0.41	0.17	-0.21
1-propanol	n/a	n/a	-0.58
1-butanol	n/a	n/a	-0.89
2-m-1-propanol	n/a	n/a	-0.42

* Not regressed.

* The full drawn lines are in fact interpolations of the model estimates at the experimental measurements.

is used in *all* four systems, and similar for heptane and octane. The remaining solute-solvent parameters (diethyl adipate, ethyl acetate, and butyl acetate) are limited to just one data set. The resulting parameters are given in Table 6–3 (second column, marked $f_{1j}^{0,a}$), and reveal that there is a trend in the alkane parameters, as they appear to decrease with increasing carbon number. Applying a model for a selected set of data, which show these kinds of trends, is expected to produce parameters that show a similar pattern. The model is not quite able to match the experimental data points. The reason for this lies with the inconsistent patterns in the 3-methyl-1-butanol sets. If these are removed from the regression, i.e., only data sets from Figure 6–3(a–c), the results differ remarkably compared to before. The third column shows the resulting parameters, $f_{1j}^{0,b}$. The values still decrease with increasing chain length for the alkane parameters, but are shifted upwards. The heptane and octane parameters are now positive, and the ethyl acetate value is now negative. Thus, a significant change occurs when excluding the data set with unsystematic trends. Figure 6–4 shows the resulting model-data agreement for all four systems, using the anthracene–3-methyl-1-butanol parameter regressed previously. The experimental data is correlated much better, when excluding the data containing 3-methyl-1-butanol as the one solvent component. Perhaps most notably is the excess solubilities in hexane–butyl acetate and hexane with ethyl acetate. The new parameter set also performs much better in the diethyl adipate sets, where the unsymmetric variation is now captured much better. While the remaining systems are correlated much better, the result is worsened significantly in the system, which was excluded from the optimization. This suggests that the excess solubility profiles of the excluded data is inconsistent with the remaining. As noted above, this does not imply that the data is thermodynamically inconsistent, but this unsystematic behavior does not facilitate application of a model based on a thermodynamic framework, since parameters of a model, which can be interpreted from a physical or thermodynamic point of view, must follow a systematic trend. If there is no systematic variation, it is unrealistic that any model can describe those data consistently. Even if the magnitude of the excess solubilities are small, the effects of discrepancies can be severe. The cases treated above are examples of anomalous behavior. From a modeling perspective, this means it is important to make systematic evaluations of the data from which model parameters are estimated. The excess solubility approach is a good way of detecting potentially inconsistent or unreliable data.

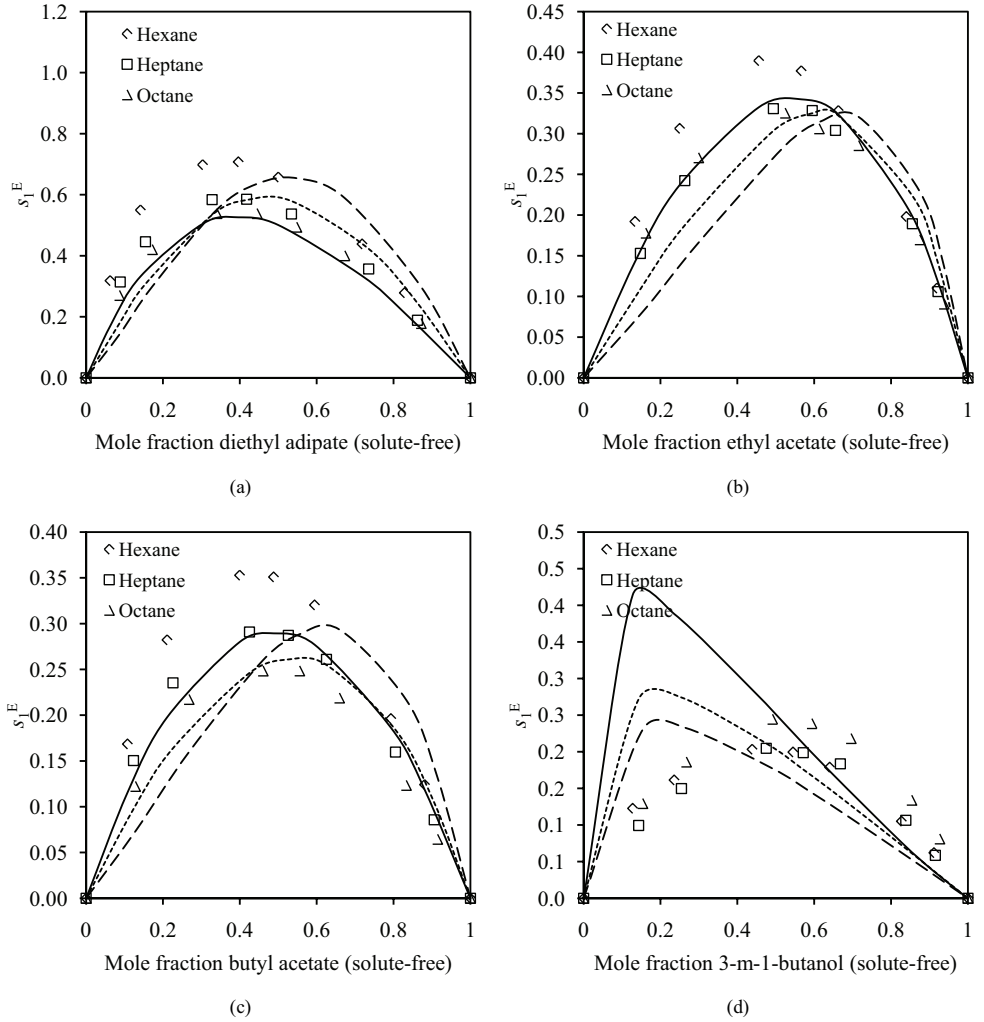

Figure 6–3. Excess solubility profiles and model estimates of anthracene in various solvent mixtures, with model parameters regressed from all data sets. Hexane: −, heptane: **..**, octane: −−. The model, with parameters regressed from all data sets, fails to give a consistent qualitative excess solubility estimate in all systems, since the data in subplot (d) does not vary consistently with increasing chain length of the solvent species.

If the analysis of systems is expanded to cover other types of solvent mixtures, the results may very accordingly. Figure 6–5 shows the effects of including 1-propanol, 1-butanol, and 2-methyl-1-propanol with the three alkane species, using the data of Zvaigzne et al.[40,41] and regressing all solute-solvent parameters globally. Their values are given in Table 6–3, column four. Unlike the previous estimates, the current parameters do not vary vary consistently with carbon chain length. Although the excess solubilities in these additional systems vary in a systematically, with octane having the larger value,

and hexane the smaller, the model is unable to capture the variation of the excess solubility. Most remarkably is the completely different variation in the model performance in the 1-propanol and 1-butanol systems. The estimates of anthracene excess solubilities in octane–1-propanol and octane–1-butanol differ significantly from those in the hexane and heptane systems, which are quite similar. The reason for this does not lie with the magnitude of the solute-solvent parameters, but is reflected by the variation of the solvent-solvent activity coefficient derivative, which goes into the model. Figure 6–6 shows the variation of the f_{23}^{+} for the solvent binaries. This is given by rearranging Equation (4–23),

$$f_{23}^{+} = -\frac{\dfrac{1}{x_2}\left(\dfrac{\partial \ln \gamma_3}{\partial x_3}\right)^{+}_{T,P,n_2}}{1 + x_3\left(\dfrac{\partial \ln \gamma_3}{\partial x_3}\right)^{+}_{T,P,n_2}}. \tag{6–9}$$

This is calculated using the Wilson equation with parameters regressed from experimental VLE data, as detailed in Chapter 5. The f_{23}^{+} is indicative of the weight of the nonideality contribution from the solvent mixtures at specific solvent compositions. Thus, if this property is large, then the excess solubility estimate from the model is highly contributed from this. On the other hand, if the value is small, the solvent mixture does not contribute significantly. Figure 6–6 shows that the variation of f_{23}^{+} in hexane–propanol and heptane–propanol is quite similar, with a strong peak in the region near pure alkane. The behavior of the octane–propanol binary is remarkably different, and is almost symmetric w.r.t. solvent composition. The behavior of 1-butanol with the three alkane solvents is similar. With 2-methyl-1-propanol the variation of f_{23}^{+} with hexane and octane is different than that with heptane. The result of this solute-free behavior, is that the model is unable to use the same set of parameters for describing excess solubilities in all these systems, when the solvent-solvent term is obtained from sources independent of the solid. The anthracene–hexane parameter appears to be to small in mixtures with diethyl adipate, ethyl acetate, and butyl acetate, while too large in mixtures with 1-propanol, 1-butanol, and 2-methyl-1-propanol. Similarly for heptane and octane. Apparently there is an inconsistency between the solute-free nonideality behavior (f_{23}^{+}, or more generally: $g^{\mathrm{E}}(2,3)$) and the excess solubility. The plots in Figure 6–6 reveal that the anomaly does not necessarily result from an inadequate excess solubility model, but rather that the behaviors of the solvent mixtures are incompatible with the solubility data.

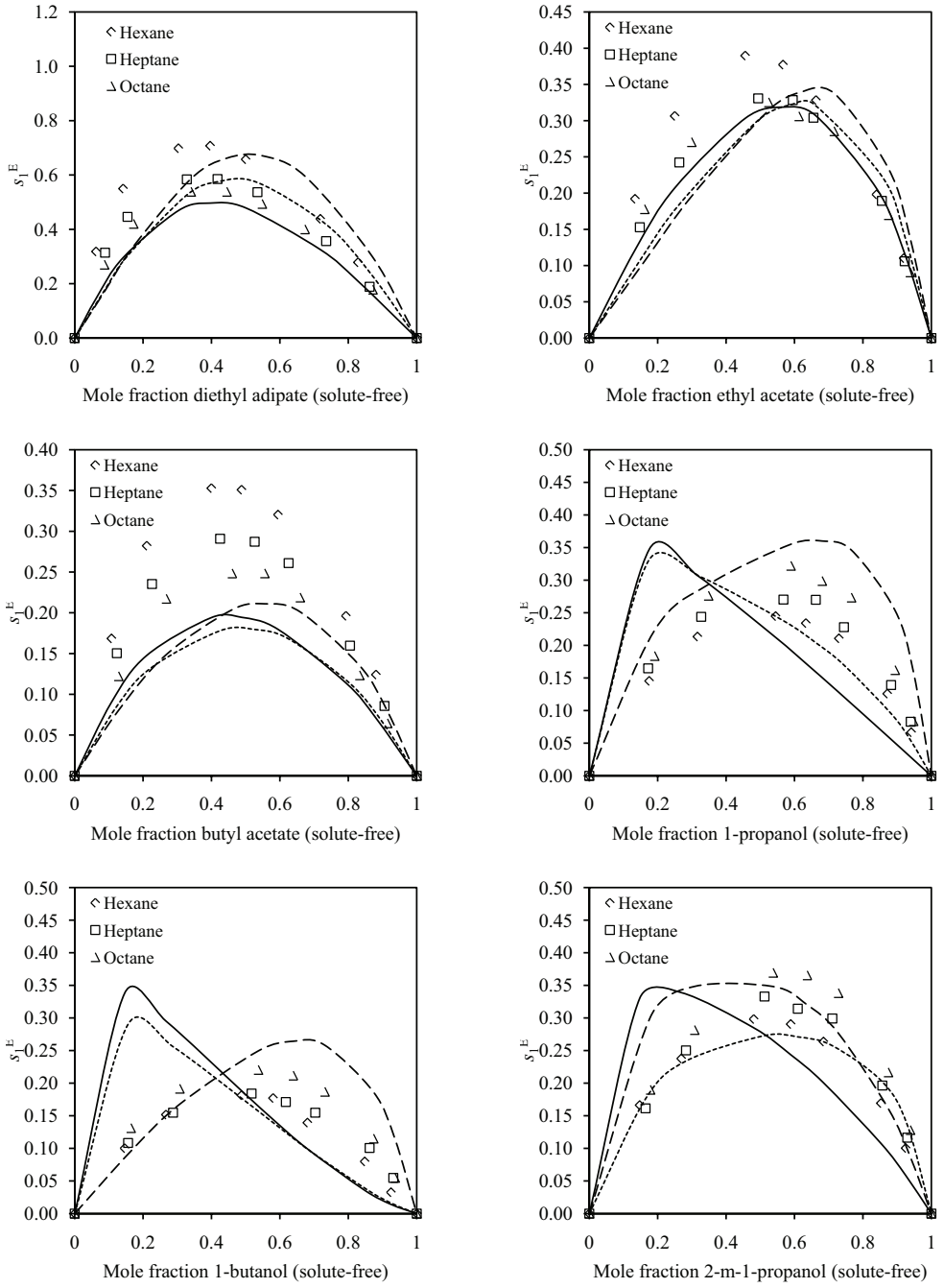

Figure 6–5. Excess solubility profiles and model estimates of anthracene in various solvent mixtures, with model parameters regressed only from data with consistent trends.

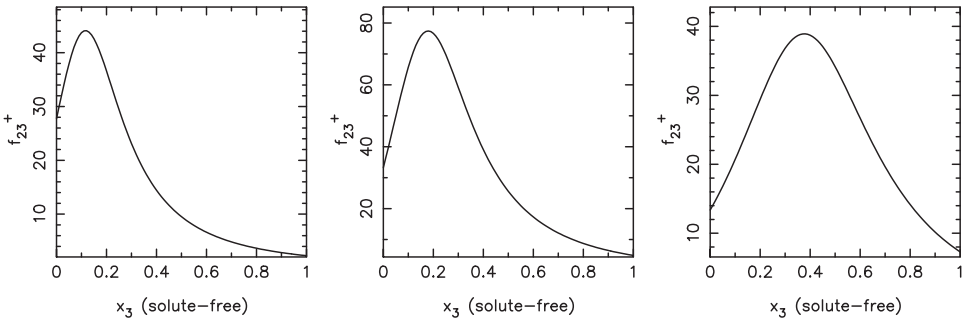

(a) Hexane(2)–propanol(3).[42] (b) Heptane(2)–propanol(3).[43] (c) Octane(2)–propanol(3).[44]

Figure 6–6. Variation of f_{23}^{+} for solvent mixtures calculated from the Wilson equation. The shape of this property is skewed towards the alkane-rich side for propanol with hexane and heptane, but almost symmetric for propanol with octane. This feature effects the excess solubility estimate in these solvent mixtures.

The systematic variation of the solubility should be followed by a systematic variation in the solvent mixture, since the FST model is highly dependent on this quantity. The results suggest that the model chosen for the solvent mixture may not be optimal. Although the parameters are regressed from experimental VLE data, the Wilson equation does not give a $g^{\mathrm{E}}(2,3)$ which is compatible with the solubility data. A method based on molecular structures, e.g. group contribution methods such as ASOG[46] or UNIFAC,[47] will always give a systematic variation of the g^{E}, and is likely to be a more suitable choice than the Wilson equation. However, with the perspective of estimating excess solubilities in potentially unmeasured systems, it is not possible to make comparisons of the solvent g^{E} and the excess solubilities. Furthermore, as discussed briefly in Chapter 5, UNIFAC is capable of predicting liquid-liquid equilibria in strongly nonideal mixtures, even in mixtures which are known not to have liquid-liquid phase separations. Basing the representation of the solvent nonideality on the Wilson ensures that no miscibility issues are encountered. This is another reason for using the Wilson equation.

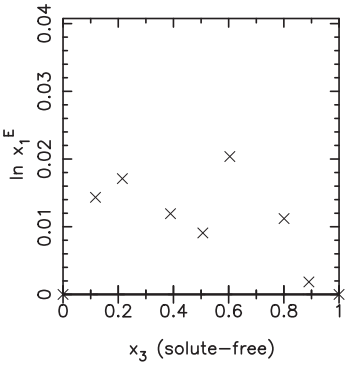

Figure 6–7. Scattering of excess solubilities of anthracene(1) in octanol(2) and 2-ethyl-1-hexanol(3) at 298 K,[45] suggesting data which is not suitable for parameter regression.

While the illustrations above might suggest that the method lacks merit, this is not the general case. As will be shown in the examples to come, the model is fully capable of describing a wide variety of behavior. The magnitudes of the excess solubilities in the plots of Figure 6–5 do not indicate that the effects of mixing is severe. An excess solubility of 0.3 corresponds to a correction of ~ 1.3 on mole

fraction basis, thus a 30% error compared to ideal mixing. The effects, which are correlated, appear to only minor, and may from a process design view point be negligible. As will be shown below, better results are obtained when correlating excess solubilities of a much larger magnitude. This suggests an advantage – when regressing parameters – of excluding data, when their excess solubilities are below a certain threshold. The solubilities in a substantial set of published mixed solvent systems conform to ideal mixing, and the excess solubilities are therefore negligible. In fact, much data – when represented as excess solubilities – appear as scatter about zero. An example is depicted in Figure 6–7, which shows the excess solubility of anthracene in octanol–2-ethyl-1-hexanol mixtures with data reported by Powell et al. [45] There are many sets similar to that in Figure 6–7, with small positive and negative effects. Adjusting values of $\mathbf{f}^0$ to describe effects that are almost not present is not likely to produce values with any physical significance, but merely satisfies the mathematical constraint of minimizing an objective function.

In the following section, results are presented pertaining to a variety of solutes. The solute-solvent parameters are temperature dependent by virtue of their definition in terms of correlation functions. The binary- and UNIFAC-based values of $\mathbf{f}^0$ has an explicit temperature dependence, but this is not the case when regressing the solute-solvent characteristics from ternary data. Figure 6–8 shows the temperature range of all systems studied, and the distribution is quite narrow. Almost 60% of all compiled data is at 25 °C, and 90% is between $20 - 30\,^{\circ}\mathrm{C}$. Therefore, the solute-solvent parameters, when regressed from data, are assumed temperature independent.

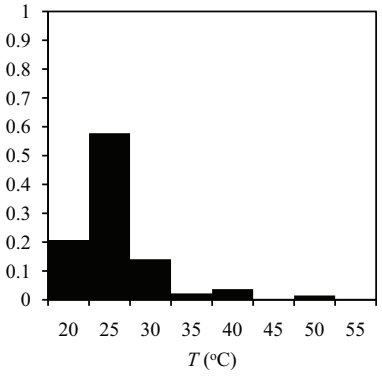

Figure 6–8. Temperatures of all solid-liquid data sets in data base, showing a narrow distribution around 25 °C.

This does not imply that the model estimate of the excess solubility (with parameters regressed from ternary data) is independent of temperature. The solvent-solvent f_{ij}^{+} and activity coefficient derivatives have explicit temperature dependencies qua their relations to g^{E}-models, and will therefore vary with temperature.

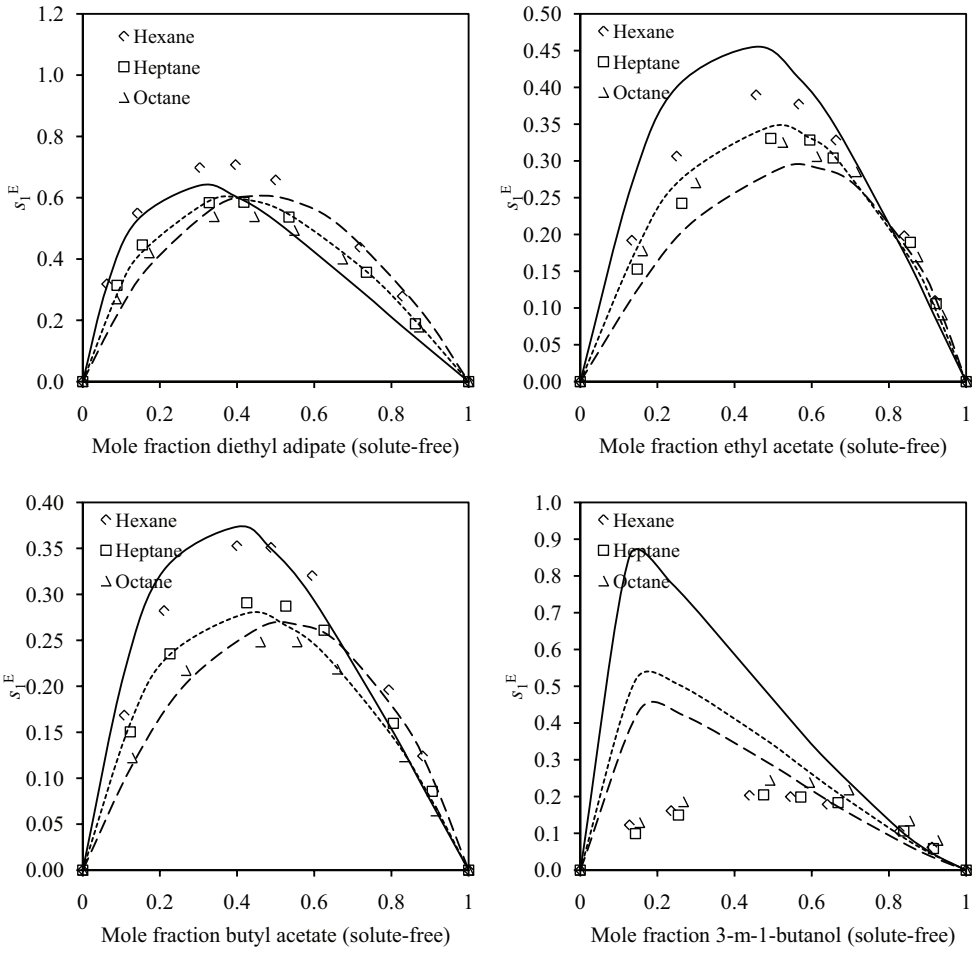

Figure 6–4. Excess solubility profiles and model estimates of anthracene in various solvent mixtures, with model parameters regressed only from data with consistent trends. Excluding the (apparently) inconsistent data from Figure 6–3 causes the model to give an overall improved description of the remaining data.

Table 6–4. Systems of solutes and solvents; n indicates the number of experimental observations and T is the temperature of the measurements. Parameters are listed, obtained from ternary solubility data, binary data, and from UNIFAC. Standard deviations (S.D.) are provided for the former. AAD is the error in solubility assuming ideal mixture (0), as calculated with parameters regressed from mixture data (I), parameters pure solvent data (II), parameters from UNIFAC (III), solubilities from UNIFAC (IV), and excess solubilities from UNIFAC (V).

Solute (1)	Solvent (2)	Solvent (3)	Ref.	n	T (°C)	$f_{12}^{0,t}$	S.D.	$f_{12}^{0,b}$	$f_{12}^{0,U}$	$f_{13}^{0,t}$	S.D.	$f_{13}^{0,b}$	$f_{13}^{0,U}$	AAD					
														0	I	II	III	IV	V
Anthracene	Hexane	Diethyl adipate	[38]	9	25	0.77	0.02	4.33	3.99	4.75	0.06	0.13	0.79	0.31	0.03	0.21	0.19	0.16	0.35
Anthracene	Cyclohexane	Diethyl adipate	[38]	9	25	1.17	0.01	3.93	3.26	4.75	0.06	0.13	0.79	0.31	0.03	0.19	0.15	0.17	0.51
Anthracene	Dimethyl adipate	Cyclohexane	[48]	9	25	2.41	0.02	0.47	1.29	1.17	0.01	3.93	3.26	0.34	0.03	0.30	0.23	0.17	0.49
Anthracene	Dimethyl adipate	Methylcyclohexane	[48]	9	25	2.41	0.02	0.47	1.29	0.56	0.01	3.81	2.99	0.32	0.03	0.35	0.26	0.14	0.39
Anthracene	1-Propanol	Diglyme	[49]	9	25	2.38	0.02	5.85	9.18	1.76	0.02	-0.07	2.43	0.33	0.01	0.29	1.05	0.16	0.49
Anthracene	2-Propanol	Diglyme	[49]	9	25	3.15	0.01	6.58	9.15	1.76	0.02	-0.07	2.43	0.37	0.03	0.27	0.82	0.23	0.45
Anthracene	2-Butanol	Diglyme	[49]	9	25	2.82	0.01	5.87	7.01	1.76	0.02	-0.07	2.43	0.32	0.04	0.26	0.58	0.18	0.43
Anthracene	2-Propanol	Acetonitrile	[50]	9	25	3.15	0.01	6.58	9.15	1.29	0.00	5.18	9.27	0.31	0.04	0.79	2.25	0.24	0.28
Anthracene	1-Butanol	Acetonitrile	[50]	9	25	2.86	0.03	5.25	7.03	1.29	0.00	5.18	9.27	0.33	0.02	0.67	2.00	0.25	0.30
Anthracene	2-Butanol	Acetonitrile	[50]	9	25	2.82	0.01	5.87	7.01	1.29	0.00	5.18	9.27	0.34	0.05	0.66	1.80	0.27	0.29
Anthracene	2-Methyl-1-propanol	Acetonitrile	[50]	9	25	3.54	0.03	6.31	7.01	1.29	0.00	5.18	9.27	0.34	0.03	0.72	1.84	0.27	0.29
Anthracene	3-Methyl-1-butanol	Acetonitrile	[50]	9	25	2.49	0.03	5.44	5.62	1.29	0.00	5.18	9.27	0.32	0.01	0.84	2.11	0.23	0.26
Anthracene	2-Methyl-1-butanol	Acetonitrile	[50]	9	25	2.69	0.03	5.29	5.62	1.29	0.00	5.18	9.27	0.33	0.01	0.78	2.05	0.24	0.26
Anthracene	1-Pentanol	Acetonitrile	[50]	9	25	2.87	0.03	4.62	5.64	1.29	0.00	5.18	9.27	0.34	0.01	0.67	1.99	0.25	0.32
Anthracene	2-Pentanol	Acetonitrile	[50]	9	25	3.64	0.03	5.25	5.62	1.29	0.00	5.18	9.27	0.37	0.02	0.66	1.85	0.29	0.28
Anthracene	2-Methyl-1-pentanol	Acetonitrile	[50]	9	25	3.29	0.03	4.87	4.64	1.29	0.00	5.18	9.27	0.36	0.01	0.76	2.11	0.27	0.27
Anthracene	4-Methyl-2-pentanol	Acetonitrile	[50]	9	25	3.04	0.03	5.30	4.63	1.29	0.00	5.18	9.27	0.35	0.02	0.82	2.08	0.26	0.27
Pyrene	1-Propanol	2-m-2-butanol	[51]	9	26	2.85	0.01	6.87	12.40	-2.77	1.95	6.15	8.16	0.01	0.01	0.04	0.05	0.03	0.19
Pyrene	2-Propanol	2-m-2-butanol	[51]	9	26	3.23	0.01	7.63	12.36	-2.77	1.95	6.15	8.16	0.02	0.01	0.01	0.02	0.00	0.08
Pyrene	1-Butanol	2-m-2-butanol	[51]	9	26	3.43	0.01	6.13	9.54	-2.77	1.95	6.15	8.16	0.00	0.00	0.01	0.01	0.00	0.21
Pyrene	2-m-1-propanol	2-m-2-butanol	[51]	9	26	4.03	0.01	7.40	9.51	-2.77	1.95	6.15	8.16	0.01	0.01	0.01	0.01	0.01	0.21
Pyrene	1-Pentanol	2-m-2-butanol	[51]	9	26	-2.90	1.58	5.35	7.68	-2.77	1.95	6.15	8.16	0.02	0.00	0.08	0.10	0.02	0.27
Pyrene	2-Pentanol	2-m-2-butanol	[51]	9	26	4.37	0.01	6.08	7.66	-2.77	1.95	6.15	8.16	0.00	0.00	0.01	0.01	0.00	0.09
Pyrene	3-m-1-butanol	2-m-2-butanol	[51]	9	26	3.41	0.01	6.39	7.66	-2.77	1.95	6.15	8.16	0.00	0.00	0.00	0.01	0.00	0.09
Pyrene	4-m-2-pentanol	2-m-2-butanol	[51]	9	26	9.35	44.37	6.14	6.34	-2.77	1.95	6.15	8.16	0.01	0.00	0.00	0.01	0.00	0.12
Pyrene	1-Propanol	Acetonitrile	[52]	9	25	2.85	0.01	6.82	12.41	0.93	0.00	6.11	12.83	0.29	0.02	1.03	5.35	0.23	0.45
Pyrene	2-Propanol	Acetonitrile	[52]	9	25	3.23	0.01	7.58	12.37	0.93	0.00	6.11	12.83	0.30	0.03	1.11	5.20	0.24	0.40
Pyrene	1-Butanol	Acetonitrile	[52]	9	25	3.43	0.01	6.08	9.55	0.93	0.00	6.11	12.83	0.32	0.02	0.91	4.40	0.26	0.44
Pyrene	2-Butanol	Acetonitrile	[52]	9	25	4.06	0.01	6.76	9.52	0.93	0.00	6.11	12.83	0.33	0.01	0.96	4.30	0.27	0.42
Pyrene	2-m-1-propanol	Acetonitrile	[52]	9	25	4.03	0.01	7.35	9.52	0.93	0.00	6.11	12.83	0.34	0.01	1.04	4.31	0.27	0.41
Pyrene	3-m-1-butanol	Acetonitrile	[52]	9	25	3.41	0.01	6.34	7.67	0.93	0.00	6.11	12.83	0.33	0.01	1.13	4.84	0.25	0.40
Pyrene	2-Pentanol	Acetonitrile	[52]	9	25	4.37	0.01	6.03	7.67	0.93	0.00	6.11	12.83	0.37	0.03	0.92	4.29	0.30	0.42

Continues on next page

Continued from last page

Solute (1)	Solvent (2)	Solvent (3)	Ref.	n	T (°C)	$f_{12}^{0,t}$	S.D.	$f_{12}^{0,b}$	$f_{12}^{0,U}$	$f_{13}^{0,t}$	S.D.	$f_{13}^{0,b}$	$f_{13}^{0,U}$	AAD					
														0	I	II	III	IV	V
Naphthalene	Water	Methanol	[53]	6	25	2.46	0.30	22.51	90.23	16.93	23.73	5.46	7.77	0.04	0.04	0.67	28.97	0.11	0.35
Naphthalene	Water	Ethanol	[53]	9	25	2.46	0.30	22.51	90.23	17.33	4.95	4.50	6.86	0.35	0.12	4.59	6E+06	0.20	0.39
Naphthalene	Water	Methanol	[35]	14	25	2.46	0.30	22.63	90.23	16.93	23.73	5.52	7.77	0.45	0.07	2.09	3660	0.21	0.16
Naphthalene	Water	Ethanol	[35]	15	25	2.46	0.30	22.63	90.23	17.33	4.95	4.58	6.86	0.66	0.41	9.86	1E+07	0.32	0.36
Naphthalene	Water	2-Propanol	[35]	12	25	2.46	0.30	22.63	90.23	15.93	4.14	4.59	4.82	0.74	0.79	185	1E+13	0.37	0.48
Naphthalene	Water	1,2-Propanediol	[35]	15	25	2.46	0.30	22.63	90.23	81.15	145.41	6.50	5.27	0.59	0.47	0.40	1.91	1.20	0.55
Naphthalene	Water	Acetone	[35]	15	25	2.46	0.30	22.63	90.23	12.90	1.95	1.73	3.57	0.78	1.00	13.45	5E+09	0.62	0.73
Naphthalene	Water	Dimethylsulfoxide	[35]	16	25	2.46	0.30	22.63	90.23	-18.06	2.32	2.50	4.29	0.68	1.22	0.86	0.87	0.15	0.41
Naphthalene	Water	Ethylene glycol	[13]	18	25	2.46	0.30	22.75	90.23	-47.66	87.32	8.49	17.68	0.38	0.23	0.65	0.82	0.34	0.18
Naphthalene	Ethylbenzene	Benzene	[54]	6	25	-1.91	7607.60	0.32	0.23	-0.33	26.41	0.29	-0.12	0.00	0.00	0.01	0.01	0.00	0.06
Naphthalene	Toluene	Benzene	[54]	7	25	-0.48	5907.30	0.33	0.04	-0.33	26.41	0.29	-0.12	0.00	0.00	0.00	0.00	0.00	0.09
Naphthalene	Carbon tetrachloride	Benzene	[54]	6	25	-1.31	599.62	0.73	0.93	-0.33	26.41	0.29	-0.12	0.00	0.00	0.02	0.02	0.01	0.09
Naphthalene	Hexadecane	Benzene	[54]	6	25	-7.21	2060.60	1.39	0.41	-0.33	26.41	0.29	-0.12	0.03	0.02	0.07	0.05	0.02	0.06
Naphthalene	Cyclohexane	Benzene	[54]	8	25	1.02	64.13	2.09	1.79	-0.33	26.41	0.29	-0.12	0.07	0.00	0.05	0.03	0.03	0.20
Naphthalene	Hexane	Benzene	[54]	8	25	0.80	62.13	2.56	2.04	-0.33	26.41	0.29	-0.12	0.07	0.00	0.08	0.05	0.01	0.20
Beta carotene	Acetone	Cyclohexane	[55]	6	20	4.46	0.18	7.89	34.71	1.95	0.08	2.16	-15.64	0.50	0.10	0.51	73.25	0.34	24.38
Beta carotene	Acetone	Hexane	[55]	6	20	4.46	0.18	7.89	34.71	1.35	0.09	4.54	-11.06	0.45	0.29	1.87	275	0.76	49.99
Beta carotene	Acetone	Toluene	[55]	6	20	4.46	0.18	7.89	34.71	3.11	1.59	-0.50	-20.14	0.29	0.08	0.10	1.75	0.79	14.38
Beta carotene	MEK	Cyclohexane	[55]	8	20	7.33	0.48	4.45	20.41	1.95	0.08	2.16	-15.64	0.58	0.32	0.29	1.80	0.04	12.42
Beta carotene	MEK	Hexane	[55]	5	20	7.33	0.48	4.45	20.41	1.35	0.09	4.54	-11.06	0.44	0.22	0.24	0.57	0.12	24.49
Beta carotene	MEK	Toluene	[55]	5	20	7.33	0.48	4.45	20.41	3.11	1.59	-0.50	-20.14	0.31	0.18	0.26	0.27	0.23	4.87
Beta carotene	1,2-Dimethoxyethane	Cyclohexane	[56]	12	20	2.81	0.15	5.19	41.41	1.95	0.08	1.74	-15.64	0.52	0.14	0.23	149	0.35	8.04
Beta carotene	1,2-Dimethoxyethane	Hexane	[56]	12	20	2.81	0.15	5.19	41.41	1.35	0.09	4.60	-11.06	0.46	0.12	1.46	634	0.79	21.93
Beta carotene	Cyclohexanone	Cyclohexane	[57]	11	20	6.16	0.40	1.94	4.39	1.95	0.08	1.74	-15.64	0.40	0.08	0.20	0.64	0.08	12.38
Beta carotene	Cyclohexanone	Hexane	[57]	12	20	6.16	0.40	1.94	4.39	1.35	0.09	4.60	-11.06	0.43	0.11	0.22	0.55	0.14	24.89
Beta carotene	Diglyme	Cyclohexane	[58]	9	20	1.89	0.16	4.35	34.40	1.95	0.08	2.06	-15.64	0.49	0.27	0.47	10.06	0.21	5.98
Beta carotene	Diglyme	Hexane	[58]	10	20	1.89	0.16	4.35	34.40	1.35	0.09	4.50	-11.06	0.48	0.08	1.35	75.47	0.14	10.66
Beta carotene	Diglyme	1-Hexene	[58]	11	20	1.89	0.16	4.35	34.40	1.12	0.17	3.01	-20.31	0.32	0.14	0.93	11.22	0.19	12.84
Beta carotene	Acetone	1-Hexene	[58]	10	20	4.46	0.18	8.20	34.71	1.12	0.17	3.01	-20.31	0.54	0.13	0.62	14.12	0.34	33.69
Beta carotene	Cyclohexanone	1-Hexene	[58]	12	20	6.16	0.40	1.94	4.39	1.12	0.17	3.01	-20.31	0.40	0.12	0.20	0.60	0.10	18.90
Aminopyrine	Water	Ethanol	[60]	11	25	5.59	0.04			1.86	0.25			0.55	0.07				
Aminopyrine	1,4-Dioxane	Water	[61]	13	25	-0.09	0.07			5.59	0.04			0.55	0.09				
Antipyrine	Water	Ethanol	[60]	11	25	0.35	0.01			-0.24	0.06			0.17	0.04				
Antipyrine	1,4-Dioxane	Water	[61]	13	25	-0.09	0.02			0.35	0.01			0.22	0.04				
4-Hydroxybenzoic acid	Water	1,4-Dioxane	[3]	13	25	14.58	0.43	7.24	21.60	-1.31	0.68	-3.17	0.40	0.78	0.18	0.68	3.41	0.66	1.84
Testosterone	Cyclohexane	Chloroform	[59]	15	25	26.73	0.96	11.27	41.61	5.90	0.55	-4.07	0.87	0.57	0.07	0.49	0.40	0.39	10.22

Continues on next page

Continued from last page

Solute (1)	Solvent (2)	Solvent (3)	Ref.	n	T (°C)	$f_{12}^{0,t}$	S.D.	$f_{12}^{0,b}$	$f_{12}^{0,U}$	$f_{13}^{0,t}$	S.D.	$f_{13}^{0,b}$	$f_{13}^{0,U}$	AAD					
														0	I	II	III	IV	V
4-Hexylresorcinol	Hexane	Ethyl acetate	[1]	6	26	15.04	64.39	13.30	85.09	8.38	55.47	-6.50	-20.15	0.61	0.59	0.58	686	0.45	2.60
4-Hexylresorcinol	Ethyl myristate	Ethyl acetate	[1]	6	26	-102.17	687.59	-3.27	-2.62	8.38	55.47	-6.50	-20.15	0.02	0.34	0.09	0.21	0.04	0.07
4-Hexylresorcinol	Hexane	Ethyl myristate	[1]	6	26	15.04	64.39	13.30	85.09	-102.17	687.59	-3.27	-2.62	0.60	0.60	0.61	0.64	0.47	2.59
Sulfamethazine	Water	1,4-Dioxane	[62]	19	25	16.38	0.10	16.21		1.70	0.12	3.82		0.78	0.10	0.35			
Sulfamethazine	Water	Ethanol	[25]	11	25	16.38	0.10	16.21		5.32	0.23	5.20		0.76	0.17	0.17			
Sulfamethazine	Ethyl acetate	Ethanol	[25]	14	25	1.87	0.39	4.00		5.32	0.23	5.20		0.50	0.15	0.27			
Sulfamethoxypyridazine	Water	1,4-Dioxane	[62]	18	25	12.81	0.28	12.09		5.57	0.64	-0.87		0.83	0.51	0.67			
Sulfamethoxypyridazine	Ethanol	Water	[28]	7	20	2.89	0.51	4.70		12.81	0.28	11.86		0.60	0.60	0.51			
Sulfamethoxypyridazine	Ethanol	Water	[28]	7	25	2.89	0.51	4.78		12.81	0.28	12.08		0.60	0.51	0.46			
Sulfamethoxypyridazine	Ethanol	Water	[28]	7	30	2.89	0.51	5.06		12.81	0.28	11.88		0.62	0.44	0.37			
Sulfamethoxypyridazine	Ethanol	Water	[28]	7	35	2.89	0.51	4.92		12.81	0.28	11.86		0.61	0.37	0.29			
Sulfamethoxypyridazine	Ethanol	Water	[28]	7	40	2.89	0.51	5.34		12.81	0.28	12.24		0.63	0.30	0.24			
Sulfamethoxypyridazine	Ethanol	Ethyl acetate	[28]	5	20	2.89	0.51	4.70		2.93	0.84	3.92		0.39	0.07	0.14			
Sulfamethoxypyridazine	Ethanol	Ethyl acetate	[28]	5	25	2.89	0.51	4.78		2.93	0.84	4.08		0.36	0.03	0.22			
Sulfamethoxypyridazine	Ethanol	Ethyl acetate	[28]	5	30	2.89	0.51	5.06		2.93	0.84	4.20		0.37	0.04	0.23			
Sulfamethoxypyridazine	Ethanol	Ethyl acetate	[28]	5	35	2.89	0.51	4.92		2.93	0.84	4.18		0.33	0.05	0.35			
Sulfamethoxypyridazine	Ethanol	Ethyl acetate	[28]	5	40	2.89	0.51	5.34		2.93	0.84	4.06		0.31	0.09	0.38			
Sulfamethoxypyridazine	Water	Ethanol	[27]	13	25	12.81	0.28	12.10		2.89	0.51	4.78		0.70	0.45	0.40			
Sulfamethoxypyridazine	Ethyl acetate	Ethanol	[27]	14	25	2.93	0.84	4.08		2.89	0.51	4.78		0.44	0.04	0.35			
Sulfamethoxypyridazine	Ethyl acetate	Hexane	[27]	4	25	2.93	0.84	4.08		-3.52	5.87	21.28		0.09	0.01	22.87			
Sulfanilamide	Water	Ethanol	[25]	12	25	10.91	0.64	8.64		-0.09	2.13	3.76		0.62	0.66	0.41			
Sulfanilamide	Ethyl acetate	Ethanol	[25]	10	25	4.99	4.45	3.41		-0.09	2.13	3.76		0.44	0.18	0.24			
Sulfanilamide	Water	1,4-Dioxane	[63]	16	25	10.91	0.64	8.64		3.10	0.96	-1.20		0.77	0.32	0.61			
Paracetamol	1,4-Dioxane	Water	[61]	11	25	4.05	0.25	0.95		7.19	0.05	7.49		0.67	0.40	0.23			
Paracetamol	Water	Ethanol	[64]	11	30	7.19	0.05	7.01		2.54	0.37	0.27		0.54	0.32	0.25			
Paracetamol	Water	Ethanol	[17]	13	25	7.19	0.05	7.37		2.54	0.37	0.72		0.61	0.25	0.32			
Paracetamol	Ethyl acetate	Ethanol	[17]	13	25	5.22	0.67	4.72		2.54	0.37	0.72		0.43	0.14	0.13			
Paracetamol	Water	1,4-Dioxane	[17]	17	25	7.19	0.05	7.37		4.05	0.25	0.97		0.79	0.42	0.50			
Paracetamol	Ethyl acetate	Methanol	[65]	14	25	5.22	0.67	4.92		-1.09	0.21	1.25		0.45	0.11	0.66			
Paracetamol	Methanol	Water	[65]	7	25	-1.09	0.21	1.25		7.19	0.05	8.64		0.20	0.32	0.42			
Paracetamol	Ethanol	Methanol	[65]	3	25	2.54	0.37	0.96		-1.09	0.21	1.25		0.00	0.03	0.03			
Paracetamol	Acetone	Toluene	[18]	13	20	3.18	0.15	1.57		3.93	0.82	11.39		0.28	0.09	0.46			
Paracetamol	Acetone	Toluene	[18]	13	25	3.18	0.15	1.52		3.93	0.82	11.57		0.30	0.07	0.39			
Paracetamol	Acetone	Toluene	[18]	13	30	3.18	0.15	1.49		3.93	0.82	11.93		0.34	0.07	0.29			
Paracetamol	Water	Acetone	[18]	10	20	7.19	0.05	7.63		3.18	0.15	1.57		0.62	0.11	0.22			
Paracetamol	Water	Acetone	[18]	15	23	7.19	0.05	7.56		3.18	0.15	1.55		0.71	0.13	0.21			

Continues on next page

Continued from last page

Solute (1)	Solvent (2)	Solvent (3)	Ref.	n	T (°C)	$f_{12}^{0,t}$	S.D.	$f_{12}^{0,b}$	$f_{12}^{0,U}$	$f_{13}^{0,t}$	S.D.	$f_{13}^{0,b}$	$f_{13}^{0,U}$	AAD					
														0	I	II	III	IV	V
Paracetamol	Water	Acetone	[18]	10	25	7.19	0.05	7.51		3.18	0.15	1.52		0.62	0.10	0.20			
Paracetamol	Water	Acetone	[18]	15	30	7.19	0.05	7.38		3.18	0.15	1.49		0.70	0.13	0.17			
Phenacetin	Water	1,4-Dioxane	[63]	13	40	13.86	0.20	13.21		2.06	0.53	2.65		0.76	0.23	0.27			
Phenacetin	Water	1,4-Dioxane	[63]	13	35	13.86	0.20	13.34		2.06	0.53	2.66		0.76	0.23	0.27			
Phenacetin	Water	1,4-Dioxane	[63]	13	30	13.86	0.20	13.34		2.06	0.53	2.78		0.75	0.20	0.24			
Phenacetin	Water	1,4-Dioxane	[63]	13	25	13.86	0.20	13.51		2.06	0.53	2.92		0.76	0.21	0.23			
Phenacetin	Water	1,4-Dioxane	[63]	13	20	13.86	0.20	13.63		2.06	0.53	3.01		0.76	0.21	0.22			
Phenacetin	Water	1,4-Dioxane	[21]	13	25	13.86	0.20	13.12		2.06	0.53	2.93		0.71	1.06	0.93			
Phenacetin	Water	Ethanol	[21]	11	25	13.86	0.20	13.12		1.29	1.57	3.26		0.66	1.06	0.95			
Phenacetin	Ethyl acetate	Ethanol	[21]	11	25	0.57	3.51	3.14		1.29	1.57	3.26		0.30	0.09	0.47			
Theophylline	Water	1,4-Dioxane	[31]	21	25	5.44	0.19	6.51		5.38	1.02	4.02		0.74	0.35	0.28			
Theophylline	Water	Methanol	[13]	13	25	5.44	0.19	6.89		7.60	7.90	5.33		0.37	0.16	0.23			
Theophylline	Water	Acetonitrile	[13]	17	25	5.44	0.19	6.89		1.17	0.44	7.61		0.59	0.35	2.98			
Desmosterol	Hexane	Ethanol	[10]	10	20	1.43	0.02	7.07	18.37	4.15	0.03	7.71	30.92	0.64	0.10	4.78	8686	0.39	11.35
Desmosterol	Hexane	Ethanol	[10]	10	25	1.43	0.02	6.85	17.04	4.15	0.03	7.51	30.70	0.64	0.09	4.31	6106	0.45	10.33
Desmosterol	Hexane	Ethanol	[10]	10	30	1.43	0.02	6.64	15.82	4.15	0.03	7.31	30.48	0.64	0.10	3.79	4352	0.53	9.62
Desmosterol	Hexane	Ethanol	[10]	10	40	1.43	0.02	6.08	13.66	4.15	0.03	6.77	30.05	0.61	0.06	3.24	2779	0.56	8.09
Desmosterol	Hexane	Ethanol	[10]	10	50	1.43	0.02	5.09	11.82	4.15	0.03	6.35	29.64	0.55	0.29	3.15	2304	0.52	6.25
Cholesterol	Hexane	Ethanol	[10]	10	20	2.46	0.03	4.45	16.41	4.20	0.04	4.96	27.72	0.66	0.08	0.65	2312	0.22	2.20
Cholesterol	Hexane	Ethanol	[10]	10	25	2.46	0.03	4.63	15.17	4.20	0.04	5.05	27.56	0.66	0.08	0.69	1634	0.26	2.41
Cholesterol	Hexane	Ethanol	[10]	10	30	2.46	0.03	4.39	14.03	4.20	0.04	5.03	27.40	0.65	0.07	0.75	1330	0.24	2.37
Cholesterol	Hexane	Ethanol	[10]	10	40	2.46	0.03	4.34	12.03	4.20	0.04	4.89	27.09	0.63	0.14	0.85	897	0.23	2.44
Cholesterol	Hexane	Ethanol	[10]	10	50	2.46	0.03	4.23	10.32	4.20	0.04	4.88	26.79	0.62	0.19	0.88	627	0.25	2.36
Cholesterol	1,4-Dioxane	Ethanol	[33]	6	20	2.88	0.25	0.93	35.42	4.20	0.04	6.12	27.72	0.26	0.29	0.33	238	0.07	0.70
Cholesterol	Benzene	1,4-Dioxane	[33]	6	20	2.33	0.15	0.70	-1.84	2.88	0.25	0.93	35.42	0.17	0.14	0.16	0.18	0.59	0.97
Cholesterol	Benzene	Hexane	[33]	7	20	2.33	0.15	0.70	-1.84	2.46	0.03	4.46	16.42	0.42	0.26	0.28	0.18	0.32	2.77
Cholesterol	Ethanol	Hexane	[33]	6	20	4.20	0.04	6.12	27.72	2.46	0.03	4.46	16.42	0.58	0.26	0.18	1111	0.34	2.20
Cholesterol	Ethanol	Benzene	[33]	9	20	4.20	0.04	6.12	27.72	2.33	0.15	0.70	-1.84	0.59	0.19	0.03	28.38	0.19	1.06
Cholesterol	1,4-Dioxane	Hexane	[33]	6	20	2.88	0.25	0.93	35.42	2.46	0.03	4.46	16.42	0.54	0.10	0.11	21486	0.17	1.93
Mefenamic Acid	Water	Ethanol	[12]	11	25	1.44	0.32	15.69		4.47	0.67	3.06		0.41	0.21	9.14			
Mefenamic Acid	Ethyl acetate	Ethanol	[12]	10	25	2.34	0.95	1.56		4.47	0.67	3.06		0.45	0.14	0.14			

6.4. Excess solubilities in binary solvent mixtures

Anthracene

The first solute which will be highlighted is a continuation of the discussion above. Anthracene belongs to the family of polycyclic aromatic hydrocarbons (PAHs), which consists of fused aromatic rings, causing a rigid molecular structures. For this reason $\Delta c_{P,m,i} = 0$ is a reasonable choice. Anthracene is perhaps the most abundantly studied solute in mixed solvents, primarily due to Acree Jr. and various coworkers from the 1980s and on. More than 200 data sets have been compiled, with solvent mixtures typically composed of hydrocarbons, alkanols, ethers, or ketones. Based on reflections on the discussion above, it was decided to establish a lower limit of the AAD-0 for inclusion in the analysis. If the average deviation from ideal mixing was less than 0.3 (AAD-0), the data set was not included in the analysis. Thus, systems with AAD-0 less than 0.3 were systematically eliminated. Remaining of the original 226 data sets are the 17 systems shown in Table 6–4. Common to all is, that one solvent species is either a linear or branched alkanol. The other solvent species in the pairs are either alkane, ether, or nitrile-based. This procedure ensures that data contributing less to estimating parameters are not included in the optimization, and therefore the parameter values which are produced should reflect actual solute-solvent behavior. The effect of excluding data with small excess solubilities is that the remaining sets seems

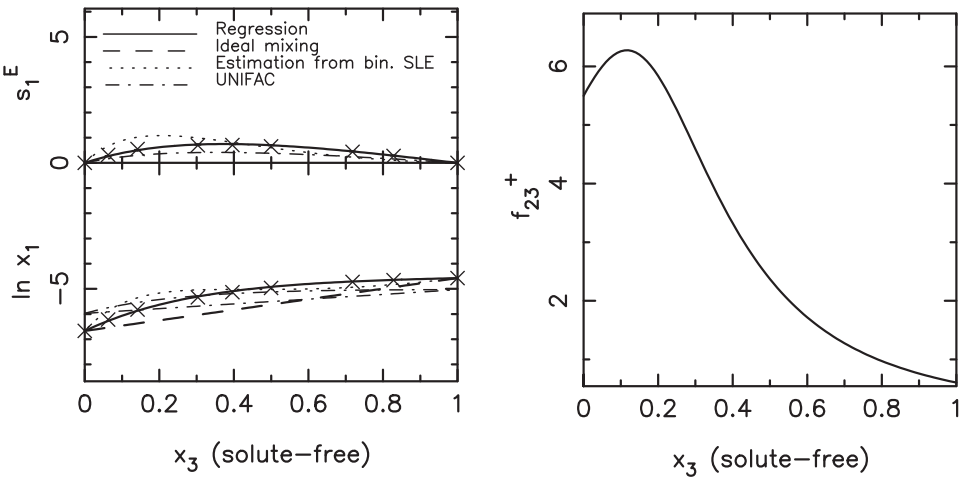

Figure 6–9. Excess solubilities of anthracene(1) in hexane(2) and diethyl adipate(3) and f_{23}^+ of the solvent binary at 25 °C. The profile of the experimental excess solubility is asymmetric, which is supported by the asymmetric profile of the f_{23}^+ of the solvent mixture.

to show a good degree of compatibility between the nonideality in the solvent mixture (characterized by f_{23}^+) and the excess solubilities of the solids. This means, that mixtures where the excess solubility profile is asymmetric also have asymmetric variations of f_{23}^+. Figure 6–9 illustrates this. Solubilities and

excess solubilities are displayed on the vertical axis. The symbols denote experimental measurements. The solid curve gives the results with the regressed parameters $\mathbf{f}^0$ obtained regression of ternary mixture data. The dashes give the ideal mixture solubility from equating to zero the excess solubility. The dotted lines give the results with $\mathbf{f}^0$ obtained from applying the Porter equation to single solvent solubilities. Dash-dot lines shows the results when UNIFAC is used to solve the isofugacity criterion in Equation (3–13). Thus, it is not results of using UNIFAC for $\mathbf{f}^0$. Regressing $\mathbf{f}^0$ from data gives an AAD-I of 0.03. Generally, the errors from regressing solute-solvent parameters are less than 0.05, indicating that the model-data agreement is excellent. The solute-solvent parameters obtained from binary data and UNIFAC are consistent with each other, but the anthracene–hexane parameter is larger than the fitted value, whereas the anthracene–diethyl adipate is much smaller, indicated by Table 6–4. Consequently, the model does not give as good estimates of the data. Figure 6–9 shows, that the experimental measurements are overestimated near pure hexane, but underestimated near pure ethyl adipate, when applying the binary-based parameter set. These results are general of all the anthracene sets in Table 6–4.

The regressed solute-solvent parameters are also listed in Table 6–4. The systems remaining after exclusion do not facilitate a significant analysis of the parameter values w.r.t. carbon chain length, as was done above. However, a few homologous series are present and are shown in Table 6–5. The first

Table 6–5. Values of f_{12}^0 for anthracene(1) with varying solvents. The solute-solvent parameters often increase or decrease with increasing chain length/carbon number, but this is not always the case, which is also seen in this table.

Solvent(2)	f_{12}^0	Solvent(2)	f_{12}^0	Solvent(2)	f_{12}^0
1-propanol	2.38	2-propanol	3.15	2-methyl-1-propanol	3.54
1-butanol	2.86	2-butanol	2.82	2-methyl-1-butanol	2.49
1-pentanol	2.87	2-pentanol	3.64	2-methyl-1-pentanol	3.29

two columns reveal, that there is a tendency for the f_{12}^0 to increase with carbon number. However, this trend is not repeated for the branched alkanols in columns 3-4 or 5-6.

Applying UNIFAC for computing x_1 as function of solvent composition often gives results which are in disagreement with the experimental solubilities. UNIFAC often overestimates solubilities in hydrocarbon solvents, while underestimating in diglyme (an ether). As a consequence, the mixed solvent solubilities are estimated wrongfully as well. UNIFAC gives good estimates in alkanols and just a slight overestimation in acetonitrile. However, the excess solubilities are consequently too small in magnitude for all anthracene mixtures in Table 6–4.

Pyrene

Pyrene is available for investigation in 15 mixtures of 11 different solvent species. The majority of systems are comprised of mixtures of alkanols, in addition to a few systems with alkanols and acetonitrile. Pyrene dissolves almost equally in all of these solvents around 0.01 in mole fraction, thus

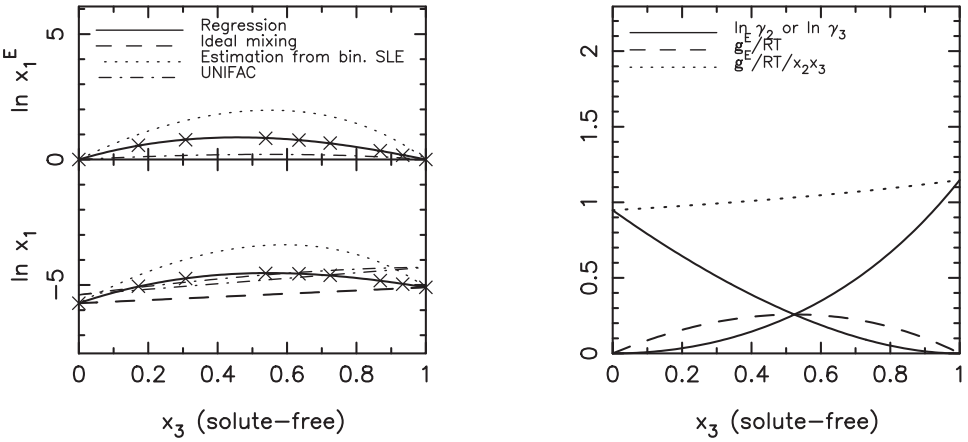

Figure 6–10. Solubility of pyrene(1) in 2-methyl-1-propanol(2)–acetonitrile(3) and excess free energy of the solvent mixture. Most pyrene systems are almost ideal, with negligible excess solubilities, but this is an example of a system with significant departure from ideal mixing.

verging on the limit of infinite dilution. This limit is typically set at 0.01 in mole fractions,[67] but may vary, depending on the system. The excess solubilities are vanishingly small in the alkanol mixtures, since these form almost completely ideal solutions, and the error of assuming ideal mixture gives AADs of these systems less than 0.02. Therefore, these systems do not pose any significant departures from ideal behavior. Regressing $\mathbf{f}^0$ from mixture data gives similar results for the alkanol mixtures, as do the cases where $\mathbf{f}^0$ is obtained from single solvent data or UNIFAC. If UNIFAC is used to solve Equation (3–13) for the solubilities, results are worsened, since UNIFAC usually underestimates the solubilities in alkanols. Therefore, the mixed solvent solubility estimates are also off.

The seven mixtures with acetonitrile in Table 6–4 behave differently, since the excess solubilities in these mixtures are much more significant. Figure 6–10 illustrates this with 2-methyl-1-propanol with acetonitrile. The left plot shows solubility and excess solubility profiles of the solute as function of solvent composition. The notation $\ln x_1^{\mathrm{E}}$ is here used to denote excess solubility. The right plot shows the activity coefficients and excess free energy of the solvent binary. The excess solubility has a maximum of around 1.0, which corresponds to a correction factor from ideal mixing of nearly 3. Using $\mathbf{f}^0$ regressed from ternary mixture data gives an almost perfect fit, yielding an AAD of 0.01. Using solubilities in individual solvents, Equation (4–46), results in overestimation of the mixing behavior.

The solute-solvent parameters are nearly double those found from regressions. UNIFAC is unable to give accurate estimates of either solubility nor excess solubility, since the excess solubility estimates from UNIFAC are too small in comparison with experiment.

Naphthalene

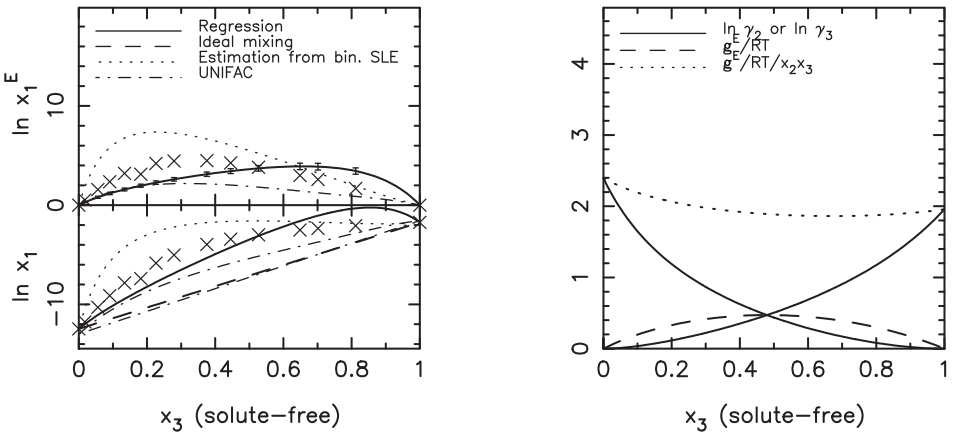

Figure 6–11. Solubility of naphthalene(1) in water(2)–acetone(3) and excess free energy of the solvent mixture. Both plots show considerable nonideal behavior, but the model is unable to give a good estimate of the experimental excess solubility data.

Naphthalene also belongs to the PAH family of hydrocarbons. This means that $\Delta c_{P,m,i} = 0$ is a reasonable approximation. Heric and Posey [54] reported solubilities of naphthalene in mixtures of benzene with varying hydrocarbons. The solubility is around 0.1 in mole fraction, varying slightly between solvent species. The solvent mixtures are nearly ideal (in the Lewis-Randall sense). Because of this, estimation using solute-solvent parameters from regression and single solvent solubility performs adequate. The solubility of naphthalene in pure water is around 10^{-6}, and addition of organic cosolvents increases this value significantly. Dickhut et al. [53] measured the solubilities of naphthalene in water and small alkanols, but measurements were limited to almost pure water, making the effect of mixing solvents difficult to observe. Later, Lepree et al. [35] measured similar systems, including propylene glycol and acetone as cosolvents across the entire range of compositions. The nonideality in the solvent systems is usually large (except for water–methanol, which is nearly ideal), increasing the contribution from the solvent derivative term in the model significantly. This means, that even small values of f_{1j}^0 are likely to result in large excess solubility estimates. The solvent mixture water–acetone forms an interesting example of the method. Figure 6–11 shows the agreement with data. The excess solubility is positive, with maximum value of around 2. The model has severe difficulties describing the behavior of this system, even when regressing parameters to mixed solvent data. The naphthalene–water parameter is too

small in magnitude to capture the variation, and to compensate, the value of the naphthalene–acetone is too large, resulting in overshoot in the acetone-rich side of the plot, while underestimating in the water-rich end. The reason for this is found in another system, where the naphthalene–water pair is present. Consider Figure 6–12, which shows the system naphthalene–water–dimethylsulfoxide (DMSO). The

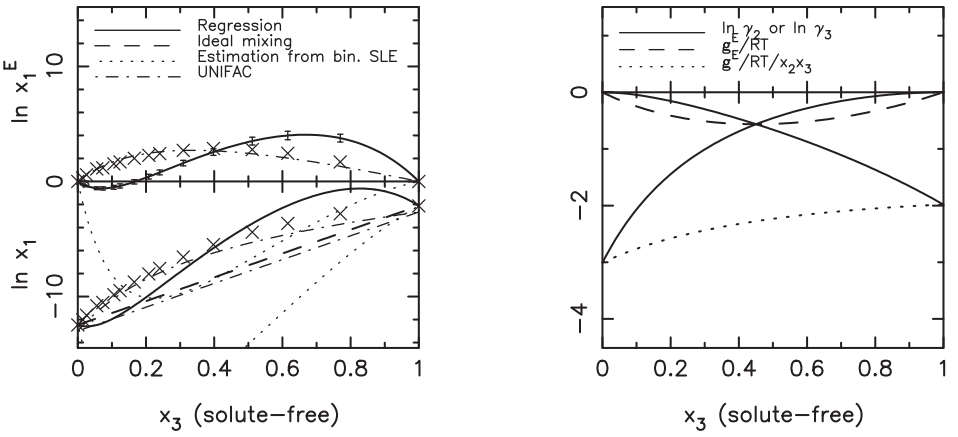

Figure 6–12. Solubility of naphthalene(1) in water(2)–DMSO(3) and excess free energy of the solvent mixture. Both plots reveal, that also both of these systems are considerably nonideal. However, the sign of the excess solubility data is now opposite to the excess Gibbs energy of the solvent mixture, which causes severe problems when applying the model for regression and prediction.

experimental excess solubility data is, as previously, distinctly positive, and similarly to the previous system, the model is unable to capture the variation of the solubility data. The naphthalene–water parameter appears to be of opposite sign to what would be expected from the data. The model gives a negative excess solubility near pure water, while overshooting the data towards the DMSO-end of the plot. The excess free energy of the solvent mixture determines this behavior, and unlike previously, the system water–DMSO forms a solution with strong negative deviations from Raoult's law. The water–acetone systems has positive deviations, as seen on the right plot of Figure 6–11. This implies that the derivative of the activity coefficient has opposite sign in the water–DMSO mixture compared to water–acetone, and this makes the model unable to describe the data. Water and ethylene glycol (Figure 6–13) also forms a solution with negative deviations from Raoult's law. The excess solubility in this solvent binary is clearly positive, and of opposite sign to the solvent g^{E}. This means that a positive value of the naphthalene–water parameter is inconsistent with solubility data for this particular system, giving a small region of negative excess solubility, as can be seen on Figure 6–13. It is not possible to match this behavior with any parameter set. The problem of incompatible signs of $g^{\mathrm{E}}(2,3)$ and excess solubilities is not a common phenomenon, but does pose a general problem. It reflects the problem discussed above, where the solvent mixture was incompatible with the experimental excess solubilities. There is no im-

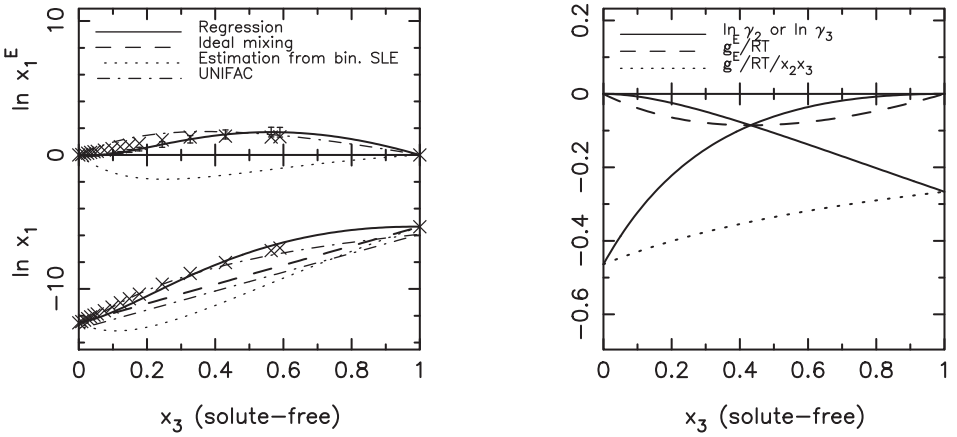

Figure 6–13. Solubility of naphthalene(1) in water(2)–ethylene glycol(3) and excess free energy of the solvent mixture. An example of another system, where the solvents form a mixture with negative deviations from Raoult's law, which is conflicting with the excess solubility data of naphthalene in the solvent mixture.

mediate remedy for this problem, since this is not just a matter of finding a more compatible VLE set to regress parameters for a g^{E}-model from. The water–DMSO binary have clear negative deviations from Raoult's law, which is incompatible with the solubility data. Using the Margules or UNIFAC models for the solvent binaries produces similar results. This example illustrates a shortcoming of the method, and one for which there is not obvious solution. However, one way might be to include the term, which was discarded from Equation (4–19). This term might contribute such, that the model estimate of the excess solubility remains positive. This path has not been explored further at this point, since it involves additional regression of mixed solvent solubility data.

Beta carotene

Treszczanowicz et al.[55–58] measured the solubilities of beta carotene in mixture of polar compounds (ketones, ethers) and nonpolar hydrocarbons. The availability of thermophysical property data is limited, and the ideal solubility can be computed with Equation (3–13) using $\Delta c_{P,m,i} = 0$, since its value is unknown. The ideal solubility is low, around 10^{-5}, but slightly higher than the solubility in the polar solvents and lower than the solubility in the nonpolar solvents. Regressing $\mathbf{f}^0$ from data gives good agreement with experimental data. The binary-based values of $\mathbf{f}^0$, from Equation (4–46), are generally in good agreement for beta carotene with the nonpolar hydrocarbons, but the polar solvent species do not conform well with Equation (4–46), and generally overpredict the values. Comparisons with data show that although the quantitative description is worsened, the overall estimation is still reasonably good. A few exceptions being hexane with acetone, 1,2-dimethoxyethane, and diglyme repespectively,

and 1-hexene with acetone and diglyme, respectively. Figure 6–14 shows an example with MEK and cyclohexane. Beta carotene ($C_{40}H_{56}$) is larger than molecules normally treated with UNIFAC, and the

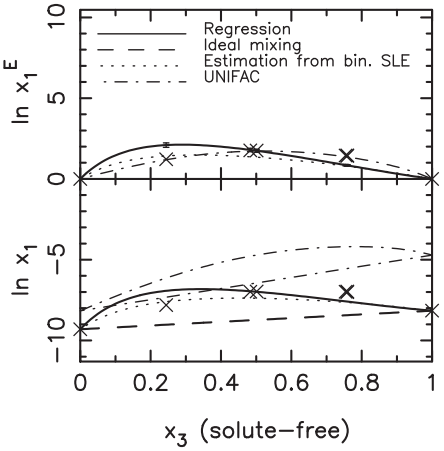

Figure 6–14. Beta carotene(1) with methyl ethyl ketone(2) and cyclohexane(3) at 20 °C.[58] UNIFAC applied for solubility estimates in the solvent mixture is generally unsuccessful, since the solubility in pure MEK is overpredicted. However, UNIFAC gives a reasonable estimate of the excess solubility, suggesting that UNIFAC may useful for estimating mixing effects in solvent mixtures.

$\mathbf{f}^0$ obtained from UNIFAC for each solvent in a mixture are of opposite sign to each other, and too large in magnitude. However, UNIFAC for beta carotene is an extrapolation to molecular structures beyond the proven range of the model. Solving the isofugacity criterion shows that UNIFAC often overpredicts the pure solvent solubilities by several orders of magnitude. The exceptions are 1,2-dimethoxyethane (where the solubility estimate is within an order of magnitude) and diglyme, which is underestimated by several orders of magnitude. The errors arising from using UNIFAC for calculating the excess solubility are often comparable with the FST model with regressed solute-solvent parameters, suggesting that UNIFAC could be a viable method for determining the effects of mixing solvents.

The systems above are characterized by solutes having well established thermophysical characteristics, e.g., there are no solid-state transitions. The following sections will be concerned with solutes which, from a thermophysical point of view, are less well defined. They belong to a class of solids typically found in pharmaceutical products. This means that the systems contain water, and therefore often show significant excess solubilities. Furthermore, the selection of an appropriate expression for the ideal solubility, i.e., choice of $\Delta c_{P,m,i}$, is not always obvious. For each solute below, a form of Equation (3–13) is selected partly based on availability of thermophysical property information and partly based on past experience with the respective solutes as described in the literature. The absence of heat capacity data means choosing either Equation (3–15) ($\Delta c_{P,m,i} = 0$) or (3–16) ($\Delta c_{P,m,i} = \Delta s_{m,i}$). Consistency

among values of $\mathbf{f}^0$ estimated by minimizing the objective function, Equation (4–43), and values obtained from Equation (4–46) (single-solvent data), for parameter transferability, is sought. Comparisons are made between results obtained using different choices for $\Delta c_{P,m,i}$, even though such an analysis will not be feasible in the general case.

4-Hydroxybenzoic acid

Wu and Martin[3] measured solubilities of 4-hydroxybenzoic acid in water and dioxane. $\Delta c_{P,m,i} = \Delta s_{m,i}$ to calculate the ideal solubility is used, since the $\mathbf{f}^0$ calculated from this gives the lowest AAD. The excess solubilities are large, reaching almost 4, which corresponds to a factor of more than 50 on mole fraction basis. Regressing two parameters to the 11 (excluding the single-solvent solubilities) measurements gives an AAD of 0.18, which increases to 0.68 when using the binary-based values. Figure 6–15 shows the agreement with data. The $\mathbf{f}^0$ produced by UNIFAC are inconsistent with those

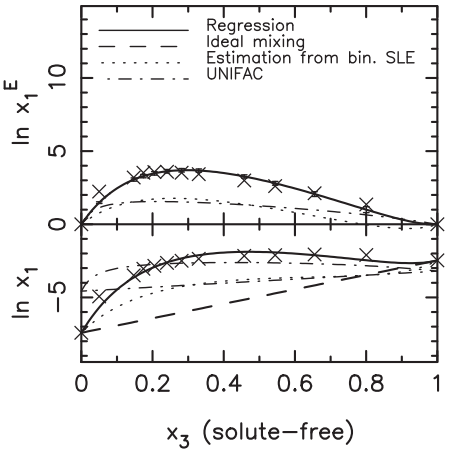

Figure 6–15. 4-hydroxybenzoic acid(1) in water(2)–dioxane(3) mixtures at $25\,^\circ\mathrm{C}$.[3] This is an example of a highly nonideal system, where the model with regressed parameters performs quantitatively, whereas the predicted excess solubilities are underestimated.

obtained from data. The solute-water parameter value is more than 20, whereas the binary-based value is 7.24, indicating that UNIFAC clearly underestimates the solubility in pure water. The UNIFAC-based values of $\mathbf{f}^0$ gives an AAD of 3.41, whereas solving Equation (3–13) gives an AAD of 1.84 on the actual solubilities, and 0.66 in the excess solubility factors.

Testosterone

As with the previous solute, Equation (3–16) is also here used to calculate the ideal solubility. There is just a single data set with testosterone as solute. This is in the nearly ideal mixture of cyclohexane

and chloroform. Regressing $\mathbf{f}^0$ from ternary data gives $\mathbf{f}^0 = \{26.71, 5.90\}$ and an average error of just 0.07, while the binary-based values, $\mathbf{f}^0 = \{11.27, -4.07\}$, gives 0.49. Figure 6–16 shows the model-data agreement. The values obtained from UNIFAC $\{41.61, 0.87\}$ are more consistent with those fitted to the data, and therefore also has a slightly lower AAD, 0.40. The large testosterone–cyclohexane parameter from UNIFAC indicates that the pure-solvent solubility is mismatched. The excess solubility estimates from UNIFAC is similar to using the model with binary-based parameters. UNIFAC estimates the solubility in pure chloroform quite well, but overestimates the solubility in pure cyclohexane.

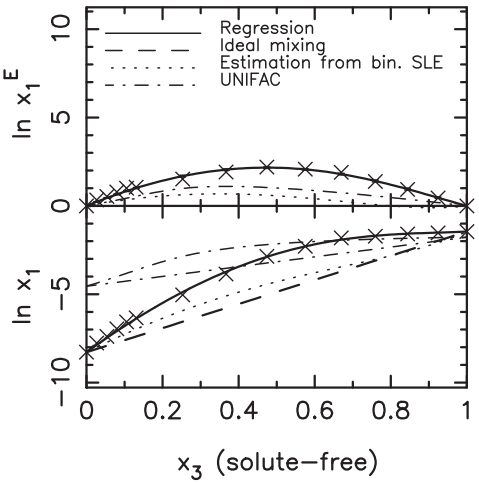

Figure 6–16. Solubilities of testosterone(1) in cyclohexane(2) and chloroform(3) and $25\,^\circ\mathrm{C}$.[59]

Aminopyrine and antipyrine

The agreement of the model with data is nearly quantitative when the $\mathbf{f}^0$ is regressed from Equation (4–43) using all of the available ternary solubility data for a particular solute. An illustration is the solute aminopyrine in the binary mixtures of water–ethanol and water–dioxane as shown in Figure 6–17. The asymmetry of the solubility is fully captured by the model using the same $\mathbf{f}^0$ parameter for aminopyrine with water. Similar results are found for antipyrine in the same solvent mixtures.

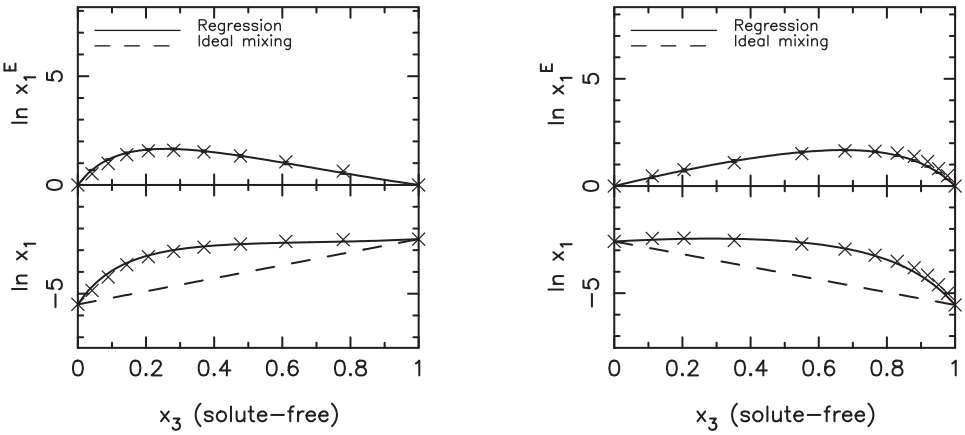

Figure 6–17. Solubilities of aminopyrine(1) in water(2)–ethanol(3) (left) and in dioxane(2)–water(3) (right), both at 25 °C. The heats of fusion and melting points are unknown for both these solutes wherefore only regressions are possible.

Sulfamethazine, sulfamethoxypyridazine, and sulfanilamide

For sulfamethazine, comparison of $\mathbf{f}^0$ values obtained with Equations (3–15) and (3–16) suggests that superior results are obtained from Equation (3–15), which also was used in previous works.[27,68] For sulfamethoxypyridazine, there is significant uncertainty in the heat of melting data. Escalera et al.[27] report 33948 J/mol, while Bustamente and Escalera[28] report 22300 J/mol. Previous treatments of sulfamethoxypyridazine[26–28,68] and sulfanilamide[63,68] consistently employed Equation (3–15). This yields $\mathbf{f}^0$ values from binary data to be somewhat more consistent with the ternary fitting when Equation (3–16) is employed, but the difference is not substantial. In the end, therefore, Equation (3–15) was employed. All of these substances have been reported to have polymorphs,[69] but insufficient information about their properties $(T_{t,i}, \Delta h_{t,i})$ is available to deal with this situation.

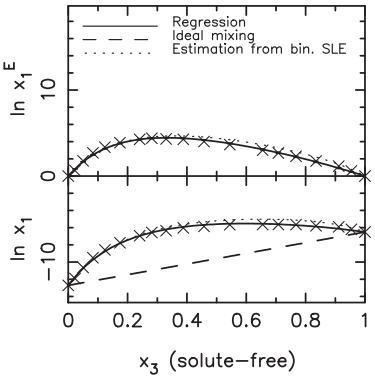

Figure 6–18. Solubility and excess solubility of sulfamethazine(1) in water(2)–dioxane(3) at 25 °C. Excellent agreement is found when applying the FST model with parameters regressed from data and predicted from solubilities in single solvents.

Figure 6–18 shows excess solubility estimates for sulfamethazine in water with dioxane. As Table 6–4

shows, the value of f_{12}^0 for sulfamethazine(1) and water(2) predicted from binary solubility information is quite close to the value obtained from ternary data. Also, f_{12}^0 for water is much greater than for the other solvents: Ethanol, ethyl acetate, and dioxane. The form of Equation (6–6) suggests that the larger parameter influences the results the most. Thus, if an estimate of the dominant parameter agrees with the value from fitting ternary data, the predictions are usually good. Here, the sulfamethazine–water parameter dominates the excess solubility calculation so the predictions are accurate. The case of the ethyl acetate–ethanol binary is different. The ethanol–sulfamethazine parameter is essentially the same as the fitted value, but it is not much larger than the estimated ethyl acetate–sulfamethazine parameter, which is more than twice the ternary-based parameter. The result is a slightly greater discrepancy of prediction and data for the ethyl acetate–ethanol system than on the water–ethanol system. This is shown

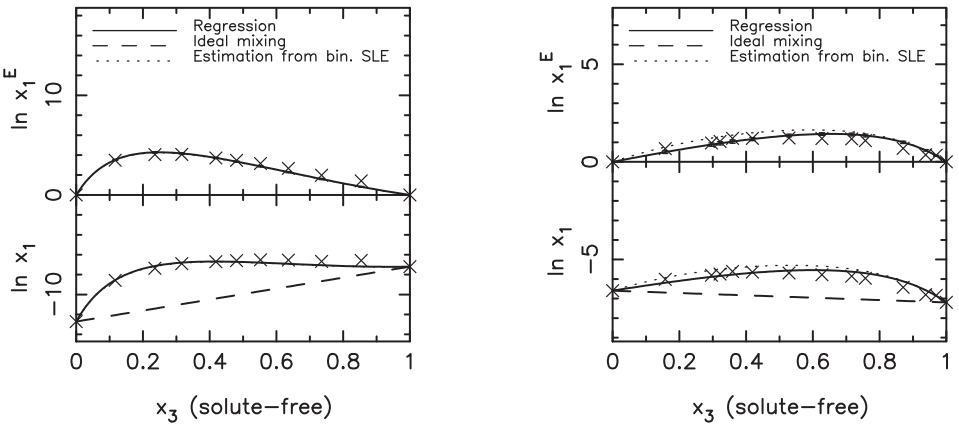

Figure 6–19. Sulfamethazine(1) solubilities in water(2)–ethanol(3) (left) and ethanol(2)–ethyl acetate(3)(right), both at $25\,^{\circ}\mathrm{C}$. The asymmetric profiles of both systems are generally captured well with the model, although there is a small overestimation in the ethanol–ethyl acetate system using the model in prediction mode.

in Figure 6–19. Figure 6–20 shows sulfamethoxypyridazine solubility in mixtures of water-dioxane and water-ethanol. The sulfamethoxypyridazine–water parameter predicted from Equation (4–46) is in good agreement with that fitted to ternary data. On the other hand, neither the ethanol nor the dioxane parameters are as well predicted from binary data, since the estimated line deviates from the data and the fitted lines at organic-rich compositions. The dioxane parameter is greater and the dioxane disagreement is greater giving greater discrepancy here than for the aqueous ethanol system.

The system sulfamethoxypyridazine(1)–ethyl acetate(2)–hexane(3) is fitted well but predicted poorly, as indicated in Table 6–4. The binary-based value of f_{13}^0 is 21.28, whereas fitting of ternary data gives -3.52. There can be several reasons for this discrepancy. The fit is from only two data points, which

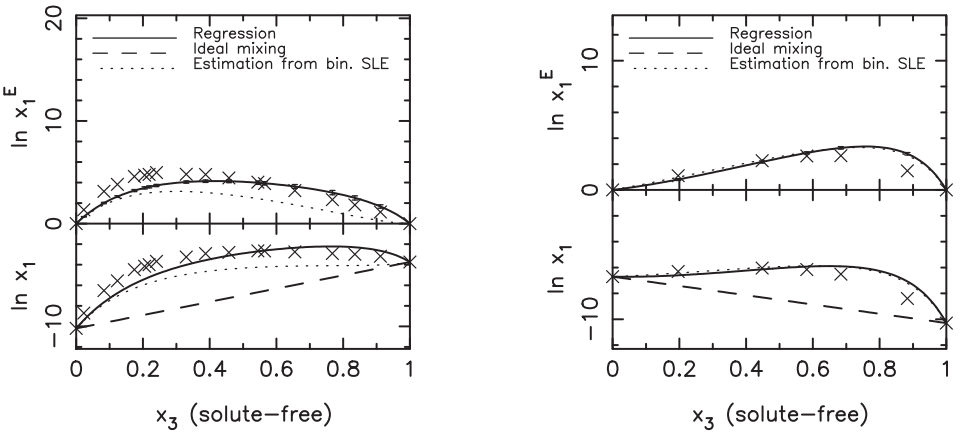

Figure 6–20. Sulfamethoxypyridazine(1) solubilities in water(2)–dioxane(3) at $25\,^{\circ}\mathrm{C}$ (left) and ethanol(2)–water(3) at $20\,^{\circ}\mathrm{C}$ (right). Both solvent mixtures form strongly nonideal solutions, and the excess solubilities in them are significant. The latter system is predicted well, while the model is unable to accurately capture the magnitude of the experimental excess solubility data when using.

is normally insufficient, though they are near equimolar in the solvents. The excess free energy of the sulfamethoxypyridazine–hexane binary might not be symmetric as the Porter equation requires. Finally, the cause may be from the solubility of sulfamethoxypyridazine in hexane being extremely small and the results of Equation (4–46) being very sensitive to measurement error in such cases.

There are three sulfanilamide cases, two aqueous and one nonaqueous. Descriptions of the aqueous systems are good because the water–sulfanilamide parameter dominates, and its values from fitting ternary data and estimation from binary data agree quite well. The excess solubilities for the ethyl acetate–ethanol case are symmetric while the fitted and predicted results show asymmetry. However, the magnitudes are close to experiment at midrange solvent compositions, giving acceptable prediction over the whole range.

Paracetamol

The literature is rich in studies of paracetamol solubility, including ideal solubilities calculated from both Equations (3–15) and (3–16), as well as from (3–14) with measured $\Delta c_{P,m,i}$ values. Equation (3–16) produces results in closer agreement with data than (3–15), whereas (3–15) does not produce as good agreement. With $\Delta c_{P,m,i}$ equal to $99.8\,\mathrm{J/mol/\,K}$ at the melting point,[70] Equation (3–14) is also accurate. Using $\mathbf{f}^0$ values estimated from binary data gives close agreement in solubilities with those from ternary regressions for both Equations (3–16) and (3–14). In the pharmaceutical literature, solid

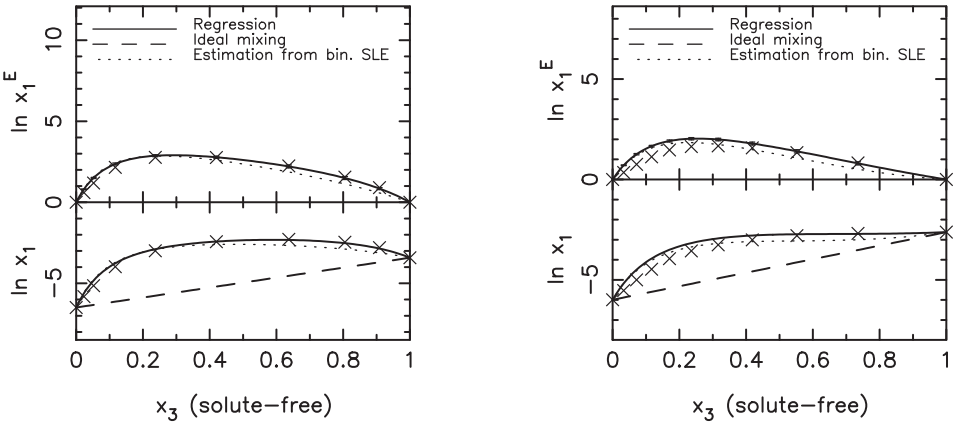

Figure 6–21. Paracetamol(1) in water(2)–acetone(3) at 20 °C (left) and water(2)–ethanol(3) at 25 °C (right). The model is able to describe all aqueous paracetamol systems well with parameters from regression and values predicted from single solvent solubilities. Two representative systems are shown here.

paracetamol is usually found in one of two forms: Form I (commercially available monoclinic), and Form II (orthorhombic), although results have also appeared for alternative forms.[71] Since transition enthalpies have not been reported, such effects have not been taken into account here.

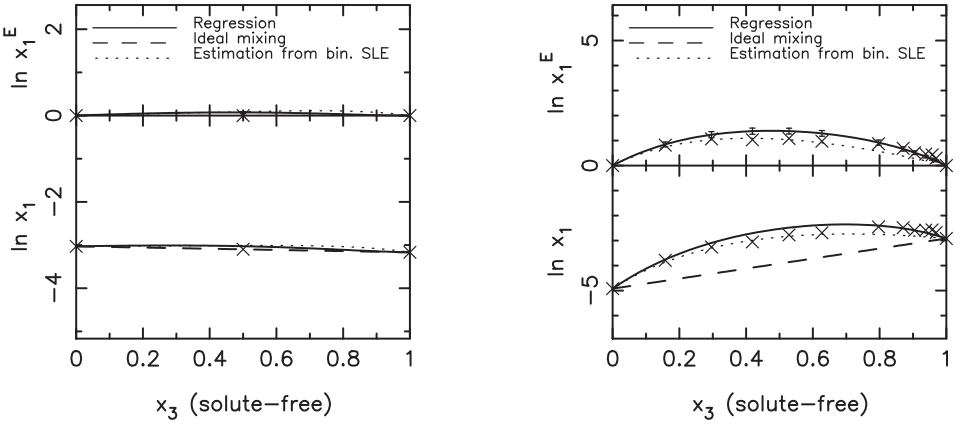

Figure 6–22. Paracetamol(1) in ethanol(2)–methanol(3) (left) and ethyl acetate(2)–ethanol(3) (right), both at 25 °C. The solvent mixture in the former systems forms an almost ideal solution, consistent with almost no excess solubility. The latter is much more nonideal, and generally captured well with the model.

Solubilities have been found for 17 paracetamol systems, nine of which are aqueous. The water cases

demonstrate again the importance of good agreement between the prediction and regression results for the dominant solvent component. The paracetamol–water parameter fitted to all systems is 7.19 ± 0.22, whereas the values estimated from binary data range from $7.01 - 7.63$. The water–methanol mixture is an exception where the value is 8.64, but the description of the water-rich solubility data is not very good in that case. This difference could suggest experimental error. Yet, all nine aqueous systems (two are shown in Figure 6–21) are relatively well represented by the model, irrespective of whether the $\mathbf{f}^0$ parameters are obtained from ternary or binary data. Figure 6–22 shows the solubilities of paracetamol in two nonaqueous binary systems: Methanol–ethanol and ethyl acetate–ethanol. In the first, where there is only a single data point, the excess solubility is very small, consistent with the solvent solution being nearly ideal. Thus, the results are relatively independent of the f_{1j}^0 values. The other system shows greater nonideality. Interestingly, both binary parameter values are less than those ternary values from regression of the entire set of solubilities. However, since in the midrange the ternary parameters overestimate the solubility, the binary-based predictions give better overall agreement with the measured data. Among the systems investigated, the solubility of paracetamol in toluene with acetone is somewhat better predicted than expected because the acetone–paracetamol parameter from binary data is less than that from ternary data, partly compensating for the erroneous toluene parameter.

Phenacetin

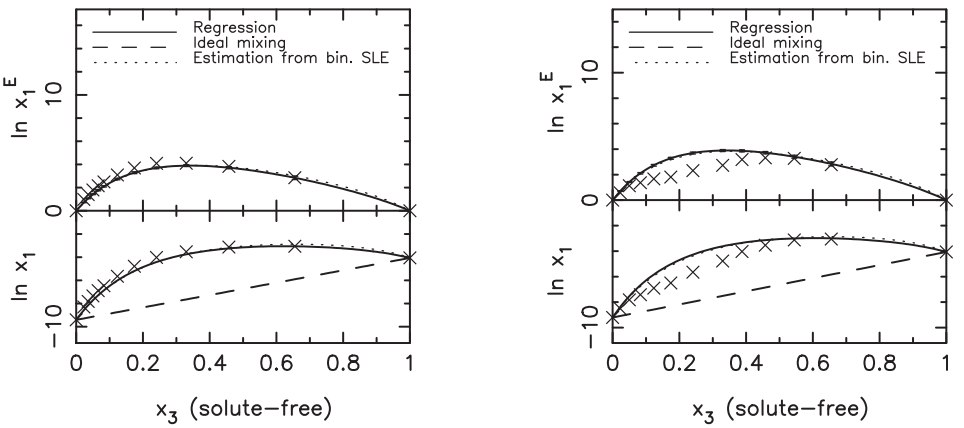

Figure 6–23. Phenacetin(1) in water(2)–dioxane(3). Left and right sets both at $25\,^\circ\mathrm{C}$, but from different sources. The data is not consistent, wherefore the model overestimates one system and underestimates the other. This is not uncommon when comparing data from different investigators.

Phase transitions for phenacetin below the melting point are unknown. This is consistent with the investigations of Pena et al..[21] Though Yalkowsky et al.[72] used Equation (3–15), Equation (3–16) seems

to be better. Application of the model to phenacetin solubilities in aqueous mixtures is successful though there are some discrepancies with data from Pena et al. Figure 6–23 shows two different measurements for the water–dioxane system. Both binary- and ternary-based parameter values slightly underestimate the data of Reillo et al.[63] (left plot), while overestimating that of Pena et al. (right plot). This is not unusual when examining data from independent investigators. Figure 6–24 shows results for ethanol with ethyl acetate, where parameter estimates from binary data are both greater than those from ternary data, leading to errors in the predictions.

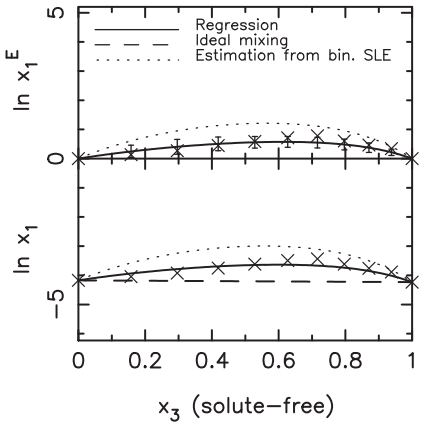

Figure 6–24. Phenacetin(1) in ethyl acetate(2)–ethanol(3) at 25 °C. The model is able to correlate the data, but prediction is unsuccessful in this nonideal solvent mixture.

Theophylline

The behavior of theophylline in the solid phase is complex. Below 340 K, monohydrous theophylline is stable while above 340 K, crystalline theophylline is stable, as determined by Fokkens et al.[73] using DSC and vapor pressure studies. This hydration behavior of theophylline is complicated by the fact that the state of the hydrate depends on the water activity of the crystallization medium.[74] In contact with methanol–water or 2-propanol–water mixtures at water activities less than 0.25, the anhydrate is the only solid phase observed, no matter which solid form was initially added. At water activities greater than 0.25 in either solvent mixture, the monohydrate is obtained as the most stable form. Finally, the monohydrous form can be observed metastably at lower temperatures, leading to the wrong solid for solubility. Most available thermophysical data on theophylline are for the anhydrous form, but the proper thermophysical data for calculating theophylline solubilities in water and in organics would not be the same if the solids differ. Most of the solubility studies of anhydrous theophylline in the literature[29,31,32,75] have used Equation (3–16), which is used here, though a few[72,73] have adopted Equation

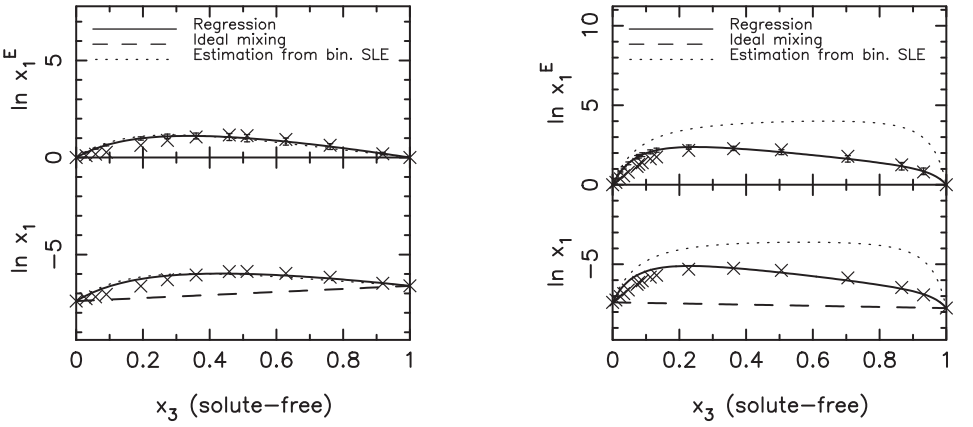

Figure 6–25. Theophylline(1) in water(2)–methanol(3) (left) and water(2)–acetonitrile(3) (right), both at $25\,^{\circ}\mathrm{C}$.[13] The aqueous theophylline solubility data is generally well described, except for the system containing acetonitrile. In here, the model is unable to accurately predict the excess solubilities, though the regressed values match the experimental data well.

(3–15). Theophylline data, in the three aqueous mixtures, are well represented by both approaches, except for acetonitrile, where the solubility is very small as seen in Figure 6–25 and the predictions give solubilities somewhat higher than experiment.

Desmosterol and cholesterol

Data on desmosterol solubility in mixed solvents exist for the case of hexane with ethanol from 293 to 323 K from Chen et al..[10] They used Equation (3–15), but there is little difference when Equation (3–16) is used. Since the ternary regressions are only for these solvents, the fits are quantitative. However, since the parameters from pure solvent solubilities generally exceed the ternary-based fits, the desmosterol solubilities in mixtures are overpredicted. It might be that the desmosterol binaries with hexane–ethanol are not symmetric enough for the Porter model of Equation (4–45) to apply, due to the great difference in size and shape of the solute desmosterol from the two solvents. The ideal solubility is rather large, $x_1^{\mathrm{id}} \approx 0.2$ at 293 K. The solubility in pure hexane is 0.006 and 0.004 in pure ethanol, implying that the activity coefficients of desmosterol are high. As a result, estimation of $\mathbf{f}^0$ from UNIFAC overestimates significantly compared to those obtained from binary and ternary solubility data. Solving the isofugacity criterion using UNIFAC reveals that the pure solvent solubilities are overestimated dramatically, whereby the mixed solvent solubilities cannot be estimated accurately at all. Moreover, UNIFAC underpredicts the excess solubility, except for a small region close to pure ethanol. The excess solubility estimate is best at low temperatures, and progressively worsens as the temperature increases.

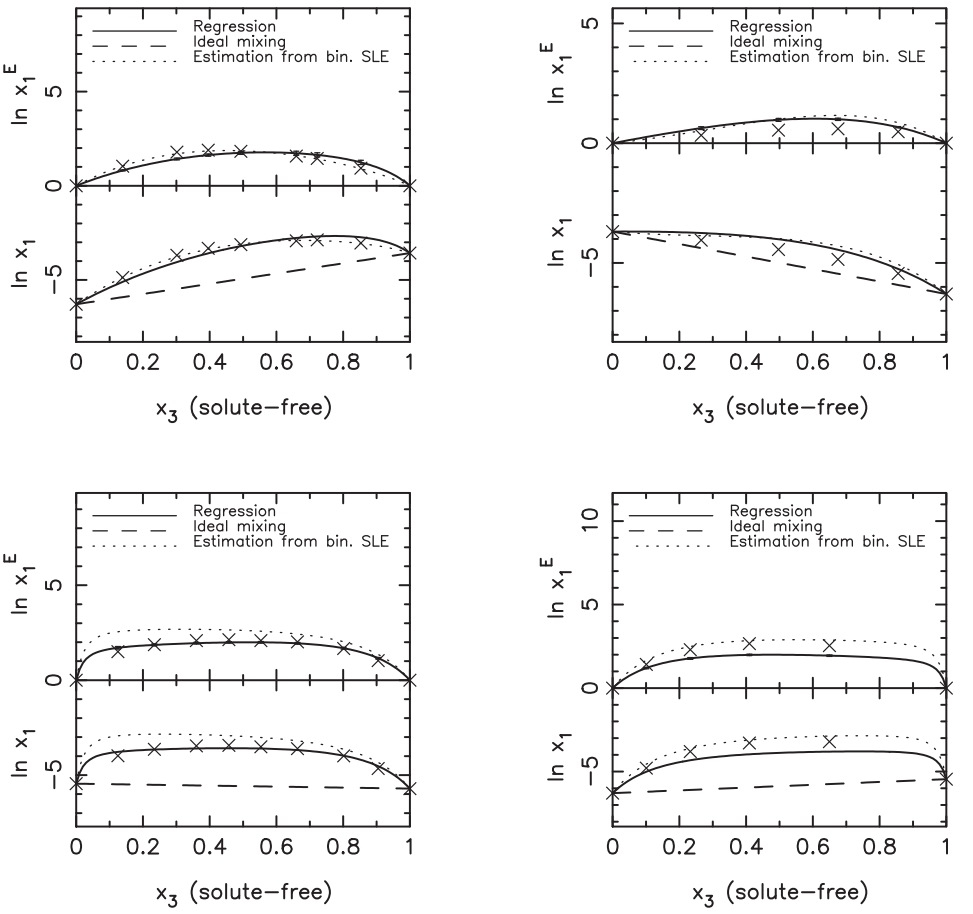

Figure 6–26. Cholesterol(1) in ethanol(2)–benzene (upper left), dioxane(2)–ethanol(3) (upper right), and hexane(2)–ethanol (bottom plots), all at 20 °C. Examples of different cholesterol systems. The two bottom plots show solubilities and excess solubilities in hexane–ethanol mixtures from two different data sources. The data is inconsistent with each other, and the model is therefore unable to accurately describe both, landing in between the two. The situation is similar to that described in connection with phenacetin in Figure 6–23.

Several treatments of cholesterol are reported in the literature. The heat capacity change on melting and temperatures of phase transitions below the melting point have been established by Domańska et al.,[9] potentially allowing use of Equation (3–14). Chen et al.[10] also reduced data on cholesterol solutions by treating $\Delta c_{P,m,i}$ as an adjustable parameter to be estimated from fitting solubility data. Most cholesterol systems are represented successfully. Figure 6–26 illustrates the results for mixtures of benzene with ethanol and dioxane with ethanol. The solubilities of cholesterol in hexane-ethanol binaries are reported by Chen et al.[10] and by Weicherz and Marschik.[33] The data do not agree as can be seen from the bottom

plots of Figure 6–26. Regressions underestimate the results of Weicherz and Marschik while matching the data of Chen et al.. On the other hand, binary predictions using Equation (4–46) overestimate the data of Chen et al. and produce a nearly quantitative agreement with the data of Weicherz and Marschik. Such discrepancies complicate conclusions about experimental accuracy. UNIFAC generally overestimates $\mathbf{f}^0$, as in the example above. The cholesterol–hexane parameter varies from 16.41 at 293 K to 10.32 at 323 K, disagreeing strongly with those found from solubility data, which range from 2.46 to 4.63. Similarly for cholesterol with ethanol. The binary- and ternary-based parameter lie between 4.20 and 5.05, but UNIFAC estimates values around 27. With dioxane the parameter is 35.42, whereas those from binary and ternary data give 0.93 and 2.88, respectively. Unlike those from data, the cholesterol–benzene parameter from UNIFAC is slightly negative. Consequently, the error when applying the model with UNIFAC-based $\mathbf{f}^0$-parameters is large, except for the case of cholesterol with benzene and hexane. Using the set of $\mathbf{f}^0$ from UNIFAC gives a lower AAD than fitting ternary mixture data in this set.

Mefenamic acid

Mefenamic acid undergoes a phase transition from a form identified as I to a form II at $140 - 150\,^\circ\mathrm{C}$. Form II melts at $230\,^\circ\mathrm{C}$[76] while form I is observed in solubility measurements[12] at temperatures less than $140\,^\circ\mathrm{C}$. Unfortunately, the heat of transition is unknown, preventing the inclusion of its effect into predictions of the ideal solubility. The ideal solubility of mefenamic acid is very small with values from Equations (3–15) and (3–16) differing by a factor of more than four. While the solubility in water is small, solubilities in ethanol and ethyl acetate are in the same range as the ideal values. Further, there is a large difference in the binary- and ternary-based parameter values for water–mefenamic acid. The discrepancy could be due to the binary system being asymmetric or to error in the extremely low aqueous solubility, which strongly affects the solute-water parameter value. Regardless, the result is that both regression and prediction of mixed aqueous solvent solubility are problematic. The $\mathbf{f}^0$ values from binary data are in quantitatively better agreement with those from ternary fitting when Equation (3–15) is employed, but Equation (3–16) is in better agreement with the excess solubility variation with mixed solvent composition, so Equation (3–16) is employed. The nonaqueous system of ethyl acetate–ethanol shows quite good agreement between binary- and ternary-based estimates, suggesting that the Porter equation is valid for the solute-solvent binaries.

Thus far, the results have concerned excess solubilities of solids in binary solvent mixtures. The solubility behavior of many (but not all) solutes where generally described well using parameter estimates from both ternary data (regression) and binary data (prediction), as well as UNIFAC (prediction).

In the following section, a provisional investigation of the excess solubilities in mixtures with three

solvent species will be given. Many of the same principles that applies to binary solvent mixtures (i.e. nonideality of the solvent mixture, and its influence on the excess solubilities) also apply to solubilities in ternary solvent mixtures. Results using solute-solvent parameters fitted to quaternary mixture data are compared with those obtained from single solvent data.

6.5. Excess solubilities in ternary solvent mixtures

While solubilities of solids in binary solvents mixtures are less abundant than in pure solvents, there is still a significant amount of measured data in the open literature. Much less abundant are measurements in four component systems, i.e., solutes with three solvents. Even more, most of the data available are with solutes such as anthracene and pyrene, which show little or no excess solubilities in both binary and ternary solvent mixtures. Thus, the data available for testing is quite fragmented. Table 6–7 shows the sets of data gathered for testing the model. The entries in Table 6–7 have been organized such that they appear according to the nature of the solvent mixture. Many of the solvent systems are very nonideal, which means that the model is likely to estimate a significant excess solubility. The model for excess solubilities in ternary solvent mixtures is given in Chapter 4, Equation (4–38), and here

$$s_1^{\mathrm{E}} = \frac{x_2x_3f_{23}^{+} + x_2x_4f_{24}^{+} + x_3x_4f_{34}^{+}}{1 + x_2x_3f_{23}^{+} + x_2x_4f_{24}^{+} + x_3x_4f_{34}^{+}} \left[1 + x_2f_{12}^{0} + x_3f_{13}^{0} + x_4f_{14}^{0}\right]. \tag{6–10}$$

UNIFAC has been used to estimate the necessary derivatives of solvent activity coefficients for the f_{ij}^{+} in the model in most of the systems. Only for the ternary of water–ethanol–propylene glycol (used below) were VLE data available for all three binaries, so parameters for the Wilson equation could be estimated. Below, results are reported. Investigations will aid in determining if the solute-solvent parameters, f_{1j}^{0}, are transferable between estimates from regression of mixture data and those found from use of Equation (4–46) using single solvent solubilities.

6.5.1. Mixtures of an ether with and alkanol and an alkane

The first examples are anthracene in MTBE with isooctane and varying alkanols. The values of f_{1j}^{0} regressed from the mixed solvent solubility data (columns $8-10$ in Table 6–7) do not agree with those found from single solvent solubilities, using the Porter equation (columns $11-13$). The values from mixed solvent data are generally smaller than those found from binary data, and for anthracene–isooctane the value is negative when regressed to data, while (relatively) large and positive, 4.66, when predicted from binary data. Columns $14-16$ show the average absolute deviation in mole fraction, defined identically to that previously. As before, AAD-0 denotes that the excess solubility is assumed zero (ideal mixture), AAD-1 denotes model estimate with parameters fitted to mixed solvent data, while

AAD-2 indicates model estimate with parameters from solubilities in pure solvents. The discrepancies in the values of $\mathbf{f}^0$ is also reflected in the AADs. Assuming ideal mixture ($s_1^{\mathrm{E}} = 0$) gives values around $0.2 - 0.3$. When fitting the model to mixture data lowers that to $0.03 - 0.04$, while using the binary-based values of f_{1j}^0 produce values around 2. This is similar to the solubility results of anthracene in nonideal binary solvent mixtures. The values of f_{1j}^0 found from binary data are usually large in comparison with those from regression, because the solubility in these systems is relatively low ($x_1 \sim 10^{-3}$) compared to the ideal solubility of anthracene, which is 0.011. Plots with four variables (though only three independent) are difficult to present in a convenient fashion, and a surface plot (such as Figure 6–27) appears to be the best way for a systematic depiction. Figure 6–27 shows the excess solubility of anthracene in the solvent mixture as function of solute-free composition. In each of the endpoint of the surface triangle, the excess solubility is zero, conforming to the estimation in a pure solvent. In between, the surface rises, suggesting nonnegative excess solubility. The magnitude of the model estimate, with binary-based parameters, is indicated by the left-hand side colorbar. The model estimate, with solute-solvent parameters from binary data, is the surface plot, while experimental measurements are marked with points. The pair of 1-propanol–isooctane has the greatest contribution to the mixture excess solubility, and is also the solvent pair with greatest degree of nonideality associated.. The peak in that binary is nearly 3.0, unlike the other two binary sides, which are less nonideal. The experimental points fluctuate around 0.25. The surface shows that the addition of MTBE lowers the excess solubility, since MTBE form solutions with both the alkanol as well as alkane, which are more nonideal. The effect of interchanging the alkanol species (i.e., the remaining systems) is negligible. This is indicated by the remaining entries in Table 6–7.

6.5.2. Mixtures of dioxane, alkanol, and an alkane

Addition of dioxane to mixtures of alkanols and alkanes decreases the excess solubility of anthracene in these systems, since dioxane forms less nonideal mixtures with both solvent species. The discrepancy between the different estimation methods for the anthracene–dioxane parameter is small, compared to the differences found in previous systems. Here, they differ by a factor of nearly two. Interestingly, the fitted value is larger than the predicted. The remaining values are in disagreement with each other. The fitted values of $\mathbf{f}^0$ for anthracene with cyclohexane, isooctane, and heptane are negative, while those from binary data are positive*. Regressed from data, the anthracene–dioxane parameter is 1.25, the anthracene–butanol parameter is 0.19, and finally the anthracene–cyclohexane parameter is negative, -0.46. This set yields an average error of 0.12. The values from binary solubility data are $\{0.57, 5.25, 3.93\}$, respectively, and gives an error of 0.99. The AADs of assuming ideal mixture lie

* The solute-solvent parameters for anthracene with cyclohexane is identical to that with heptane. This is because the solubilities in these solvents are the same.[77,78]

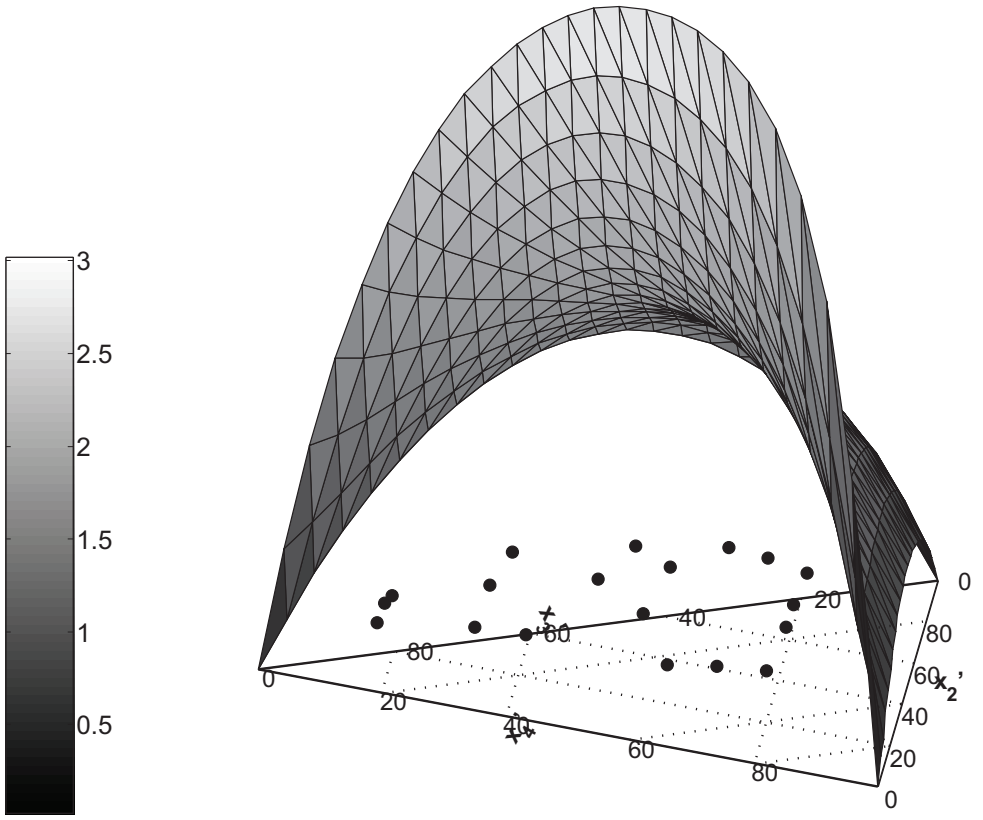

Figure 6–27. Surface plot showing excess solubility of anthracene(1) in mixtures of MTBE(2), 1-propanol(3), and isooctane(4). The shaded surface represents model estimates using binary-based parameters, and experimental observations are marked with •. The magnitude of the model estimate is indicated with the color bar to the left.

around 0.45, while the model with parameters from binary data give around 1.20. The errors when fitting to mixture data are significantly larger than usual; $0.10 - 0.15$ (values less than 0.05 is expected, since this is the error in many similar systems in Table 6–7). For the majority of the other three-solvent systems the errors drop to around 0.05 with fitting. Figure 6–28 illustrates the behavior for anthracene in dioxane–2-butanol(3)–cyclohexane(4). The model assigns significant excess solubility to all combinations of solvent pairs, which is not supported by experiment.

6.5.3. Mixtures of alkanes and alkanols

The solvent systems covered in this subsection are characterized by having two strongly nonideal pairs and one almost ideal pair of solvents. Anthracene is again the primary solute, but there are also measurements of pyrene. The f_{1j}^0 between solute and alkane is constantly negative, which is also the

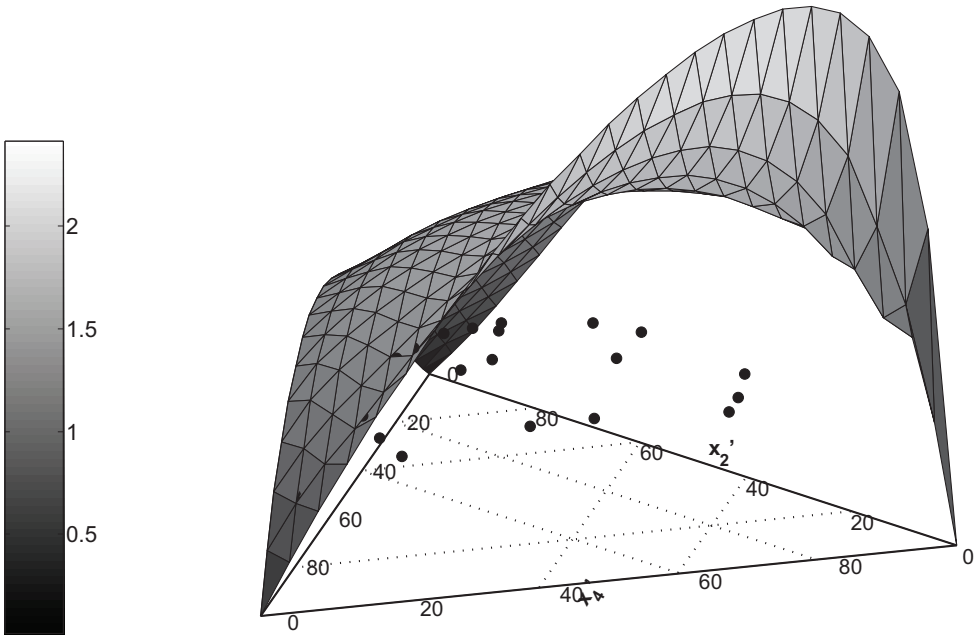

Figure 6–28. Surface plot showing excess solubility of anthracene(1) in mixtures of dioxane(2), 2-butanol(3), and cyclohexane(4). The model, with solute-solvent parameters predicted from single solvent solubilities, overestimates the experimental data significantly.

case for anthracene with alkanes in binary solvent mixtures. When regressed from two-solvent mixtures the f_{12}^0 between anthracene(1) and heptane(2) is -0.83, while the value from three-solvent systems is -0.16. The solute-solvent parameters available for comparison are tabulated in Table 6–6. Although a few discrepancies remain, the overall suggestion is that the parameters regressed from binary and ternary solvent mixture are consistent. In addition, they both differ significantly from those found from pure solvent combined with the Porter equation. Figure 6–29 shows an illustrative example of anthracene with cyclohexane–2-propanol–1-pentanol. The figure shows that the alkanol–alkanol side of the phase diagram is almost completely ideal, while the two alkane–alkanol sides show distinct departure from ideal mixture. As previously, the measurements are located well below the estimated surface with parameters from binary data.

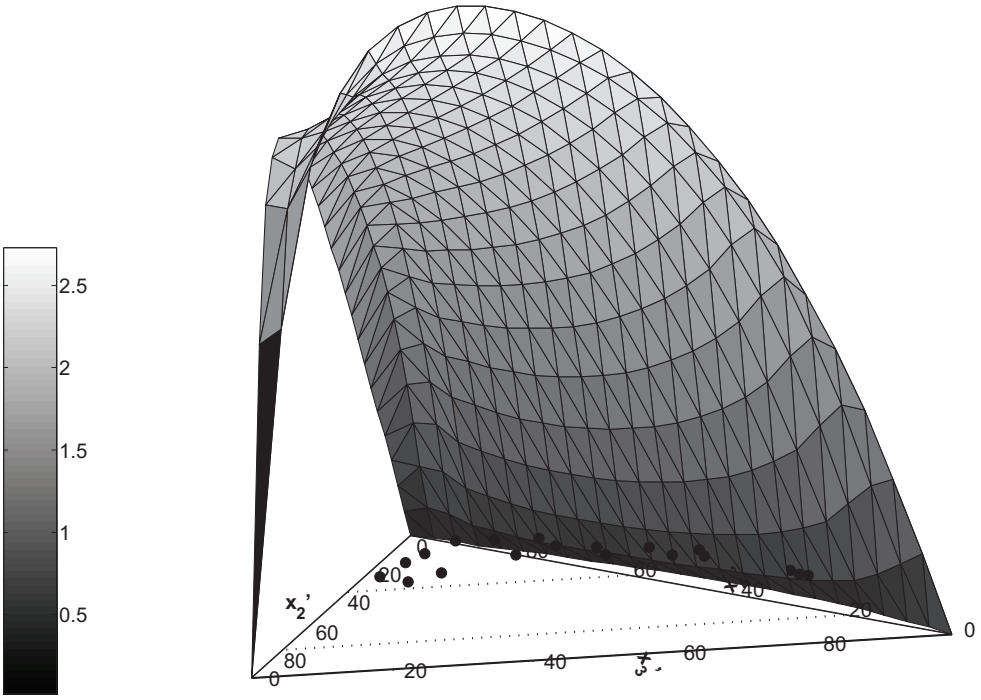

Figure 6–29. Surface plot showing excess solubility of anthracene(1) in mixtures of cyclohexane(2), 2-propanol(3), and 1-pentanol(4). The model-calculated excess solubilities near pure cyclohexane are orders of magnitude above the experimental values. This causes the model to overestimate across nearly the entire composition range, except in the alkanol-alkanol binary (along the x_3-x_4 axis).

Table 6–6. Comparison of f_{12}^0 between anthracene and solvents found from pure solvent (b) and regression of mixtures of two (t) and three (q) solvents, and their corresponding standard deviations.

Solvent	$f_{12}^{o,b}$	$f_{12}^{o,t}$	S.D.	$f_{12}^{o,q}$	S.D.
1,4-Dioxane	0.57	1.33	0.03	1.25	0.07
MTBE	2.58	0.08	0.12	0.30	0.17
Ethyl acetate	1.66	0.81	0.02	0.75	0.72
Heptane	3.91	-0.83	0.01	-0.16	0.14
Cyclohexane	3.93	-0.31	0.01	-0.46	0.07
Isooctane	4.68	-1.05	0.01	-1.09	0.08
Methanol	7.63	-0.55	0.16	3.03	0.20
Ethanol	6.35	0.82	0.23	1.44	0.28
1-Propanol	5.85	0.28	0.01	0.59	0.09
1-Butanol	5.25	0.06	0.01	0.19	0.10
1-Pentanol	4.62	2.32	0.12	-0.41	0.15
2-Propanol	6.58	1.25	0.01	1.23	0.09
2-Butanol	5.87	0.86	0.01	0.78	0.10
2-Methyl-1-propanol	6.31	0.63	0.01	0.94	0.14

6.5.4. Mixtures with halogenated alkanes

For benzoic acid in carbon tetrachloride with hydrocarbons, as measured by Acree Jr. and Bertrand,[79] the $\mathbf{f}^0$ obtained from binary data (again) do not agree well with those regressed to mixture data. However, this does not impact the excess solubility estimate since the solvent mixtures are nearly ideal. Thus, the average error drops significantly compared to the above studies: 0.18 and 0.20, respectively. The solubilities of naphthalene in mixture of benzene, dioxane, and chloroform, measured by Negadi,[80] largely follow ideal mixing. The dioxane–chloroform pair forms a solution with large negative deviations from Raoult's law. The benzene–chloroform pair is slightly less negative, while the benzene–dioxane is slightly positive. However, due to the high solubilities of naphthalene in these systems (x_1 varies from 0.3 to 0.6 in the composition range studied), the $\mathbf{f}^0$ from binary data are small. The reason is that the ideal solubility varies from 0.32 to 0.62 in the temperature range Negadi studied. Hence, the model describes the excess solubility behavior quite well, but the effects are very small. Assuming ideal mixture gives errors around $0.03 - 0.06$, just slightly above the results of fitting the $\mathbf{f}^0$ to mixture data.

6.5.5. Aqueous systems

The mixtures with water are traditionally those exhibiting great excess solubilities due to the strong interactions between water and organic components (solvents and solutes). Moreover, the aqueous solubilities are usually very small, so the effects of mixing can be severe. The aqueous systems compiled in this work consists of eight paracetamol-water–acetone–toluene mixtures at different temperatures, one mixture of paracetamol with water, ethanol, and propylene glycol, and finally phenobarbital in that same mixture. The solubilities of paracetamol in water–acetone–toluene mixtures by Granberg and Rasmuson [18] are measured near pure acetone, which form completely miscible solutions with both water and toluene, although water and toluene form immiscible solutions over most of the phase diagram.[18] Generally, the model is able to qualitatively describe the mixing effects in this system. This is indicated partly by comparing the values of $\mathbf{f}^0$ as regressed from data and estimated from pure solvent solubilities. The paracetamol–acetone parameter is almost identical using either method. Similarly for the paracetamol–toluene parameter. The f_{1j}^0 with water is less well described, but remains qualitatively correct. Another reason why the model is fairly successful is reflected by the AADs, which for the values of $\mathbf{f}^0$ from binary data are around 0.31. This drops to 0.24 when fitting the parameters to mixture data, while ideal mixture renders about 0.60 error. The error in the solubility results when fitting the f_{1j}^0 is not impressive. The reason for this is likely to lie with the solvent-solvent effects. UNIFAC is used to generate activity coefficient derivatives for the solvent-solvent f_{ij}^+ that goes into the model. Since water forms strongly nonideal solutions with acetone and toluene, the variation of the f_{ij}^+ with solvent composition can be strong, thereby causing difficulties for the solute-solvent parameters to compensate. In fact, even when

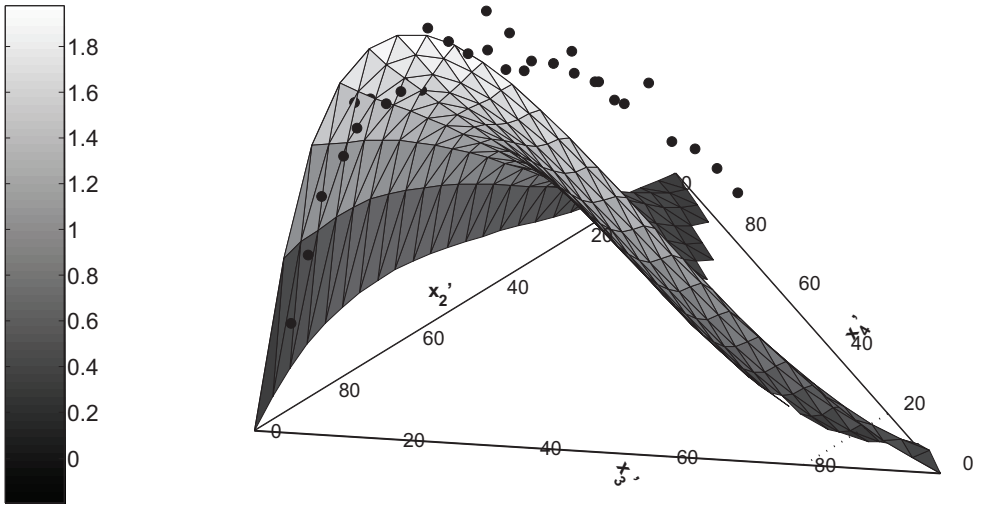

Figure 6–30. Surface plot showing excess solubility of paracetamol(1) in mixtures of water(2), ethanol(3), and propylene glycol(4). The model estimate is based on solute-solvent parameters, and describes the data qualitatively. The excess Gibbs energy of this solvent mixture is characterized with the Wilson equation, using parameters regressed from the individual solvent binaries, unlike the previous mixtures, which were described with the UNIFAC equation.

fitting just the data at $25\,^{\circ}\mathrm{C}$ the error remains at 0.24.

Paracetamol with water, ethanol, and propylene glycol forms an interesting example. The data of Jouyban et al.[81] indicate large positive deviations from ideal mixing. Using the binary-based parameter set, and the Wilson equation for the solvent mixture, the model is able to qualitatively describe the data. The overall error with this is 0.33. Figure 6–30 shows the model-data agreement. The variation of the experimental data is captured reasonably well, especially in the water-rich end of the phase diagram. The paracetamol–water parameter regressed from data agrees reasonably well with that found from binary data, whereas the remaining two differ significantly. As the water concentration decreases, the model increasingly underestimate the data because the pair of ethanol–propylene glycol has a large region of negative excess solubility. Along the pure ethanol–propylene glycol edge of the plot there is a small region of positive excess solubility ($x'_4 < 0.1$), whereafter the model estimate slightly negative deviations from ideal mixing. Using the regressed parameters, this negative region is further decreased. The fitted paracetamol–glycol parameter is 13.00, while the binary-based value is 1.05. Figure 6–31 shows the result when applying the fitted values of $\mathbf{f}^0$. The effect of the now increased value of f^0_{14} is dramatic, and means that the surface now is much more concave than before, and describes the data sufficiently.

Peterson and Hopponen[82] reported phenobarbital solubilities in water–ethanol–propylene glycol mix-

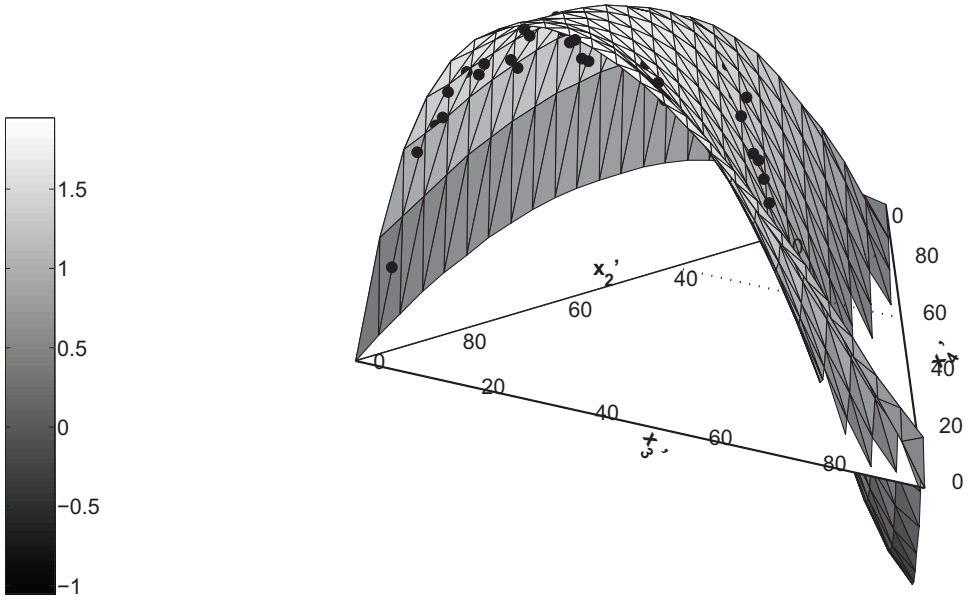

Figure 6–31. Surface plot showing excess solubility of paracetamol(1) in mixtures of water(2), ethanol(3), and propylene glycol(4) with solute–solvent parameters fitted to mixture data. This gives a quantitative agreement with the experimental excess solubility data.

tures, which stand out from the paracetamol sets. First of all, the values of $\mathbf{f}^0$ found are mainly negative. For the solute–propylene glycol and solute–ethanol parameters there is agreement between the $\mathbf{f}^0$ from mixture data and those from binary data, but the water parameter disagrees strongly. Its value from binary data is 5.66, which is in agreement with many previously found solute–water values, but the f_{1j}^0 regressed is -10.4. Figure 6–32 shows the model estimate versus the experimental data. The experimental points form a plane which intersects the (x_2', x_3', x_4')-plane, and the positive solute-water parameter from binary data is inconsistent with this. The (large) negative value fitted to the data is able to describe the data quite well, giving an average error of 0.12.

When estimating the parameters from single solvent solubilities, i.e., using the Porter for each pair, the results are worsened in many cases. Generally, the solubility data seems to be dividable in two overall classes: i) nonaqueous solvent mixtures and ii) aqueous mixtures. For the nonaqueous the excess solubilities are generally small. Assuming ideal mixture $(s_1^{\mathrm{E}} = 0)$ yields an average error in the range $0.2 - 0.4$. Using the binary-based parameters usually results in AADs around $1 - 3$. The high degree of nonideality in the solvent mixture facilitates a large degree of nonideality in the solute–solvent interactions, i.e., excess solubilities, but unlike the organic systems, previously addressed, the excess solubilities are significant (> 1). Therefore, the model is able to estimate the excess solubility without

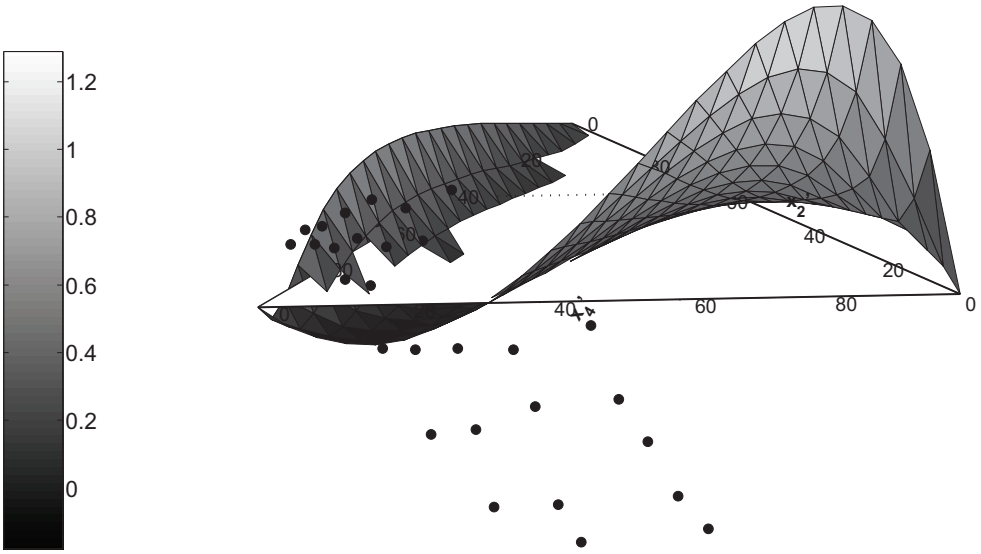

Figure 6–32. Surface plot showing excess solubility of phenobarbital(1) in mixtures of propylene glycol(2), ethanol(3), and water(4). The model estimate changes sign, showing both negative and positive deviations from ideal mixing. The experimental data confirms this behavior partly, especially toward the region of pure ethanol.

mixture data much better than the nonaqueous mixtures. The agreement with data is comparable to fitting the $\mathbf{f}^0$ to mixture data in the aqueous systems.

It is not clear that the FST model is capable of describing the excess solubility behavior in mixtures with three solvent species using the parameters obtained from combining the Porter equation with solubilities in single solvents. There is a clear tendency to overestimate the experimental data. There seems to be two items which relate to this:

- The mixing effects in multisolvent systems are different than in binary solvent systems. This implies that the assumption of equating f_{1j}^0 with f_{1j}^+ is a better approximation in binary solvent systems compared to ternary solvent systems.
- The solvent-solvent term in the model is incorrect. This is related to the assumptions make during the extension of the model from two to three solvents.

It is difficult to conclude what if either (or both) of these statements are correct. The former argument implies that the variation of f_{1j}^+ with solvent composition is different than in binary solvent systems. This statement is not without reasoning. In a binary mixture (of two solvents, since the solute is diluted) there is only one pair interaction between solvents, while in a ternary solvent mixture, there are three

pairs and one triplet. The effects of this on the pair correlation functions (which f_{ij}^{+} are composed of) are difficult to explain. Gray and Gubbins [83] discuss the decomposition of three-body interactions in terms of multipoles, induction, overlap and how these can be decomposed into binaries. However, it is not clear how the effects of these propagate into the molecular correlation functions. Regarding the second item listed above, the model was derived on the basis of the binary solvent model, and was done so with some significant assumptions. These are:

1. The model was not derived rigorously from fluctuation solution theory, but was based on a compromise between rigor and simplicity. The latter was emphasized, and the result was a simple model, which can be reduced to the binary solvent model in the limiting case of two solvents.

2. The solvent-solvent f_{ij}^{+} behave as if in a mixture comprised solely of i and j, i.e., disregarding the presence of the third solvent component.

Deriving a model for excess solubilities in ternary solvent mixtures from fluctuation solution theory, using the principles outlined in Chapter 4, requires taking the inverse of a 4×4 matrix, which results in complicated expressions. These will inevitably involve products of correlation function integrals, which cannot be estimated without extensive regression from experimental data. The perspectives in the method applied in these investigations are the utilization of simple models for delimited problems. Furthermore, the model parameters should have a clear physical interpretation and be obtainable from sources other than regression of mixture data. The consequences of the assumption of the terms W and Z influencing the results *can* be investigated to some extent. They contain H_{ij} for all solute-solvent combinations, and does therefore contribute (positive or negative) to the model estimate. An attempt to include them in the model estimate, as purely empirical coefficients, by fitting them to the mixture data for a few data sets suggests a model of the form

$$\begin{aligned} s_1^{\mathrm{E}} =& \frac{x_2x_3f_{23}^{+} + x_2x_4f_{24}^{+} + x_3x_4f_{34}^{+} + x_3x_4f_{34}^{+} + x_2x_3W_{123} + x_2x_4W_{124} + x_3x_4W_{133}}{1 + x_2x_3f_{23}^{+} + x_2x_4f_{24}^{+}} \\ & \times \left[1 + x_2f_{12}^{0} + x_3f_{13}^{0} + x_4f_{14}^{0}\right]. \end{aligned}$$

Consider the example anthracene with cyclohexane, 2-propanol, and 1-pentanol. Using the binary-based parameters the AAD is 2.70, and fitting values of W for all three triplets gives $\{-2.02, -2.07, 1.07\}$, respectively. This lowers the AAD to 0.35. Using the regressed values of $\mathbf{f}^0$ and refitting W, Q, and Z lowers this statistic to 0.01. Secondly, the anthracene–dioxane–butanol–cyclohexane system gives and AAD of 0.99 using the binary-based parameter set. Fitting the W-terms for this system lowers it to 0.07, i.e., and average error of 0.07. For paracetamol with water, ethanol, and propylene glycol, the AAD using $\mathbf{f}^0$ from binary data is 0.33, which drops to 0.15 when fitting the extra three parameters. For phenobarbital, in the same solvent mixture, the numbers are 0.63 and 0.56, respectively. The errors

in the anthracene sets were lowered significantly when including the extra parameters, but this is not the case in the aqueous systems. Here, addition of adjustable parameters did not improve the results significantly, since results are already good.

Following this is an analysis of a way of estimating the solute-solvent characteristics from reference solvents. The reference solvent approach has been investigated before,[84–86] but in the context of using UNIFAC for infinite dilution activity coefficients. Here, an attempt based on transferability of molecular correlation functions is attempted.

Table 6–7. Systems of solutes and three solvents; T is the temperature of measurement and n indicates the number of experimental observations, excluding pure solvent solubilities. AAD is the error in solubility assuming ideal mixture (AAD-0), as calculated with parameters regressed from mixture data (AAD-1), and pure solvent data (AAD-II). Parameters are listed, obtained from binary data and quaternary solubility data. Standard deviations (S.D.) are provided for the latter.

Solute (1)	Solvent (2)	Solvent (3)	Solvent (4)	T (°C)	n	Ref.	f_{12}^0	f_{13}^0	f_{14}^0	$f_{12}^{0,b}$	$f_{13}^{0,b}$	$f_{14}^{0,b}$	AAD		
													0	I	II
Ether–alkanol–alkane															
Anthracene	MTBE	1-Propanol	Isooctane	25	19	[87]	0.30	0.59	–1.09	2.58	5.85	4.66	0.24	0.04	2.43
Anthracene	MTBE	2-Propanol	Isooctane	25	19	[87]	0.30	1.23	–1.09	2.58	6.58	4.66	0.29	0.04	2.45
Anthracene	MTBE	1-Butanol	Isooctane	25	19	[87]	0.30	0.19	–1.09	2.58	5.25	4.66	0.18	0.03	1.86
Anthracene	MTBE	2-Butanol	Isooctane	25	19	[87]	0.30	0.78	–1.09	2.58	5.87	4.66	0.23	0.04	1.85
Dioxane–alkanol–alkane															
Anthracene	1,4-Dioxane	1-Propanol	Cyclohexane	25	19	[78]	1.25	0.59	–0.46	0.57	5.85	3.93	0.44	0.15	1.09
Anthracene	1,4-Dioxane	2-Propanol	Cyclohexane	25	19	[78]	1.25	1.23	–0.46	0.57	6.58	3.93	0.48	0.16	1.08
Anthracene	1,4-Dioxane	1-Butanol	Cyclohexane	25	19	[78]	1.25	0.19	–0.46	0.57	5.25	3.93	0.40	0.12	0.99
Anthracene	1,4-Dioxane	2-Butanol	Cyclohexane	25	19	[78]	1.25	0.78	–0.46	0.57	5.87	3.93	0.44	0.15	0.94
Anthracene	1,4-Dioxane	2-m–1-propanol	Cyclohexane	25	19	[78]	1.25	0.94	–0.46	0.57	6.31	3.93	0.45	0.14	1.02
Anthracene	1,4-Dioxane	1-Propanol	Isooctane	25	19	[88]	1.25	0.59	–1.09	0.57	5.85	4.66	0.39	0.12	1.60
Anthracene	1,4-Dioxane	2-Propanol	Isooctane	25	19	[88]	1.25	1.23	–1.09	0.57	6.58	4.66	0.44	0.12	1.60
Anthracene	1,4-Dioxane	1-Butanol	Isooctane	25	19	[88]	1.25	0.19	–1.09	0.57	5.25	4.66	0.34	0.13	1.43
Anthracene	1,4-Dioxane	2-Butanol	Isooctane	25	19	[88]	1.25	0.78	–1.09	0.57	5.87	4.66	0.40	0.13	1.37
Anthracene	1,4-Dioxane	2-m–1-propanol	Heptane	25	19	[88]	1.25	0.94	–0.16	0.57	6.31	4.66	0.38	0.10	1.41
Anthracene	1,4-Dioxane	1-Propanol	Heptane	25	19	[77]	1.25	0.59	–0.16	0.57	5.85	3.93	0.41	0.11	1.25
Anthracene	1,4-Dioxane	2-Propanol	Heptane	25	19	[77]	1.25	1.23	–0.16	0.57	6.58	3.93	0.46	0.12	1.27

Continues on next page

Continued from last page

Solute (1)	Solvent (2)	Solvent (3)	Solvent (4)	T (°C)	n	Ref.	f_{12}^{0}	f_{13}^{0}	f_{14}^{0}	$f_{12}^{0,b}$	$f_{13}^{0,b}$	$f_{14}^{0,b}$	AAD		
													0	I	II
Anthracene	1,4-Dioxane	1-Butanol	Heptane	25	19	[77]	1.25	0.19	–0.16	0.57	5.25	3.93	0.35	0.10	1.19
Anthracene	1,4-Dioxane	2-Butanol	Heptane	25	19	[77]	1.25	0.78	–0.16	0.57	5.87	3.93	0.40	0.13	1.12
Anthracene	1,4-Dioxane	2-m–1-propanol	Heptane	25	19	[77]	1.25	0.94	–0.16	0.57	6.31	3.93	0.41	0.12	1.17
		Alkane–2×alkanol													
Anthracene	Cyclohexane	1-Propanol	1-Pentanol	25	19	[89]	–0.46	0.59	–0.41	3.93	5.85	4.62	0.17	0.05	2.70
Anthracene	Cyclohexane	2-Propanol	1-Pentanol	25	19	[89]	–0.46	1.23	–0.41	3.93	6.58	4.62	0.22	0.07	2.70
Anthracene	Cyclohexane	1-Butanol	1-Pentanol	25	19	[89]	–0.46	0.19	–0.41	3.93	5.25	4.62	0.12	0.05	2.49
Anthracene	Cyclohexane	2-Butanol	1-Pentanol	25	19	[89]	–0.46	0.78	–0.41	3.93	5.87	4.62	0.16	0.05	2.50
Anthracene	Isooctane	1-Propanol	1-Pentanol	25	19	[90]	–1.09	0.59	–0.41	4.66	5.85	4.62	0.13	0.04	2.98
Anthracene	Isooctane	2-Propanol	1-Pentanol	25	19	[90]	–1.09	1.23	–0.41	4.66	6.58	4.62	0.18	0.05	2.96
Anthracene	Isooctane	1-Butanol	1-Pentanol	25	19	[90]	–1.09	0.19	–0.41	4.66	5.25	4.62	0.10	0.03	2.79
Anthracene	Isooctane	1-Butanol	1-Pentanol	25	19	[87]	–1.09	0.19	–0.41	2.58	6.31	4.66	0.24	0.13	2.52
Anthracene	Isooctane	2-Butanol	1-Pentanol	25	19	[90]	–1.09	0.78	–0.41	4.66	5.87	4.62	0.14	0.03	2.71
Anthracene	Cyclohexane	1-Propanol	2-m–1-propanol	25	19	[91]	–0.46	0.59	0.94	3.93	5.85	6.31	0.20	0.08	2.91
Anthracene	Cyclohexane	2-Propanol	2-m–1-propanol	25	19	[91]	–0.46	1.23	0.94	3.93	6.58	6.31	0.24	0.10	2.96
Anthracene	Cyclohexane	1-Butanol	2-m–1-propanol	25	19	[91]	–0.46	0.19	0.94	3.93	5.25	6.31	0.16	0.08	2.76
Anthracene	Cyclohexane	2-Butanol	2-m–1-propanol	25	19	[91]	–0.46	0.78	0.94	3.93	5.87	6.31	0.19	0.08	2.78
Anthracene	1-Propanol	1-Butanol	Isooctane	25	19	[92]	0.59	0.19	–1.09	5.85	5.25	4.66	0.14	0.17	3.57
Anthracene	1-Propanol	2-Butanol	Isooctane	25	19	[92]	0.59	0.78	–1.09	5.85	5.87	4.66	0.13	0.16	3.61
Anthracene	2-Propanol	1-Butanol	Isooctane	25	19	[92]	1.23	0.19	–1.09	6.58	5.25	4.66	0.16	0.13	3.53
Anthracene	2-Propanol	2-Butanol	Isooctane	25	19	[92]	1.23	0.78	–1.09	6.58	5.87	4.66	0.18	0.16	3.57

Continues on next page

Continued from last page

Solute (1)	Solvent (2)	Solvent (3)	Solvent (4)	T (°C)	n	Ref.	f_{12}^{0}	f_{13}^{0}	f_{14}^{0}	$f_{12}^{0,b}$	$f_{13}^{0,b}$	$f_{14}^{0,b}$	AAD		
													0	I	II
Pyrene	1-Propanol	1-Butanol	Cyclohexane	26	19	[93]	0.07	–0.33	–0.06	6.87	6.13	5.02	0.20	0.03	3.22
Pyrene	2-Propanol	1-Butanol	Cyclohexane	26	19	[93]	0.77	–0.33	–0.06	7.62	6.13	5.02	0.22	0.01	3.35
Pyrene	1-Propanol	2-Butanol	Cyclohexane	26	19	[93]	0.07	0.51	–0.06	6.87	6.81	5.02	0.21	0.02	3.35
Pyrene	2-Propanol	2-Butanol	Cyclohexane	26	19	[93]	0.77	0.51	–0.06	7.62	6.81	5.02	0.26	0.02	3.35
Alkanol–2×alkane															
Anthracene	1-Propanol	Isooctane	Cyclohexane	25	19	[94]	0.59	–1.09	–0.46	5.85	4.66	3.93	0.20	0.08	3.98
Anthracene	2-Propanol	Isooctane	Cyclohexane	25	19	[94]	1.23	–1.09	–0.46	6.58	4.66	3.93	0.24	0.08	4.08
Anthracene	1-Butanol	Isooctane	Cyclohexane	25	19	[94]	0.19	–1.09	–0.46	5.25	4.66	3.93	0.13	0.04	2.89
Anthracene	2-Butanol	Isooctane	Cyclohexane	25	19	[94]	0.78	–1.09	–0.46	5.87	4.66	3.93	0.19	0.04	2.88
Pyrene	1-Propanol	Cyclohexane	Heptane	26	19	[95]	0.07	–0.06	0.02	6.87	5.02	5.02	0.27	0.02	5.18
Pyrene	2-Propanol	Cyclohexane	Heptane	26	19	[95]	0.77	–0.06	0.02	7.62	5.02	5.02	0.32	0.03	4.57
Pyrene	1-Butanol	Cyclohexane	Heptane	26	19	[95]	–0.33	–0.06	0.02	6.13	5.02	5.02	0.20	0.04	3.96
Pyrene	2-Butanol	Cyclohexane	Heptane	26	19	[95]	0.51	–0.06	0.02	6.81	5.02	5.02	0.27	0.04	3.08
Pyrene	2-m–1-propanol	Cyclohexane	Heptane	26	19	[95]	0.70	–0.06	0.02	7.39	5.02	5.02	0.27	0.03	3.45
Alkane–ketone–alkanol															
Anthracene	Isooctane	Acetone	1-Propanol	25	19	[96]	–1.09	1.63	0.59	4.60	2.48	5.77	0.41	0.15	1.34
Anthracene	Isooctane	Acetone	2-Propanol	25	19	[96]	–1.09	1.63	1.23	4.60	2.48	6.45	0.40	0.08	1.54
Anthracene	Isooctane	Acetone	Ethanol	25	19	[96]	–1.09	1.63	1.44	4.60	2.48	6.15	0.38	0.08	1.76
Anthracene	Isooctane	Acetone	Methanol	25	19	[96]	–1.09	1.63	3.03	4.60	2.48	7.69	0.46	0.14	2.49
Aqueous systems															
Paracetamol	Water	Acetone	Toluene	0	9	[18]	5.48	–4.99	6.64	3.51	–3.84	7.17	0.55	0.24	0.30

Continues on next page

Continued from last page

Solute (1)	Solvent (2)	Solvent (3)	Solvent (4)	T (°C)	n	Ref.	f_{12}^{0}	f_{13}^{0}	f_{14}^{0}	$f_{12}^{0,b}$	$f_{13}^{0,b}$	$f_{14}^{0,b}$	AAD		
													0	I	II
Paracetamol	Water	Acetone	Toluene	5	9	[18]	5.48	–4.99	6.64	3.43	–4.02	6.94	0.57	0.25	0.30
Paracetamol	Water	Acetone	Toluene	10	9	[18]	5.48	–4.99	6.64	3.34	–4.21	6.78	0.59	0.24	0.31
Paracetamol	Water	Acetone	Toluene	15	9	[18]	5.48	–4.99	6.64	3.23	–4.45	6.73	0.61	0.24	0.31
Paracetamol	Water	Acetone	Toluene	16	9	[18]	5.48	–4.99	6.64	3.21	–4.51	7.20	0.59	0.24	0.31
Paracetamol	Water	Acetone	Toluene	20	9	[18]	5.48	–4.99	6.64	3.12	–4.70	6.85	0.61	0.24	0.31
Paracetamol	Water	Acetone	Toluene	25	9	[18]	5.48	–4.99	6.64	3.01	–5.02	7.04	0.62	0.24	0.32
Paracetamol	Water	Acetone	Toluene	30	9	[18]	5.48	–4.99	6.64	2.90	–5.32	7.38	0.62	0.24	0.32
Paracetamol	Water	Ethanol	1,2-Propanediol	25	36	[81]	5.48	5.78	13.00	7.48	0.80	1.05	0.75	0.14	0.33
Phenobarbital	1,2-Propanediol	Ethanol	Water	25	36	[82]	–6.20	–1.45	–10.40	–5.12	–4.15	5.66	0.55	0.12	0.63
Halogenated alkanes															
Benzoic acid	Carbon tetrachl.	Cyclohexane	Hexane	25	7	[79]	–0.76	1.65	0.69	2.70	5.47	5.74	0.06	0.01	0.20
Benzoic acid	Carbon tetrachl.	Cyclohexane	Heptane	25	8	[79]	–0.76	1.65	–1.20	2.70	5.47	5.49	0.03	0.00	0.18
Naphthalene	Benzene	1,4-Dioxane	Chloroform	25	6	[80]	–1.17	–0.53	–0.47	0.45	0.31	–0.18	0.06	0.02	0.09
Naphthalene	Benzene	1,4-Dioxane	Chloroform	40	6	[80]	–1.17	–0.53	–0.47	0.52	0.38	–0.02	0.03	0.01	0.12
Naphthalene	Benzene	1,4-Dioxane	Chloroform	55	6	[80]	–1.17	–0.53	–0.47	0.70	0.56	0.24	0.02	0.02	0.15

6.6. Predicting solute-solvent parameters from reference solvents

Presently, the solute-solvent parameters are estimated from either regressing experimental solubility data, Porter equation with single solvent solubilities, or perhaps UNIFAC. The estimates are in a fair amount of cases consistent with values found from regression of ternary mixture data, but there are also many cases where the agreement is less good. Estimation from binary data is limited by the melting temperatures and heats of melting (and perhaps change in heat capacity) frequently being unavailable for a large number of solutes, or is flawed by uncertainty in measurements. Models, which are based on molecular structure, e.g. group contribution methods, can predict these values, but the uncertainty in the estimates is usually high, especially for polyfunctional molecules. Furthermore, the availability of group parameters is often sparse in these cases, further limiting the application range.

In this section, the use of a scheme for estimating solute-solvent parameters f_{1j}^0 from a known value in another solvent – a *reference* solvent – is investigated. Thus, if relations connecting f_{12}^0 for a solute (1) in a solvent (2) to that of 1 in another solvent can be established, it opens for a powerful and very general way of estimating solid-liquid equilibria. Thus, parameters can be predicted without knowledge of the thermophysical properties characterizing the fusion process. First step is to recognize that the parameters are the coefficients that appears in the Taylor expansion of the chemical potential, Equation (4–10),

$$f_{12}^0 = -\lim_{x_2\to 1}\frac{\partial}{\partial x_1}\left(\frac{\mu_1}{\mathsf{R}T}+1-\frac{1}{x_1}\right)_{T,P,n_2} = -\lim_{x_2\to 1}\left(\frac{\partial \ln\gamma_1}{\partial x_1}\right)_{T,P,n_2}. \tag{6–11}$$

The method used here is based on relating these derivatives in binary and ternary mixtures to total correlation function integrals. However, they can also be expressed in terms of direct correlation function integrals. For a binary, O'Connell[97] showed that

$$-\lim_{x_2\to 1}\left(\frac{\partial \ln\gamma_1}{\partial x_1}\right) = \frac{(1-C_{11}^0)(1-C_{22}^0)-(1-C_{12}^0)^2}{1-C_{22}^0}. \tag{6–12}$$

where C_{ij} is the direct correlation function integral, defined in Equation (2–32), superscript 0 denotes infinite dilution of solute, 1. This expression can be simplified by writing Equation (2–41) for a binary at infinite dilution of 1

$$\lim_{x_1\to 0}\rho\bar{v}_1 = \lim_{x_1\to 0}\frac{1-\sum_{j=1}^{2}x_jC_{1j}}{1-\sum_{i=1}^{2}\sum_{j=1}^{2}x_ix_jC_{ij}} = \frac{1-C_{12}^0}{1-C_{22}^0}. \tag{6–13}$$

The reduced liquid bulk modulus is defined as $B_{ij} \equiv 1 - C_{ij}$. This means, that

$$f_{12}^0 = B_{11}^0 - (\rho_2 \bar{v}_1^0)^2 B_{22}. \tag{6–14}$$

Below are listed two assumptions in order to apply Equation (6–14):

1. Dense substances, such as solids, usually have small excess molar volumes, indicating that the partial molal volumes are well approximated by the molal volumes.

2. If the solute forms a pure solid phase, the solute-solute direct correlation function integral in a single solvent might be unaffected by the nature of the medium in which the solid is dissolved, i.e., that C_{11}^0 is solvent-independent.

The former is reasonable in many systems of organics. Though the excess volumes of aqueous mixtures are usually larger than purely organic systems, the relative values are still quite small. The latter item is related to the strong density dependence of the correlation functions. If the solid phase is pure, i.e., the interaction with the solvent is smaller than the solute-solute interaction. Then C_{11}^0 is likely to depend only on the nature of the solute, and the right-hand side of Equation (6–14) is independent of solute-solvent interactions, and depends only on properties of pure solute and solvent. This hypothesis can be examined from previously determined values of f_{12}^0. For a solid in pure solvents 2 and R this means

$$C_{11}^0(2) = C_{11}^0(R) \qquad \Rightarrow \qquad f_{12}^0 = f_{1R}^0 + (\rho_2 v_1)^2 B_{22} - (\rho_R v_1)^2 B_{RR}. \tag{6–15}$$

Table 6–8 shows values of f_{12}^0 for a number of solute-solvent pairs, where the values found from regression matched those from single solvent data, and the solubility data was described quantitatively. The direct correlation function integrals of the pure solvents were obtained from the equation of state of Huang and O'Connell.[103] The seventh column of Table 6–8 shows that C_{11}^0 is not constant. The C_{ij} is a product of solution density and the integral of direct correlation function, and it might be that the integral itself is independent of the solvent, i.e.,

$$\begin{aligned} &\int c_{11}^0(2)\mathrm{d}\mathbf{r} = \int c_{11}^0(R)\mathrm{d}\mathbf{r} \\ \Rightarrow \quad &\frac{C_{11}^0(2)}{\rho_2} = \frac{C_{11}^0(R)}{\rho_R}. \end{aligned} \tag{6–16}$$

or, in dimensionless units,

$$C_{11}^0(2)\frac{v_2}{v_1} = C_{11}^0(R)\frac{v_R}{v_1}. \tag{6–17}$$

These recurrence relations predict solute-solvent parameters for a solute in all solvents, given a known value of f_{12}^0 in a reference solvent. The requirements for input are

Table 6–8. Pure species molar volumes[a] and solute-solute direct correlation function integrals from solute-solvent characteristics. The table shows that the recurrence relations sought in the section are generally unsuccessful, since neither quantities in the two right-most columns are constant for a particular solute in a single (pure) solvent.

Solute (1)	Solvent (2)	f_{12}^0	v_1 $(\mathrm{cm}^3/\mathrm{mol})$	v_2 $(\mathrm{cm}^3/\mathrm{mol})$	B_{22}^0	C_{11}^0	$C_{11}^0 v_2/v_1$
Sulfamethazine	Water	16.38	197.0	18.1	14	-1633	-150
Sulfamethazine	Ethanol	5.32	197.0	58.6	21	-246	-73
Sulfamethazine	Dioxane	1.7	197.0	85.7	20	-105	-46
Paracetamol	Water	7.19	115.7	18.1	14	-564	-88
Paracetamol	Acetone	3.18	115.7	73.8	30	-75	-48
Paracetamol	Ethanol	2.54	115.7	58.6	21	-85	-43
Phenacetin	Water	13.86	154.6	18.1	14	-1009	-118
Phenacetin	Dioxane	2.06	154.6	85.7	20	-66	-36
Cholesterol	Hexane	2.47	338.3	131.4	44	-292	-114
Cholesterol	Ethanol	4.22	338.3	58.6	21	-715	-124
Cholesterol	Benzene	2.11	338.3	89.5	43	-615	-163
Pyrene	Acetonitrile	0.93	172.0	52.9	16	-164	-50
Pyrene	2-m-2-butanol	-2.77	172.0	109.6	52	-123	-79
Naphthalene	Water	2.37	125.0	18.1	14	-653	-94
Naphthalene	Ethanol	17.45	125.0	58.6	21	-114	-53
Naphthalene	Benzene	-0.33	125.0	89.5	43	-82	-59

[a] References for v_1^0: Sulfamethazine,[98] paracetamol,[65,99] phenacetin,[98] cholesterol,[100] pyrene,[101] and naphthalene.[101] Solvent molar volumes taken from the DIPPR compilation.[102]

1. Knowledge of f_{1R}^0.
2. Pure solvent direct correlation function integrals for computing B_{22}^0 and B_{RR}^0. These can be obtained from existing models in the literature,[103,104] or from compressed liquid density data.
3. Molar volumes of pure solvents at system temperature.
4. Molar volumes of the solute (or partial molal volumes of the solute, if available).

The right-most column of Table 6–8 show the results of applying Equation (6–17). From Table 6–8 it is clear, that the value of $C_{11}^0(2)v_2/v_1$ is not transferable from solvent to solvent. The variation from one solvent to another is large. However, there appears to be a systematic trend in the variation of $C_{11}^0 v_2/v_1$. The solute-water property is usually twice that of solute with ethanol, and threefold that of solute with dioxane.

This information can be useful. Water, ethanol, and dioxane are the most abundant solvents for pharmaceutical solutes. However, extension to additional solvents require more data. For practical usage, a problem occurs in the formulation of Equations (6–15) and (6–17): They contain squares of molar volume ratios. Since the molar volume of a solid is usually very large, compared to traditional

solvents, these ratios can be significant (they may vary as much as an order of magnitude), making the squared values even larger, and therefore extremely sensitive towards even small errors in molar volumes. This can be seen by writing Equation (6–15) as

$$f_{12}^0 - f_{1R}^0 = (v_1/v_2)^2 B_{22} - (v_1/v_R)^2 B_{RR}. \tag{6–18}$$

The f_{1j}^0 typically range in ± 20, whereas the molar volume ratios can be very large. This means, that the result is a small difference of large numbers. This is not desirable, since this makes the predicted parameters, f_{1R}^0, too sensitive to the input data.

6.7. Summary

This chapter has seen the application of the FST method, outlined in Chapter 4, applied to excess solubilities in solvent mixtures. A thorough examination showed the importance of characterizing the solvent mixture appropriately, since incompatibilities between solvent-solvent nonideality and excess solubilities, can lead to wrongful estimation of parameters. This was also illustrated with a few examples of naphthalene in water–DMSO and water–ethylene glycol. An extensive list of pharmaceutical solutes were addressed, and the results showed that results are generally successful when estimating the solute-solvent parameters from single solvent solubilities. Estimation of parameters using UNIFAC often leads to overestimation. Using UNIFAC to generate activity coefficient for solving the equilibrium relations, showed that UNIFAC often is unable to give accurate estimates of solubilities in single solvents, whereby the mixed solvent solubility behavior is also inaccurately described. Curiously, UNIFAC gives much better results when forming excess solubilities.

The model developed for excess solubilities in ternary solvent mixtures was also applied. The results were less good compared to the binary solvent cases. However, results for the aqueous mixtures revealed, that the method performs better in aqueous mixtures. This is encouraging, since excess solubilities are often large in these systems.

Finally, a relation which links the solute-solvent parameter to that in another solvent was tested. It was found that the resulting expression was too sensitive towards molar volumes, so that a small difference in large numbers governed the estimate of the solute-solvent parameters.

References

1. A. B. Ochsner and T. D. Sokoloski. *J. Pharm. Sci.*, 74:634–637, 1985.
2. A. Martin, P. L. Wu, and A. Beerbower. *J. Pharm. Sci.*, 73:188–194, 1984.
3. P. L. Wu and A. Martin. *J. Pharm. Sci.*, 72:587–592, 1983.
4. S. Gracin and Å. C. Rasmuson. *J. Chem. Eng. Data*, 47:1379–1383, 2002.
5. J. E. Coon, W. B. Sediawan, J. E. Auwaerter, and E. McLaughlin. *J. Sol. Chem.*, 17:519–534, 1988.
6. K. Sakai. *J. Chem. Eng. Data*, 37:249–251, 1992.
7. N. Garti, L. Karpuj, and S. Sarig. *Thermochim. Acta*, 35:343–348, 1980.

References

8. S. Pal and S. P. Moulik. *Ind. J. Biochem. Biophys.*, 21:12–16, 1984.

9. U. Domańska, C. Klofutar, and S. Paljk. *Fluid Phase Equil.*, 97:191–200, 1994.

10. W. Chen, B. Su, H. Xing, Y. Yang, and Q. Ren. *Fluid Phase Equil.*, 287:1–6, 2009.

11. L. C. Labowitz. *Thermochim. Acta*, 3:419, 1972.

12. S. Romero, B. Escalera, and P. Bustamente. *Int. J. Pharm.*, 178:193–202, 1999.

13. D. Khossravi and K. A. Connors. *J. Pharm. Sci.*, 81:371–379, 1992.

14. I. Kotula and B. Marciniak. *J. Chem. Eng. Data*, 46:783–787, 2001.

15. A. A. Sunier. *J. Phys. Chem.*, 34:2582, 1930.

16. D. J. W. Grant, M. Mehdizadeh, A. H. L. Chow, and J.E. Fairbrother. *Int. J. Pharm.*, 18:25–38, 1984.

17. S. Romero, A. Reillo, B. Escalera, and P. Bustamente. *Chem. Pharm. Bull.*, 44(5):1061–1064, 1996.

18. R. A. Granberg and Å. C. Rasmuson. *J. Chem. Eng. Data*, 45:478–483, 2000.

19. S. H. Neau, S. V. Bhandarkar, and E. W. Hellmuth. *Pharm. Res.*, 14:601, 1997.

20. C. Bustamente and P. Bustamente. *J. Pharm. Sci.*, 85:1109–1111, 1996.

21. M. A. Pena, A. Reillo, B. Escalera, and P. Bustamante. *Int. J. Pharm.*, 321:155–161, 2006.

22. P. B. Choi and E. McLaughlin. *Ind. Eng. Chem. Fundam.*, 22:46–51, 1983.

23. C. Sunwoo and H. Eisen. *J. Pharm. Sci.*, 60:238–244, 1971.

24. F. I. Khattab. *Thermochim. Acta*, 61:253–268, 1983.

25. P. Bustamente, R. Ochoa, A. Reillo, and J. B. Escalera. *Chem. Pharm. Bull.*, 42:1129–1133, 1994.

26. P. Bustamente, B. Escalera, A. Martin, and E. Selles. *J. Pharm. Sci.*, 78:567–573, 1994.

27. J. B. Escalera, P. Bustamente, and A. Martin. *J. Pharm. Pharmacol.*, 46:172–176, 1994.

28. P. Bustamente and B. Escalera. *J. Pharm. Pharmacol.*, 47:550–555, 1995.

29. H. M. Lin and R. A. Nash. *J. Pharm. Sci.*, 82: 1018–1026, 1993.

30. C. A. S. Bergstrom, U. Norinder, K. Luthman, and P. Artursson. *Pharm. Res.*, 19:182–188, 2002.

31. A. Martin, J. Newburger, and A. Adjei. *J. Pharm. Sci.*, 69:487–491, 1980.

32. A. Martin, A. N. Paruta, and A. Adjei. *J. Pharm. Sci.*, 70:1115–1120, 1981.

33. J. Weicherz and H. Marschik. *Biochem. Z.*, 249: 312, 1932.

34. C. I. Monarrez, J. H. Woo, P. G. Taylor, A. M. Tran, and W. E. Acree Jr. *J. Chem. Eng. Data*, 48: 720–722, 2003.

35. J. M. Lepree, M. J. Mulski, and K. A. Connors. *J. Chem. Soc., Perk. Trans.*, 2:1491–1497, 1994.

36. J. M. Prausnitz, R. N. Lichtenthaler, and E. Gomez de Azevedo. *Molecular thermodynamics of fluid-phase equilibria*. Prentice-Hall, 3rd edition, 1999.

37. W. E. Acree Jr. *J. Chem. Soc. Faraday Trans.*, 87: 461–464, 1991.

38. A. I. Zvaigzne and W. E. Acree Jr. *Phys. Chem. Liq.*, 24:31–42, 1991.

39. A. I. Zvaigzne and W. E. Acree Jr. *J. Chem. Eng. Data*, 39:708–710, 1994.

40. A. I. Zvaigzne, I. L. Teng, E. Martinez, J. Trejo, and W. E. Acree Jr. *J. Chem. Eng. Data*, 38:389–392, 1993.

41. A. I. Zvaigzne, J. Wolfe, and W. E. Acree Jr. *J. Chem. Eng. Data*, 39:541–543, 1994.

42. M. Ronc and G. A. Ratcliff. *Can. J. Chem. Eng.*, 54:326, 1976.

43. H. C. Van Ness, A. Soczek, G. L. Peloquin, and R. L. Machado. *J. Chem. Eng. Data*, 12:217–224, 1967.

44. T. Hiaki, K. Takahashi, T. Tsuji, M. Hongo, and Kojima K. *J. Chem. Eng. Data*, 40:271–273, 1995.

45. J. R. Powell, McHale M. E. R., A. S. M. Kauppila, Oterom P., and Acree Jr. W.E. Jayasekera, M. *J. Chem. Eng. Data*, 40:1270–1272, 1995.

46. G. M. Wilson and C. H. Deal. *Ind. Eng. Chem. Res. Fundam.*, 1:20–23, 1962.

47. Aa. Fredenslund, R. L. Jones, and J. M. Prausnitz. *AIChE J.*, 21:1086–1099, 1975.

48. A. I. Zvaigzne, B. Smith, Y. Cordero, and W. E. Acree Jr. *Phys. Chem. Liq.*, 25:51–58, 1991.

49. J. R. Powell, K. S. Coym, and W. E. Acree Jr. *J. Chem. Eng. Data*, 42:395–397, 1997.

50. K. M. de Fina, S. Abernathy, K. Alexander, C. Olugbuyi, A. Vance, and W. E. Acree Jr. *J. Chem. Eng. Data*, 48:402–404, 2003.

51. M. E. R. Mchale, K. S. Coym, K. A. Fletcher, and W. E. Acree Jr. *J. Chem. Eng. Data*, 42:511–513, 1997.

52. C. I. Monarrez, J. H. Woo, P. G. Taylor, A. M. Tran, and W. E. Acree Jr. *J. Chem. Eng. Data*, 48: 736–738, 2003.

53. R. M. Dickhut, A. W. Andren, and D. E. Armstrong. *J. Chem. Eng. Data*, 34:438–443, 1989.

54. E. L. Heric and C. D. Posey. *J. Chem. Eng. Data*, 9:35, 1964.

55. T. Treszczanowicz, A. J. Treszczanowicz, T. Kasprzycka-Guttman, and A. Kulesza. *J. Chem. Eng. Data*, 46(4):792–794, 2001.

56. T. Treszczanowicz, T. Kasprzycka-Guttman, and A. J. Treszczanowicz. *J. Chem. Eng. Data*, 48: 1517–1520, 2003.

57. T. Treszczanowicz, A. J. Treszczanowicz, T. Kasprzycka-Guttman, and A. Kulesza. *J. Chem. Eng. Data*, 46:1494–1496, 2001.

58. T. Treszczanowicz, T. Kasprzycka-Guttman, and A. J. Treszczanowicz. *J. Chem. Eng. Data*, 52: 261–264, 2007.

59. A. Martin, P. L. Wu, A. Adjei, M. Mehdizadeh, K. C. James, and C. Metzler. *J. Pharm. Sci.*, 71: 1334, 1982.

60. A.N. Paruta. *J. Pharm. Sci.*, 56:1565–1569, 1967.

61. A.N. Paruta and S.A. Irani. *J. Pharm. Sci.*, 54: 1334–1338, 1965.

62. P. Bustamente, B. Escalera, A. Martin, and E. Selles. *J. Pharm. Pharmacol.*, 45:253–257, 1993.

63. A. Reillo, B. Escalera, and E. Selles. *Pharmazie*, 48:904–907, 1993.

64. S. Prakongpan and T. Nagai. *Chem. Pharm. Bull.*, 31:340–343, 1984.

65. C. V. S. Subrahmanyam, M. S. Reddy, J. V. Rao, and P. G. Rao. *Int. J. Pharm.*, 78:17–24, 1992.

66. W. E. Acree Jr. *J. Chem. Eng. Data*, 46:885–887, 2001.

67. E. A. Guggenheim. *Mixtures*. Oxford University Press, 1952.

68. A. Regosz, T. Pelplinska, P. Kowalski, and Z. Thiel. *Int. J. Pharm.*, 88:437, 1992.

69. S. S. Yang and J. K. Guillory. *J. Pharm. Sci.*, 61: 26, 1972.

70. S. Gracin, T. Brinck, and Å. C. Rasmuson. *Ind. Eng. Chem. Res.*, 41:5114–5124, 2002.

71. P. Di Martino, A. M. Guyot-Hermann, P. Conflant, M. Drache, and J. C. Guyot. *Int. J. Pharm.*, 128: 1, 1996.

72. S. H. Yalkowsky, S. C. Valvani, and T. J. Roseman. *J. Pharm. Sci.*, 72:866, 1983.

73. J. G. Fokkens, J. G. M. van Amelsfoort, C. G. de Blaey, C. J. andde Kruif, and J. Wilting. *Int. J. Pharm.*, 14:79, 1983.

74. H. Zhu, C. Yuen, and D. J. W. Grant. *Int. J. Pharm.*, 135:151, 1996.

75. A. G. Gonzales, M. A. Herrador, and A. G. Asuero. *Int. J. Pharm.*, 108:149, 1994.

76. T. Umeda, N. Ohnishi, T. Yokoyama, T. Kuroda, Y. Kita, K. Kuroda, E. Tatsumi, and Y. Matsuda. *Chem. Pharm. Bull.*, 33:2073, 1985.

77. K. J. Pribyla, M. A. Spurgin, I. Chuca, and W. E. Acree Jr. *J. Chem. Eng. Data*, 45:965–967, 2000.

78. K. J. Pribyla, M. A. Spurgin, I. Chuca, and W. E. Acree Jr. *J. Chem. Eng. Data*, 45:971–973, 2000.

79. W. E. Acree Jr. and G. L. Bertrand. *J. Pharm. Sci.*, 70:1033–1036, 1981.

80. M. L. Negadi. *Etude de la Solubilité du naphthaléne dans les Solvants Ternaires. Approche par les méthodes UNIFAC et ASOG et la modèle d'une solution simple*. PhD thesis, Universite de Tlemcen, Algeria, 1989.

81. A. Jouyban, O. Azarmir, S. Mirzaei, D. Hassanzadeh, T. Ghafourian, W. E. Acree Jr., and A. Nokhodchi. *Chem. Pharm. Bull.*, 56:602–606, 2008.

82. C. F. Peterson and R. E. Hopponen. *J. Am. Pharm. Assoc. Sci. Ed.*, 42:540–542, 1953.

83. C. G. Gray and K. E. Gubbins. *Theory of molecular fluids*, volume 1: Fundamentals. Oxford University Press, 1984.

84. J. Abildskov and J. P. O'Connell. *Fluid Phase Equil.*, 228-229:395–400, 2005.

85. J. Abildskov and J. P. O'Connell. *Mol. Sim.*, 30: 367–378, 2004.

86. J. Abildskov and J. P. O'Connell. *Ind. Eng. Chem. Res.*, 42:5622–5634, 2003.

87. K. J. Pribyla, C. Ezell, T. T. Van, and W. E. Acree Jr. *J. Chem. Eng. Data*, 45:974–976, 2000.

88. K. J. Pribyla, T. T. Van, C. Ezell, and W. E. Acree Jr. *J. Chem. Eng. Data*, 45:968–970, 2000.

89. B. A. Martine, B. H. Blake-Taylor, and W. E. Acree Jr. *J. Chem. Eng. Data*, 53:556–558, 2008.

90. B. H. Blake-Taylor, B. A. Martine, and W. E. Acree Jr. *J. Chem. Eng. Data*, 53:970–972, 2008.

91. A. Proctor, B. H. Blake-Taylor, and W. E. Acree Jr. *J. Chem. Eng. Data*, 53:2910–2912, 2008.

92. T. Deng, S. D. Childress, K. M. De Fina, T. L. Sharp, and W. E. Acree Jr. *J. Chem. Eng. Data*, 43:1065–1067, 1998.

93. E. M. Debase and W. E. Acree Jr. *J. Chem. Eng. Data*, 46:991–993, 2001.

94. T. Deng and W. E. Acree Jr. *J. Chem. Eng. Data*, 43:1059–1061, 1998.

95. E. M. Debase and W. E. Acree Jr. *J. Chem. Eng. Data*, 46:1297–1299, 2001.

96. A. Shayanfar, S. Soltani, F. Jabbaribar, E. Tamizi, W. E. Acree Jr., and A. Jouyban. *J. Chem. Eng. Data*, 53:890–893, 2008.

97. J. P. O'Connell. *Mol. Phys.*, 20(1):27–33, 1971.

98. A. F. M. Barton. *CRC handbook of solubility parameters and other cohesion parameters*. CRC Press, 2nd edition, 1989.

References

99. B. Y. Shekunov, M. Hanna, and P. York. *J. Cryst. Gr.*, 198-199:1345–1351, 1999.

100. U. Domańska, A. Pobudkowska, and P. Gierycz. *Fluid Phase Equil.*, 289:20–31, 2010.

101. H. Davis and S. Gottlieb. *Fuel*, 8:37, 1962.

102. DIPPR 801 project. Design institute for physical properties, americal institute for chemical engineers, 2005-2010.

103. Y. H. Huang and J. P. O'Connell. *Fluid Phase Equil.*, 37:75–84, 1987.

104. P. M. Mathias and J. P. O'Connell. *Chem. Eng. Sci.*, 36:1123–1132, 1981.

7. Summary and discussion for Part I

The present method for predicting solubilities of solid solutes in mixed solvents should be attractive to engineers and thermodynamicists, since the method may be used in a variety of forms, depending upon the available input data. A key point is that solubilities in mixed solvents can often be predicted from solubilities in pure solvents alone, though the quality of the estimates without multisolvent data depends upon the following factors:

1. A g^{E}-model must be known for the binary solvent mixtures (also when regressing parameters).
2. Estimates must be made of the f_{1j}^{0} parameters for both solute-solvent pairs.
3. Thermophysical properties of the pure solid solute must be obtainable.

While having activity coefficient derivatives of the mixed solvent is necessary, the particular g^{E}-model selected does not strongly affect the results. However, there must be systematic variation in the g^{E} of the solvent mixtures with molecular structure. When sufficient data have been available, solubility estimates using both the Wilson and modified Margules equations have been done. Normally the results are very similar. The model is limited in that the sign of the excess solubility must be consistent with sign of excess free energy for the solvent pair. This means that if the solvent-solvent g^{E} changes sign, the excess solubility in that mixture must do so also in order to qualitatively describe the data. This behavior is not always observed in the pharmaceutical cases reported here, but some examples were observed with aqueous naphthalene mixtures. For reliability, the most important aspect seems to be accurate determination of the solute-solvent parameters, f_{1j}^{0} , especially parameters of larger value in magnitude. If this quantity is accurate, predictions will commonly be reliable. The bigger parameter is often associated with the more nonideal solute-solvent pair or the solvent with the lowest solute solubility. Often this is water. Thus, having accurate measurements of low solubilities, especially in water, can determine accuracy in predicting mixed solvent solubilities.

Estimating the solute-solvent parameter from single solvent solubilities with the Porter equation delivers useful results, although the accuracy is sometimes less than then case when regressing them from

mixed solvent solubility data. This suggests that the assumed symmetric composition dependence of the Porter equation is incorrect. Perhaps using additional temperature dependent solubility data to assess and mitigate measurement errors. The temperature range of the data studied is rather narrow, and focus is on systems at or near room temperature. Alternatives to the Porter equation include models such as UNIFAC, though it is frequently not directly applicable to e.g. pharmaceutical systems, though other methods to circumvent this difficulty exist.[1–3] Explorations[4] of the properties of UNIFAC derivatives at infinite dilution suggest that this could have several attractive features, but the methods are more complicated than the present approach. Extensions of UNIFAC parameter tables continue to appear,[5,6] but several pharmaceuticals, and substances with similar polyfunctionality, will remain untractable for quite some time. Recently, a modification to UNIFAC ("Pharma" UNIFAC[7]) was proposed, which incorporates functional groups not previously covered by UNIFAC. UNIFAC estimates relies on a good combinatorial part, Equation (5–19). This has mostly been tested for chain-like species, such as homologous series of organic compounds, and not pharmaceuticals. Moreover, regression of UNIFAC group parameters require large data compilations, so this method is not attractive for molecular structures with new stoichiometries.

Having values of the pure solute properties to estimate ideal solubility is required. First, at least $T_{m,i}$ and $\Delta h_{m,i}$ must be known. It is found that results are better when $\Delta c_{P,m,i}$ is also known, especially if its value is large or if $T_{m,i} - T$ is significant. Phase transitions below the melting point are relevant, but they seem not to make much difference according to the cases reported here, as seen in the systems containing sulfamethazine, sulfamethoxypyridazine, sulfanilamide, paracetamol, cholesterol, and mefenamic acid. All of these solutes have been claimed to undergo a solid phase transition below the melting point. The apparent insensitivity is probably due to the effects being taken into account in obtaining the parameter values. Also the magnitude of the transition enthalpies are usually much less than the enthalpy of fusion. For cholesterol, Garti et al.[8] reports a value of the transition enthalpy of $2.845\,\mathrm{kJ/mol}$ while the fusion enthalpy is $28.034\,\mathrm{kJ/mol}$. However, that does not mean the effects should be ignored, particularly when there are polymorphs[9] and hydrates. For example, the aqueous solubility of theophylline anhydrate is nearly double that of the hydrated solid.[9]

The ability of the model to quantitatively describe the mixed solvent solubility data has been assessed by the average absolute relative deviation, AAD, which is defined in Equation (6–7). Figure 7–1 shows the distribution of AADs using the values arising from regressing the solute-solvent parameters globally to the mixed solvent solubility data. The majority of the errors resulting from regressions (AAD-I) are below 0.2. Those from using single solvent solubilities (AAD-II) are more spread out. About half of

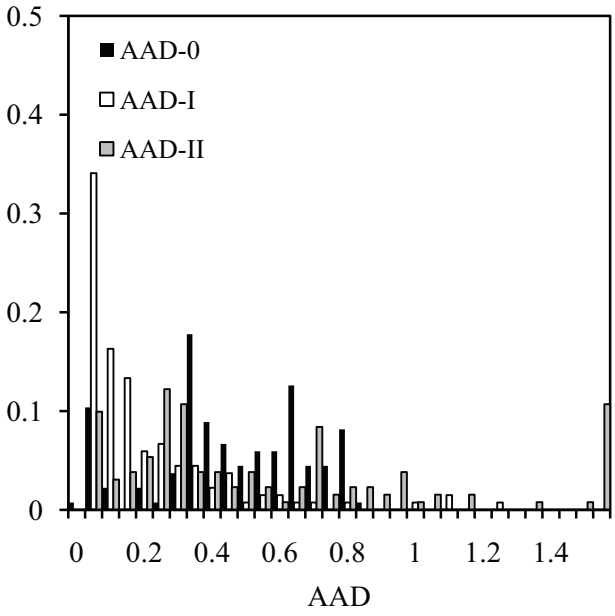

Figure 7–1. Distribution of AADs from FST model. Values with AAD > 1 are summed into one column

the errors are located below 0.4, while about 10% have AADs larger than 1.0. These large errors result from those solutes (primarily anthracene and pyrene), where the solvent mixtures form strongly nonideal solutions, but the excess solubilities are small, thus causing an overestimation.

Application of UNIFAC has been studied in three cases:

1. For estimation of $f_{12}^0 = -(\partial \ln \gamma_1 / \partial x_1)_{T,P,n_2,x_2=1}$.
2. Solving Equation (3–13) for x_1.
3. Solving Equation (3–13) for s_1^{E}

Results have shown that UNIFAC often overestimates limiting values of activity coefficient derivatives, making it less suitable for inclusion within the FST model framework. UNIFAC does seem to estimate $\mathbf{f}^0$ better for solutes with small excess solubilities. Although the mixture solubilities are often not described well, due to wrongful estimates of solubilities in pure solvents, the mixing effects are many times described reasonably well. Figure 7–2 shows the distribution of AADs from using UNIFAC for excess solubilities (AAD-IV) and actual solubilities (AAD-V). As the figure shows, most of the errors from case three are located below 0.3, while those from the second case are less likely to give good estimates of mixture solubilities.

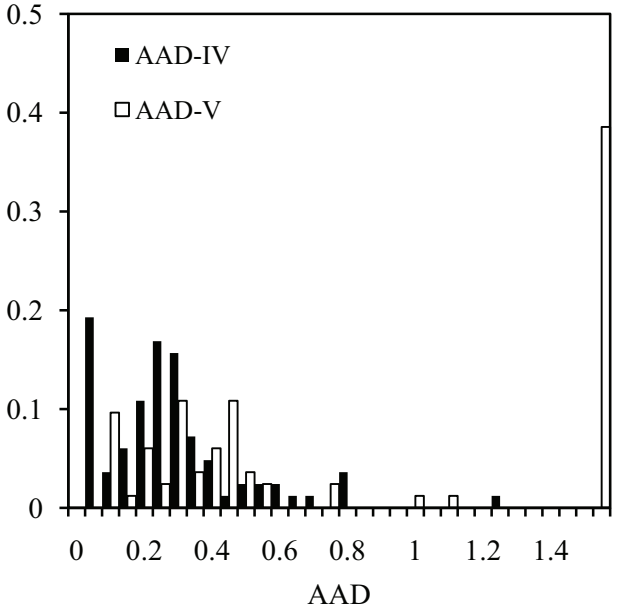

Figure 7–2. Distribution of AADs from UNIFAC. Values with AAD > 1 are summed into one column

The model assumes the connection between the "excess" solubility and the "excess" Henry's law constant; Equation (3–33) is for infinitely dilute solutes $(x_1 \leq 0.01)$ in pure solvents and mixtures. Frequently this is not the case. In fact, many of the pharmaceutical solute-solvent mixtures have experimental solubility points at higher concentrations. This is especially the case in mixtures of organic solvents, while aqueous systems typically have very dilute solubilities in the water-rich end and higher concentrations towards the organic end of the solvent composition range. Yet, the method does well for several of such cases too.

Several reflections can be made regarding the parameter estimation procedure. The preliminary analysis done for anthracene in mixtures of alkanes and various polar components revealed that reducing (i.e., correlating) excess solubilities of small magnitude must be done using carefully selected input data. Consistency (or compatibility) between the experimental solubility data and the g^{E} of the solvent mixture must be sought. The analysis of the excess solubilities of the pharmaceutical solutes (typically aqueous systems) showed that solute-solvent systems with large deviations from ideality are often easier to describe quantitatively. This suggests that parameter estimation is best done when the solvent mixture forms a strongly nonideal solution, as is often the case with aqueous systems.

Excluding data sets with excess solubilities below a certain threshold reflects an important aspect of parameter estimation. Including as much data as possible, regardless of its magnitude, can have a severe effect on the final parameters.

Altering the formulation of the optimization, i.e., minimizing Equation (4–43), can also have an effect on the result. The current objective function focuses on minimizing the residuals of excess solubilities with large magnitude. Other objective functions have also been explored, where the residuals are weighted with the experimental value, i.e.,

$$F' = \min_{\mathbf{z}} \sum_{k=1}^{m} \left(\frac{\delta s_1^{\mathrm{E}}}{s_1^{\mathrm{E}}} \right)_k^2 . \tag{7–1}$$

This means, that all data points are weighted equally in the optimization, regardless of their absolute values. This has an interesting impact on the case with naphthalene–water–DMSO. Regressing the water parameter using Equation (4–43) gives 2.46, which is inconsistent with the water–DMSO case, but consistent with the remaining aqueous systems. If Equation (7–1) was minimized instead the parameter becomes -0.79, which is more consistent with the aqueous DMSO and ethylene glycol systems, but less inconsistent with the remaining aqueous systems. This tradeoff is unfortunate. In addition, excess solubilities in systems which are nearly ideal, often appear as scatter, as depicted in Figure 6–7. If the measurements in dilute systems give inconsistent excess solubilities, then regressing parameters from that set, and weighted equal to sets with larger magnitudes of excess solubilities, the resulting parameters usually range in between the two, unable to accurately describe either. There is no obvious remedy for this situation. One option may, however, be found in the derivation of the excess solubility model. When arriving at Equation (4–27), the term W was omitted from the equations. This term contained multiple H_{ij}, which could not be factored into f_{ij}, meaning that its value would appear as an adjustable parameter pertaining to each triplet of solute and two solvent species. This is not desirable, since the transferability of this parameter is nil. No attempts were made to include it in the analysis of excess solubilities in binary solvent mixtures.

A provisional extension of the excess solubility model developed for binary solvent mixtures was applied for excess solubilities in ternary solvent mixtures. This led to a model, which were able to qualitatively describe the excess solubility behavior in many aqueous systems, but was less successful in systems comprised of organic solvents.

Finally, it is possible to conceive of estimating the $\mathbf{f}^0$ parameters in Equation (4–20) for liquid mixtures by molecular simulation. This possibility has been explored via integration of the molecular radial

distribution function.[10–14] While progress is being made, achieving prediction without data is unlikely. Computer simulation of dense mixtures takes considerable computational resources, is time-consuming, and robust techniques for spatial integration are still under development.

A chemical phenomenon not addressed in this thesis is the effect of the solute in nearly highly nonideal (or near immiscible) solvent mixtures. There may be situations, where adding organic solute to a solution which is on the verge of partial miscibility may cause the system to separate in two phases. It is not a phenomenon, which has been observed in the data presented here, but the situation may arise in aqueous organic mixtures. In these systems, the hydrophobic interactions between water with organic solvent and water with organic solute may cause the creation of a new phase with the two organics (micellar formation).[15] This is likely to occur in the water-rich end of the solvent composition range, since water should act as the chemical environment. However, the solubilities in (and near) pure water are usually very small (sometimes down to 10^{-6} in mole fraction), and therefore the amount of solute in the aqueous phase is extremely small, and the effect may be difficult to obtain using these quantities. It is therefore likely, that the effect is more pronounced with more water soluble solutes, such as amino acids.

References

1. H. Modaressi, E. Conte, J. Abildskov, R. Gani, and P. Crafts. *Ind. Eng. Chem. Res.*, 47:5234, 2008.
2. J. Abildskov and J. P. O'Connell. *Mol. Sim.*, 30: 367–378, 2004.
3. J. Abildskov and J. P. O'Connell. *Fluid Phase Equil.*, 228-229:395–400, 2005.
4. J. Abildskov, R. Gani, P. Rasmussen, and J. P. O'Connell. *Fluid Phase Equil.*, 181:163–186, 2001.
5. K. Balslev and J. Abildskov. *Ind. Eng. Chem. Res.*, 41:2047–2057, 2002.
6. R. Witting, J. Lohmann, and J. G. Gmehling. *Ind. Eng. Chem. Res.*, 42:183, 2003.
7. A. Diedrichs and J. G. Gmehling. *Ind. Eng. Chem. Res.*, 50:1757–1769, 2011.
8. N. Garti, L. Karpuj, and S. Sarig. *Thermochim. Acta*, 35:343–348, 1980.
9. M. Puddipeddi Pudipeddi and A. T. M. Serajuddin. *J. Pharm. Sci.*, 94:929, 2005.
10. S. Christensen, G. H. Peters, F. Y. Hansen, and J. Abildskov. *Fluid Phase Equil.*, 261:185–190, 2007.
11. S. Christensen, G. H. Peters, F. Y. Hansen, J. P. O'Connell, and J. Abildskov. *Fluid Phase Equil.*, 260:169, 2007.
12. S. Christensen, J. Abildskov, G. H. Peters, F. Y. Hansen, and J. P. O'Connell. *Mol. Sim.*, 33:449, 2007.
13. R. Wedberg, G. H. Peters, and J. Abildskov. *Fluid Phase Equil.*, 273:1, 2008.
14. R. Wedberg, G. H. Peters, J. P. O'Connell, and J. Abildskov. *Mol. Sim.*, 36:1243–1252, 2010.
15. Charles Tanford. *The hydrophobic effect: Formation of micelles and biological membranes.* Krieger Publishing Company, 2nd edition, 1991.

PART II

SOLUBILITIES OF GASES IN IONIC LIQUIDS

8. Introduction to ionic liquid systems

The focus in Part I of the thesis was on (excess) solubilities of solids in solvent mixtures. While often successful, the method was empirical in nature, since data was needed to directly quantify the model parameters, and parameters obtained from different methods could be conflicting. In this part of the thesis, another approach for quantifying fluctuation solution theory is applied. A model for the pair correlation function integrals is introduced, thereby allowing calculation of a variety of thermodynamic properties from the fluctuation solution theory framework. Details about the specific model and application is given in Chapter 9. Here, the purpose of applying a FST-based framework for gas solubilities in ionic liquid systems is presented. The chapter begins by introducing the concept of ionic liquids and their properties. Then, a brief review of some existing methods is given, and the motivations for pursuing another method is presented.

8.1. Ionic liquids

Ionic liquids are salts composed of weakly coupled ions, i.e., electrolytes. Typically, one ion has a delocalized charge and one is a an unsymmetric organic. These features prevent the formation of a stable crystal lattice, so that these solvents remain in their liquid form at room temperatures. They are combinations of nitrogen-containing cations and anions, which vary from small, simple inorganic molecules (halides) to large organic structures (such as pentadecafluorooctanoate). Figure 8–1 shows chemical structures of two common ionic liquids: 1-butyl-3-methylimidazolium hexafluorophosphate (or [bmim][PF_6]) and 1-hexyl-3-methylimidazolium bis (triflouromethylsulfonyl) imide (or [hmim][Tf_2N]). The structures are usually large, making their IUPAC-derived names very long. For the sake of legibility it is therefore convenient to address them by the abbreviations of the ions of which the ionic liquids are composed, e.g. [bmim][PF_6]. Although somewhat systematic, this rarely reveals the chemical structure of the ionic liqid. Many common ionic liquids are based on the imidazolium-cation; a five-membered double-bonded ring containing two nitrogen atoms, and the pyridinium-cation; a six-membered double-membered ring containing one nitrogen atom. Other commonly found cations are based on quaternary ammonium or phosphonium. Potentially, millions of ionic liquid structures can be constructed. Even

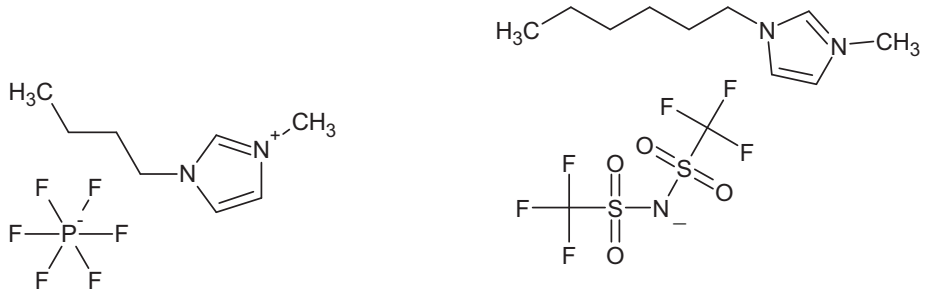

Figure 8–1. Structures of two common ionic liquids based on the imidazolium cation: [bmim][PF_6] (left) and [hmim][Tf_2N] (right). The IUPAC-derived names of most ionic liquids are long, and not particularly legible. Therefore, it is customary to use standardized abbreviations based on the anion and cation of the ionic liquid.

with the cations being most common, a myriad of ionic liquid structures have emerged in the open literature, and continue to appear.

8.1.1. Chemical processing using ionic liquids

Throughout the history of ionic liquids, since their discovery in 1914,[1] there has been a significant number of industrial investigations into the use of ionic liquids, as described well in a recent review article by Plechkova and Seddon.[2] Since World War II there has been a huge number of reports (academic and industrial) of ionic liquids as electrolytes and reaction enhancing solvents, but successful industrial processing has been limited to just a few.[2] The first was operated by the Texas Eastman Division from 1996 to 2004.[2] The ionic liquid acted as a weak Lewis base in the isomerization of 3,4-epoxybut-1-ene to 2,5-dihydrofuran. Perhaps the most successful, though not the first commercial process, is the BASIL^{TM}(Biphasic Acid Scavenging utilising Ionic Liquids) process introduced by BASF in 2002.[3] This concerns production of phosphin, which is a precursor for production of a generic photoinitiator for coating surfaces against UV light. Replacing the traditional solvent triethylamine with the ionic liquid 1-methylimidazole resulted in an increase in the space-time yield from $8\,\mathrm{kg/m^3/h}$ to $690\,000$ and almost doubling the yield from 50% to 98%. Other examples have later followed.[2] All in all, there is a real room for production and processing involving ionic liquids as replacements for traditional volatile organic solvents.

8.1.2. Favorable properties of ionic liquids

Dealing with mixture properties facilitates interest in physical properties of the pure components as well as mixtures. While $P\rho T$ relations of conventional hydrocarbon-based organics and water have

been addressed throughout most of the 20th century, interest in these properties for ionic liquids was for long not as strong. Lately, a large number of publications and methods concerning volumetric and thermophysical properties of pure ionic liquids have appeared. With division into cations and anions, the properties of ionic liquids can be varied by simple changes of structure of the ions. This means that their properties can (in principle) be adjusted to suit the requirements of a particular process. Properties such as melting point, viscosity, density, and hydrophobicity are important from a process point-of-view. Ionic liquids are largely rigid molecules, which has given rise to development of a number of group contribution methods, inspired by the success of standard thermodynamic treatments (such as ASOG[4] and UNIFAC[5]). Coupled with the high degree of "tunability" of these solvents (e.g. cation-anion pairing) these methods are highly attractive, since ionic liquid candidates with promising properties can easily be generated to optimize a specific process. The term "designer solvents" have often been used in connection with ionic liquids.[6]

The great interest in ionic liquids as solvents arises from a set of very favorable physical properties common to most ionic liquids. The two of most importance are:

Extremely low volatility. Most ionic liquids have vapor pressures less than $10^{-9}\,\mathrm{bar}$.[7]

Thermal stability. Most ionic liquids exists as liquids over large temperature ranges $(473 - 673\,\mathrm{K})$ without decomposing.[8]

These properties make ionic liquids interesting for chemical processing. A thermally stable solvent, combined with a nonexisting volatility, and hence no volatility, means that they have often been classified* as "green" solvents.[6] In addition, ionic liquids can facilitate higher yields and reduce manufacturing costs in catalytic reactions such as hydrogenation, hydroformylation, hydrosilytation, Diels-Alder, Friedel-Crafts, nucleophilic substitution reactions, and enzymatic (or biocatalytic) reactions.[6,9,10] Furthermore, ionic liquids dissolves water, organics, and inorganics alike, and can therefore also be used as media for incompatible reagents. Perhaps one of the most studied accounts of ionic liquids is the solubilities of gases in them. The reasons for this seems to be:[11]

Solvents for reactions involving gases. Ionic liquids are particularly attractive towards homogenously catalyzed reactions involving gases. Ionic liquids can immobilize organometallic compounds, and thereby reduce the loss of precious metals[9] from solution. Furthermore, the mass transfer of reactions involving substrates and gases are often limited by resistance of the gas in the solvent. If the solubility is large enough, this effect can be reduced significantly.

* However, issues regarding the actual toxicity of ionic liquids remain, so this classification is somewhat ambiguous.

Storage of gases. Hazards from high-pressure containers, especially when dealing with highly toxic chemicals, are reduced significantly since ionic liquid do not have vapor pressures.

Separation from solutions involving ionic liquids. This may involve separation of gaseous mixtures, since the solubility of gases in ionic liquids can vary significantly. Since ionic liquids do not contaminate air streams, even at elevated temperatures, their potential for replacing traditional industrial solvents is enormous. Another aspect is the separation of solutes (such AIs) from ionic liquid solutions using supercritical fluids, e.g. carbon dioxide.

For these purposes, it is relevant to address the modeling issues regarding solubilities of gases in ionic liquids; the main task of this part of the thesis. Because of the potential for designing ionic liquids as solvents, group contribution methods seem particularly attractive (i.e., predictive methods). This requires more than good correlations, and places strong demands on the method. This means, that gas solubility methods (or models) that are based on rigorous thermodynamics are likely to be better suited than models of an empirical nature.

8.2. Volumetric properties of pure ionic liquids

Before we address solubilities of gases in ionic liquids, some recent developments in modelling pure ionic liquid systems are described. The properties of fundamental interest for liquids are the relations between pressure, density (or molar volume), and temperature, based on the isothermal compressibility of the solution, κ, and isobaric expansivity, β,

$$\begin{gathered} \mathrm{d}v = \left(\frac{\partial v}{\partial T}\right)_P \mathrm{d}T + \left(\frac{\partial v}{\partial P}\right)_T \mathrm{d}P = v\left[\beta \mathrm{d}T - \kappa \mathrm{d}P\right] \\ \beta \equiv \frac{1}{v}\left(\frac{\partial v}{\partial T}\right)_P, \quad \kappa \equiv -\frac{1}{v}\left(\frac{\partial v}{\partial P}\right)_T. \end{gathered} \tag{8–1}$$

It is not uncommon to assume that both β and κ are constants, leading to variations in volume being linear with state conditions.

The literature on $P\rho T$ relations for ionic liquids is dominated by methods of a very empirical nature, or "short-cut" methods. In the following paragraphs, two existing methods for volumetric properties of ionic liquids will be introduced. These are based on a large degree of empirism, and appear as the two best established methods.

Ye and Shreeve [12] developed a method for estimating densities of ionic liquids by means of a group contribution method. They found a simple relation for the liquid density at room temperature at ambient conditions. The molar volume of an ionic liquid was successfully represented as the sum of volumes of

its constituent groups. For the salt C_pA_q, the density is estimated from an expression on the form

$$\rho(T^0, P^0) = \frac{1}{v(T^0, P^0)} = [pv_C + qv_A]^{-1}\,. \tag{8–2}$$

The method worked well for a large selection of ionic liquids. Ye and Shreeve estimated molar volume contributions for a set of cat- and anions, as well as a few minor groups attached to the larger fragments, such as nitrile C≡N. Later, Gardas and Coutinho [13] extended the method to also cover ranges in temperature and pressure. They did so by assuming that the volume varied linearly with temperature and pressure, as above. They regressed data to find $\beta = 6.652 \cdot 10^{-4}\,\mathrm{K}^{-1}$ and $\kappa = 5.919 \cdot 10^{-4}\,\mathrm{MPa}^{-1}$, and saw that these could describe the behavior of a wide range of ionic liquids. The method requires a single liquid (measured) reference $P\rho T$ point.

Jacquemin et al. [14–16] developed a method for estimating volumetric properties at ambient pressures as function of temperature,

$$v(T, P^0) = v_c^* + v_a^* = \sum_{i=0}^{2} D_{c,i}\delta T^i + \sum_{i=0}^{2} D_{a,i}\delta T^i, \quad \delta T = T - T^0, \tag{8–3}$$

where $(T^0, P^0) = (298\,\mathrm{K}, 1\,\mathrm{bar})$ is a known reference point. The D_c and D_a in the above equation are characteristics of each cat- and anion, the values of which are regressed from data. Using an expression similar to the Tait equation, they were able to extend the method to higher pressures as well,

$$v(T, P) = \frac{v_c^*}{1 - G_c \ln \dfrac{H_c(T) + P}{H_c(T) + P^0}} + \frac{v_a^*}{1 - G_a \ln \dfrac{H_a(T) + P}{H_a(T) + P^0}}. \tag{8–4}$$

Again, C_c and G_a are scalar quantities characterizing single ions. The values of H_c and H_a are expressed as functions of temperature

$$H_c(T) = \sum_{i=0}^{2} H_{c,i}\delta T^i, \qquad H_a(T) = \sum_{i=0}^{2} H_{a,i}\delta T^i. \tag{8–5}$$

The agreement with experiment was excellent, even when predicting. Unfortunately, the method requires a substantial number of parameters for a single ion; as many as seven: $D_{c,i}$ and $H_{c,i}$ for $i = 0, 1, 2$ as well as G_c – and similar for the anion. In contrast to most equations of state, this method gives the molar volume (or density) analytically without iteration as function of T and P. However, computation of pressure, given T and ρ, is iterative. Occasionally, the "reverse" computation of pressure changes associated with experimentally realistic density changes can yield negative pressures. [17]

8.3. Methods for high-pressure gas-liquid equilibrium

8.3.1. $\phi - \phi$ methods

There are a wide variety of modeling approaches to ionic liquid phase equilibria in the open literature, covering application of the majority of traditional engineering approaches to vapor-liquid equilibria. One example is the $\phi - \phi$ method, where a single equation of state is used to represent nonideality in both vapor and liquid phases

$$\forall i: \quad y_i \phi_i^V(T, \rho^V, \mathbf{y}) = x_i \phi_i^L(T, \rho^L, \mathbf{x}), \tag{8–6}$$

where y_i and x_i are vapor and liquid mole fractions, respectively. The equation of state is then used to calculate the densities of the vapor and liquid phase, ρ^V and ρ^L, respectively, as well as the fugacity coefficients of both phases. A great convenience of the $\phi - \phi$ approach is that it does not require explicit specification of a reference fugacity. That means that only a model connecting T and P across the density range is required. Unfortunately, this is also the major deficiency of this approach. The density of the vapor (or gas) phase is small, whereas the liquid phase – especially with ionic liquids – has a much larger density. Correlation of properties across such a large density range puts severe demands on the equation of state. Shariati and Peters [18] used the Peng-Robinson equation of state to represent the phase behavior of fluoroform and [emim][PF_6], but were unable to accurately describe the same ionic liquid with carbon dioxide. Shiflett and Yokozeki [19] employed the Redlich-Kwong equation for carbon dioxide solubilities in [bmim][BF_4] and [bmim][PF_6] at pressures below $20\,\mathrm{bar}$. Also the GC-EOS [20] have been applied for bubble point calculations for carbon dioxide with several ionic liduids.[21] The agreement with experiment was excellent for pressures up to $200\,\mathrm{bar}$, in some cases even $1000\,\mathrm{bar}$. An recurring inconvenience regarding application of cubic equations of state is that they require vapor-liquid critical temperatures and pressures, which for almost all ionic liquids are completely hypothetical since these do not vaporize. When regarding these as mere parameters for a model it can be of less importance whether they possess actual physical meaning. However, this is not the case with critical parameters (T_c, P_c, ω). They force an equation of state to exhibit the well-known relation at the critical point

$$\left(\frac{\partial P}{\partial \rho}\right)_T = \left(\frac{\partial^2 P}{\partial \rho^2}\right)_T = 0. \tag{8–7}$$

If the critical point is hypothetical then the equation of state is forced to exhibit a phenomenon which is not real. Fortunately, there are other equations of state which do not require critical variables. The statistical-associated fluid theory (SAFT) framework for pure species and mixtures have been applied for ionic liquid systems on many occasions, and a short review is given by Tan et al..[22] Andreu and Vega [23]

used a four-term equation, "Soft-SAFT". Although based on rigorous theory, a series of problems can arise when applying SAFT (in any of its many forms) to ionic liquid systems, e.g. establishing appropriate association schemes. Ionic liquids generally do not self-associate, but do form solvates with other molecules. Aparicio et al.[24] compared the experimental data and molecular dynamics simulation results, concluding that the model had difficulties capturing the complex association phenomena encountered in these systems. In addition to the problem of selecting appropriate association sehemces, the SAFT combining rules can be unsuccessful and highly sensitive toward binary interaction parameters. Karakatsani et al.[25] used the tPC-SAFT, and found that accurate ternary mixture properties require binary parameters fitted to ternary data. This suggests that the combining rules used within SAFT may not always be reliable for multicomponent systems. Kim et al.[26] used a group contribution lattice-fluid equation of state for predicting carbon dioxide solubilities in a variety of ionic liquids at pressures up to $10\,\mathrm{bar}$, occasionally up to $100\,\mathrm{bar}$. The model-data agreement was generally good, but extension to higher pressures is not available.

8.3.2. $\gamma - \phi$ methods

Perhaps the most widely used method, and a form which is adopted in this work, is the $\gamma - \phi$ approach. The independent variables chosen is often the set T, P, and mole fractions ($\mathbf{x}$ and $\mathbf{y}$). The fugacities of species are here given by

$$y_i \phi_i^V(T, P, \mathbf{y}) P = x_i \gamma_i(T, P, \mathbf{x}) f_i^0(T). \tag{8–8}$$

Separate thermodynamic models are used for nonidealities in liquid and vapor phases. That means:

1. An equation-of-state must be chosen for the vapor phase to calculate ϕ_i^V.
2. A model, experimental measurement, or other method of estimation, must be chosen for the standard state (reference) fugacity, f_i^0.
3. A model must be chosen for the liquid-phase activity coefficient, γ_i.

Vapor phase nonidealities can be significant, especially at high pressures, but from a modeling perspective it is less problematic than the liquid phase. There are several options for vapor nonideality, including second virial coefficients, equations of state, and multiparameter expressions. Much work has been done in advancing correlations for the second virial coefficient. Perhaps most notably are the pioneering works of Pitzer and Curl,[27] Tsonopoulos,[28] and Hayden and O'Connell.[29] These methods rely on the existence of a critical point (T_c, P_c, v_c) which is used in correlations based on a corresponding-states principle. While ionic liquids themselves do not exhibit criticality, this is of little problem with addressing their vapor phases, since their vapor pressures usually are of the order of a few pascals and

may therefore well be neglected. Cubic equations of state are often sufficient for dealing with non-idealities in the vapor phase, especially for phases of pure gas. Furthermore, most of the gases to be covered are small molecules, which a cubic equation, such as SRK, will have little problems dealing with. Their application is, however, more tedious than the virial equation, since density appears explicitly in the calculation of fugacity coefficients; this is not the case with the virial equation of state. Finally, multiparameter equations of state have been proposed for highly accurate descriptions of vapor phase properties. The models are usually simple in application, but their parameterization come from a huge compilation of a multitude of data and data sources. This means that, their application is not generally straightforward for gases with few measurements.

The second item listed above, the reference state fugacity, is one which typically refers to either pure species (Raoult's law; the Lewis-Randall state) or pure solvent (Henry's law). The choice of reference state is usually set by the problem at hand: In low-pressure, subcritical systems, where solubilities are usually high, Raoult's law will be adequate, whereas in systems with supercritical solutes, and small solubilities, Henry's law will usually be the more suitable selection.

The pressure dependence of properties of condensed matter is often negligible. Ionic liquid systems may exhibit pressure variations well above $100\,\mathrm{bar}$, and at these conditions the effects of pressure on liquid-phase nonideality can be significant. Since most activity coefficient models do not include pressure explicitly, the pressure dependence is usually accounted for explicitly by a Poynting correction factor. That means, that the phase equilibrium problem can be formulated as

$$y_i\phi_i^V(T,\rho^V,\mathbf{y})P = x_i\gamma_i(T,P^0,\mathbf{x})f_i^0(T)\exp\int_{P^0}^{P}\frac{\bar{v}_i(T,P,\mathbf{x})}{\mathsf{R}T}\mathrm{d}P. \tag{8–9}$$

For the gas–ionic liquid binary system, the standard state is frequently chosen as pure solvent, meaning

$$P^0 = P_2^0(T); \quad \lim_{x_1\to 0}\gamma_1 = 1; \quad f_1^0 = H_1 = \lim_{x_1\to 0}\frac{f_1}{x_1}. \tag{8–10}$$

In this case, the two species refer to different standard states (unsymmetric convention), and it is customary to denote γ_1 with γ_1^*. The Henry's law constant, H_1, can be obtained from binary vapor-liquid equilibrium data in the region $x_1 \approx 0$ along with assumed expressions for γ_1 and $\bar{v}_1$. Thus, in a plot of $\ln f_1/x_1$ versus x_1 the intercept is $\ln H_1$, as depicted in Figure 8–2 for the system carbon monoxide–[bmim][CH_3SO_4]. At higher concentrations of 1 $\ln f_1/x_1$ is the summation of $\ln H_1$, $\ln\gamma_1$ (typically negative), and the Poynting factor, $\ln$ POY (typically positive). These are also indicated in Figure 8–2. This formulation, and variants of it, has been applied for reduction of phase equilibrium data in multi-

tude. The other plot of Figure 8–2 shows the system carbon dioxide–[hmim][Tf_2N]. Here, the behavior

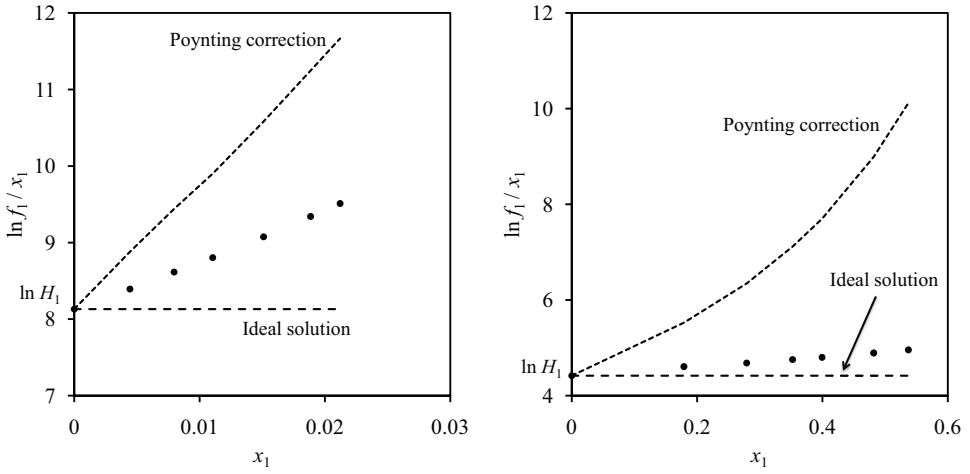

Figure 8–2. Left plot: Fugacity of carbon monoxide(1) in [bmim][CH_3SO_4](2) at 293 K with data from Kumełan et al..[30] Right plot: Carbon dioxide(1) in [hmim][Tf_2N](2) at 373 K with data from Kumełan et al..[31] These plots reveal that the nonideality effect arising from mixing solute and solvent (activity coefficient, γ_1) must remain negative, since the Poynting factor overcorrects the ideal solution fugacity. This can be unfortunate, since the liquid fugacity then contains a ratio of two terms, which often cancels to a significant extent.

is quite different. The vapor phase is significantly more nonideal than the carbon monoxide (second virial coefficient is $-71\,\mathrm{cm^3/mol}$ versus $22\,\mathrm{cm^3/mol}$ for carbon monoxide at the temperatures indicated), but the liquid-phase nonideality is small. Maurer and coworkers[30–34] have used this formulation for reducing data on a wide variety of gases (eg. hydrogen, oxygen, carbon monoxide, carbon dioxide, methane, xenon) in ionic liquids. While reduction was often successful, in terms of experimental solubilities, the partial molal volumes of the gases, estimated as part of data reduction, were occasionally negative. This phenomenon, which does not make sense in physical terms, can be explained in terms of the interpretation of the data, which is connected to the limiting behavior of the liquid-phase nonideality, which we will address later in this section. If we assume that the composition dependence of γ_1 can be described with the Porter equation near $x_1 \approx 0$ (which is usually a good assumption), the fugacity in the liquid phase becomes

$$\ln \frac{f_1^L}{x_1} = \frac{A}{\mathsf{R}T}(x_2^2 - 1) + \ln H_1(T) + \frac{\bar{v}_1(T, \mathbf{x})}{\mathsf{R}T}(P - P_2^0). \tag{8–11}$$

This equation is the *Krichevskii-Ilinskaya* equation,[35] and were among the first attempts to properly describe high-pressure gas-liquid equilibria. If 1 is dilute, then the activity coefficient term drops out of

the equation, and we obtain the *Krichevskii-Kasarnovsky*[36] equation

$$\ln \frac{f_1^L}{x_1} \approx \ln H_1(T) + \frac{\bar{v}_1^\infty(T)}{\mathsf{R}T}(P - P_2^0). \tag{8–12}$$

A major deficiency of using the Krickvskii-Ilinskaya and Krichevskii-Kasarnovsky formulations is the separation of pressure and composition dependencies in deviations from ideal behavior. As was mentioned above, the terms in the formulation of the liquid fugacity are of opposite sign and often cancel to a great extent. Figure 8–2 illustrates this by the Poynting correction factor overestimating the experimental data. To compensate, the contribution from the activity coefficient must remain negative. This situation is often seen in ionic liquid gas-solvent systems. The Krichevskii-Kasarnovsky formulation has also been applied been applied to reduce experimental solubility data[37,38] in the dilute region. The slope of $\ln f_1/x_1$ versus pressure should then yield the partial molal volume of the gas, when the system is close to its reference state. However, as shown by Orentlicher and Prausnitz,[39] the situation at high pressures can be significantly different. The starting point is the Krichevskii-Ilinskaya formulation which results in a relation when $x_1 \approx 0$ that is different than the Krichevskii-Kasarnovsky equation

$$\lim_{x_1 \to 0} \ln \frac{f_1^L}{x_1} = \ln H_1 + \left(\bar{v}_1^\infty - \frac{2A}{H_1/\phi_1^0 - P_2^0} \right) \frac{P - P_2^0}{\mathsf{R}T}. \tag{8–13}$$

The derivation is give in the appendix at the end of this chapter, and shows the results from separating the contributions from pressure and composition to the liquid-phase fugacity. Orentlicher and Prausnitz found that for hydrogen in carbon monoxide at $88\,\mathrm{K}$

$$\bar{v}_1^\infty = 34.4\,\mathrm{cm}^3/\mathrm{mol} \qquad \text{and} \qquad \frac{2A}{H_1/\phi_1^0 - P_2^0} = 35\,\mathrm{cm}^3/\mathrm{mol},$$

and for hydrogen in propane at $282\,\mathrm{K}$

$$\bar{v}_1^\infty = 63\,\mathrm{cm}^3/\mathrm{mol} \qquad \text{and} \qquad \frac{2A}{H_1/\phi_1^0 - P_2^0} = 48.5\,\mathrm{cm}^3/\mathrm{mol}.$$

The two terms are similar and therefore cancel to a great extent. Then, from an engineering point of view, it is clearly advantageous to have a single model which accounts for both effects.

There are also situations where surprisingly simple treatments can prevail. A Henry's law formulation of Carvalho and Coutinho,[40] expressed in terms of molalities, is surprisingly successful for systems of carbon dioxide in a range of ionic liquids. Since ionic liquids themselves to not possess vapor pressures, the vapor is composed entirely of 1. This simplifies the isofugacity criterion slightly, and we may write

for the pressure

$$P = \ln \gamma_1(T, P^0, \mathbf{x}) + \int_{P^0}^{P} \frac{\bar{v}_1(T, P, \mathbf{x})}{\mathsf{R}T} \mathrm{d}P - \ln \phi_1^V(T, P) + \ln H_1(T) + \ln x_1. \tag{8–14}$$

Carvalho and Coutinho lumped together all contributions to nonideality into one "effective" Henry's law constant, expressed as a function of temperature. Imposing a simple, Antoine-like, expression for the temperature dependence of this effective Henry's contant, they were able to describe the solubility behavior of carbon dioxide to more than $50\,\mathrm{bar}$ and molalities up to $3\,\mathrm{mol/kg}$*. This means, that solubilities can be predicted using only temperature, since parameters for the functional expression of the temperature dependence can be found from regression of carbon dioxide with other ionic liquids. Although a potentially powerful method, there are some limitations. The assumptions made for developing the method are

1. Liquid-phase nonideality is not affected by composition.

2. Pressure effects to the liquid-phase fugacity are neglected.

3. Pressure effects to vapor-phase nonideality are neglected.

These statements are consistent with cancelation of the first three terms in Equation (8–14), a phenomenon which is not infrequent. The terms can, one-by-one, be significant, and the data analysis of Kumełan et al.[34] suggests that there truly are nonidealities in both vapor and liquid phases of many gas-ionic liquid systems, especially those with more soluble gases (e.g. carbon dioxide and xenon). Relying on cancelation of three factors can lead to unacceptable and unnecessary risk. Furthermore, there are a number of severe limitations to this approach:

1. The method cannot be extended to mixtures of solvents.

2. There is an upper limit to the concentration for which the method is applicable. For the systems by Carvalho and Coutinho this limit is about $3\,\mathrm{mol/kg}$.

3. There is an upper limit to the pressure which can be applied. For the systems considered the limit is about $50\,\mathrm{bar}$.

The method is therefore not very general, and much data is required for estimation of parameters for new gases.

* For an ionic liquid with a molecular weight of $200\,\mathrm{g/mol}$ this corresponds to a mole fraction of about 0.4 With $400\,\mathrm{g/mol}$ the limit is 0.6.

8.4. Summary

Much activity is seen in this field, but despite numerous investigations using advanced and empirical models, it appears that phase equilibria involving ionic liquids are difficult to describe generally using conventional equations of state and excess free energy models. Many of the works are not easily generalized since they can be inaccurate for multicomponent systems, or rely on vapor-liquid critical constants, which are hypothetical and therefore not experimentally accessible. More specifically, there seems to be a need for:

1. A simple, but reliable, method for solubilities of gases in ionic liquids. The method should require a minimum of parameters that can be resolved into group contributions in order to decrease the amount of input data.

2. A method based on a rigorous thermodynamic platform, which allow integration with other property calculations, e.g. pressure-density relations of pure liquids.

These items are not currently offered by one single method, for reasons which have been explained in this chapter. Though traditional equations of state, such as the cubic, offer (relatively) simple relations between P, ρ, and T for pure species, and can be extended to gas solubilities as well, they rely on hypothetical phenomena and parameters. In addition, the sensitivities towards binary interaction parameters makes cubic equations of state an unattractive approach. Models, which are more advanced (e.g. SAFT), have great potential in terms of secondary properties, but share with the cubic equations of state a high degree of sensitivity towards binary interactions. Furthermore, models which describes hydrogen bonding explicitly are faced with establishing reliable rules for association schemes. These are not always obvious, and may require tedious comparison with experimental data for selection of a better scheme.

Excess Gibbs energy models definitely require mixture data for regression of parameters, but their estimates can often be more reliable, since they are confined to only liquid-phase properties. Unfortunately, these do not contain any dependence on pressure, so Poynting factors are necessary. As was shown above, the effect of pressure on liquid-phase nonideality can be significant at high pressures, and neglecting this can lead to wrongful estimates of secondary properties, such as partial molar volumes.

A key point of the literature is that the effects of the nonideality contributions should either be evaluated independently or combined,[39,41,42] since it is not uncommon for the composition nonideality to significantly cancel the pressure nonideality, especially at higher temperatures. Therefore, it is advantageous to have a single model which accounts for both effects simultaneously.

What is attempted here, is development and use of a method based on fluctuation solution theory, originally developed by Mathias.[43] It combines the effect of pressure and composition in γ_i, for computing liquid-phase fugacities. It is completely general, and applicable to all gas-solvent systems, including nonionics. Furthermore, the method can be reduced to an equation of state, linking $P\rho T$ properties of pure liquids. In the following chapters, the method and its thermodynamic relations are outlined, and applied for properties of pure liquids and solubilities of gases in ionic liquids.

8.A. Pressure-composition effects on liquid-phase fugacity

Consider the Krichevskii-Ilinskaya[35] equation for a gas (1) in a solvent (2)

$$\ln \frac{f_1^L}{x_1} = \ln \gamma_1^* + \ln f_1^0 = \frac{A}{\mathsf{R}T}(x_2^2 - 1) + \frac{\bar{v}_i(P - P_2^0)}{\mathsf{R}T} + \ln H_1. \tag{8–15}$$

Here, superscript 0 denotes a property of the pure species. If the solubility of 1 is sufficiently low, deviations from composition nonideality can be ignored, and the limiting value is the Krichevskii-Kasarnovsky[36] formulation for the fugacity at infinite dilution

$$\ln \frac{f_1^L}{x_1} = \frac{\bar{v}_i^\infty (P - P_2^0)}{\mathsf{R}T} + \ln H_1(T). \tag{8–16}$$

However, at high pressures, the value of γ_1 at finite small concentrations of x_1 is not 1, but is a function of pressure.[39,41] The limiting value of the term $x_2^2 - 1$ can be found from

$$x_2^2 - 1 = \frac{x_2^2 - 1}{x_1} \left(\frac{P - P_2^0}{x_1} \right)^{-1} (P - P_2^0). \tag{8–17}$$

If we now take the limit of the right-hand side, we find for the first term

$$\lim_{x_1 \to 0} \frac{x_2^2 - 1}{x_1} = \lim_{x_1 \to 0} \frac{x_1^2 - 2x_1}{x_1} = -2. \tag{8–18}$$

The limit of the second term is

$$\lim_{x_1 \to 0} \frac{P - P_2^0}{x_1} = \lim_{x_1 \to 0} \frac{P - f_2^0/\phi_2}{x_1}. \tag{8–19}$$

The value of this is not explicitly clear. The total pressure can be calculated as

$$\begin{aligned} P &= \frac{f_1}{\phi_1} + \frac{f_2}{\phi_2} = \frac{x_1 H_1}{\phi_1} + \frac{(1 - x_1) f_2^0}{\phi_2} \\ &= \frac{f_2^0}{\phi_2} + x_1 \left(\frac{H_1}{\phi_1} - \frac{f_2^0}{\phi_2} \right), \end{aligned} \tag{8–20}$$

where f_2^0 is the reference fugacity of 2. Plugging this into the above limit, we see

$$\lim_{x_1 \to 0} \frac{P - P_2^0}{x_1} = \lim_{x_1 \to 0} \left(\frac{H_1}{\phi_1} - \frac{f_2^0}{\phi_2} \right) = \frac{H_1}{\phi_1^0} - P_2^0. \tag{8–21}$$

Thus, combining to find the limit of $x_2^2 - 1$,

$$\lim_{x_1 \to 0} (x_2^2 - 1) = (-2) \left(\frac{H_1}{\phi_1^0} - P_2^0 \right)^{-1} (P - P_2^0). \tag{8–22}$$

In accordance with the remaining Krischevskii-Ilinskaya equation, we obtain the relation when 1 is dilute at elevated pressures

$$\lim_{x_1 \to 0} \ln \frac{f_1^L}{x_1} = \ln H_1 + \left(\bar{v}_1^\infty - \frac{2A}{H_1/\phi_1^0 - P_2^0} \right) \frac{P - P_2^0}{\mathsf{R}T} \tag{8–23}$$

Thus, the slope of the left-hand side versus pressure does not just give the partial molal volume of 1, but a combination of the partial molal volume and the solute-solvent nonideality. The two terms are often of similar magnitude, which may describe why negative partial molal volumes can sometimes be found from data, when ignoring pressure nonideality.

References

1. P. Walden. *Bull. Acad. Impér. Sci. St. Pétersbourg*, 8:405–422, 1914.
2. N. V. Plechkova and K. R. Seddon. *Chem. Soc. Rev.*, 37:123–150, 2008.
3. BASF. Acid scavenging, 2002. URL `www.basionics.com/en/ionic-liquids/`.
4. G. M. Wilson and C. H. Deal. *Ind. Eng. Chem. Res. Fundam.*, 1:20–23, 1962.
5. Aa. Fredenslund, R. L. Jones, and J. M. Prausnitz. *AIChE J.*, 21:1086–1099, 1975.
6. M. J. Earle and K. R. Seddon. *Pure Appl. Chem.*, 72:1391–1398, 2000.
7. L. P. N. L. Rebelo, J. N. Canongia, J. M. S. S. Esperança, and F. Eduardo. *J. Phys. Chem. B*, 107: 6040–6043, 2005.
8. C. P. Fredlake, J. M. Crostwaite, D. G. Hert, S. N. V. K. Aki, and J. F. Brennecke. *J. Chem. Eng. Data*, 49:954–964, 2004.
9. P. Wasserscheid and W. Keim. *Angew. Chem., Intl. Ed.*, 39:3773–3789, 2000.
10. B. Chen, Z. Guo, T. Tan, and X. Xu. *Biotechnol. Bioeng.*, 99:18–29, 2008.
11. J. L. Anderson, J. K. Dixon, and J. F. Brennecke. *Acc. Chem. Res.*, 40:1208Ű–1216, 2007.
12. C. Ye and J. M. Shreeve. *J. Phys. Chem. A*, 111: 1456–1461, 2007.
13. R. L. Gardas and J. A. P. Coutinho. *Fluid Phase Equil.*, 263:26–32, 2007.
14. J. Jacquemin, P. Husson, V. Mayer, and I. Cibulka. *J. Chem. Eng. Data*, 52:2204–2211, 2007.
15. J. Jacquemin, P. Nancarrow, D. W. Rooney, M. F. Costa Gomes, P. Husson, V. Mayer, A. A. H. Pádua, and C. Hardacre. *J. Chem. Eng. Data*, 53: 2133–2143, 2008.
16. J. Jacquemin, R. Ge, P. Nancarrow, D. W. Rooney, M. F. Costa Gomes, and C. Hardacre. *J. Chem. Eng. Data*, 53:716–126, 2008.
17. J. Abilskov, M. D. Ellegaard, and J. P. O'Connell. *Fluid Phase Equil.*, 295:215–229, 2010.
18. A. Shariati and C. J. Peters. *J. Supercrit. Fluids*, 25:109–117, 2003.
19. M. B. Shiflett and A. Yokozeki. *Ind. Eng. Chem. Res.*, 44:4453–4464, 2005.
20. S. Skjold-Jørgensen. *Fluid Phase Equil.*, 16:317–351, 1984.
21. B. Breure, S. B. Bottini, G. J. Witkamp, and C. J. Peters. *J. Phys. Chem. B*, 51:14265–14270, 2007.
22. S. P. Tan, H. Adidharma, and M. Radosz. *Ind. Eng. Chem. Res.*, 47:8063–8082, 2008.
23. J. S. Andreu and L. F. Vega. *J. Phys. Chem. B*, 112: 15398–15406, 2008.
24. S. Aparicio, R. Alcalde, M. J. Davila, B. Garcia, and J. M. Leal. *J. Phys. Chem. B*, 112:11361–11373, 2008.

25. E. K. Karakatsani, I. G. Economou, M. C. Kroon, M. D. Bermejo, C. J. Peters, and G. J. Witkamp. *Phys. Chem. Chem. Phys*, 10:6160–6168, 2008.

26. Y. S. Kim, W. Y. Choi, J. H. Jang, K. P. Yoo, and C. S. Lee. *Fluid Phase Equil.*, 228-229:439–445, 2005.

27. K. S. Pitzer and R. F. Curl. *J. Am. Chem. Soc.*, 79: 2369, 1957.

28. C. Tsonopoulos. *AIChE J.*, 20:263–272, 1974.

29. J. G. Hayden and J. P. O'Connell. *Ind. Eng. Chem. Proc. Des. Dev.*, 14:209–216, 1975.

30. J. Kumełan, Á. Pérez-Salado Kamps, D. Tuma, and G. Maurer. *Fluid Phase Equil.*, 260:3–8, 2007.

31. J. Kumełan, Á. Pérez-Salado Kamps, D. Tuma, and G. Maurer. *J. Chem. Thermodyn.*, 38:1396–1401, 2006.

32. J. Kumełan, A. Á. Pérez-Salado Kamps, D. Tuma, and G. Maurer. *J. Chem. Eng. Data*, 51:1802–1807, 2006.

33. J. Kumełan, Á. Pérez-Salado Kamps, D. Tuma, and G. Maurer. *J. Chem. Eng. Data*, 51:1364–1367, 2006.

34. J. Kumełan, D. Tuma, and G. Maurer. *Fluid Phase Equil.*, 275:132–144, 2009.

35. I. R. Krichevskii and A. A. Ilinskaya. *Zh. Fiz. Khim.*, 19:621–, 1945.

36. I. R. Krichevskii and J. S. Kasarnovsky. *J. Am. Chem. Soc.*, 57:2168–2171, 1935.

37. X. Yuan, S. Zhang, J. Liu, and X. Lu. *Fluid Phase Equil.*, 257:195–200, 2007.

38. F. Y. Jou and A. E. Mather. *Int. J. Thermophys.*, 28: 490, 2007.

39. M. Orentlicher and J. M. Prausnitz. *Chem. Eng. Sci.*, 19:775–782, 1964.

40. P. J. Carvalho and J. A. P. Coutinho. *J. Phys. Chem. Lett.*, 1:774–780, 2010.

41. R. E. Gibbs and H. C. Van Ness. *Ind. Eng. Chem. Fundam.*, 10:312–315, 1971.

42. P. M. Mathias and J. P. O'Connell. *Chem. Eng. Sci.*, 36:1123–1132, 1981.

43. P. M. Mathias. *Thermodynamic properties of high-pressure liquid mixtures containing supercritical components*. PhD thesis, University of Florida, Gainesville, FL, USA, 1978.

9. Fluctuation solution theory method

In this chapter, the thermodynamic framework for gas solubilities is set up. Initially, it is shown how to derive thermodynamic expressions from a model of the correlation function integrals. This continues into establishing the equilibrium relations, which are then connected to fluctuation solution theory properties.

9.1. Properties from correlation function integrals

Given the nature of the correlation functions $h(r)$ and $c(r)$ (or their integrals), modeling efforts favors the short-ranged direct correlation function, since this function is more well-behaved with less fluctuations at large separations. The feasibility of this was demonstrated in a number of publications,[1–3] showing that the integrals of the direct correlation function, in the liquid region, are largely temperature independent and can therefore be suitably reduced using only a size-dependent parameter. However, these early investigations considered only pure liquids, and was therefore not applied to mixtures. One of the most successful efforts to correlate integrals of the direct correlation function was done by Mathias,[4] who derived a hard-sphere augmented model from first-order perturbation theory.

Molecular correlation functions depend strongly on density and temperature, which are the variables arising naturally from the canonical ensemble. Calculation of a thermodynamic property from fluctuation solution theory – using these variables – is done by specifying the density in terms of a dummy variable $t \in [0; 1]$ and a reference state density ρ_i^0

$$\forall i: \quad \rho_i(t) = \rho_i^0 + (\rho_i - \rho_i^0)t. \tag{9–1}$$

The reference state can be arbitrarily, but needs to be a the same temperature as the final state density, $\rho_i(t = 1)$. The change of a thermodynamic quantity, $\Psi(T, \boldsymbol{\rho})$, arising from an isothermal change in density (or t) is given by

$$\Psi - \Psi^0 = \int_0^1 \frac{\mathrm{d}\Psi}{\mathrm{d}t}\mathrm{d}t, \qquad \Psi^0 = \Psi(T, \boldsymbol{\rho}^0). \tag{9–2}$$

Taking the partial derivative of Ψ at constant T leads to

$$\Psi - \Psi^0 = \int_0^1 \left\{ \sum_{i=1}^{M} \left(\frac{\partial \Psi}{\partial \rho_i} \right)_{T,\rho_{j\neq i}} \frac{\partial \rho_i(t)}{\partial t} \right\} \mathrm{d}t = \sum_{i=1}^{M} (\rho_i - \rho_i^0) \int_0^1 \left\{ \sum_{i=1}^{M} \left(\frac{\partial \Psi}{\partial \rho_i} \right)_{T,\rho_{j\neq i}} \right\} \mathrm{d}t. \quad (9\text{–}3)$$

Inserting the expression for the pressure, given by Equation (2–38), into the above expression, an isothermal change in density (from $\rho_i^0 \rightarrow \rho_i$) gives the resulting change in pressure

$$\frac{P - P^0}{\mathsf{R}T} = \sum_{i=1}^{M} (\rho_i - \rho_i^0) \int_0^1 \left\{ 1 - \sum_{j=1}^{M} x_j C_{ji}(t) \right\} \mathrm{d}t. \quad (9\text{–}4)$$

The corresponding expression for the activity coefficient of species i in solution becomes

$$\ln \gamma_i = \ln \rho_i - \ln \rho_i^0 - \sum_{j=1}^{M} (\rho_j - \rho_j^0) \int_0^1 \frac{C_{ji}(t)}{\rho(t)} \mathrm{d}t, \quad (9\text{–}5)$$

where $\rho(t) = \sum_i \rho_i(t)$. Fluctuation solution theory offers the derivatives of Ψ with respect to density for use with these equations. In Appendix 9.A these properties are derived from a model for the direct correlation function integral. That model is obtained from previous investigators,[5–7] and expresses the direct correlation function integral, C_{ij}, between species i and j as

$$C_{ij}(T, \boldsymbol{\rho}) = C_{ij}^{h.s.}(T, \boldsymbol{\rho}) - 2\rho \left[B_{ji}(T) - B_{ji}^{h.s.}(T) \right] \quad (9\text{–}6)$$

The notation $h.s.$ denote a hard-sphere property, calculable from any hard-sphere equation of state. The B_{ij} and $B_{ij}^{h.s.}$ appearing here resemble second virial coefficients for simple molecules, and are obtained from functional expressions of a corresponding-states correlation in temperature. The expressions utilize characteristic temperatures and volumes for each pure species

$$\frac{B_{ii}^{h.s.}}{V_i^*} = \frac{\frac{2\pi}{3}\sigma_i^3}{V_i^*} \begin{cases} a_1 / \tilde{T}_{ii}^{a_2} & \tilde{T}_{ii} > 0.73 \\ b_1 \exp\left[b_2 \tilde{T}_{ii} \right] & \tilde{T}_{ii} < 0.73 \end{cases}, \quad (9\text{–}7a)$$

$$\frac{B_{ji}}{V_{ji}^*} = c_1 + \frac{c_2}{\tilde{T}_{ji}} + \frac{c_3}{\tilde{T}_{ji}^2} + \frac{c_4}{\tilde{T}_{ji}^3} + \frac{c_5}{\tilde{T}_{ji}^8}. \quad (9\text{–}7b)$$

The coefficients and some additional details regarding the model are given in Appendix 9.A. For mixtures, the characteristic variables used for the corresponding-states correlations, are obtained from com-

mon semiempirical combining rules[8]

$$\tilde{T}_{ji} = \frac{T}{\sqrt{T_i^* T_j^*}(1 - k_{ji})}; \quad V_{ji}^* = \left(\frac{[V_i^*]^{1/3} + [V_j^*]^{1/3}}{2} \right)^3 . \tag{9–8}$$

If needed, the binary interaction parameter k_{ji} between unlike molecular species must be determined from binary data. However, as has been pointed out on several occasions[6,7] results are not very sensitive to its value (± 0.1), and zero is frequently adequate. With this model, integration of Equations (9–4) and (9–5) in an M-component mixture from a reference state $(P^0, \boldsymbol{\rho}^0)$ to final state $(P, \boldsymbol{\rho})$ is straightforward. The model above separates the effect of temperature and density in the second term on the right-hand side, which allows for a straightforward integration. At constant T, the pressure is

$$\frac{P - P^0}{\mathsf{R}T} = \frac{P^{h.s.}(T, \boldsymbol{\rho}) - P^{h.s.}(T, \boldsymbol{\rho}^0)}{\mathsf{R}T} + \sum_i^M \sum_j^M \left[\rho_i \rho_j - \rho_i^0 \rho_j^0\right] \left[B_{ji}(T) - B_{ji}^{h.s.}(T)\right]. \tag{9–9}$$

The species activity coefficient becomes

$$\ln \gamma_i(T, \boldsymbol{\rho}) = \frac{\mu_i^{h.s.}(T, \boldsymbol{\rho}) - \mu_i^{h.s.}(T, \boldsymbol{\rho}^0)}{\mathsf{R}T} + 2 \sum_j^M \left[\rho_j - \rho_j^0\right] \left[B_{ji}(T) - B_{ji}^{h.s.}(T)\right]. \tag{9–10}$$

Relevant hard-sphere expressions for $C_{ji}^{h.s.}$, $\mu_i^{h.s.}$, and $P^{h.s.}$ are given in the appendix at the end of the chapter. Note, that the activity coefficient now has an explicit density dependence, which combined with the pressure equation can give an implicit pressure dependence.

9.2. Thermodynamic framework for high-pressure gas-solvent equilibrium

With the formalism for obtaining properties and thermodynamic quantities in place, the task of this chapter is: To derive the thermodynamic framework for high-pressure gas solubilities. We consider a supercritical solute (1) dissolved in a liquid solvent (2). The fundamental relation for phase equilibrium is the equality of liquid- and vapor-phase fugacities

$$\forall i: \quad f_i^V(T, P, \mathbf{y}) = f_i^L(T, P, \mathbf{x}). \tag{9–11}$$

Since ionic liquids generally have negligible vapor pressures, the solvents are considered nonvolatile. This means only one relation exists in Equation (9–11). Thus, the vapor phase is assumed to be pure 1, with a fugacity

$$f_1^V(T, P) = \phi_1^V(T, P)P. \tag{9–12}$$

ϕ_i^V can be calculated from any vapor-phase equation of state. However, for the conditions and components considered here, the second virial coefficient should be adequate to account for nonideality in the vapor phase, whence

$$\ln \phi_i^V(T, P, \mathbf{y}) = \frac{P}{\mathsf{R}T} \sum_k^M \left[2y_k B_{ik}(T) - \sum_m^M y_m B_{mk}(T) \right]. \tag{9–13}$$

Thus, for a pure gas phase

$$\ln \phi_1^V(T, P) = \frac{B_{11}(T)P}{\mathsf{R}T}. \tag{9–14}$$

It should be emphasized, that the B_{ij} appearing in Equation (9–6) is *not* identical to that in Equation (9–14), which is the conventional, and well-known, second virial coefficient. The correlation of Hayden and O'Connell [9] is used to estimate its value for each solute.

Solubilities of gases in liquids at high pressures are usually small. This means, that Henry's law is a suitable standard state for the liquid-phase fugacity of the solute. Deviations from ideal behavior in the liquid phase are given by the density dependent activity coefficient, so that the mixture fugacity of 1 in the liquid phase is

$$f_1^L(T, P, \mathbf{x}) = f_1^L(T, \boldsymbol{\rho}) = x_1 \gamma_1(T, \boldsymbol{\rho}) f_1^0(T). \tag{9–15}$$

where the activity coefficient is given by Equation (9–10). The standard state fugacity is the Henry's constant

$$f_1^0(T) = H_1(T) \equiv \lim_{x_1 \to 0} \frac{f_1^L}{x_1}. \tag{9–16}$$

The full standard state specification includes pressure and (P^0) and solvent density (ρ^0) at the system temperature. Typically, an experimentally measured point at low pressure could be used. Other options might be to utilize a more predictive approach, since models are appearing for ionic liquid densities (as discussed in the introduction). The equation of state, connecting P and ρ, is given by Equation (9–9). In the application given here, the standard state pressure is the saturated vapor pressure of the solvent at the system temperature, meaning that $P^0 = 0$. The reference density of the solvent is found by extrapolating low-pressure data to zero, i.e., $\rho^0 = \rho(T, P = 0)$. For practical purposes, density data given at $1\,\mathrm{bar}$ can also be used, with negligible difference.

9.2.1. Phase equilibrium computations

Equilibrium is reached with the state variables satisfy the isofugacity relations, Equations (9–11) and (9–9). For a binary the total number of state variables are four: T, P, x_1 (or x_2), and ρ. Since two independent equations relate these four, we must specify at least two of the independent variables. A

number of different phase equilibrium computations can be made. Previously, Mathias and O'Connell[6] and Campanella et al.[7] specified T and P (the isothermal flash), and calculated x_1 and y_1*. Here, we have adopted a slightly different approach; we specify temperature, T, and composition, x_1, and solve the equilibrium relations for pressure, P, and final density, ρ. This means setting up the equations

$$\begin{aligned} g_1 &= \phi_1^V(T,P)P - x_1\gamma_1(T,\boldsymbol{\rho})H_1(T) \\ g_2 &= \frac{P-P^0}{\mathsf{R}T} - \frac{P^{h.s.}(T,\boldsymbol{\rho}) - P^{h.s.}(T,\boldsymbol{\rho}^0)}{\mathsf{R}T} - \sum_i^M \sum_j^M \left[\rho_i\rho_j - \rho_i^0\rho_j^0\right]\left[B_{ji}(T) - B_{ji}^{h.s.}(T)\right] \end{aligned} \tag{9–17}$$

and solving $\mathbf{g} = \mathbf{0}$. This requires taking derivatives of $\mathbf{g}$ with respect to P and ρ

$$\begin{bmatrix} \left(\frac{\partial g_1}{\partial P}\right)_\rho & \left(\frac{\partial g_1}{\partial \rho}\right)_P \\ \left(\frac{\partial g_2}{\partial P}\right)_\rho & \left(\frac{\partial g_2}{\partial \rho}\right)_P \end{bmatrix} = \\ \begin{bmatrix} \phi_1^V + P\left(\frac{\partial \phi_1^V}{\partial P}\right)_\rho & -x_1\gamma_1 H_1\left(\frac{\partial \ln\gamma_1}{\partial \rho}\right)_P \\ \frac{1}{\mathsf{R}T} & -\frac{1}{\mathsf{R}T}\left(\frac{\partial P^{h.s.}}{\partial \rho}\right)_P - 2\rho\sum_{i,j} x_i x_j\left[B_{ji}(T) - B_{ji}^{h.s.}(T)\right] \end{bmatrix} \tag{9–18}$$

The variables are then found iteratively from a standard Newton method, where at the kth iteration (see Appendix A)

$$\begin{bmatrix} P \\ \rho \end{bmatrix}_{(k+1)} = \begin{bmatrix} P \\ \rho \end{bmatrix}_{(k)} - \begin{bmatrix} \left(\frac{\partial g_1}{\partial P}\right)_\rho & \left(\frac{\partial g_1}{\partial \rho}\right)_P \\ \left(\frac{\partial g_2}{\partial P}\right)_\rho & \left(\frac{\partial g_2}{\partial \rho}\right)_P \end{bmatrix}_{(k)}^{-1} \begin{bmatrix} g_1 \\ g_2 \end{bmatrix}. \tag{9–19}$$

This procedure is repeated until convergence is attained. Ultimately, the $\gamma - \phi$ method relies heavily on the standard state fugacity, H_1, which is often a strong function of temperature. There are – without any prior knowledge – two ways of estimating its value

1. Extrapolation of liquid fugacities in the dilute region.
2. Semiempirical temperature expression.

Both require mixture data. The former is part of the standard Krichevskii-framework; it requires obtaining values of f_1/x_1 across a limited composition range, similar to Figure 8–2†. We choose the latter approach, which assumes that the dependence of each solute-solvent Henry's constant, in any solvent R, is given by an expression similar to

$$\ln H_{1,R}(T) = a_{0,R} + \frac{a_{1,R}}{T} + a_{2,R}\ln T. \tag{9–20}$$

* In these applications, the solvents were volatile, leaving an additional equilibrium constraint on the state variables (for vapor composition y_1) † This can be done by calculating the vapor phase fugacity from Equation (9–12).

The exact mathematical form of the expression is not unimportant. A simple linear function might on occasion be favorable, but does not constrain the enthalpy of dissolution accurately. For gases in liquids, we have the relation for the molar change in enthalpy of dissolution

$$\Delta h_1 = -R\left(\frac{\partial \ln x_1}{\partial 1/T}\right)_P = -RT^2\left(\frac{\partial \ln H_1}{\partial T}\right)_P. \tag{9–21}$$

Inserting the expression above yields

$$\Delta h_1 = -R(-a_{1,R} + a_{2,R}T), \tag{9–22}$$

which is consistent with data.[8,10] The coefficients for the Henry's law constant ($\mathbf{a}$) can then be found from minimizing an objective function, given by relevant state variables, such as

$$\min_{\mathbf{a}} s = \frac{1}{2}\sum_j (\delta P)_j^2, \tag{9–23}$$

where δP is the difference in pressure between that obtained from Equation (9–19) and the experimental value. Depending on what variables are specified for solving Equation (9–19), the choice of objective function can vary. Mathias and O'Connell[6] and Campanella et al.[7] chose to minimize the difference in liquid mole fraction of 1, x_1. Ideally, the overall results should be reasonably insensitive towards what variables are specified and the objective function. In practice, however, one may find that the objective function is slightly more sensitive towards some variables compared to others.

A phase equilibrium computation requires the model parameters, T_i^*, V_i^*, and the binary interaction parameter k_{ji}. While the latter can be determined from binary data alone, the two former can be found from pure component data. Equation (9–9) is the equation of state, connecting P, ρ, and T, and may be used for reduction of compressed liquid densities. This is explored in the next chapter, before continuing to the gas-liquid results in Chapter 11.

9.A. The Mathias model for direct correlation function integrals

The basis for a model connecting the direct correlation function integral to relevant state variables is the compressibility relation for a fluid, which in the matrix notation of Chapter 2, is given by

$$\left(\frac{\partial P/\mathrm{R}T}{\partial \rho}\right)_T = \mathbf{i}^{\mathsf{T}}(\mathbf{I} - \mathbf{XC})\mathbf{Xi}, \tag{9–24}$$

where $\mathbf{X}$ is the diagonal matrix of which the elements are $X_{ii} = x_i$, $\mathbf{C}$ is the matrix of DCFIs, and $\rho = \sum_i \rho_i$. If we assume that the variation of pressure with density can be captured by the virial equation, truncated after the second term,

$$\frac{P}{\mathsf{R}T} = \rho + \rho^2 B_{\text{mix}}(T) + \dots \qquad B_{\text{mix}} = \mathbf{i}^{\mathsf{T}}\mathbf{XBXi} \tag{9–25}$$

with B_{ij} being the cross-virial coefficient between i and j, then $\mathbf{C}$ can be found from differentiation with respect to density. The first derivative is*

$$\left(\frac{\partial P/\mathsf{R}T}{\partial \rho}\right)_T = \mathbf{i}^{\mathsf{T}}\mathbf{Xi} + 2\rho\mathbf{i}^{\mathsf{T}}\mathbf{XBXi}. \tag{9–26}$$

Comparing the two compressibility relations give

$$\begin{aligned} &\mathbf{i}^{\mathsf{T}}(\mathbf{I} - \mathbf{XC})\mathbf{Xi} = \mathbf{i}^{\mathsf{T}}\mathbf{Xi} + 2\rho\mathbf{i}^{\mathsf{T}}\mathbf{XBXi} \quad \text{or equivalently} \\ &\mathbf{C} = -2\rho\mathbf{B}. \end{aligned} \tag{9–27}$$

The virial equation with just two terms is strictly only valid in the low-density region. Unfortunately, higher-order virial coefficients are not generally known within reasonable accuracy for real fluids, thereby limiting the practical usage of the virial equation significantly. However, if we redo this derivation for hard sspheres, then after subtracting this from the "true" virial, the result is

$$\mathbf{C} - \mathbf{C}^{h.s.} = -2\rho[\mathbf{B} - \mathbf{B}^{h.s.}] \quad \Rightarrow \quad \mathbf{C} = \mathbf{C}^{h.s.} - 2\rho[\mathbf{B} - \mathbf{B}^{h.s.}] \tag{9–28}$$

Since the hard-sphere equation of state contain repulsive forces, truncating the expansion after the second coefficient, at temperatures below the critical, is in good agreement with observed experimental data.[11] Furthermore, reliable expressions exists for the second virial coefficient, and the hard-sphere expressions can be obtained analytically from a hard-sphere equation of state. Here, the Carnahan-Starling form is chosen.[12,13] The hard-sphere second virial coefficient is given analytically by

$$B_{ji}^{h.s.}(T) = \frac{\pi}{3}\left(\sigma_i^3(T) + \sigma_j^3(T)\right), \tag{9–29}$$

where σ_i is the diameter of the hard-sphere molecule representing i. Mathias[4] found that a simple, but empirical, expression based on the principle of corresponding states, for the variation of σ_i with temperature could represent liquids at conditions below their critical points. This is the expression given in Equation (9–7a). This double-function was able to accurately describe the fluid behavior at low and high reduced temperatures. The virial coefficient was given by an expression similar to that

* $\mathbf{i}^{\mathsf{T}}\mathbf{Xi}$ is another way of writing 1.

of Tsonopoulos,[14] and is shown in Equation (9–7b). Mathias and O'Connell[6] fitted the coefficients $(\mathbf{a}, \mathbf{b}, \mathbf{c})$ to observations of liquid argon, krypton, and xenon, and the reported values are

$$\mathbf{a}^{\mathsf{T}} = [0.6539, 0.1607]\,, \quad \mathbf{b}^{\mathsf{T}} = [0.8277, -0.2211]\,, \quad \mathbf{c}^{\mathsf{T}} = [0.3625, -0.7141, -1.7544, 0.4708, -0.0042]\,.$$

Figure 9–1 shows the variation of the B and $B^{h.s.}$ with temperature for a pure component.

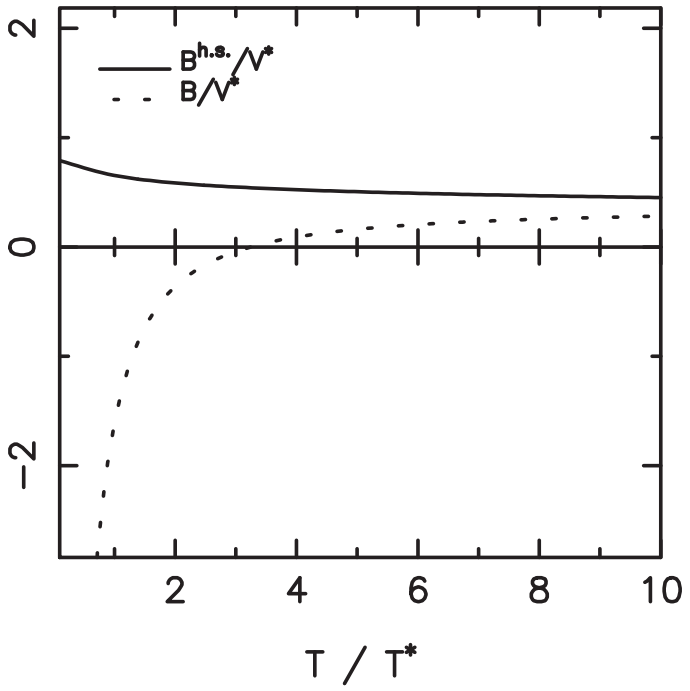

Figure 9–1. Plot of B and $B^{h.s.}$ versus reduced temperature using the correlation of Mathias and O'Connell.

9.B. Hard-sphere expressions

The multicomponent Carnahan-Starling equation of state, which was given by Mansoori et al.[13] relates pressure, chemical potential, and direct correlation function integral to a set of reduced densities, $\{\zeta_m\}$, defined by

$$\zeta_m = \frac{\pi}{6}\sum_i^M \rho_i \sigma_i^m = \frac{\pi}{6}\rho \sum_i^M x_i \sigma_i^m. \tag{9–30}$$

The pressure is

$$\frac{P^{h.s.}}{\mathsf{R}T} = \frac{6}{\pi}\left[\frac{\zeta_0}{1-\zeta_3} + \frac{3\zeta_1\zeta_2}{(1-\zeta_3)^2} + \frac{3\zeta_2^3}{(1-\zeta_3)^3} - \frac{\zeta_3\zeta_2^3}{(1-\zeta_3)^3}\right]. \tag{9–31}$$

Similarly, for the chemical potential of i

$$\frac{\mu_i^{h.s.}}{\mathsf{R}T} = \ln\rho_i - \ln(1-\zeta_3) + \frac{\pi\sigma_i^3}{6}\frac{P^{h.s.}}{\mathsf{R}T} + \frac{3\zeta_2\sigma_i}{1-\zeta_3} + \frac{3\zeta_1\sigma_i^2}{1-\zeta_3} + \frac{9\zeta_2^2\sigma_i^2}{2(1-\zeta_3)^2}$$
$$+ 3\left(\frac{\zeta_2\sigma_i}{\zeta_3}\right)^2\left[\ln(1-\zeta_3) + \frac{\zeta_3}{1-\zeta_3} - \frac{\zeta_3^2}{2(1-\zeta_3)^2}\right] - \left(\frac{\zeta_2\sigma_i}{\zeta_3}\right)^3\left[2\ln(1-\zeta_3) + \frac{\zeta_3(2-\zeta_3)}{1-\zeta_3}\right] \tag{9–32}$$

The direct correlation function integral is obtained from differentiation of the pressure with respect to density. One finds that for the (i,j) pair

$$\begin{aligned}-\frac{C_{ij}^{h.s.}}{\zeta_0} =& \frac{(\sigma_i+\sigma_j)^3}{1-\zeta_3} + \frac{2\sigma_i\sigma_j\zeta_2[(\sigma_i+\sigma_j)^2+\sigma_i\sigma_j] + 3\zeta_1(\sigma_i\sigma_j)^2(\sigma_i+\sigma_j)}{(1-\zeta_3)^3} \\ &+ 9\frac{(\sigma_i\sigma_j\zeta_2)^3}{(1-\zeta_3)^3} + \frac{\zeta_2(\sigma_i\sigma_j)^2}{(1-\zeta_3)^3}\left\{9\zeta_2(\sigma_i+\sigma_j) + 6\zeta_1\sigma_i\sigma_j + \frac{6+\zeta_3(-15+9\zeta_3)}{\zeta_3}\right. \\ &\left. - \zeta_2(\sigma_i+\sigma_j)\frac{6+\zeta_3(-15+12\zeta_3)}{\zeta_3^2} + \zeta_2^2\sigma_i\sigma_j\frac{6+\zeta_3(-21+\zeta_3(26-14\zeta_3))}{\zeta_3^3(1-\zeta_3)}\right\} \\ &+ \ln(1-\zeta_3)\frac{6\zeta_2(\sigma_i\sigma_j)^2}{\zeta_3^3}\left\{\zeta_3 - (\sigma_i+\sigma_j)\zeta_2 + \frac{\zeta_2^2\sigma_i\sigma_j}{\zeta_3}\right\}.\end{aligned} \tag{9–33}$$

The symmetry of this expression should be noted. In the limiting case of a pure fluid, the above equation reduces to

$$-C^{h.s.} = 2\zeta_3\frac{4-\zeta_3}{(1-\zeta_3)^4}. \tag{9–34}$$

References

1. S. W. Brelvi and J. P. O'Connell. *AIChE J.*, 18: 1239–1243, 1972.
2. S. W. Brelvi and J. P. O'Connell. *Can. J. Chem.*, 50:3135–3143, 1972.
3. K. E. Gubbins and J. P. O'Connell. *J. Chem. Phys.*, 60:3449–3453, 1974.
4. P. M. Mathias. *Thermodynamic properties of high-pressure liquid mixtures containing supercritical components*. PhD thesis, University of Florida, Gainesville, FL, USA, 1978.
5. P. M. Mathias and J. P. O'Connell. *Equations of State in Engineering and Research*, chapter 5, pages 97–108. Am. Chem. Soc., 1979.
6. P. M. Mathias and J. P. O'Connell. *Chem. Eng. Sci.*, 36:1123–1132, 1981.
7. E. A. Campanella, P. M. Mathias, and J. P. O'Connell. *AIChE J.*, 33:2057–2066, 1987.
8. J. M. Prausnitz, R. N. Lichtenthaler, and E. Gomez de Azevedo. *Molecular thermodynamics of fluid-phase equilibria*. Prentice-Hall, 3rd edition, 1999.
9. J. G. Hayden and J. P. O'Connell. *Ind. Eng. Chem. Proc. Des. Dev.*, 14:209–216, 1975.
10. E. C. W. Clarke and D. N. Glew. *Trans. Faraday Soc*, 62:539–547, 1966.
11. L. Haar and S. H. Shenker. *J. Chem. Phys.*, 55: 4951, 1971.
12. N. F. Carnahan and K. E. Starling. *J. Chem. Phys.*, 51:635–636, 1969.
13. G. A. Mansoori, N. F. Carnahan, K. E. Starling, and T. W. Leland. *J. Chem. Phys.*, 54:1523–1525, 1971.
14. C. Tsonopoulos. *AIChE J.*, 20:263–272, 1974.

10. Application to pure liquids

This chapter presents results for data reduction and parameter estimation for pure ionic liquids and pure gases, which is used in the gas–liquid equilibrium calculations.

10.1. Data reduction method

The equation of state, Equation (9–9), for a pure component, reduces to

$$\frac{P - P^0}{\mathsf{R}T} = \frac{P^{h.s.}(T,\rho) - P^{h.s.}(T,\rho^0)}{\mathsf{R}T} + \left[\rho^2 - (\rho^0)^2\right]\left[B(T) - B^{h.s.}(T)\right]. \qquad (10\text{–}1)$$

The pure component characteristics for the model are determined from regression of isothermally compressed liquid density data $(P\rho T)$. The reference point (P^0, ρ^0) is a low-pressure experimental point, which is taken as the observation with the lowest pressure within an isotherm of P vs. ρ. Values of T^* and V^* are obtained by minimizing the function q,

$$\min_{T^*,V^*} q = \frac{1}{2}\sum_k (\delta P)_k^2, \qquad (10\text{–}2)$$

where δP is the difference in observed pressure and that calculated using Equation (10–1). This procedure is standard[1,2] in the engineering literature, and standard deviations of parameter estimates are obtained as a convenient byproduct of the optimization.[3] The function

$$q' = \frac{1}{2}\sum_k (\delta\rho)_k^2 \qquad (10\text{–}3)$$

could also have been minimized. This requires solving the equation of state for total density, ρ, given pressure, P. It is slightly more computationally demanding, and requires taking derivatives of an iteration variable. Derivatives of Equation (10–2) do not require iteration, since P is given analytically in terms of ρ. Below, results for correlation of the ionic liquid density data are given. In addition to the ionic solvents, results are also given for the gaseous solutes (in their liquid state) which will be required for further developments in the next chapter.

10.2. Volumetric properties as function of T and ρ

Table 10–1 shows the data base on ionic liquids that has been compiled. A total of 17 references, spanning 28 different ionic liquid structures is compiled. Most of the ionic liquid structures are based on the imidazolium cation (or derivatives thereof), while the remaining cover the phosphonium, pyridinium, pyrrolidinium, and piperidinium cations. The pressure range typically span from a few bars to several hundreds (ΔP), in three cases even more than 2000, as is indicated in column four of Table 10–1. Columns 5-8 contain the regressed parameter values along with their standard deviations. The standard deviation of V^* is usually smaller than that of T^*, which is indicative of the objective function being more sensitive towards V^* than T^*. Generally, the V^* found from different sources are similar, whereas the T^* values tend to disagree, which is illustrated by the six entries of [bmim][BF_4]. The values of V^* range from $652 - 684\,\mathrm{cm^3/mol}$, while T^* varies from 442 to $849\,\mathrm{K}$; a doubling of the smallest value. The data set giving $T^* = 442\,\mathrm{K}$ is also that with an average absolute percentage error in pressure (AAPE(P)) much larger than average. The AAPE(P) defined as

$$\mathrm{AAPE}(P) = \frac{100\%}{n}\sum_j^n \left|\frac{\delta P}{P}\right|_j, \tag{10–4}$$

given density. A similar statistic is defined for the error in density,

$$\mathrm{AAPE}(\rho) = \frac{100\%}{n}\sum_j^n \left|\frac{\delta \rho}{\rho}\right|_j. \tag{10–5}$$

While calculation of pressure from density is explicitly analytical for equations of state, the reverse calculation is rarely analytical. This often results in a nonlinear problem, where the density is calculated iteratively using a standard Newton-Raphson method, where at the kth iteration

$$\rho^{(k+1)} = \rho^{(k)} - \left[P\left(\frac{\partial P}{\partial \rho}\right)_T^{-1}\right]^{(k)}. \tag{10–6}$$

The calculation requires an initial value of ρ, and derivatives of P.

Table 10–1. Data reduction of ionic liquids. Standard deviations are provided for the estimated parameter values, as well as the error in pressure and density.

Substance (abbr.)	Ref.	n	ΔP (bar)	T^* (K)	S.D. (K)	V^* ($\mathrm{cm^3/mol}$)	S.D.	AAPE(P) (%)	AAPE(ρ) (%)
[bmim][BF_4]	[4]	45	2–399	652.1	7.6	652.8	0.5	1.56	0.01
[bmim][BF_4]	[5]	77	1–100	761.4	8.0	656.9	0.4	5.25	0.01

Continues on next page

Continued from last page

[bmim][BF_4]	6	20	1–200	442.2	2.0	684.8	41	6.43	0.03
[bmim][BF_4]	7	67	1–599	761.2	4.3	656.4	0.2	1.84	0.01
[bmim][BF_4]	8	189	1–2000	849.2	3.6	660.3	0.2	3.87	0.12
[bmim][BF_4]	9	40	1–400	790.3	6.5	665.3	0.4	3.18	0.02
[bmim][PF_6]	4	45	7–401	722.5	7.9	725.1	0.3	2.38	0.02
[bmim][PF_6]	6	20	1–200	552.4	12	748.2	17	6.45	0.03
[bmim][PF_6]	10	54	1–2493	757.9	13	729.9	0.4	4.91	0.08
[bmim][PF_6]	11	14	1–2021	720.2	54	734.7	1.2	6.41	0.14
[bmim][PF_6]	8	189	1–2000	842.4	3.4	732.6	0.2	3.92	0.11
[bmim][PF_6]	9	41	1–400	829.6	9.4	751.3	0.8	9.41	0.03
[hmim][Tf_2N]	12	163	1–596	787.9	1.9	1165.2	0.2	1.15	0.01
[hmim][Tf_2N]	13	28	1–400	778.5	17	1159.5	1.3	4.10	0.07
[hmim][Tf_2N]	14	149	1–650	718.5	3.5	1160.0	0.1	1.54	0.02
[bmim][Tf_2N]	9	42	1–400	787.6	6.4	1038.9	0.6	3.36	0.03
[bmim][Tf_2N]	12	168	1–591	787.9	2.7	1036.5	0.2	1.68	0.02
[emim][Tf_2N]	15	96	1–300	759.2	4.1	906.1	0.3	3.43	0.01
[emim][Tf_2N]	9	41	1–400	846.6	6.6	938.6	0.8	5.72	0.03
[emim][BF_4]	15	96	1–300	711.7	4.1	526.2	0.1	2.92	0.01
[bmim][$C(CN)_3$]	15	96	1–300	754.5	4.2	770.0	0.2	3.78	0.01
[C_7mim][Tf_2N]	15	96	1–300	792.7	4.4	1226.2	0.5	4.78	0.02
[omim][Tf_2N]	15	96	1–300	776.1	4.8	1292.0	0.4	4.48	0.02
[emim][$EtSO_4$]	16	63	1–350	706.9	3.2	676.6	0.1	0.89	0.004
[emim][$EtSO_4$]	9	42	1–400	568.5	9.5	620.5	0.8	4.15	0.02
[C_3mim][Tf_2N]	17	165	1–596	775.4	2.5	970.8	0.2	1.85	0.01
[C_5mim][Tf_2N]	17	165	1–596	782.9	2.0	1097.6	0.2	1.55	0.01
[$(C_6H_{13})_3P(C_{14}H_{29})$][Cl]	18	134	2–650	827.8	1.8	2174.9	0.2	0.94	0.01
[$(C_6H_{13})_3P(C_{14}H_{29})$][Ac]	18	144	2–650	836.2	2.1	2284.6	0.2	1.12	0.01
[$(C_6H_{13})_3P(C_{14}H_{29})$][$Tf_2N$]	18	126	2–650	874.6	3.1	2713.4	0.6	2.19	0.02
[omim][BF_4]	5	77	1–100	729.9	6.6	908.7	0.3	2.97	0.00
[bmim][CF_3SO_3]	5	77	1–100	723.3	7.9	775.7	0.3	3.17	0.01
[bmmim][PF_6]	5	63	1–100	766.4	8.3	785.7	0.3	3.26	0.00
[hmim][PF_6]	5	77	1–100	713.5	8.3	856.4	0.4	2.98	0.01

Continues on next page

Continued from last page

[omim][PF_6]	[5]	77	1–100	768.9	5.0	980.3	0.3	3.50	0.01
[omim][PF_6]	[11]	14	1–2042	529.9	87	1013.4	19	2.64	0.08
[omim][BF_4]	[11]	15	1–2069	749.4	39	916.2	1.1	6.94	0.15
[NBuPy][BF_4]	[11]	14	1–2042	752.4	31	646.8	0.9	5.59	0.10
[bmim][$OcSO_4$]	[8]	174	1–2000	919.8	4.3	1177.9	0.4	4.89	0.14
[emim][CF_3SO_3]	[19]	91	1–350	764.5	4.3	655.8	0.3	3.98	0.02
[C_3mpy][Tf_2N]	[19]	91	1–350	795.8	2.8	1017.1	0.3	2.76	0.01
[C_4mpyr][Tf_2N]	[19]	91	1–350	792.6	3.2	1070.8	0.3	2.56	0.01
[C_3mpyr][Tf_2N]	[19]	91	1–350	792.2	3.4	1010.9	0.4	2.56	0.01
[C_3mpip][Tf_2N]	[19]	91	1–350	793	2.9	1068.0	0.3	2.09	0.01
[C_4mpyrro][Tf_2N]	[20]	36	10–400	811.2	7.4	1095.5	0.7	2.84	0.03
[N_{1114}][Tf_2N]	[20]	36	10–400	792.1	7.4	1032.6	0.5	3.49	0.03

Less fluctuation is seen in the [bmim][PF_6] sets, where T^* varies from 552 to $842\,\mathrm{K}$. As before, the set with the smallest T^* also has the largest error in P, and give pressures above $2000\,\mathrm{bar}$. The majority of entries in Table 10–1 have errors less than five percent in pressure, averaging 3.51%. A similar error statistic for the density gives values much less than 1%, with an average value of 0.034%. Usually the error in density is much lower than that in pressure, since pressure (unlike density) is a much more fluctuating quantity. Thus, from Table10–1 it seems that overall the model is capable of reducing the data to within reasonable error. Figure 10–1 (left plot) shows the (P, ρ) relation; the points give experimental measurements and the full lines indicate model estimates using T^* and V^* obtained from minimizing Equation (10–2). The measured values are described quantitatively, which is also indicated in Table 10–1. The right plot shows the variation of the liquid bulk modulus, which is given by

$$\left(\frac{\partial P/\mathsf{R}T}{\partial \rho}\right)_T = \frac{1}{\rho \kappa_T \mathsf{R}T} = 1 - C(T, \rho). \tag{10–7}$$

The points on the graphs are the experimentally determined values, transformed from (P, ρ) data using forward differences

$$\left(\frac{\partial P/\mathsf{R}T}{\partial \rho}\right)_T \approx \frac{1}{\mathsf{R}T}\frac{P_{k+1} - P_k}{\rho_{k+1} - \rho_k}, \quad k \in [1, n-1]. \tag{10–8}$$

The uncertainties arising from finite differences of P vs. ρ data might be above negligible, but the data should remain continuous and reasonably well-behaved, within a margin of scatter. This means that data which show considerable scatter seem unreliable. On the other hand, data which conform to a smooth line does not necessarily guarantee accurate measurements. Nevertheless, this procedure can

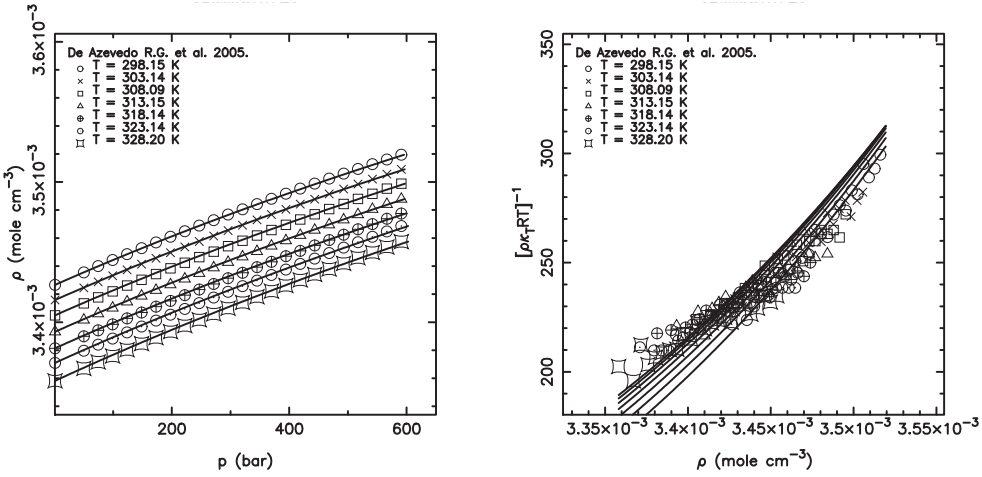

Figure 10–1. Pressure-density isotherms and liquid bulk modulus of [bmim][Tf_2N] from the data of Gomez de Azevedo et al..[12] The model gives a quantitative description of the liquid density data, and the liquid bulk modulus data (transformed from liquid density data) is also matched sufficiently.

aid in detecting potentially unreliable data. The isotherms of [bmim][Tf_2N] form smooth, continuous curves. The model does not accurately describe variations with density, but is able to match most of the data reasonably. An example of a system with discrepancies between the two representations of (P, ρ) data is that of Machida et al.,[8] of which four isotherms are shown in Figure 10–2. The (P, ρ) isotherms appears to be well behaved, a conclusion which can also be drawn by inspection of Table 10–1, where the error in pressure is just slightly above the average, 3.87%, and the corresponding error in density is 0.12%. However, inspection of $(\partial P/\partial \rho)_T$ reveals that the derivatives form a noncontinuous sequence of points. One could suspect, that the published values are not really measured, but instead being smoothed measurements.

Another case, where the model describes the data quantitatively, is the data for [bmim][PF_6] of Tekin et al..[4] The data form smooth curves on both left and right plots. The right plot, generated from Equation (10–8), shows that all data fall into one curve, which is reasonably described with the model.

Table 10–2 shows the equivalent of Table 10–1 for a handful of gases/solutes (compressed gases). However, the authors of the data cover a large range of the subcritical region as well, given the large pressure range covered in the experimental data, as indicated in the fourth column of Table 10–2. Since the treatments aims at compressed liquids, all data points were systematically excluded if $\rho/\rho_c < 1.5$, meaning that only data far from the critical region was included. This value is similar to previous treatments.[1,2] Figure 10–4 shows the agreement with the data of Michels et al.[26] from 1954. The densities of the systems in Table 10–2 are much larger than those of the ionic liquids, since these substances need to be compressed much more to remain in a liquid state at the measurement temperatures. The

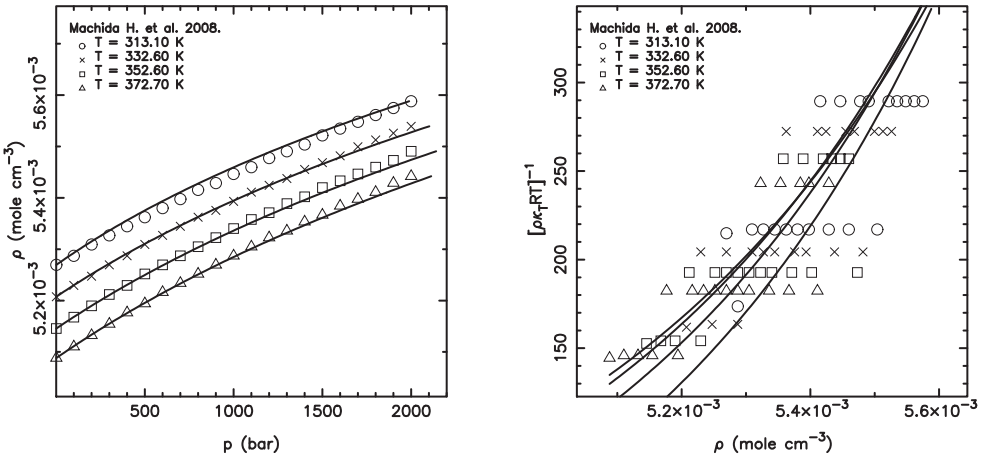

Figure 10–2. Pressure-density isotherms and liquid bulk modulus of [bmim][BF_4] from the data of Machida et al..[8] The liquid density data (left) is correlated quantitatively, but the liquid bulk modulus, calculated by taking derivatives of P with respect to ρ appears in a inconsistent way.

Table 10–2. Data reduction of compressed gases. Standard deviations are provided for the estimated parameter values, as well as the error in pressure and density.

Substance	Ref.	n	ΔP (bar)	T^* (K)	S.D. (K)	V^* (cm^3/mol)	S.D.	AAPE(P) (%)	AAPE(ρ) (%)
Carbon dioxide	[21]	55	100–300	280.60	4.15	91.06	0.59	1.88	2.50
Methane	[22]	36	500–1880	193.97	0.34	99.94	0.02	0.07	0.03
Hydrogen sulfide	[21]	55	30–400	350.66	0.55	95.22	0.04	0.96	4.84
Hydrogen	[23]	22	592–1184	34.95	4.56	52.69	0.13	0.21	0.11
Argon	[24]	56	18–2900	157.25	0.29	75.05	0.01	0.09	0.03
Krypton	[25]	48	5–1241	202.74	0.94	91.75	0.01	1.88	0.49
Xenon	[26]	90	60–2700	286.47	0.36	117.67	0.02	0.90	0.21

isotherms, when pressure is plotted against density, form much more curved lines than the ionic liquid sets. The model underestimates the bulk modulus of the fluid at higher densities, and all lines cross each other at around $0.021\,\mathrm{mol/cm^3}$. This phenomenon, usually referred to as the "cross-over" density seems common to all liquids, except water. It is a point where the compressibility of the liquid becomes independent of temperature, as discussed extensively by Huang.[27] Nevertheless, the model is able to accurately correlate the data to within 0.90% error in pressure and 0.21% in density. The errors in density in Table 10–2 are generally larger than those from 10–1. The reason for this is the variation of pressure at high densities, which is much larger than at low molar densities (where the ionic liquid data is usually taken).

Table 10–3 shows the results of estimating T^* and V^* from all data sets pertaining to a single ionic

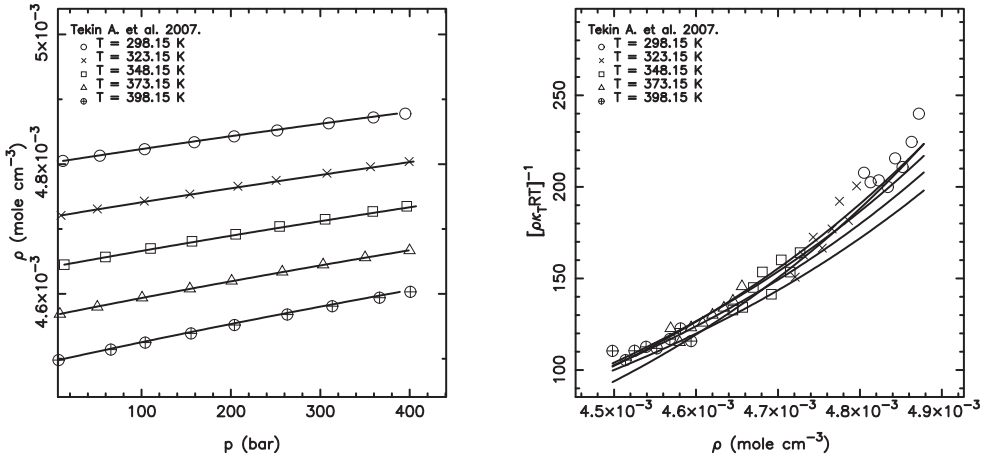

Figure 10–3. Pressure-density isotherms and liquid bulk modulus of [bmim][PF_6] from the data of Tekin et al..[4] Both plots show that the data is described quantitatively.

Table 10–3. Simultaneous reduction of all data sets for ionic liquid species.

Substance (abbr.)	n	ΔP (bar)	T^* (K)	S.D. (K)	V^* ($\mathrm{cm}^3/\mathrm{mol}$)	S.D
[C_4mpyr][NTf_2]	127	1–400	823.6	11.0	1080.3	1.6
[hmim][NTf_2]	340	1–650	747.2	4.1	1161.3	0.2
[bmim][NTf_2]	210	1–591	792.3	2.5	1037.0	0.2
[emim][Tf_2N]	137	1–400	831.4	14.0	920.7	1.9
[omim][PF_6]	91	1–2042	534.9	33.0	1012.3	6.9
[omim][BF_4]	92	1–2069	747.6	15.0	916.1	0.4
[bmim][PF_6]	363	1–2493	813.9	3.5	732.9	0.2
[bmim][BF_4]	438	1–2000	838.7	2.7	660.2	0.2

liquid, from those species in Table 10–1 where multiple data sets were found. The second column of Table 10–3 shows the total number of available data points, whereas the third gives the total pressure range studied. In most cases, the data sets are compatible, giving parameter values in close agreement with those found from reduction of the single sets. This is exemplified by [hmim][Tf_2N] using the data sets of Gomez de Azevedo et al.,[12] Kandil et al.,[13] and Esperança et al..[14] The values of V^* span the range $1159.5-1165.2\,\mathrm{cm}^3/\mathrm{mol}$, while simultaneous reduction gives $1161.3\,\mathrm{cm}^3/\mathrm{mol}$. The values of T^* vary more; within $718.8-787.9\,\mathrm{K}$, while the overall value is $747.2\,\mathrm{K}$. In both cases, the overall estimate is outside the standard deviation of the individual sets, but is still capable of giving a satisfactory fit to the data. Generally, reducing data sets simultaneously give reasonable descriptions of data from different sources. One exception is the data for [emim][Tf_2N] of Gardas et al.[15] and Jacquemin et al..[9] Figure 10.5(a) shows the raw experimental data from the two sources. It is clear that the slope of density with pressure from one set is inconsistent with the other. The data for [emim][$EtSO_4$] of Jacquemin et al.[9]

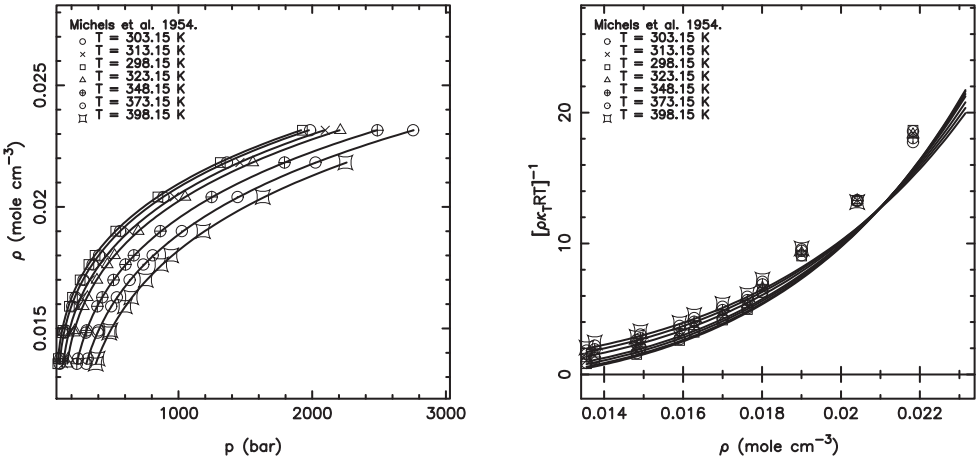

Figure 10–4. Pressure-density isotherms and liquid bulk modulus of xenon from the data of Michels et al..[26] The variation of density with pressure is much more pronounced in the case of a compressed gas, but the model describes the data excellent.

and Hofman et al.[16] are incompatible with each other, and have therefore been left out of the regression. Figure 10.5(b) shows the estimation using the data of Hofman et al.. The data ranges from 180 to about 270, whereas the data of Jacquemin et al. lie in between 50 and 125 in the same density range. The model will therefore be unable to represent simultaneously both data sets.

10.3. Density and temperature dependence

One of the great advantages of the DCFI-model of Mathias is the separation of temperature and density in the perturbation term. For a pure fluid, the DCFI is expressed by

$$C(T,\rho) = C^{h.s.}(T,\rho) - 2\rho\left[B(T) - B^{h.s.}(T)\right]. \tag{10–9}$$

This equation can be rearranged into

$$\frac{C(T,\rho) - C^{h.s.}(T,\rho)}{2\rho} = -\left[B(T) - B^{h.s.}(T)\right]. \tag{10–10}$$

The right-hand side is completely independent of density at constant temperature. Combining Equations (10–7) and (10–8) estimates of the DCFI as function of temperature can be obtained. In fact, the liquid bulk modulus plots shown above reveal the behavior of the integral as function of the state variables. Figure 10–6 shows the first four isotherms for the ionic liquid [bmpy][Tf_2N]. The full drawn lines are the model estimates, whereas the points are transformed values of the (P,ρ) data using Equation (10–8).

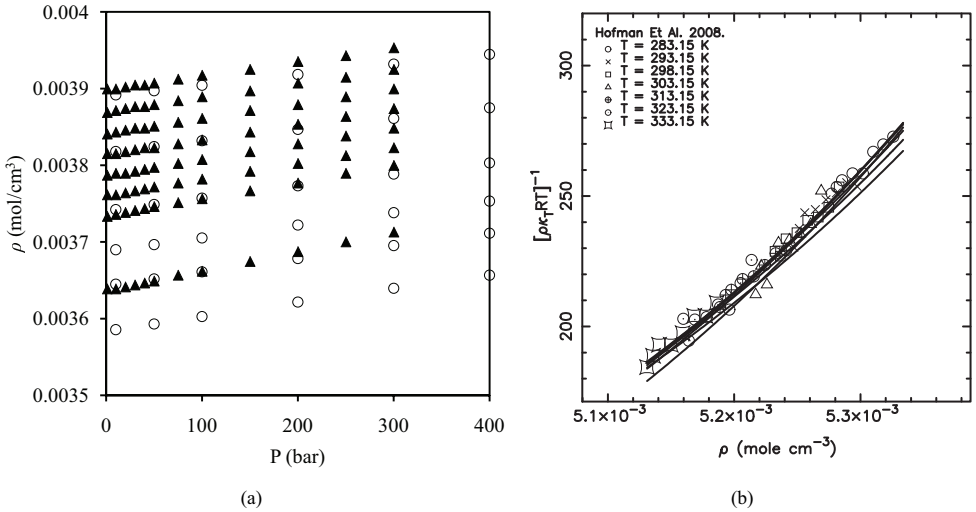

Figure 10–5. Left: Pressure-density data from Gardas et al.[15] (▲) and Jacquemin et al.[9] (○). The data from these two sources are not compatible with each other, wherefore a model is unable to give a good fit to both sets. Right: Liquid bulk modulus data and model estimate from reduction of the data of Hofman et al., where the model performs excellent.

The isotherms seem to conform very well to the "experimental points", given the magnitude of the ordinate. The agreement between the model estimate and low- and high-temperature data appears to be good, indicating that the form of Equation (10–9) is consistent with this data set. Besides the aspect of giving a correct density dependence, these plots can also be used to check for the temperature dependence. The horizontal lines, given by the model, is in reasonable agreement with the transformed experimental points for this particular system. Figure 10–6 shows a similar plot, but for [bmim][Tf_2N] with data of Gomez de Azevedo et al..[12] The isotherm at 298 K conforms reasonably, but the other isotherms appear more erratic, though a linear trend seems to govern some of the points. Similar conclusions are drawn for most of the ionic liquids studied; the transformed data points provide reasonably smooth curves when the bulk moduli form a smooth and continuous curve. For many systems, the linear trend of Figure 10–6 is also observed, which suggests that the density formulation of (10–9) is not always correct. While the model is able to describe a correct temperature dependence at the lower isothermals, the description of the highest temperature (313 K) is less good. Figure 10–7 shows a system where the temperature dependence is reasonably good, but the density variation seems nonlinear. Only the isotherm at 373 K seems to show a linear trend, although negative. Also shown in Figure 10–7 is the ionic liquid [hmim][Tf_2N]. The temperature range covered is less than the previous, but the conclusions are similar to the systems treated above, especially [bmim][Tf_2N] also from Gomez de Azevedo et al.. The temperature dependence of the low-temperature isotherms is in good agreement with the experimentally derived results,

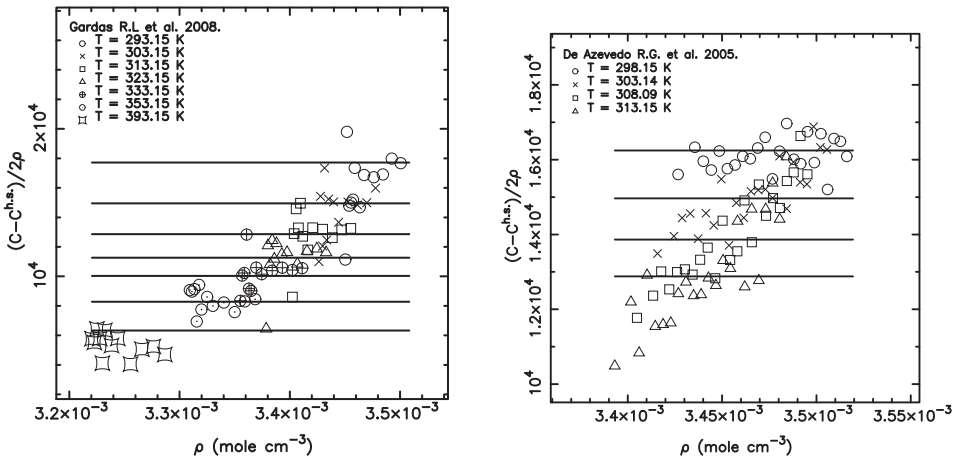

Figure 10–6. Left plot: $C - C^{h.s.}$ as function of density for [bmpy][Tf_2N] using all isotherms of Gardas et al..[19] Right plot: [bmim][Tf_2N] using four isotherms of Gomez de Azevedo et al.[12] The form of the DCFI model suggests that the quantity depicted on the ordinate is constant. This is in reasonable agreement with the experimental observations shown here.

whereas the highest temperature data is described less quantitatively. Thus far the discussion has concerned ionic liquids. For the liquified gases in Table 10–2, the left and right plots of Figure 10–8 show that the density dependence in these systems is in good agreement with the model. This is characteristic of all the systems compiled. Small variations are observed, and with much less fluctuations than the ionic liquid sets when taking the magnitude of the ordinate into account. For ionic liquids the variation of $(C - C^{h.s.})/2\rho$ is of the order $10^4\,\mathrm{cm}^3/\mathrm{mol}$, these sets vary within the order of $10^2\,\mathrm{cm}^3/\mathrm{mol}$.

The results above reveal, that it is possible to correlate compressed liquid densities over large range in pressure and density. The density data for xenon of Michels et al.[26] reach almost $3000\,\mathrm{bar}$, and the density reaches almost $0.025\,\mathrm{cm}^3/\mathrm{mol}$. This corresponds to roughly $500\,\mathrm{kg/L}$. Comparison of parameters obtained from regressions of individual data sets, as well as simultaneous reduction of all data sets pertaining to an individual ionic liquid, reveal that there is generally a good consistency between the two estimates for V^*. Results are less sensitive to T^*, and it can therefore assume quite different values, depending on the input data.

10.4. Predictive approach for ionic liquid characteristics

In order for the method to give estimate of P from ρ (or vice versa), one needs to:

1. Regress liquid density data to find T^* and V^*,

2. input a low-pressure density at each temperature as reference point.

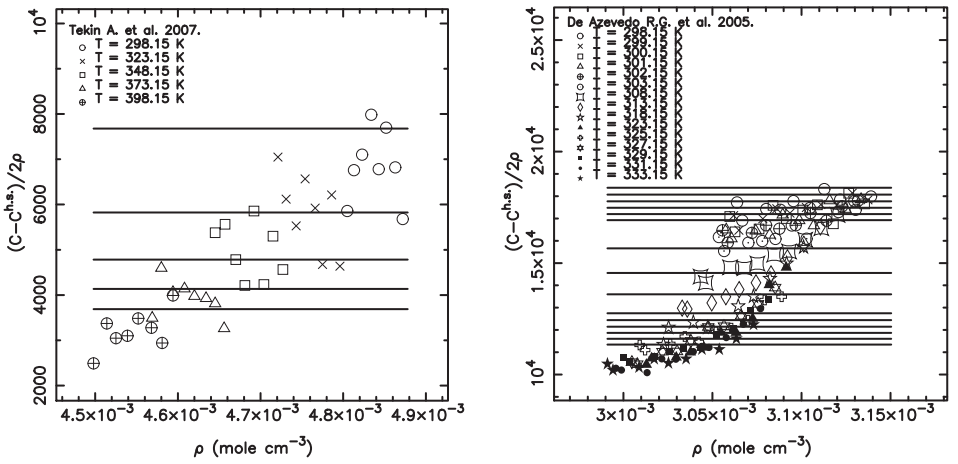

Figure 10–7. $C - C^{h.s.}$ as function of density for [bmim][PF_6](left) using data of Tekin et al.[4] and [hmim][Tf_2N] using the data of Gomez de Azevedo et al..[12] The model is in good agreement with the data.

These items prevent treatment of ionic liquids, for which no data exist. While obtaining the model characteristics, T^* and V^*, from regression of $P\rho T$ data is likely to yield parameters that are more tuned to a specific system, we seek a more predictive method. In this section, ways of predicting the model characteristics for the ionic liquid species are described. We start by exploring group contributions for the molecular parameters.

10.4.1. Group contributions

Ionic liquids are fairly rigid molecules. It therefore makes sense to assume that the characteristic volume, V^*, for an ionic liquid is proportional to the van der Waals volumes of its constituent structural groups, so that

$$V^* = k \left[\sum_{j \in a}^{\text{groups}} \nu_j^{(a)} \delta V_{w,j} + \sum_{j \in c}^{\text{groups}} \nu_j^{(c)} \delta V_{w,j} \right]. \tag{10–11}$$

Here k is a constant of proportionality, $\nu_j^{(a)}$ denotes the stoichiometry of group j on the anion of the ionic liquid, and $\delta V_{w,j}$ is its corresponding van der Waals volume contribution. Similarly, $\nu_j^{(c)}$ describes cationic group stoichiometry. The van der Waals volumes are taken from the compilation of Bondi[29] when available, while those remaining plus the proportionality constant k were regressed from values of V^* obtained from reduction of $P\rho T$ data, by solving

$$\min f = \sum_i (\delta V^*)_i^2, \tag{10–12}$$

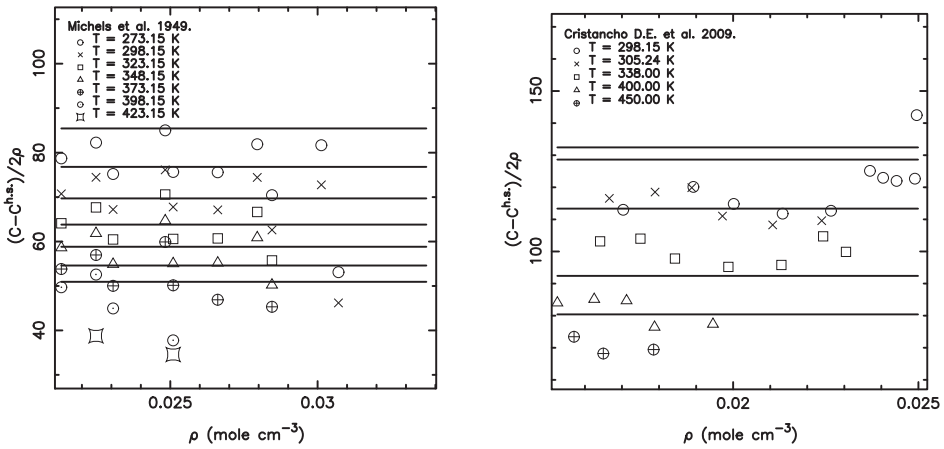

Figure 10–8. $C - C^{h.s.}$ as function of density for argon (left) and methane (right) using the data of Michels et al.[24] and Cristancho et al..[22] The magnitude of the variation in the ordinate quantity is smaller than for the ionic liquid species, and the model gives a good representation of the experimental data.

where δV^* is the difference in the regressed value of V^* of Table 10–3 and that found from the group contribution approach. This procedure is carried out to determine the missing contributions for five cationic groups (pyr, pip-N, im-2, im-3, P) and four anionic groups (BF_4, PF_6, SO_2, SO_3), in addition to k.

We find $k = 5.496$. Tables **??** and **??** show the stoichiometry of the ions and contributions from each group. The values taken from Bondi are marked by $*$. The average absolute error,

$$\mathrm{AAPE}(V^*) = \frac{100\%}{n} \sum_k^n \left| \frac{\delta V^*}{V^*} \right|_k , \tag{10–13}$$

is 1.8%. This is similar to uncertainties in experimental results, which are typically around 2%, and in agreement with the variation found in the values of V^* in Table 10–1. Table 10–5 show the regressed values of V^* and those from group contributions (columns five and six), as well as the average error between them (column seven). The biggest difference in the estimates is for [emim][EtSO4]. There are two data sets for this ionic liquid; one from Jacquemin et al.[9] and one from Hofman et al..[16] They produce widely different values of V^*, and appear to be incompatible with each other. The group contribution method is in significantly better agreement with the data of Hofman et al.[16] than Jacquemin et al..[9] Thus, the agreement with group contributions might be another way to provisionally screen for unreliable data. Removing the set of Jacquemin et al. reduces the average error in V^* to 1.4%.

It is unlikely that a method for predicting T^* from molecular structure can be developed, due to the relative insensitivity of the results to this parameter, indicated by the scatter in Table 10–1. However, an average value of $T^* = 755\,\mathrm{K}$ works remarkably well. This is illustrated in the eighth column of Table 10–5, which shows the statistic similar to that defined for V^* above, averaging 8.8%. This is in agreement with the relative standard deviation for most values of T^*. The right-most column gives the error in the pressure using the "predicted" values of T^* and V^*. By comparing to the entries in Table 10–1, we see that the model in "prediction-mode" is comparable to fitting parameters to liquid density data.

Table 10–4. Cationic and anionic contributions to V^*.

Ionic liquid	CH_3*	CH_2*	C_5H_4N*	C_5H_5N*	Pyr	pip−N	im-2	im-3	P	C*	AC*	CF_3*	C=N*	Cl*	SO_4*	N*	BF_4	PF_6	SO_3	SO_2
[bmim]	2	3	0	0	0	0	1	0	0	0	0	0	0	0	0	0	0	0	0	0
[emim]	2	1	0	0	0	0	1	0	0	0	0	0	0	0	0	0	0	0	0	0
[C_3mim]	2	2	0	0	0	0	1	0	0	0	0	0	0	0	0	0	0	0	0	0
[C_5mim]	2	4	0	0	0	0	1	0	0	0	0	0	0	0	0	0	0	0	0	0
[hmim]	2	5	0	0	0	0	1	0	0	0	0	0	0	0	0	0	0	0	0	0
[C_7mim]	2	6	0	0	0	0	1	0	0	0	0	0	0	0	0	0	0	0	0	0
[C_8mim][omim]	2	7	0	0	0	0	1	0	0	0	0	0	0	0	0	0	0	0	0	0
[$(C_6H_{13})_3P(C_{14}H_{29})$]	4	28	0	0	0	0	0	0	1	0	0	0	0	0	0	0	0	0	0	0
[bmmim]	3	3	0	0	0	0	0	1	0	0	0	0	0	0	0	0	0	0	0	0
[NBuPy]	1	3	0	1	0	0	0	0	0	0	0	0	0	0	0	0	0	0	0	0
[C_3mpy]	2	2	1	0	0	0	0	0	0	0	0	0	0	0	0	0	0	0	0	0
[C_4mpyr]	2	3	0	0	1	0	0	0	0	0	0	0	0	0	0	0	0	0	0	0
[C_3mpyr]	2	2	0	0	1	0	0	0	0	0	0	0	0	0	0	0	0	0	0	0
[C_3mpip]	2	7	0	0	0	1	0	0	0	0	0	0	0	0	0	0	0	0	0	0
[N_{1114}]	4	3	0	0	0	1	0	0	0	0	0	0	0	0	0	0	0	0	0	0
[BF_4]	0	0	0	0	0	0	0	0	0	0	0	0	0	0	0	0	1	0	0	0
[PF_6]	0	0	0	0	0	0	0	0	0	0	0	0	0	0	0	0	0	1	0	0
[Tf_2N]	0	0	0	0	0	0	0	0	0	0	0	2	0	0	0	1	0	0	0	2
[$C(CN)_3$]	0	0	0	0	0	0	0	0	0	1	0	0	3	0	0	0	0	0	0	0
[$EtSO_4$]	1	1	0	0	0	0	0	0	0	0	0	0	0	0	1	0	0	0	0	0
[Cl]	0	0	0	0	0	0	0	0	0	0	0	0	0	1	0	0	0	0	0	0
[Ac]	0	0	0	0	0	0	0	0	0	0	1	0	0	0	0	0	0	0	0	0
[CF_3SO_3]	0	0	0	0	0	0	0	0	0	0	0	1	0	0	0	0	0	0	1	0
[$OcSO_4$]	1	7	0	0	0	0	0	0	0	0	0	0	0	0	1	0	0	0	0	0
δV_w	13.67	10.23	42.98	45.5	37.29	0	30.7	27.24	46.81	3.33	28.87	21.33	14.7	11.6	35.1	4.33	31.93	46.64	30.42	26.9

Comparing with the group contribution method of Jacquemin et al.,[9,20,30] the number of parameters in the above described method is significantly less. That method treated both ions as single groups, and may require as much as up to seven parameters for each ion. Much less parameterized is the method of Gardas and Coutinho,[31] which also only required volumes of segments (or an experimental point). However, the segments were also large, and therefore the total number of parameters fitted to data was substantial. The method given here breaks down most ions into smaller groups, which are described with a single volume characteristic. Although some of the group volumes were fitted to data, most were taken directly as their van der Waals volumes.

Table 10–5. Group contribution predictions. $T^* = 755\,\mathrm{K}$, V^*_{est} from Equation (10–11) using group contributions from Tables **??** and **??**.

Substance (abbr.)	Ref.	n	ΔP (bar)	V^* ($\mathrm{cm}^3/\mathrm{mol}$)	V^*_{est}	$\delta V^*/V^*)$ (%)	$\delta T^*/T^*$ (%)	AAPE(P) (%)
[bmim][BF_4]	9	40	1–400	665.3	663	0.3	8.2	4.9
[emim][CF_3SO_3]	19	91	1–350	655.8	659.5	0.6	6.1	7.4
[bmim][BF_4]	8	189	1–2000	660.3	663	0.4	1.8	6.4
[bmim][Tf_2N]	9	42	1–400	1038.9	1041.5	0.3	36.7	3.5
[hmim][Tf_2N]	13	28	1–400	1159.5	1154	0.5	0.1	3.2
[hmim][Tf_2N]	14	149	1–650	1160	1154	0.5	15.8	3.2
[C_5mim][Tf_2N]	17	165	1–596	1097.6	1097.7	0.0	5.1	0.6
[$(C_6H_{13})_3P(C_{14}H_{29})$][Ac]	18	144	2–650	2284.6	2290.8	0.3	4.7	1.9
[hmim][PF_6]	5	77	1–100	856.4	856.4	0.0	8.8	1.9
[bmim][CF_3SO_3]	5	77	1–100	775.7	772	0.5	6.9	2.6
[emm][Tf_2N]	9	41	1–400	938.6	929	1.0	0.4	6.2
[bmim][Tf_2N]	12	168	1–591	1036.5	1041.5	0.5	13.7	1.7
[C_4mpyr][Tf_2N]	19	91	1–350	1070.8	1077.8	0.7	3.4	2.6
[omim][PF_6]	5	77	1–100	980.3	968.8	1.2	6.8	2.6
[bmim][PF_6]	8	189	1–2000	732.7	743.9	1.5	4.8	5.5
[bmim][BF_4]	6	20	1–200	684.8	663	3.2	2.9	4.5
[C_3mpyr][Tf_2N]	19	91	1–350	1010.9	1021.6	1.1	0.7	6.1
[N_{1114}][Tf_2N]	20	36	10–400	1032.6	1023.1	0.9	1.2	2.9
[bmim][PF_6]	9	41	1–400	751.3	743.9	1.0	10.4	5.4
[bmim][BF_4]	5	77	1–100	656.9	663	0.9	4.8	3.0
[C_7mim][Tf_2N]	15	96	1–300	1226.2	1210.2	1.3	4.2	6.5

Continues on next page

Continued from last page

Substance (abbr.)	Ref.	n	ΔP (bar)	V^* (cm^3/mol)	V^*_{est}	AAPE(V^*) (%)	AAPE(T^*) (%)	AAPE(P) (%)
[hmim][Tf_2N]	12	163	1–596	1165.2	1154	1.0	4.1	0.8
[bmim][PF_6]	6	20	1–200	748.2	743.9	0.6	11.1	4.0
[$(C_6H_{13})_3P(C_{14}H_{29})$][$Tf_2N$]	18	126	2–650	2713.4	2686.1	1.0	4.7	2.1
[bmim][BF_4]	7	67	1–599	656.4	663	1.0	70.7	1.7
[$(C_6H_{13})_3P(C_{14}H_{29})$][Cl]	18	134	2–650	2174.9	2196	1.0	5.1	1.7
[C_4mpyrro][Tf_2N]	20	36	10–400	1095.5	1077.8	1.6	4.4	2.4
[bmim][PF_6]	11	14	1–2021	734.7	743.9	1.3	32.8	3.4
[omim][BF_4]	5	77	1–100	908.7	888	2.3	3.0	3.1
[C_3mim][Tf_2N]	17	165	1–596	970.8	985.3	1.5	10.9	1.5
[omim][Tf_2N]	15	96	1–300	1292	1266.4	2.0	2.6	5.1
[bmmim][PF_6]	5	63	1–100	785.7	800.1	1.8	4.7	2.7
[bmim][BF_4]	4	45	2–399	652.8	663	1.6	9.7	2.5
[omim][PF_6]	11	14	1–2042	1013.4	968.8	4.4	4.5	2.0
[omim][BF_4]	11	15	1–2069	916.2	888	3.1	1.5	4.8
[emim][Tf_2N]	15	96	1–300	906.1	929	2.5	4.8	4.7
[bmim][OcSO4]	8	174	1–2000	1177.9	1149.2	2.4	42.5	6.1
[bmim][PF_6]	4	45	7–401	725.1	743.9	2.6	0.6	3.4
[bmim][PF_6]	10	54	1–2493	729.9	743.9	1.9	0.8	4.5
[bmim][$C(CN)_3$]	15	96	1–300	770	748.2	2.8	4.2	2.7
[C_3mpip][Tf_2N]	19	91	1–350	1068	1097.8	2.8	0.3	2.3
[emim][$EtSO_4$]	16	63	1–350	676.6	699.4	3.4	3.6	0.8
[NBuPy][BF_4]	11	14	1–2042	646.8	669.4	3.5	5.8	2.6
[C_3mpy][Tf_2N]	19	91	1–350	1017.1	1052.9	3.5	0.8	2.0
[emim][BF_4]	15	96	1–300	526.2	550.6	4.6	2.7	4.2
[emim][$EtSO_4$]	9	42	1–400	620.5	699.4	12.7	17.9	2.7

10.4.2. Ambient-pressure density correlation

The fluctuation solution theory method is based on integration of thermodynamic derivatives from a known reference state, the density of the solvent at specified temperature and pressure. So far a low-pressure experimental point at same temperature has been used for the results above. Inspired by existing

Table 10–6. Density correlation at 1 bar.

Substance, i (abbr.)	n	a_i ($\mathrm{cm^3/mol}$)	b_i ($\mathrm{cm^3/mol/K}$)	$\bar{a}V_i^*$ ($\mathrm{cm^3/mol}$)	$\bar{b}V_i^*/T_i^*$ ($\mathrm{cm^3/mol/K}$)
[C_2mim][BF_4]	8	124.4	0.093	124.12	0.10
[C_4mim][$C(CN)_3$]	8	176.3	0.143	168.67	0.14
[C_7mim][NTf_2]	8	269.2	0.246	272.80	0.23
[C_8mim][NTf_2]	8	281.7	0.263	285.48	0.24
[C_3mim][NTf_2]	15	217.8	0.190	222.10	0.19
[C_5mim][NTf_2]	15	245.4	0.212	247.45	0.21
[bmim][CF_3SO_3]	11	178.4	0.145	174.02	0.15
[bmmim][PF_6]	9	179.5	0.138	180.37	0.15
[hmim][PF_6]	11	194.0	0.158	193.04	0.16
[bmim][$OcSO_4$]	9	258.9	0.221	259.06	0.22
[C_2mim][CF_3SO_3]	7	150.7	0.129	148.67	0.13
[C_3mpyr][NTf_2]	7	224.7	0.202	230.29	0.19
[C_4mpyr][NTf_2]	7	237.0	0.214	242.96	0.20
[hmim][NTf_2]	29	259.0	0.225	260.13	0.22
[bmim][NTf_2]	13	231.1	0.203	234.78	0.20
[C_1C_2Im][Tf_2N]	13	203.1	0.183	209.43	0.18
[C_8mim][PF_6]	11	221.3	0.180	218.39	0.18
[C_8mim][BF_4]	11	206.3	0.166	200.17	0.17
[C_1C_4Im][PF_6]	23	169.2	0.130	167.69	0.14
[C_1C_4Im][BF_4]	33	151.5	0.121	149.47	0.13
[C_3mpy][NTf_2]*	7	224.2	0.211	237.34	0.20
[C_3mpip][NTf_2]*	7	235.3	0.214	247.46	0.21
[C_1C_2Im][$EtSO_4$]*	7	159.0	0.108	157.66	0.13

* Not included in estimation of a and b.

works in the engineering literature, we here establish a method for predicting the density of a pure ionic liquid at ambient pressure. Equation (8–1) at constant pressure (P^0) is $\mathrm{d}v = v\beta \mathrm{d}T$. Integration (assuming β is constant) yields

$$\ln \frac{v}{v^0} = \beta(T - T^0) + c \quad \Rightarrow \quad v = v^0 \exp\left[c + \beta T^0 + \beta T\right], \tag{10–14}$$

where c is a constant of integration. If we expand the exponential in a Taylor series and retain the first term, the result is

$$v(T, P^0) = a + bT. \tag{10–15}$$

Here, $a = v^0(1 + c + \beta T^0)$ and $b = v^0\beta$. Thus, at low pressures the molar volume varies linearly with temperature. We assume a corresponding states form applied to all ionic liquids, i.e.,

$$\tilde{v}_i(T, P^0) = a_i + b_i\tilde{T}_i; \quad \tilde{v}_i = \frac{v_i}{V_i^*}; \quad \tilde{T}_i = \frac{T}{T_i^*} = \frac{T}{755\,\mathrm{K}}. \tag{10–16}$$

10. Application to pure liquids

We use density data at $1\,\mathrm{bar}$ in the above expression, with values of V_i^* estimated from simultaneous reduction of all available data sets for each ionic liquid species. Table 10–6 shows the results obtained. The average value of a_i/V_i^* for the ionic liquids studied is $\bar{a} = 0.225 \pm 0.0045$ and for $b_i T_i^*/V_i^*$ the value is $\bar{b} = 0.140 \pm 0.0072$. These standard deviations correspond to 2% and 5%, respectively. This means, that it is possible to arrive at a universal expression for the density at $1\,\mathrm{bar}$ for all ionic liquids,

$$\tilde{v}_i(T, P^0) = 0.225 + 0.14\tilde{T}_i, \quad P^0 = 1\,\mathrm{bar}. \tag{10–17}$$

Specific data sets have been excluded from this approach. For instance, the data for $[N_{1114}][Tf_2N]$ of Jacquemin et al.[20] and [NBuPy][BF_4] of Gu and Brennecke[11] did not have densities at $1\,\mathrm{bar}$. In addition, the [emim][$EtSO_4$] data, also described above, showed some irregular behavior, and the data of Gardas et al.[19] for [C_3mpy][Tf_2N] and [C_3mpip][Tf_2N] were unable to be reduced within reasonable accuracy.

10.5. Summary

This chapter has seen the application of the model, previously developed by Mathias,[28] to compressed liquid densities of ionic liquids, and liquefied gases at large ranges of pressure and density. The model uses two pure component parameters, which are obtained from regression of compressed densities. In addition, the model requires a density at ambient pressure as a reference point. Reducing data sets individually and simultaneously (multiple data sets for one compound) show that the model is generally capable of describing all of these using the same set of parameters. Analysis of the model parameters revealed, that for a given species, it is possible to estimate its characteristic volume parameter from the volumes of the constituent molecular groups. Furthermore, it was shown, that it is possible to use a value of the other parameter, a characteristic temperature, common to all ionic liquids. These parameters were subsequently applied in a correlation, to estimate the reference density as function of temperature at ambient pressures, with good results.

Although it is not the primary intention to develop liquid density methods, it seems like the current method is better than previously studied methods.[32]

Now that the parameter estimation procedure has been outlined, the thesis addresses the solubilities of gases in ionic liquids. The thermodynamic relations and model equations were given in Chapter 9, and are put to practice in the next chapter.

References

1. P. M. Mathias and J. P. O'Connell. *Chem. Eng. Sci.*, 36:1123–1132, 1981.
2. E. A. Campanella, P. M. Mathias, and J. P. O'Connell. *AIChE J.*, 33:2057–2066, 1987.
3. R. Fletcher. *Practical methods of optimization*. Wiley, 1987.
4. A. Tekin, J. Safarov, A. Shahverdiyev, and E. Hassel. *J. Mol. Liq.*, 136:177–182, 2007.
5. R. L. Gardas, M. G. Freire, P. J. Carvalho, I. M. Marrucho, I. M. A. Fonseca, A. G. M. Ferreira, and J. A. P. Coutinho. *J. Chem. Eng. Data*, 52:80–88, 2007.
6. D. Tomida, A. Kamugai, K. Qiao, and C. Yokoyama. *Int. J. Thermophys.*, 27:39, 2006.
7. R. Gomes de Azevedo, J. M. S. S. Esperança, V. Najdanovic-Visak, Z. P. Visak, H. J. R. Guedes, and L. P. N. Rebelo. *J. Chem. Eng. Data*, 50:997–1008, 2005.
8. H. Machida, Y. Sato, and R. L. Smith Jr. *Fluid Phase Equil.*, 264:147–155, 2008.
9. J. Jacquemin, P. Husson, V. Mayer, and I. Cibulka. *J. Chem. Eng. Data*, 52:2204–2211, 2007.
10. K. R. Harris, L. A. Woolf, and M. Kanakubo. *J. Chem. Eng. Data*, 50:1777–1782, 2005.
11. Z. Gu and J. F. Brennecke. *J. Chem. Eng. Data*, 47: 339–345, 2002.
12. R. Gomez de Azevedo, J. M. S. S. Esperança, J. Szydlowski, Z. P. Visak, P. F. Pires, H. J. R. Guedes, and L. P. N. Rebelo. *J. Chem. Thermodyn.*, 37:888–899, 2005.
13. M. E. Kandil, K. N. Marsh, and A. R. H. Goodwin. *J. Chem. Eng. Data*, 52:2382–2387, 2007.
14. J. M. S. S. Esperança, H. J. R. Guedes, J. N. C. Lopes, and L. P. N. Rebelo. *J. Chem. Eng. Data*, 53:867–870, 2008.
15. R. L. Gardas, M. G. Freire, P. J. Carvalho, I. M. Marrucho, I. M. A. Fonseca, A. G. M. Ferreira, and J. A. P. Coutinho. *J. Chem. Eng. Data*, 52:1881–1888, 2007.
16. T. Hofman, A. Goldon, A. Nevines, and T. M. Letcher. *J. Chem. Thermodyn.*, 40:580–591, 2008.
17. J. M. S. S. Esperança, Z. P. Visak, N. V. Plechova, K. R. Seddon, H. J. R. Guedes, and L. P. N. Rebelo. *J. Chem. Eng. Data*, 51:2009–2015, 2006.
18. J. M. S. S. Esperança, H. J. R. Guedes, M. Blesic, and L. P. N. Rebelo. *J. Chem. Eng. Data*, 51:237–242, 2006.
19. R. L. Gardas, H. F. Costa, M. G. Freire, P. J. Carvalho, I. M. Marrucho, I. M. A. Fonseca, A. G. M. Ferreira, and J. A. P. Coutinho. *J. Chem. Eng. Data*, 53:805–811, 2008.
20. J. Jacquemin, P. Nancarrow, D. W. Rooney, M. F. Costa Gomes, P. Husson, V. Mayer, A. A. H. Pádua, and C. Hardacre. *J. Chem. Eng. Data*, 53: 2133–2143, 2008.
21. E. C. Ihmels and J. G. Gmehling. *Ind. Eng. Chem. Res.*, 40:4470–4477, 2001.
22. D. E. Cristancho, I. D. Mantilla, S. Ejaz, K. R. Hall, M. Atilhan, and G. A. Iglesia-Silva. *J. Chem. Eng. Data*, 55:826–829, 2009.
23. W. E. Deming and L. E. Shupe. *Phys. Rev.*, 40: 848–859, 1932.
24. A. Michels, H. Wijker, and H. Wijker. *Physica*, 7: 627–633, 1949.
25. W. B. Streett and L. A. K. Stavely. *J. Chem. Phys.*, 55:2495–2506, 1971.
26. A. Michels, T. Wassenaar, and P. Louwerse. *Physica*, 20:99–106, 1954.
27. Y. H. Huang. *Thermodynamic properties of compressed liquids and liquid mixtures from fluctuation solution theory*. PhD thesis, University of Florida, Gainesville, FL, USA, 1986.
28. P. M. Mathias. *Thermodynamic properties of high-pressure liquid mixtures containing supercritical components*. PhD thesis, University of Florida, Gainesville, FL, USA, 1978.
29. A. Bondi. *Physical properties of molecular crystals, liquids, and glases*. John Wiley & Sons, New York, 1968.
30. J. Jacquemin, R. Ge, P. Nancarrow, D. W. Rooney, M. F. Costa Gomes, and C. Hardacre. *J. Chem. Eng. Data*, 53:716–126, 2008.
31. R. L. Gardas and J. A. P. Coutinho. *Fluid Phase Equil.*, 263:26–32, 2007.
32. J. Abilskov, M. D. Ellegaard, and J. P. O'Connell. *Fluid Phase Equil.*, 295:215–229, 2010.

11. Solubilities of gases in ionic liquids

Correlations of gas–liquid equilibrium data using the method outlined in Chapter 9 is presented. This is followed by analysis of a powerful constraint that arises from applying Henry's law from a specified reference state.

11.1. Binary gas–liquid equilibria: Results

The method is applied to a series of gases for which solubility data in ionic liquids have been measured. The open literature is rich in references to experimental measurements of gas solubility data in nonionic solvents, but less plentiful for ionic liquids. Initially, this limits the variety of systems available since the pure component parameters of the model must be found from compressed liquid density data of each pure species. These were found for the ionic liquid solvents in the preceding chapter. Efforts were also made to estimate the corresponding values for the gaseous solutes, i.e., Table 10–2. However, as the density of these "traditional" chemicals varies much stronger than that of ionic liquids, it is better to base the parameter estimation on a large amount of data. While the data reduction in Chapter 10 were based on single data sources, it may be more appropriate to use the parameter values originally given by Mathias and O'Connell.[1] These were found using a much larger data base of compressed liquid densities, and summarized in Table 11–1. Also shown are the critical temperatures and volumes of the gases. Except for carbon dioxide, there is almost negligible difference between the model parameters

Table 11–1. Characteristic parameters for gases[1] and critical point.[2] The two are often closely similar, since the DCFI model is closely related to expressions for second virial coefficients based on critical parameters.

Gas	T^* (K)	V^* ($\mathrm{cm^3/mol}$)	T_c (K)	v_c ($\mathrm{cm^3/mol}$)
Hydrogen	24.6	52.5	33.1	64.5
Carbon monoxide	128.5	94.1	132.9	92.2
Oxygen	157.4	74.2	154.6	73.4
Methane	195.1	100.1	190.6	98.6
Carbon dioxide	269.5	93.2	304.1	94.1

and the corresponding critical parameters. This is expected, since the model is based on expressions derived from corresponding-states treatments of second virial coefficients (see Chapter 9), traditionally parameterized with critical parameters. However, as the species becomes more and more subcritical this difference becomes more and more significant. Since ionic liquids generally do not possess critical points, their parameter values cannot be derived from data directly and must be found from regression.

Table 11–2. Parameters for functional form of Henry's constant for gases in solvents, as regressed from gas-liquid data using the model formulation in this work.

Gas(1)	Solvent(2)	Ref.	a_0	a_1	a_2	k_{12}
Hydrogen	[bmim][PF_6]	[3]	38.0060	-954.5750	-4.6358	0
Hydrogen	[bmpy][Tf_2N]	[4]	14.1257	56.2880	-1.1646	0
Hydrogen	[bmim][CH_3SO_4]	[5]	11.3522	370.8397	-0.6644	0
Carbon monoxide	[bmim][PF_6]	[6]	7.5583	n/a	n/a	0
Carbon monoxide	[bmim][CH_3SO_4]		8.1606	n/a	n/a	0
Carbon monoxide	[bmim][CH_3SO_4]		7.5802	n/a	n/a	0.15*
Oxygen	[bmim][PF_6]	[7]	7.4683	n/a	n/a	0
Oxygen	[bmim][PF_6]	[7]	7.4853	n/a	n/a	0.15*
Methane	[hmim][Tf_2N]	[8]	4.6826	-180.7656	0.3077	0.29
Methane	[bmim][CH_3SO_4]	[9]	4.5404	61.4718	n/a	0.05
Carbon dioxide	[bmim][Tf_2N]	[10]	5.8855	-651.8464	n/a	0.02
Xenon	[hmim][Tf_2N]	[8]	5.5697	223.9173	n/a	0.225

* Using $T_2^* = 780\,\mathrm{K}$ and $V_2^* = 732.6\,\mathrm{cm}^3/\mathrm{mol}$.

In the following sections we will describe how the fluctuation solution theory method is able to describe experimental data and behavior of the gas-ionic liquid systems. Initially, we report the model-data agreement with ionic liquid parameter values found from reduction of the individual $P\rho T$ data sets. Then, we show how the model performs with parameters predicted using the methods described in the preceding chapter. However, first an outline of the procedure for computing gas solubilities is provided.

11.1.1. Computational procedure

The solution technique involves direct calculation and then iterations. Initially, the steps are to calculate:

1. The reduced temperature and volume matrices ($\tilde{T}_{ij}$ and V_{ij}^*) via the expressions in Equation (9–8),
2. Henry's law constant, H_i, with Equation (9–20),
3. elements in the matrix $\mathbf{B}$ in Equation (9–7b),
4. diagonal and off-diagonal elements of $\mathbf{B}^{h.s.}$ in Equation (9–7a), and hard-sphere diameters, σ_i.
5. Compute the reference point: Reduced reference densities, ζ_m^0, using Equation (9–30), and
6. reference state hard-sphere pressure, $P^{h.s.}(T, \boldsymbol{\rho}^0)$, and chemical potential, $\mu_1^{h.s.}(T, \boldsymbol{\rho}^0)$, using Equations (9–31) and (9–32).

Then one iteratively solves Equation (9–19) to get P and ρ, by steps of calculating:

7. Hard-sphere pressure, $P^{h.s.}(T, \boldsymbol{\rho})$, and chemical potential, $\mu_1^{h.s.}(T, \boldsymbol{\rho})$, using Equations (9–31) and (9–32), and
8. full activity coefficient, $\gamma_1(T, \boldsymbol{\rho})$, using Equation (9–10).
9. Check for convergence, and continue to next iteration if necessary.

The calculation procedure is similar to a usual bubble pressure calculation,[11] except that there is the additional iteration to find the liquid density ρ. This procedure gives the final pressure and density for a given set of parameters for the Henry's constant, **a**. The optimal set of **a** is found by laying an outer iteration loop onto the calculations above to solve Equation (9–23).

11.1.2. Hydrogen

The first solute for which results are presented is hydrogen. Hydrogen is by far the most supercritical of the solutes covered here, with $T_c = 33.1\,\mathrm{K}$. The solubility is usually smaller than less supercritical gases. Our first example is formed by the data of Kumełan et al.[3] in [bmim][PF_6]. We use the solute characteristics as described above, whereas those for the solvent are taken from the entry in Table 10–1 which results in the lowest error; those regressed from the set of Tekin et al..[12] The temperature dependence of the Henry's law constant was found by minimizing the sum of the squared pressure differences according to Equation (9–23) yielding three parameters in Equation (9–20). Their values are

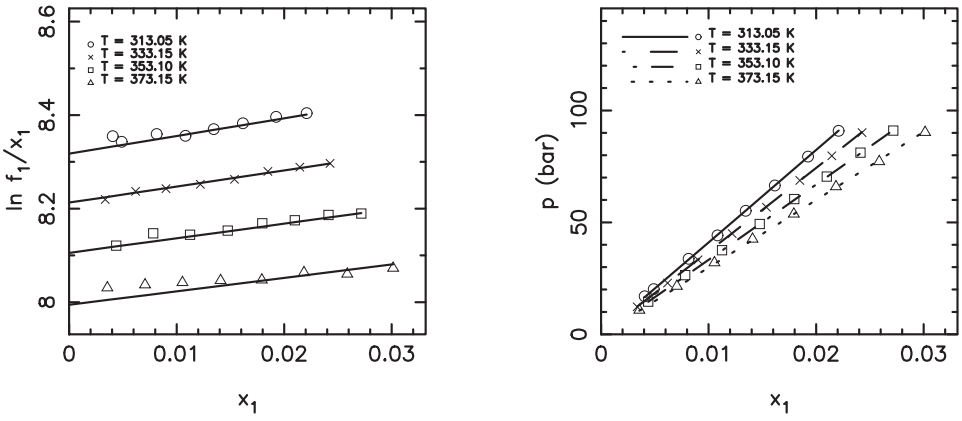

Figure 11–1. Hydrogen(1) in [bmim][PF_6](2) with data of Kumełan et al.[3] using $k_{12} = 0$. The model performance is excellent, and the data conforms to straight lines. This behavior is often seen for highly supercritical gases, such as hydrogen.

summarized in Table 11–2. Figure 11–1 compares the model output with experimental data using a binary interaction parameter, k_{12}, equal to zero. The right plot shows pressure versus mole fraction solubility, and the left plot shows the logarithm of the fugacity in the gas phase divided by the solubility

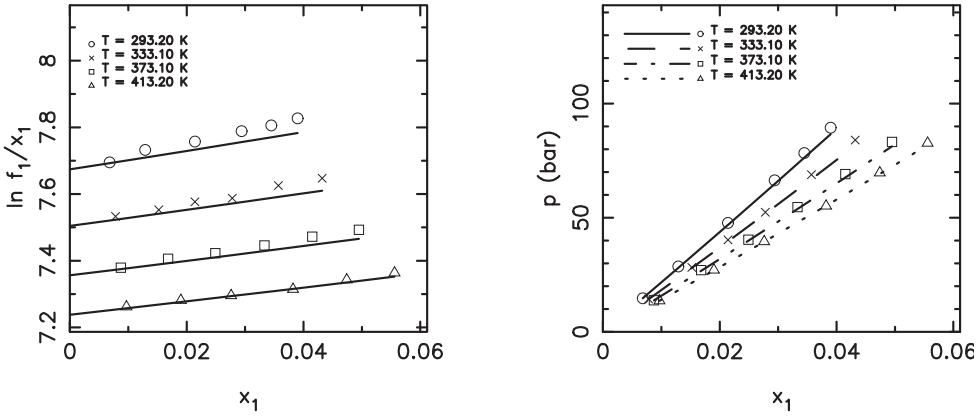

Figure 11–2. Hydrogen(1) in [bmpy][Tf_2N](2) with data of Kumełan et al.[4] using $k_{12} = 0$. As before, the model describes the data quantitatively.

of hydrogen in the liquid phase. The points are not experimental values directly, but are transformed with an assumed model for the gas-phase nonideality. The full drawn lines are model estimates of $\ln \gamma_1$ added to $\ln H_1$ for each isotherm. The lines are almost completely straight, which is commonly seen in this system.[1,13,14] Another example is seen in the system of hydrogen in [bmpy][Tf_2N] with data of Kumełan et al..[4] Like before, the agreement is quantitative with $k_{12} = 0$ and three parameters for the Henry's law expression. Generally, the gas-phase nonidealities of hydrogen are small in these systems,

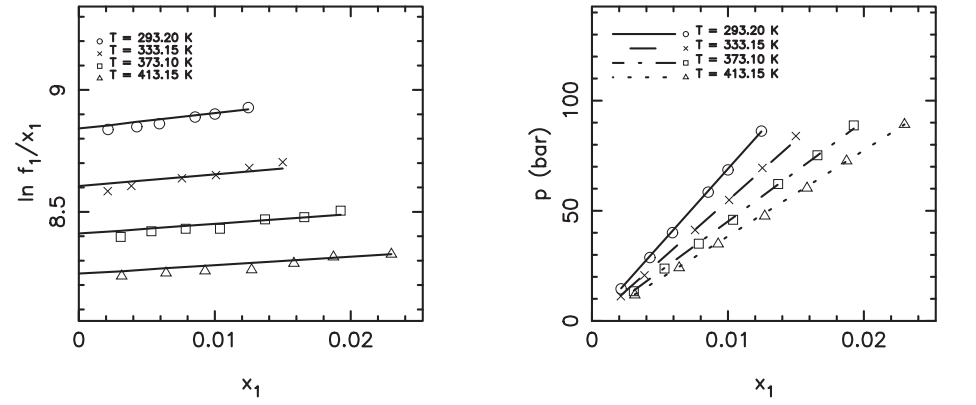

Figure 11–3. Hydrogen(1) in [bmim][CH_3SO_4](2) with data of Kumełan et al.[5] using $k_{12} = 0$. The solvent parameters for the model are estimated using the predictive approach described in Chapter 10. Nevertheless, the agreement with the experimental data is excellent.

so $\ln f_1/x_1$ usually form straight lines when plotted against x_1. Using regressed values of T_i^* and V_i^* for the solvent species generally gives a good match of the experimental solubility data when the parameters for Equation (9–20) are fitted to the data. Figure 11–3 shows the solubility calculations for the hydrogen

in [bmim][CH_3SO_4]. No $P\rho T$ data is available for the solvent, and we have therefore estimated V_2^* from group contributions, while $T_2^* = 755\,\mathrm{K}$. As before, the agreement with data is quantitative using k_{12} equal to zero.

11.1.3. Carbon monoxide

Carbon monoxide is also highly supercritical and only somewhat more soluble than hydrogen. However, unlike hydrogen, the Henry's constant of carbon monoxide is nearly independent of temperature. Figure 11–4 shows that the agreement with experimental data is quite good using a temperature independent Henry's law constant and $k_{12} = 0$. However, the slope of the lines of $\ln f_1/x_1$ seems incorrect. Regressing the value of k_{12} gives a better description, but also renders $k_{12} = 0.65$. This is outside the expected range of ± 0.3. Part of this may be caused by the models ability to use different combinations

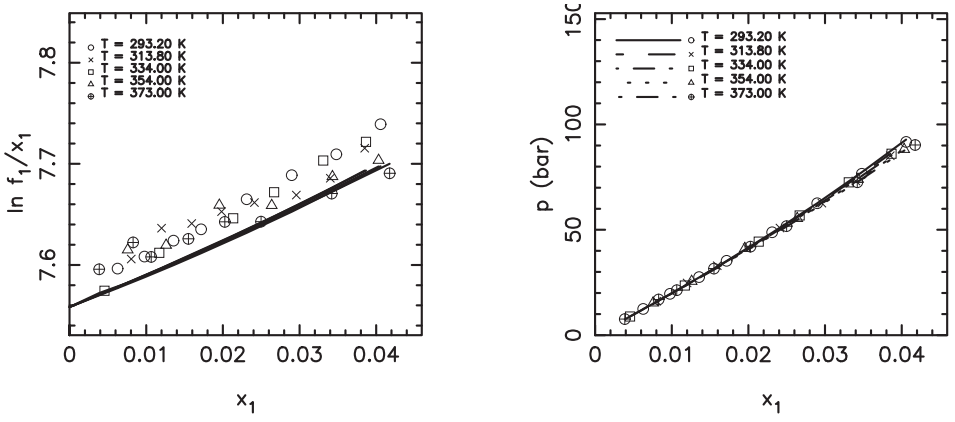

Figure 11–4. Carbon monoxide(1) in [bmim][PF_6](2) with data of Kumełan et al.[6] using $k_{12} = 0$, and a constant Henry's constant. The gas solubility data (right) is described quantitatively, but the slope of the lines on the left plot seems incorrect with the data.

of T_i^* and V_i^* to represent the volumetric behavior of pure ionic liquids, as discussed in the preceding chapter. Unlike pure compressed liquid densities, gas solubility data are very sensitive towards the value of T_i^*. Therefore, one can explore different combinations of the solvent parameters by simultaneous comparison of the descriptions of pure data as well as mixture data. We consider the case of Figure 11–4 with solvent parameters regressed from the data of Tekin et al.[12] as the benchmark. When varying T_2^* using $V_2^* = 732.6\,\mathrm{cm}^3/\mathrm{mol}$ of Machida et al.,[15] the objective function in Equation (9–23) decreases up to $T_2^* \approx 780\,\mathrm{K}$, before increasing again. The result is that different combinations of model parameters can be used, and it may take a considerable amount of compression data to determine the "best" set of values. Varying k_{12} with $T_2^* = 780\,\mathrm{K}$ and $V_2^* = 732.6\,\mathrm{cm}^3/\mathrm{mol}$ gives an optimum around $k_{12} = 0.15$. The resulting agreement with data is clearly better, as shown in Figure 11–5.

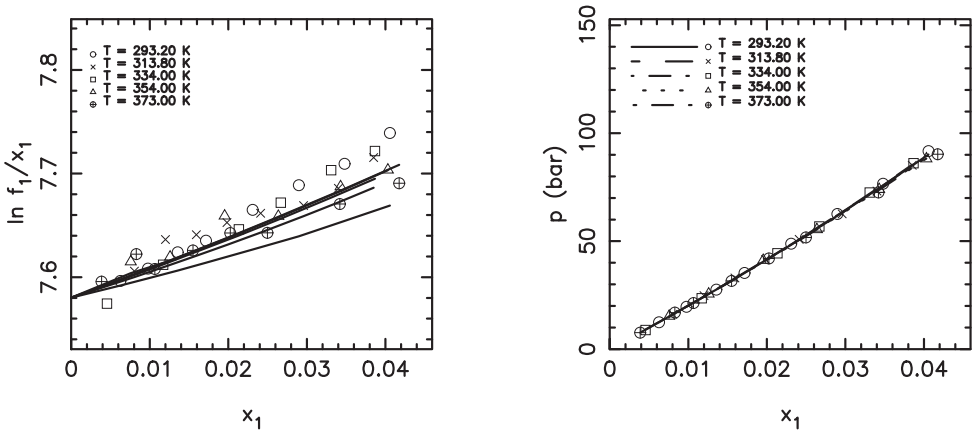

Figure 11–5. Carbon monoxide(1) in [bmim][PF_6](2) with data of Kumełan et al.[6] using $k_{12} = 0.15$ and $T_2^* = 780\,\mathrm{K}$ and $V_2^* = 732.6\,\mathrm{cm}^3/\mathrm{mol}$. Same system as before, but with other parameters. The agreement with data is similar to previously, wherefore it is difficult to evaluate the best set of parameters.

11.1.4. Oxygen

Oxygen dissolved in [bmim][PF_6] forms the next example. As was the case with carbon monoxide, the Henry's law constant is relative insensitive to temperature. The upper plots of Figure 11–6 shows that the agreement using $k_{12} = 0$ is quite good. However, as was also the case with carbon monoxide, the lines of $\ln f_1/x_1$ do not quite match the points calculated from the gas phase fugacity. Attempting to further optimize k_{12} results in a value outside the range of ± 0.3. If we again explore the sensitivity towards the solvent characteristics T_2^* and V_2^*, we again find that different combinations of values can be used. Using $T_2^* = 780\,\mathrm{K}$ and $V_2^* = 732.6\,\mathrm{cm}^3/\mathrm{mol}$, as for carbon monoxide, and $k_{12} = 0.15$ seems to be the optimum. The single parameter for the Henry's constant expression is almost the same using either approach, as seen in Table 11–2.

11.1.5. Methane

So far the gases treated have been highly supercritical, and largely insoluble in ionic liquids. Methane in [hmim][Tf_2N] is much more soluble than the systems above. We use the data of Kumełan et al.[8] and the solvent characteristics regressed from the data of Esperança et al..[16] Although the regression of the data from Gomez de Azevedo et al.[17] gives a slightly lower error in the liquid density data, we find a better description of the gas–solvent data using the data of Esperança et al.. Therefore we use the values of T_i^* and V_i^* for the solvent regressed from that data set. Figure 11–7 show the agreement with data using the full form of the Henry's law expression and $k_{12} = 0.29$. The overall description of the Px_1 data is good, but the slopes of $\ln f_1/x_1$ are not always in agreement, especially the isotherm at 293 K.

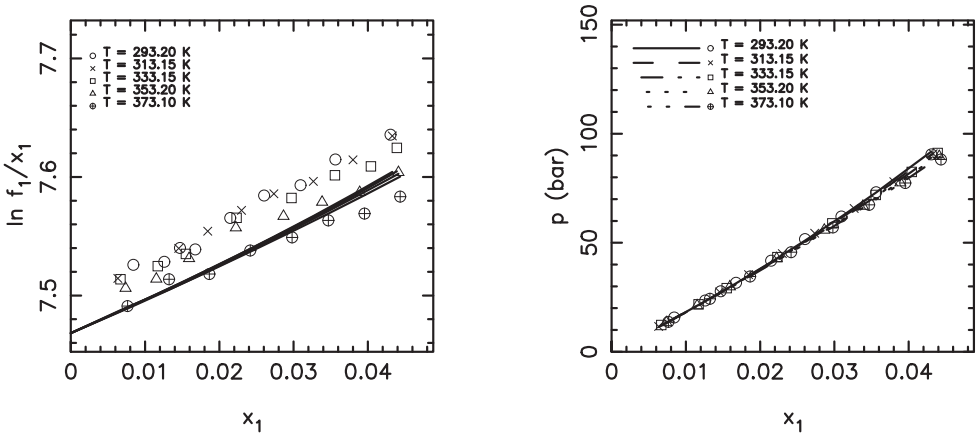

(a) Using $k_{12} = 0$ and $T_2^* = 722.5\,\mathrm{K}$ and $V_2^* = 725.1\,\mathrm{cm}^3/\mathrm{mol}$.

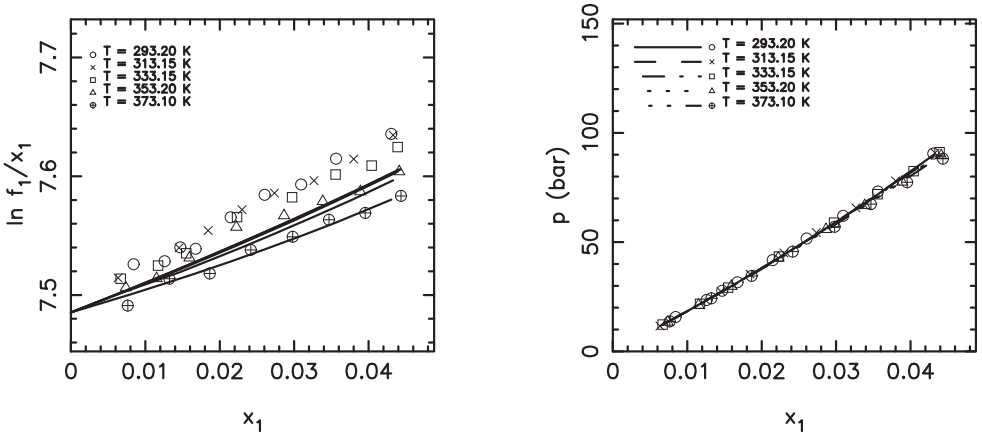

(b) Using $k_{12} = 0.15$ and $T_2^* = 780\,\mathrm{K}$ and $V_2^* = 732.6\,\mathrm{cm}^3/\mathrm{mol}$.

Figure 11–6. Oxygen(1) in [bmim][PF_6](2) with data of Kumełan et al.[7] using different combinations of parameters, suggesting that selecting the optimal set is not straightforward.

Similar agreement is seen when the solvent is [bmim][CH_3SO_4]. Using the data of Kumełan et al.[9] with two coefficients in the Henry's law expression and $k_{12} = 0.05$, Figure 11–8 shows the agreement with data. Since no compression data could be found for this solvent, its characteristics were found using the group contribution approach ($V_2^* = 755.6\,\mathrm{cm}^3/\mathrm{mol}$) and with $T_2^* = 755\,\mathrm{K}$. The Px_1 data shows negligible temperature dependence, with all data points clustering into one curve. However, the values of $\ln f_1/x_1$ calculated from the gas-phase fugacity shows considerable temperature dependence at the lower solubilities (and hence lower pressures). The behavior is somewhat similar the oxygen system described above. The previous systems had almost ideal gas phases and the lines of P versus x_1 were straight. However, methane is much more nonideal in the gas phase than e.g. oxygen (the second virial coefficient ranges from -32 at $413\,\mathrm{K}$ to $-52\,\mathrm{cm}^3/\mathrm{mol}$ at $333\,\mathrm{K}$, and $-70\,\mathrm{cm}^3/\mathrm{mol}$ at $293\,\mathrm{K}$), which

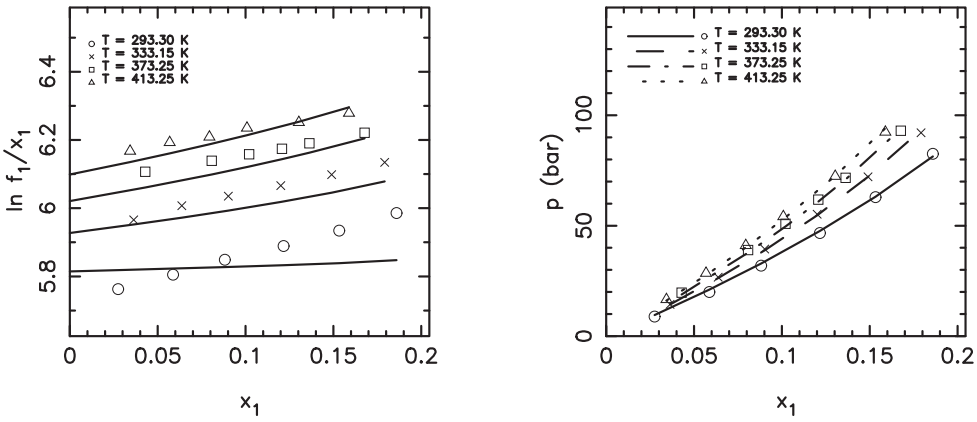

Figure 11–7. Methane(1) in [hmim][Tf_2N](2) with data of Kumełan et al.[8] using $k_{12} = 0.29$. The gas solubility data (right) is represented well, but the lines on the left plot do not match the low-temperature isotherms.

explains the curvature which is now observed in the Px_1 data.

11.1.6. Carbon dioxide

Carbon dioxide is an example of a gas, which is highly soluble in most ionic liquids. Like methane, both gas and liquid phases usually form solutions with substantial deviations from ideal behavior. The data of Lee and Outcalt[10] covers temperatures from 280 K to 340 K, and herein the virial coefficient ranges from approximately $-100\,\mathrm{cm^3/mol}$ at 340 K to $-134\,\mathrm{cm^3/mol}$ at 280 K. Figure 11–9 shows the phase diagram using $k_{12} = 0.02$ and two parameters for the Henry's law expression. The solvent characteristics do not vary much in Table 10–1, so we use the values obtained from regression of the data of Gomez de Azevedo et al..[17] The description of the Px_1 data is generally not quantitatively. While the low-pressure data is reasonably well fitted, the model generally overestimates the pressure at 320 and 340 K and underestimates at 300 K. The lines of $\ln f_1/x_1$ are in excellent agreement with the points calculated from the gas phase model at 320 K, but underestimates the fugacity at the higher temperature and overestimates at the lower temperature. Figure 11–10 shows the solubility results for carbon dioxide in [bmpy][Tf_2N]. The plots were obtained using $k_{12} = 0.225$. The solubility data (right plot) is described reasonably well, and the agreement between lines of $\ln f_1/x_1$ and the transformed experimental points is good at higher temperatures, but less good in the 333 K-case

The results shown for gases methane, carbon dioxide, and xenon reveal that the model is generally better at describing high-temperature data, indicated by the disagreement between the lines of $\ln f_1/x_1$ and the markings. In fact, data have been left out for these three solutes, since the method was completely unable to give accurate estimates of the liquid-phase fugacity. Methane has a critical temperature

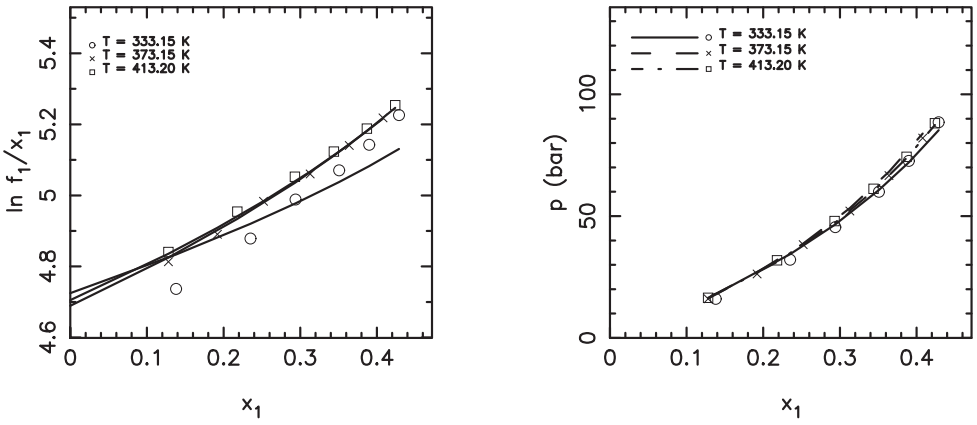

Figure 11–8. Methane(1) in [bmim][CH_4SO_4](2) with data of Kumełan et al.[9] using $k_{12} = 0.05$. Similar situation as the previous example: The low-temperature data is not represented as well as the high-temperature sets.

of 191 K, and the data originally reported by Kumełan et al.[9] at 293 K is too close to the critical point for inclusion in the optimization. Similarly was the case with the 280 K-isotherm of Lee and Outcalt for carbon dioxide with [bmim][Tf_2N]. Also the original 293 K- and 333 K-isotherms of Kumełan et al.[8] for xenon with [hmim][Tf_2N] were removed. Using separate models for the gas- and liquid-phase fugacities disables the ability to accurately describe fluid behavior at the critical point. Therefore, removal of the low-temperature data, as was done above, is necessary with this method.

11.2. Henry's law constant constraints

Using Henry's law as the standard state for the liquid-phase fugacity imposes restrictions on the variation of the Henry's constant in other solvent species. In fact, the solubility of a gas in one solvent can be predicted from a known value in another solvent; a *reference* solvent. This follows from writing the fugacity of the gas (1) at temperature T and densities $\boldsymbol{\rho}$ as $f_1^L(T,\boldsymbol{\rho}) = x_1\gamma_1(T,\boldsymbol{\rho};\boldsymbol{\rho}^r)H_{1,r}$. The notation implies that γ_1 is obtained from integrating Equation (9–5) isothermally from reference state $\boldsymbol{\rho}^r$ to final state $\boldsymbol{\rho}$. That means, that we can write the fugacity of 1 using two different standard states, r and p.

$$f_1^L(T,\boldsymbol{\rho}) = x_1\gamma_1(T,\boldsymbol{\rho};\boldsymbol{\rho}^r)H_{1,r}(T) = x_1\gamma_1(T,\boldsymbol{\rho};\boldsymbol{\rho}^p)H_{1,p}(T). \tag{11–1}$$

The states $(T,\boldsymbol{\rho})$ and $(T,\boldsymbol{\rho}^r)$ need not contain the same species. In fact, to find the properties of 1 at infinite dilution or at finite concentrations, 1 is the only species that must be common to the states. Thus,

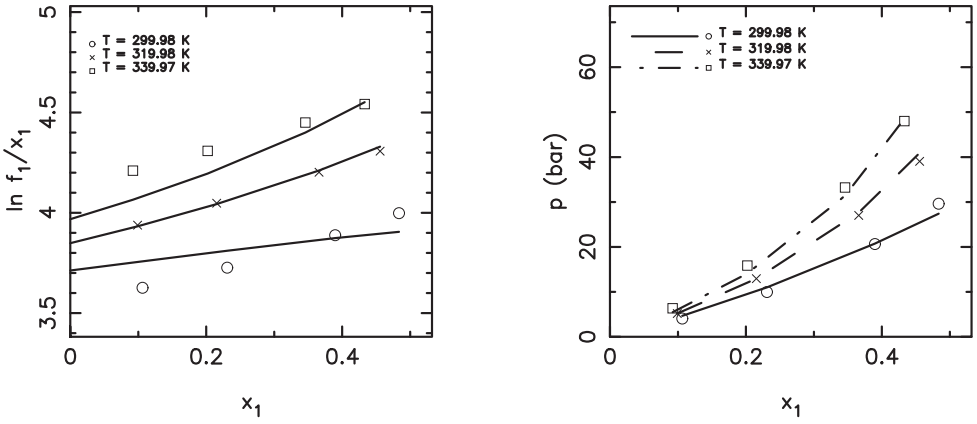

Figure 11–9. Carbon dioxide(1) in [bmim][Tf_2N](2) with data of Lee and Outcalt[10] using $k_{12} = 0.02$. As with methane, the gas solubility data is described sufficiently well, but the left plot show an incorrect variation of $\ln f_1/x_1$ at low temperature.

taking logarithms on both sides we obtain

$$\ln H_{1,r}(T) - \ln H_{1,p}(T) = \ln \gamma_1(T, \boldsymbol{\rho}^f; \boldsymbol{\rho}^r) - \ln \gamma_1(T, \boldsymbol{\rho}^f; \boldsymbol{\rho}^p) = \ln \gamma_1(T, \boldsymbol{\rho}^r; \boldsymbol{\rho}^p). \tag{11–2}$$

This equation connects the properties $H_{1,r}$, $H_{1,p}$, $\boldsymbol{\rho}^r$, and $\boldsymbol{\rho}^p$ with the parameters k_{1r} to k_{1p}. The result is that using solubility data in two solvents, automatically fixes the Henry's constant in one of the solvents, provided that the binary interaction parameters are independent of solvent, as we have seen for a number of cases above. Alternatively, k_{1p} can be estimated using known values of the other properties. The formulation allows for any one of the properties to be estimated, though it is likely that the Henry's constant or binary interaction parameter will be properties of greater interest to find.

Consider hydrogen(1) with [hmim][Tf_2N](p) and [bmim][PF_6](r). Then, since $k_{1r} = 0$, the value of k_{1p} should satisfy

$$\ln H_{1,p}(T) = \ln H_{1,r}(T) + \ln \gamma_1(T, \boldsymbol{\rho}^p; \boldsymbol{\rho}^r). \tag{11–3}$$

Using the fitted results for hydrogen–[bmim][PF_6] system, we find

$$\ln H_{1,p}(T) = 38.0060 - \frac{954.5750}{T} - 4.6358 \ln T + \ln \gamma_1(T, \boldsymbol{\rho}^p; \boldsymbol{\rho}^r). \tag{11–4}$$

The value of k_{1p} varies slightly with temperature from this equation, but an average value of 0.3 is sufficient. The resulting solubilities are shown in Figure 11–11. The gas solubilities are described well, and the lines of $\ln f_1/x_1$ are in good agreement with the values from the gas phase. When regressing parameters for the Henry's constant expression for each individual hydrogen system the results are

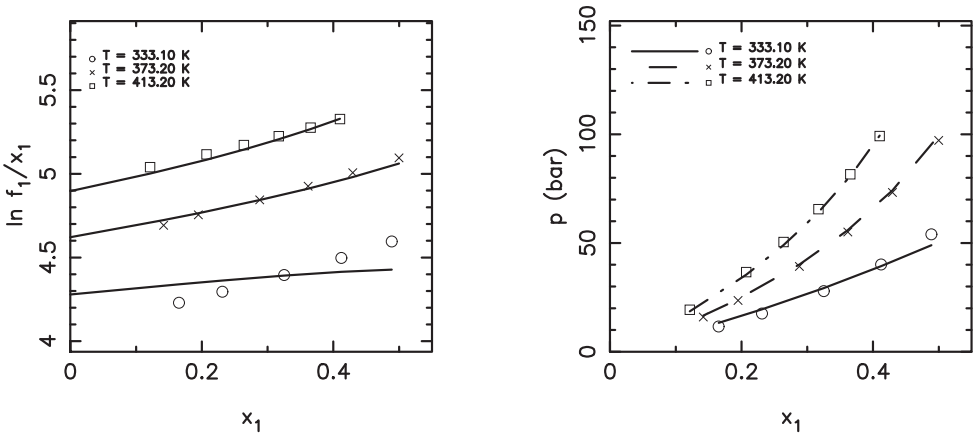

Figure 11–10. Carbon dioxide(1) in [bmpy][Tf_2N](2) with data of Kumełan et al.[4] using $k_{12} = 0.225$. The low-temperature data on the left plot is described less accurate than the high-temperature data, even though the gas solubility data is good agreement with the model estimates.

quantitative with a binary interaction parameter of zero. Therefore, the fact that $k_{12} = 0.3$ for the system above suggests that this approach might not be generally applicable for gas-ionic liquid systems. This is likely due to the Henry's law constant being fitted to the data, by minimization of Equation (9–23). That means that the optimization will prioritize high-pressure data over lower pressures, since the differences in pressure are squared. Fitting the Henry's constant to essentially high-pressure data can give serious errors in the extension to lower pressures. We recall, that the Henry's constant for 1 in 2 is defined as

$$H_{1,2}(T) = \frac{f_1}{x_1}(T, P^0, x_2 = 1), \quad P^0 = P_2^{\text{sat}}(T). \tag{11–5}$$

Since the vapor pressures of the solvent in this case is negligible, the Henry's constant should ideally be obtained from low-pressure data. Low-pressure data of hydrogen systems, around the saturation pressure of ionic liquids, is not likely to be measurable, since the quantities of hydrogen must be extremely small. However, data at slightly higher pressures might suffice.

11.3. Summary

The preceding results show that the method is most successful in describing systems with sparingly soluble gases, such as hydrogen, carbon monoxide, and oxygen in ionic solvents. In these systems, quantitative agreement with experimental data was obtained using a binary interaction – k_{12} – near zero. Results were less quantitative, though still quite good, for the more soluble gases methane, carbon dioxide, and xenon. In these systems it is difficult to find optimal values of the Henry's constant that describe the gas solubility behavior, especially at temperatures closer to the critical point. This is an inherent lim-

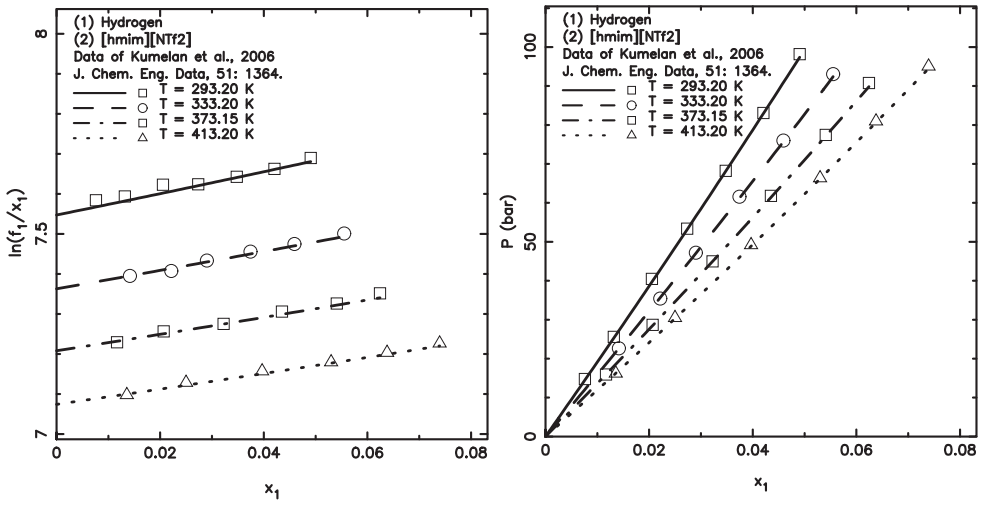

Figure 11–11. Reference solvent approach: Phase equilibria for hydrogen(1) in [hmim][Tf_2N] computed from the Henry's constant of hydrogen in [bmim][PF_6]. This method enables the prediction if phase equilibria from knowledge of solubility of the gas in another solvent.

itation in the $\gamma - \phi$ approach, when applying different thermodynamic models for gas and liquid phases. The model parameters are regressed to compressed liquid density data, and then used for gas-solvent equilibria. When no compression data for the solvent was available, group contributions for V_2^* and a constant T_2^* was able to yield satisfactory results.

The problem of selecting appropriate values of T_i^* and V_i^* is illustrated by the preceding examples. The uncertainty in T_i^* (but to a lesser extent V_i^*) when obtained *only* from regression compression data, suggests that the level of variance in especially T_i^* is substantial. This parameter is determined by the reduced temperature correlations in Equations (9–7a) and (9–7b), the coefficients of which were fitted to densities of pure compressed liquids.[1,18] Phase equilibrium data is generally more sensitive towards temperature than compressed liquid density data. Therefore, it is likely to be worthwhile to examine other ways of estimating the reduced temperature correlations. We address a possible way of treating this in the following chapter.

Finally, one may conceive of using the Henry's law constraint for representation of multiple data sets, as a means of provisional validation of gas solubility data, at least for systems the model is capable of representing one-by-one.

References

1. P. M. Mathias and J. P. O'Connell. *Chem. Eng. Sci.*, 36:1123–1132, 1981.

2. NIST National Institute for Standards & Technology. Nist chemistry webbook. URL `webbook.nist.gov/chemistry/`.

3. J. Kumełan, Á. Pérez-Salado Kamps, D. Tuma, and G. Maurer. *J. Chem. Eng. Data*, 51:11–14, 2006.

4. J. Kumełan, D. Tuma, Á. Pérez-Salado Kamps, and G. Maurer. *J. Chem. Eng. Data*, 55:165–172, 2010.

5. J. Kumełan, Á. Pérez-Salado Kamps, D. Tuma, and G. Maurer. *Fluid Phase Equil.*, 260:3–8, 2007.

6. J. Kumełan, Á. Pérez-Salado Kamps, D. Tuma, and G. Maurer. *Fluid Phase Equil.*, 228-229:207–211, 2005.

7. J. Kumełan, Á. Pérez-Salado Kamps, I. Urukova, D. Tuma, and G. Maurer. *J. Chem. Thermodyn.*, 37:595–602, 2005.

8. J. Kumełan, Á. Pérez-Salado Kamps, D. Tuma, and G. Maurer. *Ind. Eng. Chem. Res.*, 46:8236–8240, 2007.

9. J. Kumełan, Á. Pérez-Salado Kamps, D. Tuma, and G. Maurer. *J. Chem. Eng. Data*, 52:2319–2324, 2007.

10. B. Y. Lee and S. L. Outcalt. *J. Chem. Eng. Data*, 51:892–897, 2006.

11. J. M. Smith, H. C. Van Ness, and M. M. Abbott. *Introduction to chemical engineering thermodynamics*. McGraw-Hill, seventh edition, 2005.

12. A. Tekin, J. Safarov, A. Shahverdiyev, and E. Hassel. *J. Mol. Liq.*, 136:177–182, 2007.

13. P. M. Mathias and J. P. O'Connell. *Equations of State in Engineering and Research*, chapter 5, pages 97–108. Am. Chem. Soc., 1979.

14. E. A. Campanella, P. M. Mathias, and J. P. O'Connell. *AIChE J.*, 33:2057–2066, 1987.

15. H. Machida, Y. Sato, and R. L. Smith Jr. *Fluid Phase Equil.*, 264:147–155, 2008.

16. J. M. S. S. Esperança, H. J. R. Guedes, J. N. C. Lopes, and L. P. N. Rebelo. *J. Chem. Eng. Data*, 53:867–870, 2008.

17. R. Gomez de Azevedo, J. M. S. S. Esperança, J. Szydlowski, Z. P. Visak, P. F. Pires, H. J. R. Guedes, and L. P. N. Rebelo. *J. Chem. Thermodyn.*, 37:888–899, 2005.

18. P. M. Mathias. *Thermodynamic properties of high-pressure liquid mixtures containing supercritical components*. PhD thesis, University of Florida, Gainesville, FL, USA, 1978.

12. Optimization of model from data

In this chapter, we re-examine the temperature dependence of the model, since a limiting feature of the previous formulation was unable to accurately address low- and high-temperature data. The chapter starts by examining the temperature dependence on the compressed densities of pure fluids, and then moves on to addressing phase equilibria of gas-ionic liquid mixtures.

12.1. Pure liquids

It is standard procedure to parameterize equations of state, and similar methods, by fitting functional expressions to compressed liquid densities to minimize a function such as

$$\min s = \frac{1}{2}\sum_k (\delta P)_k^2. \tag{12–1}$$

We have reapplied the model for a selected set of substances, shown in Table 12–1, in order to examine the temperature dependence of liquid properties of these substances. In the optimization, data was included if $\rho/\rho_c > 1.5$ to ensure that only the liquid state is examined. For the ionic liquids, all data were included. The entries are similar to those from Tables 10–1 and 10–2. Characteristic of the ionic liquid species' high values of T^*, the reduced temperature range is small, spanning from about 0.4 to 0.5. For the nonionic species the range is significantly higher, spanning from about 0.5 to above 9.0. The values of T_i^* and V_i^* are slightly different from those originally given by Mathias and O'Connell,[1] since the data sources are not the same. The equation of state, based on the DCFI-model, assumes a hard-sphere reference fluid with deviations being linear in density,

$$\begin{aligned} P(T,\rho) &= P^0 + P^{h.s.}(T,\rho) - P^{h.s.}(T,\rho^0) + \mathsf{R}T(\rho^2 - (\rho^0)^2)\Delta B, \\ \Delta B &= B(T) - B^{h.s.} = B(T) - \frac{2\pi}{3}\sigma^3(T). \end{aligned} \tag{12–2}$$

The expressions for $B(T)$ and σ are suggested by empirical observations and their parameters fitted to compression data for argon, krypton, and xenon. In order to assess the reduced-temperature correlations, the values of B and $B^{h.s.}$ are compared with the values obtained from *optimal* set of parameters for the

Table 12–1. Reduction of liquid densities with correlations of Mathias and O'Connell.[1]

Substance	Ref.	ΔT (K)	ΔP (bar)	T^* (K)	S.D. (K)	V^* ($\mathrm{cm^3/mol}$)	S.D.	$\Delta\tilde{T}$	AAPE(P) (%)	AAPE(ρ) (%)
[bmim][PF_6]	2	298–398	7–401	722.50	7.90	725.10	0.30	0.41–0.55	2.380	0.020
[bmim][NTf_2]	3	298–328	1–591	787.90	2.70	1036.50	0.17	0.38–0.42	1.680	0.020
[hmim][NTf_2]	3	298–333	1–596	787.91	1.90	1165.23	0.20	0.38–0.42	1.150	0.010
[emim][$EtSO_4$]	4	283–333	1–350	706.90	3.20	676.60	0.10	0.40–0.47	0.890	0.004
Hydrogen sulfide	5	273–413	30–400	350.66	0.55	95.22	0.04	0.78–1.18	0.962	0.085
Carbon dioxide	5	283–358	100–300	280.60	4.22	91.06	0.60	1.01–1.28	1.954	0.478
Methane	6	298–450	500–1880	193.97	0.34	99.94	0.02	1.54–2.32	0.073	0.025
Xenon	7	303–398	60–2700	283.84	0.44	117.60	0.03	1.07–1.40	1.572	0.482
Hydrogen	8	198–323	592–1184	34.95	4.56	52.69	0.13	5.67–9.24	0.213	0.115
Argon	9	273–423	606–2900	157.25	0.29	75.05	0.01	1.74–2.69	0.092	0.032
Krypton	10	120–150	5–1241	202.74	0.94	91.75	0.01	0.59–0.74	1.880	0.029

Mathias[11] correlation, for the substances in Table 12–1. The procedure is to specify the pressure at constant temperature,

$$P(\rho,\sigma) = P^0 + P^{h.s.}(\rho,\sigma) - P^{h.s.}(\rho^0,\sigma) + \mathsf{R}T(\rho-\rho^0)\Delta B(\sigma), \tag{12–3}$$

and minimize Equation (12–1) by adjusting σ and ΔB. Thus, for each isotherm in a series of data sets, the values of σ and ΔB are obtained by solving

$$\min_{\sigma,\Delta B} s = \frac{1}{2}\sum_k (\delta P)_k^2. \tag{12–4}$$

Figure 12–1 shows contours of the logarithm of the objective function of Equation (12–1) for single isotherms of the pure fluid [bmim][Tf_2N] at four temperatures. The independent variables in these plots are σ and the term ΔB. The temperature dependence in these plots enters via Equation (9–7b), i.e., one pair of σ and ΔB per isotherm. The trends in these plots are characteristic of all fluids. They show that the two quantities are highly correlated over a significant range of conditions, as given by the series of local minima along an almost straight line. The distance between two local minima is determined by the "roughness" of the mesh, i.e., the intervals chosen for the σ and ΔB. As the interval approaches zero, the local minima approaches a continuous curve with one global extremum. The global minimum of the contours is indicated with a circle, while the point given by the original correlations is marked with a square. The latter is calculated using the optimal values of V^* and T^* obtained from regression of $P\rho T$ data, by minimizing Equation (12–1), i.e., the procedure in Chapter 10. Though some discrepancies among values of σ are observed, the differences appear to be only minor. Larger discrepancies are seen in the values for the ΔB-term. At 298 K the value obtained from the correlations is in good agreement with the optimal model estimate. As the temperature increases, the difference in ΔB appear to increase as well. At the two high temperatures the sign of the term is inconsistent with the original correlation. Figure 12–2 shows a similar plot for xenon. Here, the correlations are in good agreement with data over

all temperatures. However, unlike the ionic liquid, the global minimum of the contours does not change significantly. The values given by the correlations are given as

$$B = V^* f(T/T^*) \qquad \text{and} \qquad B^{h.s.} = V^* g(T/T^*). \tag{12–5}$$

If T^* is large, then the variation of B with temperature is largely determined by V^*. Therefore, since V^* is much smaller for xenon than the ionic liquid ($117.6\,\mathrm{cm^3/mol}$ versus $1036.6\,\mathrm{cm^3/mol}$), the variation of B with temperature is much larger for the ionic liquid than for xenon.

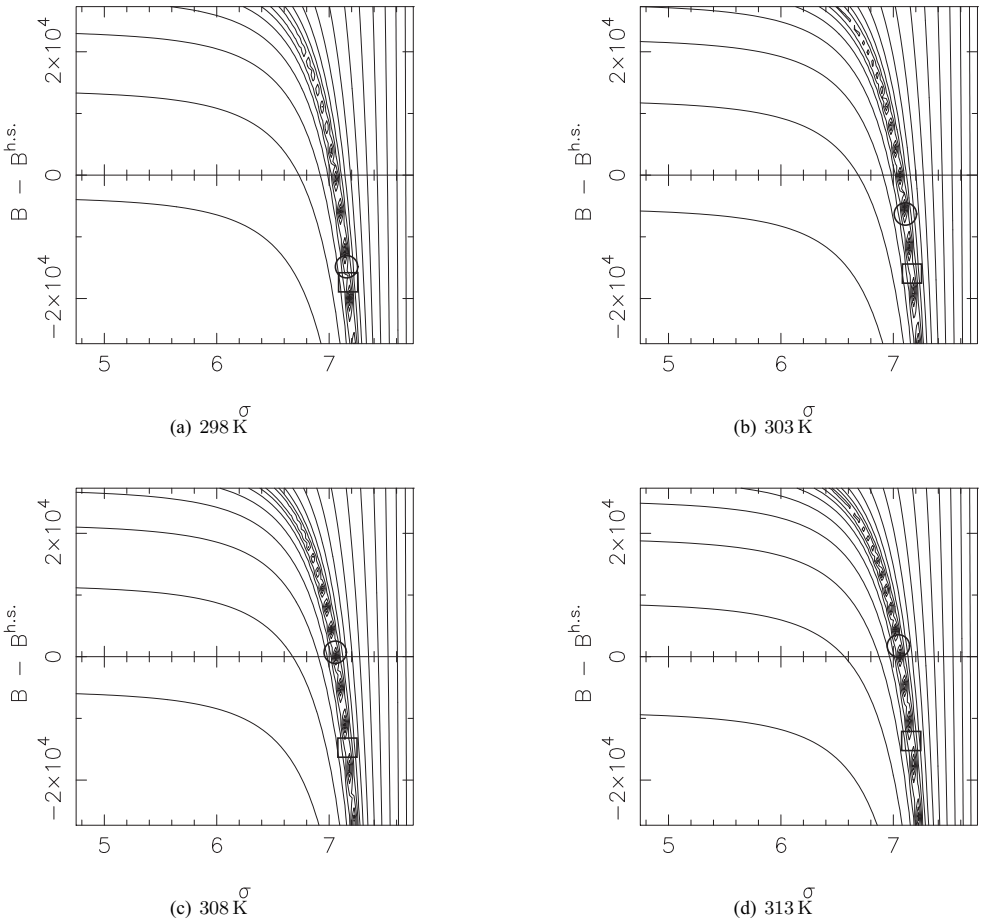

Figure 12–1. Contours of optimal parameter values of Equation (12–1) for [bmim][Tf_2N] using data of Gomez de Azevedo et al.[3] at four temperatures. ○ indicates the optimal combination and □ indicates the combination given by the original correlations.[1] As temperature increases, the discrepancy between the set regressed from $P\rho T$ data and the optimal set increases.

Identical arguments are made for hydrogen, which is given in Figure 12–4. Generally, so long as the

points are located along the series of local minima the description of the fluid behavior is quantitative. Thus, it appears that although the ΔB-term is not optimal, the variations do not significantly affect the results as long as the correlation for σ is satisfactory. This is consistent with liquid compression data being reducible using only a size-dependent parameter, as concluded by Brelvi and O'Connell.[12–14]

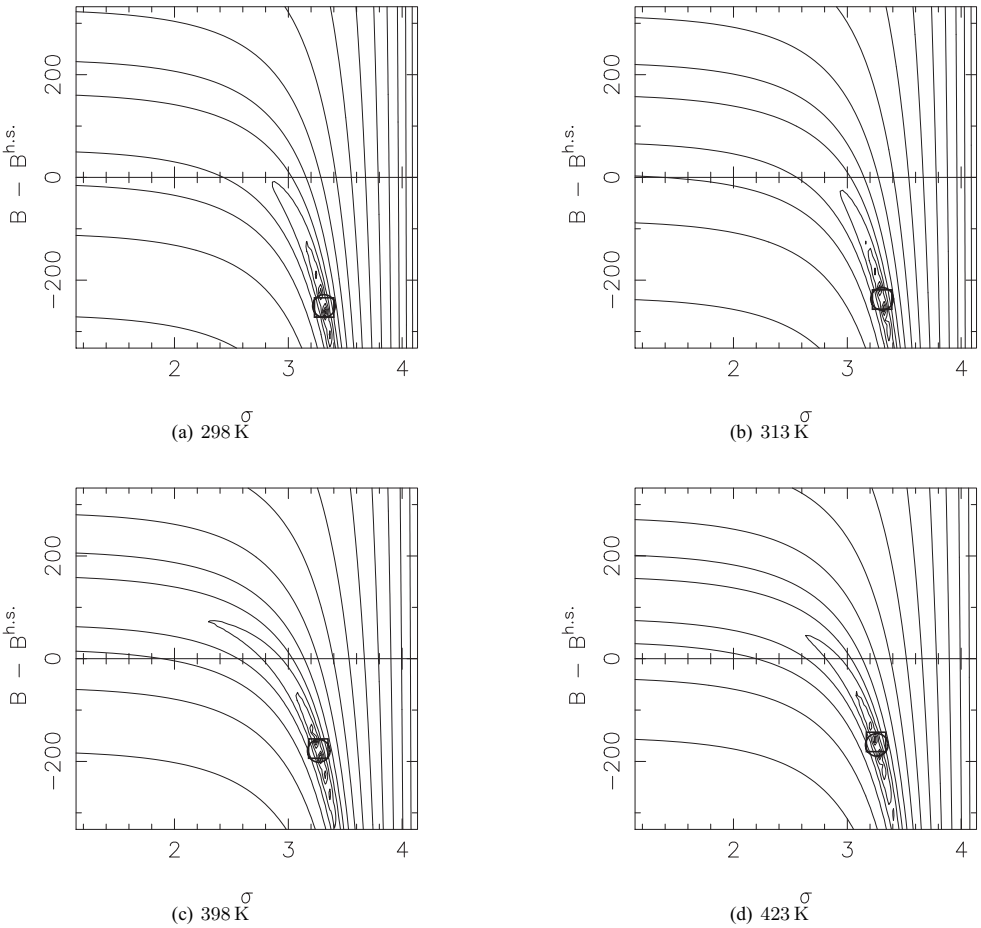

Figure 12–2. Contours of optimal parameter values of Equation (12–1) for xenon using data of Michels et al.[7] at six temperatures. ○ indicates the optimal combination and □ indicates the combination given by the original correlations.[1] Unlike the ionic liquid exemplified previously, the discrepancy between optimal set of parameters and that regressed from $P\rho T$ data does not vary with temperature, although the actual parameters do vary.

Figure 12–3 plots the contours in a surface plot for xenon at 298 K. The shape of the objective function is more clearly viewed in this way. The series of local minima that defines the "valley" has a global minimum at about $(1.5, 175)$.

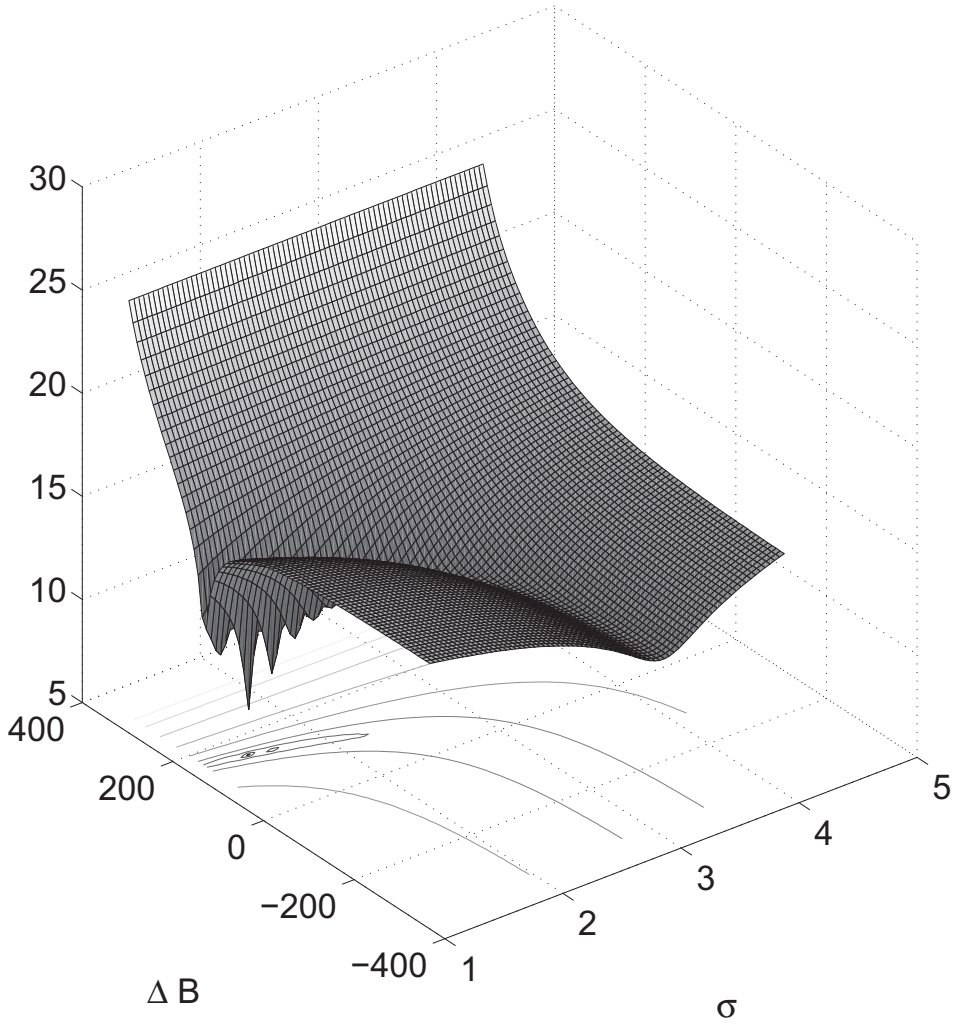

Figure 12–3. Surface-contour plot of the logarithmic objective function of Equation (12–1) for xenon using data of Michels et al.[7] at 298 K.

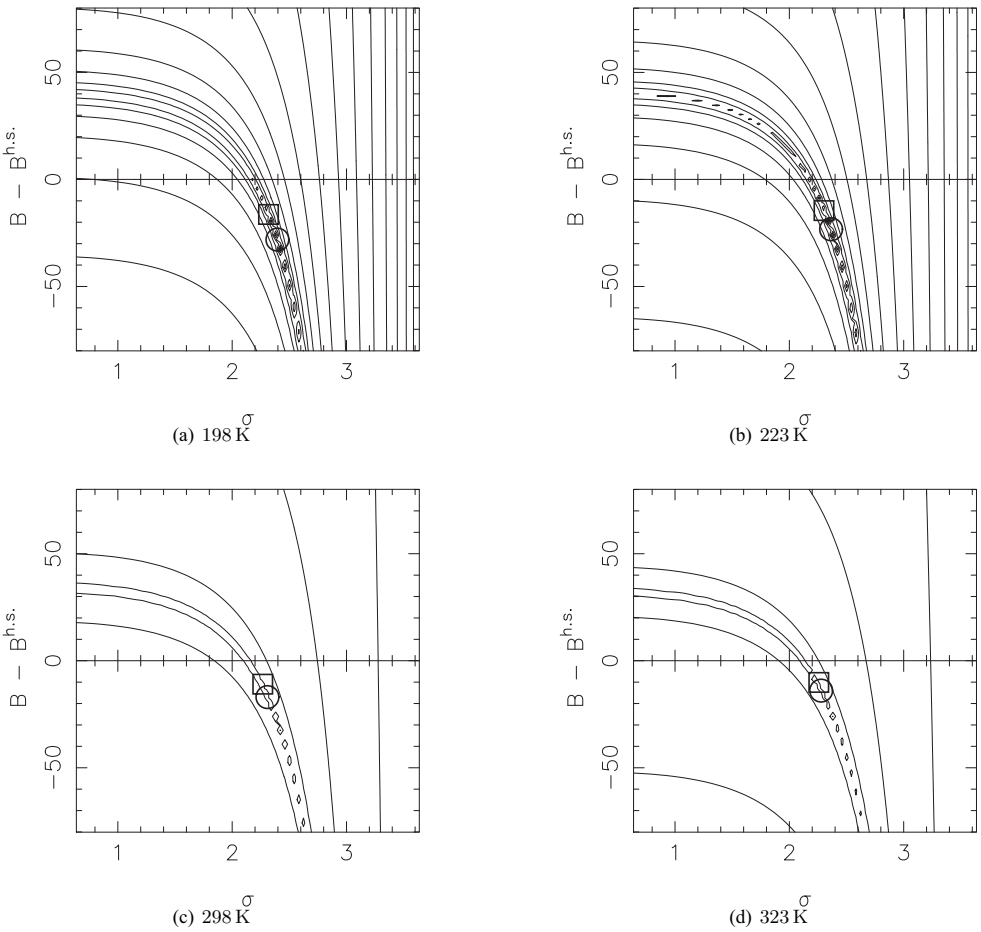

Figure 12–4. Contours of optimal parameter values of Equation (12–1) for hydrogen using data of Deming and Shupe[8] at six temperatures. ∘ indicates the optimal combination and □ indicates the combination given by the original correlations.[1]

Figure 12–5 plots the values of σ against temperature. For the ionic liquids [hmim][Tf_2N] and [bmim][Tf_2N] the variation with temperature is significant, but for the remaining substances, including nonionic species, the variation is not large. Interestingly, the value of σ for $[\mathrm{emim}][\mathrm{EtSO_4}]$ increases slightly with increasing temperature. This is inconsistent with the theory of Barker and Henderson,[15] which claims that σ will decrease with increasing temperature. $[\mathrm{bmim}][\mathrm{PF_6}]$ has a small maximum in the value of σ, but the overall variation is small. Above all, this figure illustrates that the temperature dependence generally is weak, suggesting that liquid compression data alone does not provide for a temperature correlation of σ. The reason for the model's inadequacy in representing the phase behavior of more soluble gases in ionic liquids may be linked to an inadequacy of the correlations in Equations

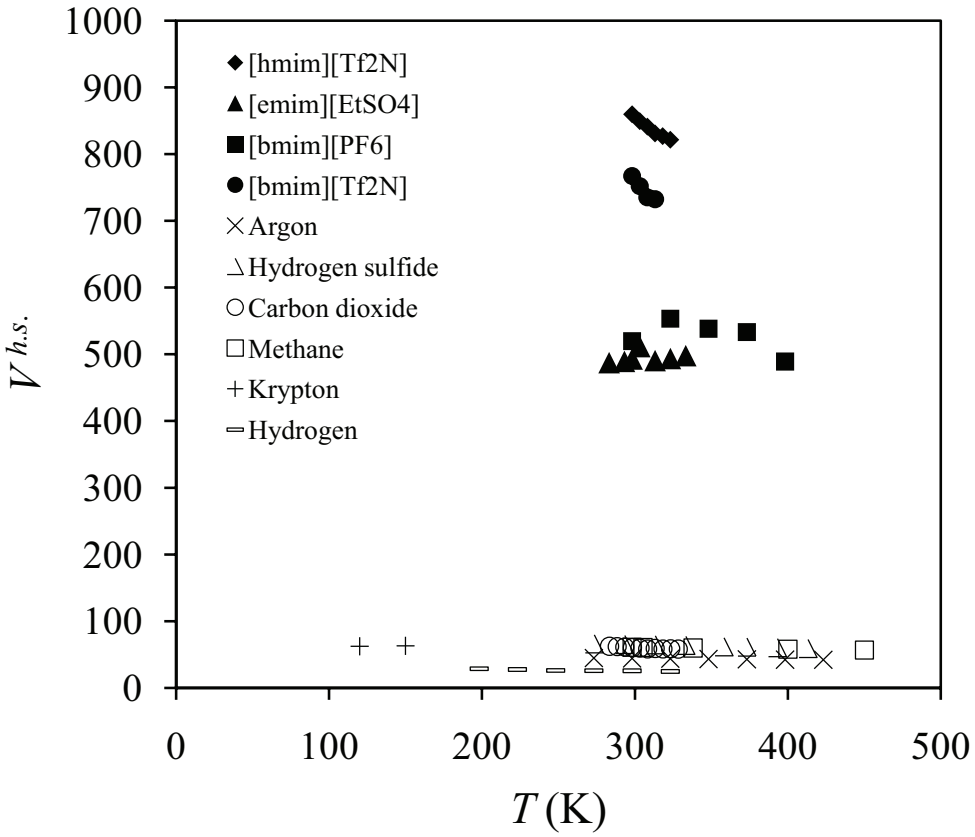

Figure 12–5. Plot of optimal hard-sphere volume, $V^{h.s.} = \frac{2\pi}{3}\sigma^3$, versus temperature for the substances in Table 12–1. Little variation with temperature is observed for most substances. This suggests, that a correlation for σ as function of (reduced) temperature based on compressed liquid densities is not optimal.

(9–7a) and (9–7b). Originally the adjustable parameters – **a**, **b**, and **c** – were fitted to data of liquid argon, krypton, and zenon[1,11] over a reduced temperature range of $0.6 - 2.8$. Since compressed liquid densities of noble gases might not be sufficient basis for temperature correlations involving other gases and ionic liquids, redoing the correlations for these parameters in Equations (9–7a) and (9–7b) may improve results for the systems treated above, where the agreement with experimental data was less quantitatively.

12.2. Optimization of temperature correlations to gas-liquid equilibrium data

The function in Equation (9–7a) is continuous, but its derivatives with respect to temperature are not. However, the double-function in Equation (9–7a) sufficiently describes a large variety of systems,[1,16] so any new correlation would need to be similar. We chose a form derived from the Barker-Henderson

theory

$$\frac{B_{ii}^{h.s.}}{V_i^*} = \frac{\frac{2\pi}{3}\sigma_i^3}{V_i^*} = z_0\left[1 - z_1 \exp\left(-z_2/\tilde{T}_{ii}\right)\right]. \tag{12–6}$$

This expression is similar to that of the PC-SAFT equation of state,[17] and its derivatives are continuous over the entire reduced temperature region. The form of $B_{ii}^{h.s.}$ in Equation (12–6) captures the strong decrease with temperature that is usually observed at low reduced temperatures. The temperature dependence of the second virial coefficient follows well established trends, and is not redone here. However, the coefficients for B_{ij} in Equation (9–7b) are also included in the reestimation, since they initially were also found from density data. Thus, the parameters **c**, **z**, and the coefficients for the Henry's law constant

Table 12–2. Regressed coefficients for $B_{ij}^{h.s.}$ in Equation (12–6) found from a combination of compressed liquid densities and gas solubility data.

Gas	Solvent	z_0	z_1	z_2	T_1^* (K)	V_1^* ($\mathrm{cm}^3/\mathrm{mol}$)	T_2^* (K)	V_2^* ($\mathrm{cm}^3/\mathrm{mol}$)
Hydrogen	[hmim][Tf_2N]	0.779	0.423	0.915	34.7	51.5	733.7	1159.1
d.o.	[bmim][PF_6]	0.778	0.427	0.916	33.9	48.3	749.5	722.1
Methane	[hmim][Tf_2N]*	0.781	0.387	0.961	51.7	101.7	709.6	1157.8
Ethane	[bmim][PF_6]*	0.781	0.392	0.958	262.0	142.5	699.5	724.8

* Using $k_{12} = 0.2$.

Table 12–3. Coefficients for Henry's law expression in Equation (9–20), when using the modified expressions for B_{ij} and $B_{ij}^{h.s.}$.

Gas (1)	Solvent (2)	a_0	a_1	a_2
Hydrogen	[hmim][Tf_2N]	11.4706	197.5243	-0.8089
d.o.	[bmim][PF_6]	18.513	6.3022	-1.7778
d.o.	[bmpy][Tf_2N]	14.0915	58.0785	-1.1604
d.o.	[bmim][CH_3SO_4]	9.3576	300.7241	-0.2536
Methane	[hmim][Tf_2N]	6.4432	-286.3700	0.1146
d.o.	[hmim][Tf_2N]*	6.1145	-285.036	0.1147
Carbon monoxide	[bmim][CH_3SO_4]	7.9368	124.7527	n/a

* Using $k_{12} = 0.2$.

for a gas-solvent system should be estimated so that the highly temperature dependent gas solubilities are described quantitatively, while the pure component densities should be correlated. In addition to the problem of selecting an appropriate temperature dependence on the model quantities, the Henry's law constant was previously estimated primarily from high-pressure data, since the objective function minimized contained the squared differences of absolute pressures. Therefore, it might be reasonable to minimize the relative differences in pressure, so that high and low pressure are weighted equally in the

objective function. Regression of parameters is therefore based on solving

$$\min s' = \frac{1}{2}\sum_{i}^{3}\frac{w_i}{n_i}\sum_{j\in i}^{n_i}\left(\frac{\delta P}{P}\right)_j^2 \tag{12–7}$$

Here $i = 1$ corresponds to $P\rho T$ data of pure 1, $i = 2$ corresponds to $P\rho T$ data of pure 2, and $i = 3$ corresponds to gas + liquid equilibrium data of 1 in 2 with computation of pressure as described above. The weights w_i can be adjusted to ensure that both pure compressed liquid density and gas solubility data are well represented. Included in the optimization are also values of T_i^*, V_i^*, and k_{ij} for the gas and solvent, giving a total of up to 16 adjustable parameters to be determined from a combination of data on the compressed liquid densities of the pure species and their binary phase equilibrium.

12.2.1. Hydrogen

The solubility of hydrogen in the ionic liquid [hmim][Tf_2N] from Kumełan et al. [18] provides our first example. Using the original correlations for $B_{ij}^{h.s.}$ and B_{ij} the model was able to describe the solubility behavior using k_{12} equal to zero. Thus, this particular system can be treated as a benchmark case for considering new correlations. Figure 12–6 shows the result from optimizing the correlations for $B_{ij}^{h.s.}$, B_{ij}, and $H_1(T)$ as well as the pure component characteristics T_i^* and V_i^* for both solute and solvent. The weights for the objective function were set so that $w_1 = w_2 = 0.01w_3$, though the results are not highly sensitive to their values. Table 12–2 gives the coefficients for the correlation of $B_{ij}^{h.s.}$. The upper plots of Figure 12–6 show the agreement for liquid density data for each pure component, while the lower plots show the gas solubility correlation. The Henry's law constant for hydrogen usually has a strong temperature dependence, so all three parameters in Equation (9–20) are employed. The resulting coefficients, found by minimizing the sum of squared pressure differences, are given in Table 12–3. The slope and intercept with the ordinate axis are in good agreement with a linear approximation, allowing the Henry's law constant to be estimated by extrapolation of $\ln f_1/x_1$ to infinite dilution rather than by the correlation in Equation (9–20). The lower right plot shows the pressure as function of mole fraction solubility, showing quantitative agreement of the model with data.

Figure 12–7 shows a similar plot, but with the ionic liquid [bmim][PF_6]. The agreement is quantitative when $k_{12} = 0$, but the temperature dependence of the Henry's law constant is not quantitatively matched. For the three lowest isotherms, the fitted Henry's constants agree well with those found by extrapolating fugacities divided by solubilities to infinite dilution. However, the isotherm at 373 K has a slightly different slope and intercept relative to the others. This causes a slight overestimation of the fugacity at high pressures, and subsequently propagates into the overall solubility estimates. The low-temperature isotherms of pure liquid hydrogen are not represented quantitatively, but this discrepancy is

from “trading off” to more closely approach the gas solubilities.

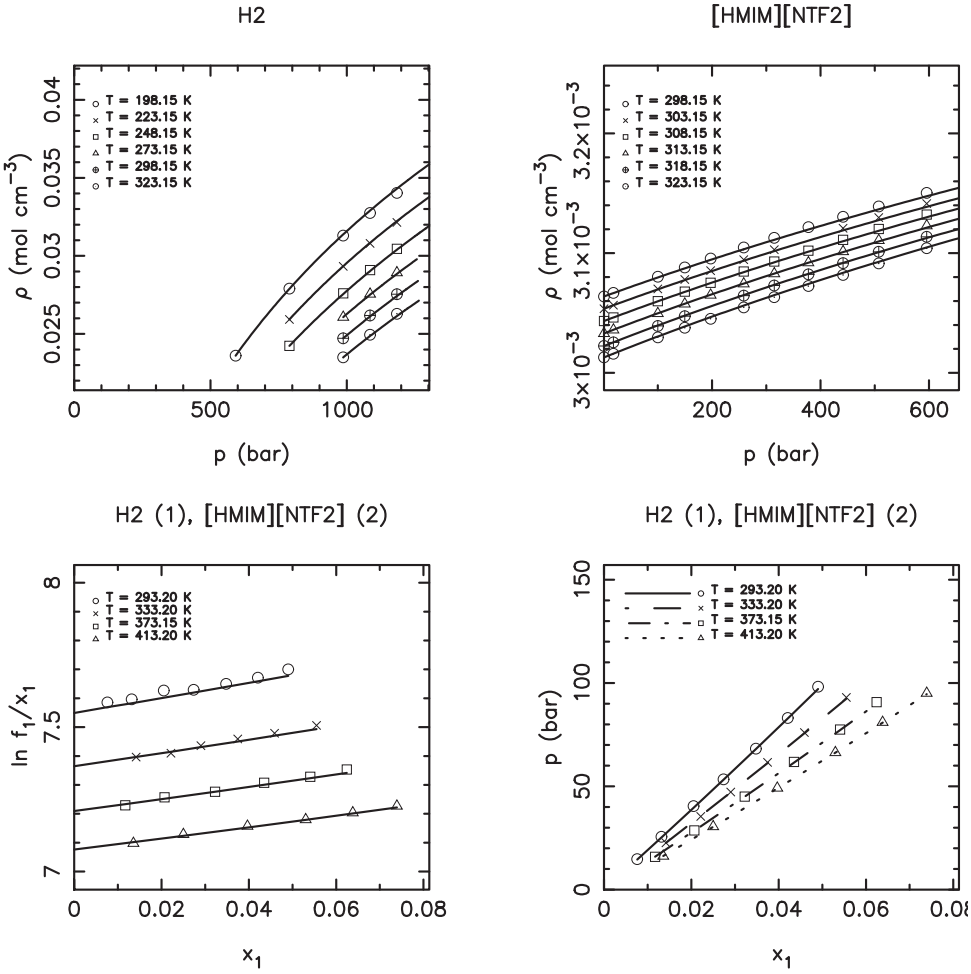

Figure 12–6. Solubility of hydrogen in [hmim][Tf_2N] and their individual pure compressed liquid densities[3,8] from optimization to pure liquids and gas-solvent data.[18] Only six of 15 isotherms for [hmim][Tf_2N] are displayed for legibility (upper right plot). The result is good, showing that the modified model is able to quantitatively describe the gas solubility data, as well as the liquid compression data.

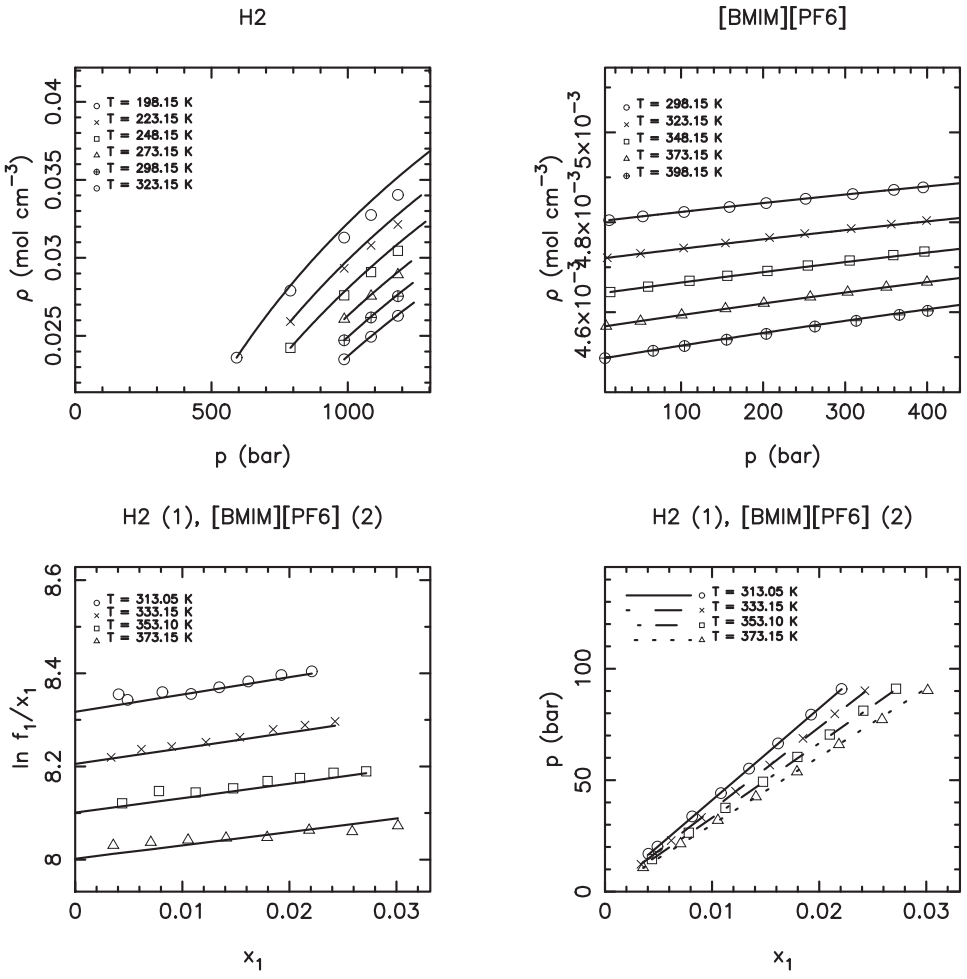

Figure 12–7. Solubility of hydrogen in [bmim][PF_6] and their individual pure compressed liquid densities[2,8] from optimization to pure liquids and gas-solvent data.[19] An excellent agreement is found between the model and the experimental data for each of the pure species liquid densities and their mutual phase equilibria.

12.2.2. Methane

The solubility of methane in [hmim][Tf_2N] was also addressed previously, but unlike the hydrogen systems, a good fit to the solubility data was only accomplished when using a binary interaction parameter of $k_{12} = 0.29$. When optimizing the parameters to match pure component $P\rho T$ data and gas-liquid data, the result is not dramatically improved, although $k_{12} = 0.20$ is sufficient for the new correlation. Fig. 12–8 plots the agreement with experiment. The isotherms of the pure fluids are generally described quantitatively, except for the highest pressures in the lowest isotherm for methane, where the model

slightly overestimates the density. The lower right plot of total pressure versus liquid mole fraction also shows good agreement between experiment and calculations. However, the lines of $\ln f_1/x_1$ (lower left plot) give model estimates that do not quantitatively match the experimental results combined with the second virial fugacity coefficient. The vapor phase of methane is much more nonideal than that of hydrogen, indicated by the relatively large and negative virial coefficients $(B_{11} \sim -50\,\mathrm{cm^3/mol})$. This

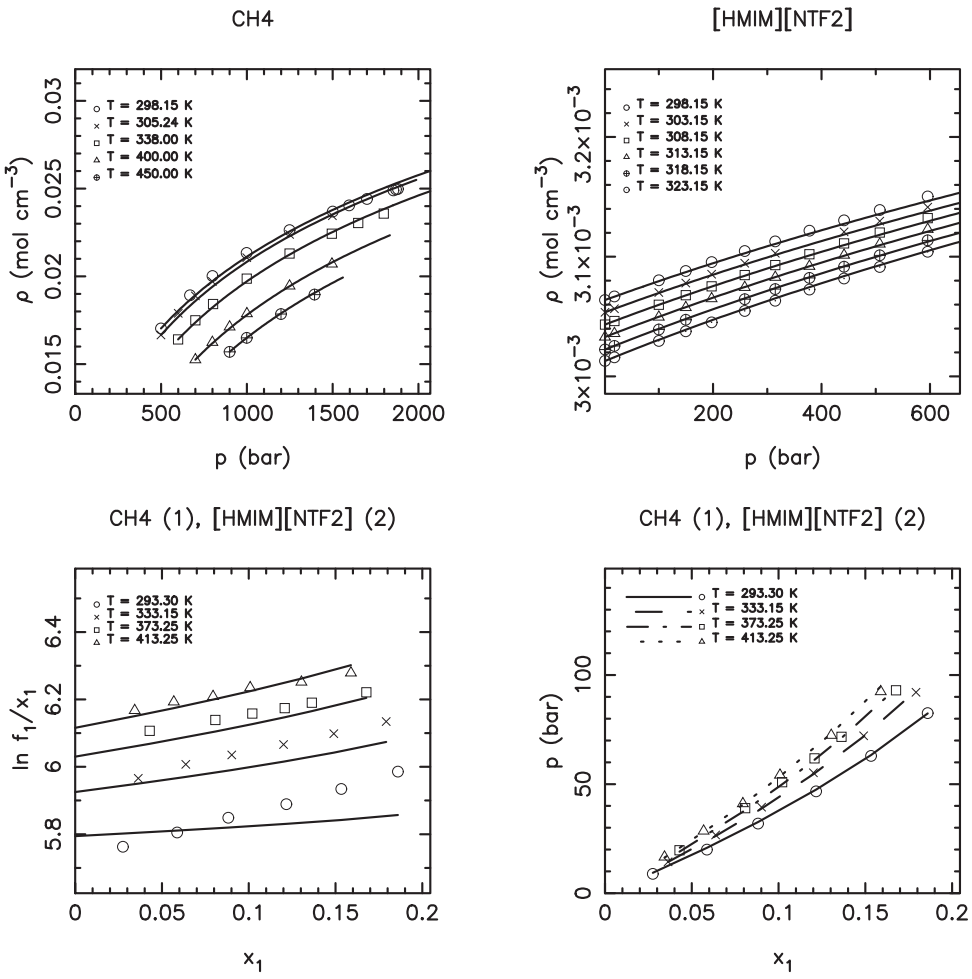

Figure 12–8. Solubility of methane in [hmim][Tf_2N] using $k_{12} = 0.2$ and their individual pure compressed liquid densities[3,6] from optimization to pure liquids and gas-solvent data.[20] Only six of 15 isotherms for [hmim][Tf_2N] are displayed for legibility (upper right plot).

means that the solubility is more dependent on the fugacity of the vapor phase, and hence the value chosen for the second virial coefficient. The value of T_1^* regressed is 51.7 K, which is significantly different than that found from liquid compression data (194 K). Curiously, increasing the value of B_{11} by 10% decreases T_1^* to 44.4 K, whereas an decrease in B_{11} by 10% increases T_1^* to 57.4 K. The objective

function remains (almost) unchanged, as do the other coefficients regressed. Thus, the gas-phase fugacity greatly influences T_1^*, and as expected the $P\rho T$ relation of pure methane is virtually unaffected by either value. Of course, the virial coefficient cannot be chosen arbitrarily, but this analysis shows how the parameters depend on the gas-phase fugacity.

The coefficients regressed for $B_{ij}^{h.s.}$, given in Table 12–2, show that the values in **z** are quite similar to those obtained from the two hydrogen systems. Furthermore, all of these parameters give variations of $B_{ij}^{h.s.}$ that closely resemble those from the original correlations of Mathias and O'Connell, confirming that Equation (12–6) is a viable replacement for Equation (9–7a).

12.2.3. Ethane

A system not treated previously is ethane with [bmim][PF_6] by Anthony et al..[21] It is hardly a high-pressure system ($P < 20\,\mathrm{bar}$), but the solubilities are quite low, much lower than the other near-critical gases, methane, xenon and carbon dioxide. The vapors of ethane are substantially nonideal, with second virial coefficients ranging from $-200\,\mathrm{cm^3/mol}$ to $-276\,\mathrm{cm^3/mol}$ at the conditions specified. Figure 12–9 shows the results using three coefficients in the expression for $H_1(T)$. The pure component densities are described reasonably, but the description of gas-liquid data is not good. The lower left plot reveals that the lines of $\ln f_1/x_1$ are linear at higher concentrations of ethane, but varies strongly as the solubility decreases. In addition, the slopes of the isotherms at 298 and 323 K are distinctly negative, whereas it is positive at 283 K. The model is unable to capture either phenomena, and lands in between, yielding almost constant values. The solubility data are ambiguous, showing hysteresis effects. This means, that solubilities at constant temperatures were measured first with increasing pressure, and then decreasing. Since the two methods do not provide the same solubilities, for whatever reason, this means that two pressures can be obtained at one specified composition. This phenomenon cannot be explained in terms of thermodynamics, and is most likely due to unequilibrated solutions. The degree of hysteresis between two values at same x_1 indicates the reliability/accuracy of the reported values. This phenomenon is particularly visible in the 283 K-isotherm, and to a lesser extent the other two. The model gives (at 283 K) a result in between the two branches of the loop, while overestimating at both 298 K and 323 K. Figure 12–10 shows the variation of $\ln f_1/x_1$ with pressure. The ambiguous data reveal that it is impossible to obtain a fugacity (Henry's constant), which satisfies the reference state at infinite dilution, since the data at same temperature show two limiting values of $\ln f_1/x_1$. The data cannot form the basis of serious decisions when comparing models. The above example is meant as an illustration of data being less suitable for data reduction. There are many data sets with similar disproving features as the ethane set here. In fact, much data published prior to 2005 have severe flaws due to previously undetected impurities in the ionic liquids when taking measurements.[22] Therefore, ionic

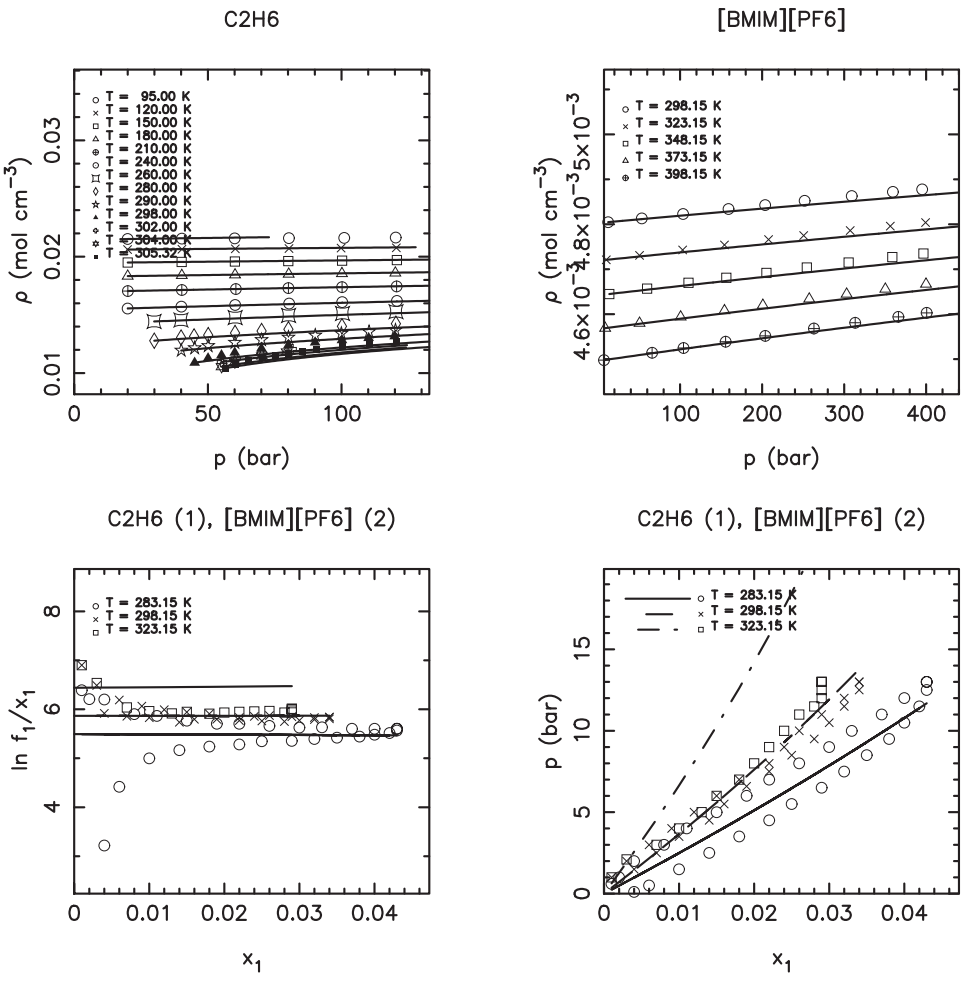

Figure 12–9. Solubility of ethane in [bmim][PF_6] using $k_{12} = 0.2$and their individual pure compressed liquid densities[2,8] from optimization to pure liquids and gas-solvent data.[21]

liquid data, especially those published before 2005, should be used with caution when applying models.

12.3. Summary

This chapter has illustrated the limitations of using compressed liquid densities for regression of coefficients for temperature correlations. This is due to the fact, that compression data usually shows little dependence towards temperature. This is, among other, illustrated by the often straight curves of the hard-sphere diameter versus temperature in Figure 12–5. A much more pronounced sensitivity is found in gas solubility data, and it was therefore convenient to attempt to optimize the original correlations, given by Mathias and O'Connell,[1] to phase equilibrium data. In order to ensure, that the model was

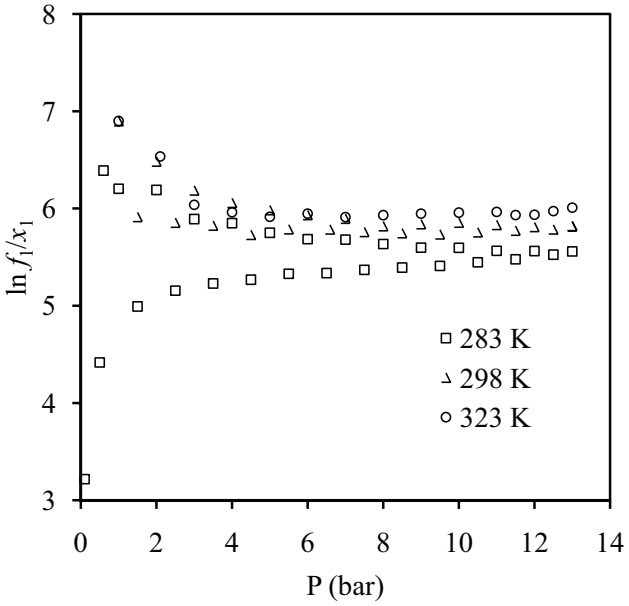

Figure 12–10. Values of $\ln f_1/x_1$ vs. P for ethane in [bmim][PF_6].[21] The points are not actual experimental values, but are transformations from experimental data using the virial equation of state for vapor phase nonideality. The behavior of the points makes it extremely difficult for a model based on a $\gamma - \phi$ method to give accurate results, due to the diverging limiting values. This phenomenon may be caused from the vapor phase model being insufficient.

still able to give accurate estimates of liquid densities, the objective function in Equation (12–7) was found suitable. In addition, it was also speculated if the Henry's law constants, when obtained using Equation (12–7) would be more consistent with low-pressure data. It is not clear that the efforts are fruitful. Although a slightly less value of the binary interaction parameter was often required (compared to using the original reduced-temperature correlations), results were not improved substantially.

References

1. P. M. Mathias and J. P. O'Connell. *Chem. Eng. Sci.*, 36:1123–1132, 1981.
2. A. Tekin, J. Safarov, A. Shahverdiyev, and E. Hassel. *J. Mol. Liq.*, 136:177–182, 2007.
3. R. Gomez de Azevedo, J. M. S. S. Esperança, J. Szydlowski, Z. P. Visak, P. F. Pires, H. J. R. Guedes, and L. P. N. Rebelo. *J. Chem. Thermodyn.*, 37:888–899, 2005.
4. T. Hofman, A. Goldon, A. Nevines, and T. M. Letcher. *J. Chem. Thermodyn.*, 40:580–591, 2008.
5. E. C. Ihmels and J. G. Gmehling. *Ind. Eng. Chem. Res.*, 40:4470–4477, 2001.
6. D. E. Cristancho, I. D. Mantilla, S. Ejaz, K. R. Hall, M. Atilhan, and G. A. Iglesia-Silva. *J. Chem. Eng. Data*, 55:826–829, 2009.
7. A. Michels, T. Wassenaar, and P. Louwerse. *Physica*, 20:99–106, 1954.
8. W. E. Deming and L. E. Shupe. *Phys. Rev.*, 40: 848–859, 1932.
9. A. Michels, H. Wijker, and H. Wijker. *Physica*, 7: 627–633, 1949.
10. W. B. Streett and L. A. K. Stavely. *J. Chem. Phys.*, 55:2495–2506, 1971.
11. P. M. Mathias. *Thermodynamic properties of high-pressure liquid mixtures containing supercritical components*. PhD thesis, University of Florida, Gainesville, FL, USA, 1978.
12. S. W. Brelvi and J. P. O'Connell. *AIChE J.*, 18: 1239–1243, 1972.
13. S. W. Brelvi and J. P. O'Connell. *AIChE J.*, 21: 171–173, 1975.

References

14. S. W. Brelvi and J. P. O'Connell. *AIChE J.*, 21: 1024–1027, 1975.

15. J. A. Barker and D. Henderson. *J. Chem. Phys.*, 47: 4714–4721, 1967.

16. E. A. Campanella, P. M. Mathias, and J. P. O'Connell. *AIChE J.*, 33:2057–2066, 1987.

17. J. Gross and G. Sadowski. *Ind. Eng. Chem. Res.*, 40:1244–1260, 2001.

18. J. Kumełan, Á. Pérez-Salado Kamps, D. Tuma, and G. Maurer. *J. Chem. Eng. Data*, 51:11–14, 2006.

19. J. Kumełan, A. Á. Pérez-Salado Kamps, D. Tuma, and G. Maurer. *J. Chem. Eng. Data*, 51:1802–1807, 2006.

20. J. Kumełan, Á. Pérez-Salado Kamps, D. Tuma, and G. Maurer. *Ind. Eng. Chem. Res.*, 46:8236–8240, 2007.

21. J. L. Anthony, E. J. Maginn, and J. F. Brennecke. *J. Phys. Chem. B*, 106:7315–7320, 2002.

22. D. Tuma, 2009. Personal communication.

13. Summary and discussion for Part II

There are two outcomes of the investigations from this thesis part:

1. A method for describing volumetric behavior of ionic liquids.

2. A method for high-pressure gas solubilities in ionic liquids.

The two are closely related, sharing a common background in fluctuation solution theory. In fact, the former application area is developed as a byproduct of exploring the gas-ionic liquid phase equilibrium problem.

If we initially focus on the behavior of pure ionic liquids, the results shown in this part reveal that the method, using simple formulations for B and $B^{h.s.}$ successfully describe volumetric properties of a wide range of ionic liquids. Due to a general insensitivity of ionic liquid characteristics toward temperature, it is possible to characterize the different $P\rho T$ relations using only a single characteristic-volume parameter. Ionic liquids are largely rigid molecular structures, which is supported by the success of a group contribution method such as that of Ye and Shreeve.[1] This means, that the characteristic volume parameter can be conceived from group contributions, using van der Waals volumes of the constituent molecular groups. This also explains why a model formulation of the DCFI of the generalized van der Waals form is successful. The resulting equation of state for pure ionic liquids is completely predictive, requiring only the molecular structure for estimation of V^* from group contributions. Unlike similar models (i.e. traditional cubic equations of state), which are of similar complexity, this model formulation does not require (hypothetical) critical parameters, although T^* and V^* can be thought of in terms of scaled critical parameters[2,3] (on which the model was in fact originally formulated[4]). This is most obvious when comparing the parameters to the corresponding critical values, which is done in Table 11–1 for a set of gaseous solutes. In this light, the discussion of hypothetical parameters might appear superficial and without major implications, such as the application of hypothetical liquid reference fugacities. However, this is not the case. Critical parameters force the equation of state to exhibit critical points, i.e., forcing $(\partial P/\partial \rho)_T$ to zero and creating an inflection point, $(\partial^2 P/\partial \rho^2)_T = 0$. This

behavior is unreal for ionic liquids and advocates for application of a method with similar complexity as the cubic equations of state, but at the same time preserving actual physical behavior. There are also advanced equations of state not based on the existence of criticality, such as those based on the statistical associated-fluid theory (SAFT). Much attention has been directed toward these methods, as discussed in Chapter 8. While accounting for hydrogen bonding explicitly, the role of association/solvation in ionic liquid systems has not yet been fully uncovered. Therefore, a large number of SAFT-based models for ionic liquid systems have emerged in recent years (see e.g. a recent review by Vega et al.[5]). However, application of these models is not straightforward and may require large amounts of data for parameter estimation. The separation of density and temperature dependent terms in the DCFI-model applied here facilitates analysis of model structure and may help reveal inadequate correlations or aid in the detection of erroneous data, as was done in Chapter 10.

The phase equilibria of gaseous solutes with ionic liquids is the driving force for the investigations done in the treatment of pure ionic liquid systems. Results show that solubilities of the highly supercritical solutes hydrogen, carbon monoxide, and oxygen, can be described well using hardly any adjustable parameters. The methods of estimating V_i^* of the ionic liquid from group contributions and fixing T_i^*, in connection with the estimation of the ionic liquid reference state, allows prediction of the solvent properties using a binary interaction parameter of zero. A complete predictive capability would allow estimation of the characteristics of the gases in addition to the binary interaction coefficients, when applicable. For the larger gases, methane, carbon dioxide, and xenon, results were not quite as good. Although gases methane and carbon dioxide could be described well, relatively large binary interaction coefficients were required.

Analysis of the results suggested that superior results for gas solubilities could be obtained if the reduced-temperature correlations – built into the model, and originally estimated from liquid density data – were optimized to gas solubility data, which are considerably more sensitive towards temperature. This was achieved by modifying the reduced temperature correlation for the hard-sphere diameter in Equation (9–7a) to Equation. (12–6) and simultaneous adjustment of the coefficients to $P\rho T$ data of pure species and their gas-liquid phase equilibrium. However, results were only slightly improved. This was done only for a few gas-solvent systems. Attempts to include multiple systems in the regression of universal parameters for Equation (12–6) were not done, since significant improvements were not observed for the single gas-ionic liquid systems. The reason for the less quantitative description is likely to come from the nonideality in the gas phase (the lighter gases form nearly ideal gas phases). Figure 13–1 shows the $P\rho T$-relations for hydrogen at 293 K and 393 K and carbon dioxide at 313 K and 393 K using the multiparameter equations of state proposed by Span and Wagner[6] and Leachman et al.,[7] and the

virial equation with second virial coefficients from Hayden and O'Connell.[8] For hydrogen there is little

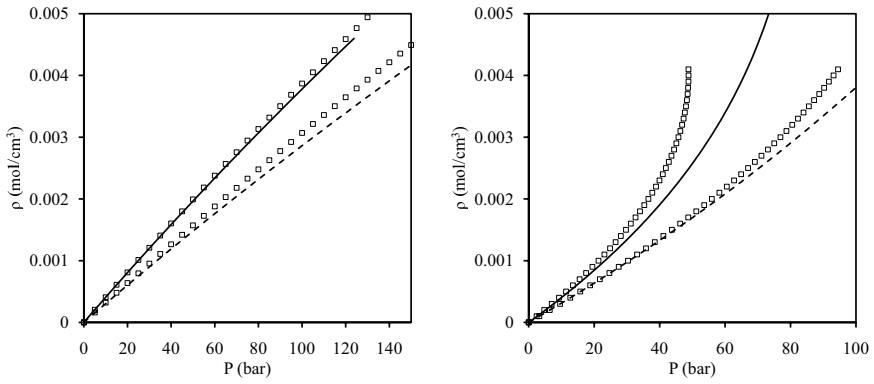

Figure 13–1. Pressure-density for hydrogen (left) and carbon dioxide (right) using multiparameter equations of state (lines) and virial equation (□).

difference between either method over most of the conditions. The virial equation slightly overpredicts, and the difference at $90\,\mathrm{bar}$ is around 40%. For carbon dioxide the high-temperature values are in good agreement with each other over most of the pressure range, whereas the low-temperature data disagrees strongly, since carbon dioxide does not become supercritical before $75\,\mathrm{bar}$. This indicates that the choice of model for the gas-phase nonideality is nontrivial, especially when dealing with gases such as carbon dioxide. For more reliable results it might be worthwhile to examine implementation of equations of state of the multiparameter type. This might be particularly important when conditions of the available data are closer to the critical point. This means, that a formulation of the $\gamma - \phi$ type, regardless of model chosen for liquid-phase nonideality, can be unsuccessful. Generally, there are two major limitations of formulating a phase equilibrium problem in this way

1. Conditions must be relatively far from the critical point.

2. Accurate estimation of the reference fugacity (Henry's law constant) is of utmost importance.

Possibly a $\phi - \phi$ method, i.e., using an equation of state for both liquid and vapor phases, will be successful. However, this puts severe demands on the density relations within the equation of state, since the range of densities covered is large. Also the vapor nonideality must be well accounted for. It is doubtful that the current method can be extended to cover both liquid and gaseous phases, and is likely to result in an advanced, and therefore usually complex, model, which for reasons discussed above and in Chapter 1 is not desirable. A limiting factor of applying this method is the strong dependency toward the reference fugacity of the gas, i.e., the Henry's constant. Its value comes alone from mixture data; either regression of parameters for an expression such as Equation (9–20) or extrapolation of low-pressure data to infinite

dilution. Models for estimating Henry's constants have been developed for traditional chemicals[9] over many years, but those in ionic liquids are beginning to appear in the open literature.[10,11] However, it is unlikely that their current accuracy will be sufficient for the framework in the $\gamma - \phi$ formulation due to the strong dependence at high pressures.

Clearly extra work is required for a treatment that separates the vapor and liquid nonidealities, so it is appropriate to inquire about the added value of such extra efforts, even beyond their rigor. The data analysis of this work, as well as Kumełan et al.,[12] suggest that there truly are nonidealities in both the vapors and liquids of many gas–ionic liquid systems, especially those with more soluble gases (e.g. carbon dioxide and xenon). Equating fugacities of a pure gas and a liquid mixture, with a Poynting correction factor for pressure nonideality of the liquid-phase fugacity, yields

$$\ln P = \ln \gamma_1 \left(T, P^0, \mathbf{x}\right) + \int_{P^0}^{P} \frac{\bar{v}_1 \left(T, P, \mathbf{x}\right)}{\mathsf{R}T} \mathrm{d}P - \ln \phi_1^V \left(T, P\right) + \ln H_1 \left(T\right) + \ln x_1. \qquad (13\text{–}1)$$

If the first three terms on the right-hand side cancel, Henry's law is obtained. This is frequently the case for carbon dioxide in ionic liquids [bmim][CH_3SO_4] and [hmim][Tf_2N].[13,14] Figure 13–2 shows the fugacity coefficient subtracted from the summation of activity coefficient and Poynting factor versus solubility using the data provided by Kumełan et al..[13] Even at very high solubilities the departure from ideal behavior remains less than 10%. While this plot is by no means general of all gas-ionic liquid

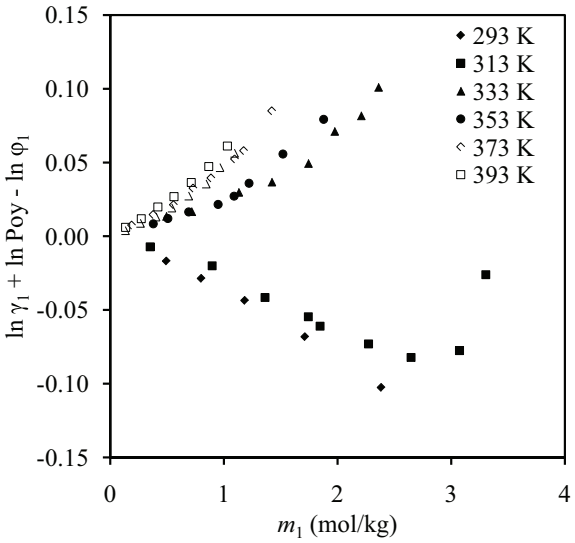

Figure 13–2. Pressure effects of nonideality versus molality of carbon dioxide in [bmim][CH_3SO_4].[13]

systems it does prove an important point; it is not always obvious when nonideality contributions cancel, making the points raised in Chapter 8 and the discussion above relevant. Relying on cancelation of three factors can lead to unacceptable and unnecessary risk. Furthermore, extension to mixtures should be more reliable when using a soundly based model, although this is not pursued here.

References

1. C. Ye and J. M. Shreeve. *J. Phys. Chem. A*, 111: 1456–1461, 2007.
2. W. B. Streett and L. A. K. Staveley. *Physica*, 71: 51–65, 1974.
3. J. M. H. Levelt. *Physica*, 26:361–377, 1960.
4. P. M. Mathias. *Thermodynamic properties of high-pressure liquid mixtures containing supercritical components*. PhD thesis, University of Florida, Gainesville, FL, USA, 1978.
5. L. F. Vega, O. Vilaseca, F. Llovell, and J. S. Andreu. *Fluid Phase Equil.*, 294:15–30, 2010.
6. R. Span and W. Wagner. *J. Phys. Chem. Ref. Data*, 25:1509–1596, 1996.
7. J. W. Leachman, R. T Jacobsen, S. G. Penoncello, and E. W. Lemmon. *J. Phys. Chem. Ref. Data*, 38: 721–748, 2009.
8. J. G. Hayden and J. P. O'Connell. *Ind. Eng. Chem. Proc. Des. Dev.*, 14:209–216, 1975.
9. D. Mackay, W. Y. Shiu, and K. C. Ma. *Handbook of property estimation methods for chemicals*, chapter 4: Henry's law constant. Lewis Publishers, 2000.
10. Y. Qin and J. M. Prausnitz. *Ind. Eng. Chem. Res.*, 45:5518–5523, 2006.
11. J. E. Bara, T. K. Carlisle, C. J. Gabriel, D. Camper, A. Finotello, D. L. Gin, and R. D. Noble. *Ind. Eng. Chem. Res.*, 48:2739–2751, 2009.
12. J. Kumełan, D. Tuma, and G. Maurer. *Fluid Phase Equil.*, 275:132–144, 2009.
13. J. Kumełan, A. Á. Pérez-Salado Kamps, D. Tuma, and G. Maurer. *J. Chem. Eng. Data*, 51:1802–1807, 2006.
14. J. Kumełan, Á. Pérez-Salado Kamps, D. Tuma, and G. Maurer. *J. Chem. Thermodyn.*, 38:1396–1401, 2006.

14. Conclusions and significance

The Kirkwood-Buff theory of solutions (or fluctuation solution theory; FST) connects derivative thermodynamic properties to spatial integrals of pair correlation functions. The theory is completely general and makes no assumptions concerning interactions between molecules. This thesis has reported application of this rigorous, yet surprisingly simple, framework for thermodynamic properties and phase equilibria of pure pure components and mixtures. This was done by invoking the FST relations in two different ways:

1. Application to solid solubilities in mixed solvent systems. This results in model expressions, where correlation function integrals enter as parameters, which were estimated from data.

2. Application to gas solubilities in ionic liquids. The correlation function integrals were approximated with a simple model, allowing for a general approach to gas-ionic liquid phase equilibria, as well as volumetric properties of the pure species.

The models require a minimum of parameters, and the models are not particular sensitive towards their values. It is hoped that these relatively simple methods can support the existing methods. These are often complicated models, which can be difficult to apply when experimental data, for regression of parameters is limited.

Below are drawn the main conclusions from this thesis. A summary of contributions to the engineering and scientific literature is also emphasized, and a few directions for further studies are briefly outlined.

14.1. Overall conclusions

The thermodynamic relations governing solid-liquid phase equilibria (of pure solids) have been presented and discussed. Expressing component activity coefficients using fluctuation solution theory lead to simple expressions for a model for excess solubilities of solid solutes in mixed solvents. Analysis of excess solubilities and their relations to excess Gibbs energies (and derivatives thereof) of the solvent mixtures, revealed the importance of the two excess quantities being consistent with each other.

14. Conclusions and significance

Regressions of model parameters – integrals of molecular pair correlation functions – from solid solubilities in binary solvent mixtures showed that the method is capable of describing a wide variety of observed phenomena, including nearly ideal solute-solvent systems and systems which deviate significantly from this. The anchoring in FST allows for the solute-solvent parameters from other sources as well. A method was deduced which allows for obtaining these parameters from solubilities in single solvents. Estimates of these are best done, when the solute is deviate strongly from the ideal solubility, i.e., the solute-solvent pair is highly nonideal. This if often the case with aqueous-organic systems. Application of UNIFAC for estimating limiting activity coefficient derivatives showed that UNIFAC is unable to give accurate estimates in many cases, most likely due to some inherent limiting features. Comparisons have shown that UNIFAC generally gives good estimates of the excess solubilities in solvent mixtures, while not necessarily yielding good estimates of solubilities in single (or for that matter mixed) solvents.

A provisional extension of the method for excess solubilities in ternary solvent mixtures showed that the resulting model is capable of correlating ternary solvent excess solubilities. However, parameters from single solvent solubilities were generally not capable of representing the mixture excess solubilities.

The main advantage is that the model resolves effects into solute-solvent and solvent-solvent effects. Solute-solvent factor is simple and linear. The solvent-solvent term is less simple, but is usually better accounted for, since binary low-pressure vapor-liquid equilibrium data (which forms the basis for the solvent-solvent effects) is straightforward in terms of data reduction, and can be done independently of the solid solute. Only a single solute-solvent parameters is required, and is in principle obtainable from solubilities in pure solvents.

Ionic liquids are a class of solvents, which have gained tremendous attention in recent years due to a unique set of favorable thermophysical properties. Application of an existing, simple two-parameter, corresponding-states based model for correlation function integrals revealed that volumetric properties could be described accurately for a variety of different ionic liquids. The method requires two pure component parameters, describing characteristic temperatures and volumes, in addition to a specified density at ambient pressure. The characteristic temperature could be approximated by a common value for all ionic liquids, while the characteristic volume could be sufficiently estimated by a simple group contribution method, utilizing the van der Waals volumes of the constituent groups. A simple relation was found connecting the density at ambient pressures to the above mentioned parameters. This gives a completely predictive method for estimating volumetric properties of pure ionic liquids, provided they can be described with the group parameter table in this work.

Using the model in a $\gamma - \phi$ approach for solubilities of gases in ionic liquids gave best results when

using an additional binary interaction parameter and the Henry's law constant for reference fugacities. Estimating values of both quantities requires mixture data. Using a binary interaction parameter of zero was often successful for highly supercritical gases (such as hydrogen and carbon monoxide), while less supercritical, and more soluble, gases (such as methane and carbon dioxide) required larger values. Almost all systems are highly sensitive towards the Henry's constant.

One key advantage of this framework is that nonideality effects due to composition as well as pressure are combined into a single model. This is contrary to traditional excess Gibbs energy models, which require Poynting factors to account for liquid-phase nonideality due to pressure effects. Analysis revealed, that the reduced-temperature correlations in the model might not be optimal. Attempts were made to optimize these correlations to gas solubility data, which is very sensitive to temperature, but results were not strongly improved.

14.2. Contributions to literature

The major contributions of this thesis to the scientific literature are summarized below.

* A simple model for solubilities in binary solvent mixtures is developed, requiring only solubilities in pure solvents and an excess Gibbs energy model for the solvent binary.

* Analysis of the connection between excess solubility and nonideality of the solvent mixture, and understanding the importance that must be given the solvent mixture nonideality.

* A completely predictive method for describing volumetric properties of ionic liquids over large ranges in pressure and density.

* Methodology for provisional screening of unreliable ionic liquid data on compressed liquid densities.

* A method for estimating gas solubilities with a minimum of parameters. Although the method requires iterative calculations, it remains quite simple. In addition, it is highly accurate for very supercritical gases, such as hydrogen and carbon monoxide.

* An analysis of the temperature insensitivity of liquid compression data, which shows that estimation of parameters for temperature-dependent properties is not advisable.

14.3. Suggestions for future work

Despite the efforts presented in this thesis, a few challenges remain. These are described briefly below.

14. Conclusions and significance

Data compatibility: The anthracene-alkane-alkanol systems clearly show, how the octane–propanol and octane–butanol binaries were incompatible with the excess solubilities of anthracene in them. The systems of naphthalene in water–DMSO and water–ethylene glycol showed other types of incompatibility issues between the solute-free mixture and the experimental solubility data. Further research should be directed towards seeking compatible behavior of the solvent mixture nonideality and the solubility data. This could be done by making consistency checks of the solvent mixtures.

Multisolvent solubilities: Though regression of experimental multisolvent solubility data yielded acceptable results, predictions using single solvent solubilities were not able to generally describe the excess solubility behavior in ternary solvent mixtures. The provisional extension of the binary-solvent model did not yield a method capable of describing the variation of the excess solubility using parameters from single solvent solubilities, as was done in the binary solvent case. Future work in this direction should focus on re-deriving the expression rigorously, and systematically attempting to evaluate the terms arising in order to simplify the method as much as possible.

Henry's constants: The main limitation of the method for gas solubilities in single ionic liquids is the estimation of the liquid-phase reference fugacity; the Henry's constant. Presently, its value come only from regression of mixture data. This means that a predictive method cannot be established, unless the Henry's constant for a gas with an ionic liquid can be estimated reliably. Further attempts should be made for estimating this from more fundamental concepts. This might allow for estimation from limited experimental data, or perhaps even predictions from theory.

Gas-phase nonideality: Another limiting feature of the method, though not one as crucial as the Henry's constant, is the description of gas-phase nonideality. The virial equation is applicable mostly for highly supercritical gases at high pressures, but may not work as well for gases such as carbon dioxide. Continued usage should focus on replacing the virial term by a more suitable model, e.g. a cubic or – if applicable – a multiparameter equation of state.

Data reliability: A methodology for provisional identification of unreliable gas solubility data can perhaps be developed by relating Henry's law constants of a gas in different solvents. This requires that the model is inherently capable of representing individual gas solubility sets. If improvements of gas phase nonideality is possible, such a method could be within reach., and should be highly welcomed by the community.

PART III

APPENDICES

Appendix A. Least squares estimation

The general optimization problem of a estimating the optimal solution by minimizing the m elements of a residual vector $\mathbf{r}$ can be constructed as

$$\min_{\mathbf{x}} q = \frac{1}{2}\mathbf{r}^{\mathsf{T}}\mathbf{r}, \qquad r_i = y_i - f(t_i, \mathbf{x}). \tag{A–1}$$

The elements of r_i consists of a predefined value (y_i, which can be an experimental value) and a model output, f, which depends on independent variables, $\mathbf{t}$, and dependent variables (or parameters) $\mathbf{x}$. We seek the minimum of q. If q is upper-unbounded, the minimum is found when the gradient is zero

$$\mathbf{g} = \mathbf{0}, \qquad \frac{\partial q}{\partial x_1} = \ldots = \frac{\partial q}{\partial x_n} = 0. \tag{A–2}$$

The gradient is expanded about the minimum in a first-order (linear) Taylor series by perturbing the state vector by a small increment $\mathbf{h}$

$$\mathbf{g}(\mathbf{x} + \mathbf{h}) \approx \mathbf{g}(\mathbf{x}) + (\mathbf{x} + \mathbf{h})^{\mathsf{T}}\mathbf{H}(\mathbf{x} + \mathbf{h}) = \mathbf{0}, \tag{A–3}$$

here $\mathbf{g}$ is the gradient, and formally defined by

$$\mathbf{g} = \mathbf{A}\mathbf{r}, \qquad A_{ji} = \frac{\partial r_i}{\partial x_j}, \tag{A–4}$$

where $\mathbf{A}$ is the Jacobian matrix, the columns of which are the first derivative vectors of $\mathbf{r}$. $\mathbf{H}$ is the Hessian matrix, of matrix of second order derivatives, and is given by

$$\mathbf{H} = \mathbf{A}\mathbf{A}^{\mathsf{T}} + \mathbf{r}\nabla^2\mathbf{r} \approx \mathbf{A}\mathbf{A}^{\mathsf{T}} \tag{A–5}$$

∇ is the gradient operator. The approximation above is usually valid if the elements of $\mathbf{r}$ are small, corresponding to a linear approximation[1] of the residuals. Solving the above equations for $\mathbf{h}$ yields

$$\mathbf{h} = -\mathbf{H}^{-1}\mathbf{g}, \qquad x_i^{(k+1)} - x_i^{(k)} = \left[\mathbf{H}^{-1}\mathbf{g}\right]_i^{(k)} \tag{A–6}$$

If f is nonlinear in $\mathbf{x}$, the procedure is iterative, and the next state is found by incrementing $\mathbf{x}$ and k until convergence. The case of a linear model is described below. In that event, estimation is not iterative and requires only a single matrix inversion.

Variances of output parameters are obtained from the variance-covariance matrix

$$\mathbf{V} = \mathsf{E}\left\{(\mathbf{x} - \boldsymbol{\mu})^{\mathsf{T}}(\mathbf{x} - \boldsymbol{\mu})\right\} = \frac{q}{m-n}\mathbf{H}^{-1}. \tag{A–7}$$

$\boldsymbol{\mu}$ is the mean value of $\mathbf{x}$, and E is the expectation operator. The propagation of errors into the estimate, $f(\mathbf{x})$, is obtained by the elements of $\mathbf{V}$ and $\mathbf{A}$

$$V(f(\mathbf{x})) = \mathbf{AVA}, \qquad V(f(x_k)) = \sum_{j,i} A_{kj} V_{ji} A_{ik}. \tag{A–8}$$

The standard deviation of the output variables are

$$\sigma_k = \sqrt{V(f(x_k))}. \tag{A–9}$$

Linear estimation

If the model f is linear in $\mathbf{x}$, the computations simplify significantly. The standard model is

$$\mathbf{f} = \mathbf{A}^{\mathsf{T}}\mathbf{x} + \mathbf{e}, \qquad \mathbf{e} \sim N(\sigma^2; 0), \tag{A–10}$$

where $\mathbf{e}$ is the errors from the model. It is customary to assume that they are normally distributed with constant variance σ^2 and zero mean, so that the least-squares estimate in the above framework can be formulated as.[2]

$$\mathbf{x} = (\mathbf{AA}^{\mathsf{T}})^{-1}\mathbf{Af}. \tag{A–11}$$

References for Appendix A

1. R. Fletcher. *Practical methods of optimization*. Wiley, 1987.

2. D. W. Marquardt. *Technomet.*, 12:591–613, 1970.

Appendix B. Publications

A number of publications have resulted from the efforts of this project. They are listed below in chronological order.

Peer reviewed

M. D. Ellegaard, J. Abildskov, J. P. O'Connell. Method for predicting solubilities of solids in mixed solvents. *AIChE Journal*. **2009**, *55(5)*, 1256-1264.

J. Abildskov, M. D. Ellegaard, J. P. O'Connell. Correlation of phase equilibria and liquid densities for gases with ionic liquids. *Fluid Phase Equilibria*. **2009**, *286(1)*, 95-106.

J. Abildskov, M. D. Ellegaard, J. P. O'Connell. Densities and isothermal compressibilities of ionic liquids – Modelling and application. *Fluid Phase Equilibria*. **2010**, *295(2)*, 215-229.

M. D. Ellegaard, J. Abildskov, J. P. O'Connell. Molecular thermodynamic modeling of mixed solvent solubility. *Industrial & Engineering Chemistry Research*. **2010**, *49(22)*, 11620-11632.

J. Abildskov, M. D. Ellegaard, J. P. O'Connell. Phase behavior of ionic liquids and organic solvents. *Journal of Supercritical Fluids*. **2010**, *55(2)*, 833-845.

M. D. Ellegaard, J. Abildskov, J. P. O'Connell. Solubilities of gases in ionic liquids using a corresponding-states approach to Kirkwood-Buff solution theory. *Fluid Phase Equilibria*. **2011**, *302(1-2)*, 93-102.

M. D. Ellegaard, J. Abildskov, J. P. O'Connell. Solid solubility in mixed solvents combining fluctuation solution theory and UNIFAC. *Fluid Phase Equilibria*. **2011**, in preparation.

Unreviewed conference proceedings

M. E. Christensen, J. P. O'Connell, J. Abildskov. New method for correlating and predicting solubilities in mixed solvents. Presented at the 23rd European Symposium on Applied Thermodynamics, Cannes, France. May 29-June 1, 2008.

Appendix B. Publications

M. E. Christensen, J. Abildskov, J. P. O'Connell. Recent progress in mixed solvent solubility. Presented at the American Institute of Chemical Engineers Annual Meeting, Philadelphia, PA, USA. November 16-21, 2008.

M. D. Ellegaard, J. Abildskov, J. P. O'Connell. Solubility of solids in mixed solvents – Modeling and data reduction. Presented at the 17th Symposium on Thermophysical Properties, Boulder, CO, USA. June 21-26, 2009.

J. Abildskov, M. D. Ellegaard, J. P. O'Connell. Solubilities, Henry's law constants and direct correlation function integrals of gases in ionic liquids. Presented at the 17th Symposium on Thermophysical Properties, Boulder, CO, USA. June 21-26, 2009.

J. Abildskov, M. D. Ellegaard, J. P. O'Connell. Densities and isothermal compressibilities of ionic liquids – Data retrieval, modelling, and application. Presented at the 17th Symposium on Thermophysical Properties, Boulder, CO, USA. June 21-26, 2009.

J. Abildskov, M. D. Ellegaard, J. P. O'Connell. Corresponding states correlation for liquid densities and gas solubilities in ionic liquids. Presented at the 24th European Symposium on Applied Thermodynamics, Compostela, Spain. June 27-July 1, 2009.

R. Ceriani, E. Conte, M. D. Ellegaard, C. A. Díaz Tovar, C. B. Gonçalves, A. J. A. Meirelles, R. Gani. GC, GC+ and atom connectivity index-based models for physical properties of lipid systems. Presented at the 24th European Symposium on Applied Thermodynamics, Compostela, Spain. June 27-July 1, 2009.

M. D. Ellegaard, J. Abildskov, J. P. O'Connell. Thermodynamic properties and gas solubilities in ionic liquids from a group contribution approach to fluctuation solution theory. Presented at Thermodynamics 2009, London, UK. September 23-25, 2009.

M. D. Ellegaard, J. Abildskov, J. P. O'Connell. Application of fluctuation solution theory to properties of ionic liquid systems. Presented at Properties and Phase Equilibria for Product and Process Design (PPEPPD), Suzhou, Jiangsu, China. May 16-21, 2010.

M. D. Ellegaard, J. Abildskov. Modellering af opløseligheder i blandede solventsystemer. Presented at Dansk Kemiingeniørkonference–DK_2, Kgs. Lyngby, Denmark. June 16-17, 2010.

This PhD-project was carried out at CAPEC, the Computer Aided Product-Process Engineering Center.
CAPEC is committed to research, to work in close collaboration with industry and to participate in educational activities. The research objectives of CAPEC are to develop computer-aided systems for product/process simulation, design, analysis and control/operation for chemical, petrochemical, pharmaceutical and biochemical industries. The dissemination of the research results of CAPEC is carried out in terms of computational tools, technology and application. Under computational tools, CAPEC is involved with mathematical models, numerical solvers, process/operation mathematical models, numerical solvers, process simulators, process/product synthesis/design toolbox, control toolbox, databases and many more. Under technology, CAPEC is involved with development of methodologies for synthesis/design of processes and products, analysis, control and operation of processes, strategies for modelling and simulation, solvent and chemical selection and design, pollution prevention and many more. Under application, CAPEC is actively involved with developing industrial case studies, tutorial case studies for education and training, technology transfer studies together with industrial companies, consulting and many more.

Further information about CAPEC can be found at www.capec.kt.dtu.dk.

Computer Aided Process Engineering Center
Department of Chemical and Biochemical Engineering
Technical University of Denmark
Søltofts Plads, Building 229
DK-2800 Kgs. Lyngby
Denmark

Phone: +45 4525 2800
Fax: +45 4525 4588
Web: www.capec.kt.dtu.dk

ISBN: 978-87-92481-47-4